Equity and Foreign Exchange Hybrid Models for Pricing Long-Maturity Financial Derivatives

Equity and Foreign Exchange Hybrid Models for Pricing Long-Maturity Financial Derivatives

PROEFSCHRIFT

ter verkrijging van de graad van doctor
aan de Technische Universiteit Delft,
op gezag van de Rector Magnificus Prof. ir. K.C.A.M. Luyben,
voorzitter van het College voor Promoties,
in het openbaar te verdedigen
op dinsdag 24 mei 2011 om 12:30 uur

door

Lech Aleksander GRZELAK

wiskundig ingenieur

geboren te Zielona Góra, Polen.

Dit proefschrift is goedgekeurd door de promotor:

Prof. dr. ir. C.W. Oosterlee

Samenstelling promotiecommissie:

Rector Magnificus	voorzitter
Prof. dr. ir. C.W. Oosterlee	Technische Universiteit Delft, promotor
Prof. dr. G. Deelstra	Université Libre de Bruxelles
Prof. dr. ir. A.W. Heemink	Technische Universiteit Delft
Prof. dr. M. Rutkowski	University of Sydney & Warsaw University of Technology
Prof. dr. J.M. Schumacher	Tilburg University
Prof. dr. ir. M.H. Vellekoop	Universiteit van Amsterdam
Drs. S. van Weeren	Rabobank International, Utrecht
Prof. dr. ir. C. Roos	Technische Universiteit Delft, reservelid

Dit onderzoek kwam tot stand met steun van Rabobank.

ISBN 978-90-8570-749-3

Cover design by Lech A. Grzelak and created by Sylwia Kuniewska.

Typeset by the author with the LaTeX Documentation System
Printed in The Netherlands by: Wöhrmann Print Service

To my family

Acknowledgements

This thesis concludes nearly four years of my PhD research at the Delft University of Technology. I would like to thank a number of people that contributed with their expertise and work to the realization of this thesis.

First of all I would like to thank Prof. Kees Oosterlee for his guidance during the research and for the long and fruitful discussions that we held during those years. It has been a great pleasure to work with Kees and learn from his experience.

I would like to thank Sacha van Weeren from Rabobank International for initiating this PhD research as a cooperation project between the university and banking industry. Sacha's constructive criticism and many comments have always been highly appreciated.

Particular thanks and gratitude go to Natalia Borovykh who always had time to deal with problems appearing during the research. I have learnt a lot from her insightful comments.

Sincere gratitude goes to Prof. Jolanta Misiewicz from the Warsaw University of Technology who sent me as an exchange student to the Delft University of Technology. I thank her for giving me this great opportunity.

I would also like to express my gratitude to all my colleagues at the Numerical Analysis group at TU Delft and at the DR&V team at Rabobank International. It was a great time of work and pleasure.

I would like to thank the members of my doctoral examination committee for their constructive comments and suggestions.

My time at Delft/Rabo was made enjoyable due to the many friends and groups that became a part of my life. I am especially grateful for time spent with Bin and Floris- it was a great pleasure to work together with you guys. I also would like to thank "small" Erik and Floris for translating the propositions and the summary into Dutch.

I am indebted to many of my colleagues who supported me. Especially, I would like to thank Łukasz and Magda for their friendship and our memorable trips around the Netherlands. I also thank my friend Olav for the excellent times we had when researching and trading the energy derivatives.

The most important thanks go to my family for their endless support and encouragement in those difficult but beautiful years of being a PhD Student.

Lech A. Grzelak
Delft, April 2011

Summary

Equity and Foreign Exchange Hybrid Models for Pricing Long-Maturity Financial Derivatives

Lech A. Grzelak

When the financial sector is in crisis, stocks go down and investors escape from the market to reduce their losses. Central banks then decrease interest rates in order to increase cash flow: this may lead to an increase in stock values, since it becomes less attractive for investors to keep their money in bank accounts. It is clear, therefore, that movements in the interest rate market can influence the behavior of stock prices. This is taken into account in the so-called *hybrid* models currently being developed.

Modelling derivative products in Finance usually starts with the specification of a system of Stochastic Differential Equations (SDEs), that corresponds to state variables like stock, interest rate, Foreign Exchange (FX) rate and volatility. By correlating the SDEs for the different asset classes one can define the hybrid models, and use them for pricing multi-asset derivatives. Even if each of the individual SDEs yields a closed-form solution, a non-zero correlation structure between the processes may cause difficulties for efficient product pricing. Typically, a closed-form solution of hybrid models is not known, and numerical approximation by means of Monte Carlo (MC) simulation or discretization of the corresponding Partial Differential Equations (PDEs) has to be employed for pricing. The speed of pricing European derivative products is crucial, especially for the calibration of the SDEs. Several theoretically attractive SDE models, that cannot fulfil the speed requirements, are not used in practice.

Over the past decade the Heston equity model with deterministic interest rates has established itself as one of the benchmark models for pricing equity derivatives. The assumption of deterministic interest rates in the plain Heston model is harmless when equity products with a short time to maturity need to be priced. For long-term equity, foreign exchange, or equity-interest rate hybrid products, however, a deterministic interest rate may be inaccurate.

In this thesis we present an approach for modelling these derivatives based on the extension of the Heston model with stochastic interest rates. The models developed allow for highly efficient pricing of simple, plain vanilla, derivative products.

Approximations of the full-scale Heston hybrid models, developed in this thesis, fit in the class of affine diffusion processes for which the characteristic function (ChF) exists. Availability of the ChF gives rise to efficient model calibration to liquid European derivative contracts.

It is challenging to define a realistic model, which generates implied volatility skews and smiles observable in the financial equity, FX and interest rate markets and links, by correlation, different asset classes, for which a ChF can be determined.

The point of departure in this thesis is the extended stochastic volatility model of Schöbel-Zhu with Gaussian interest rates which is presented in Chapter 1. The model enables us to perform, with a full matrix of correlations, efficient pricing of equity-interest rate hybrid products. Although, the hybrid model is analytically tractable and a semi-closed form ChF is available, the basic dynamics of the volatility process requires improvements.

In the remaining chapters of the thesis generalized hybrid models are considered. The stochastic volatility model of Schöbel-Zhu is replaced by the model of Heston, which provides a richer volatility structure as presented in Chapter 2. In this model the variance process may follow a *fat-tailed* non-central chi-square distribution.

The main issue when defining hybrid models that belong to the class of affine diffusion processes is the non-affine covariance structure. This, as presented in Chapter 2, can be resolved by *linearizations*. Two methods for obtaining approximations are proposed. Both approaches provide high accuracy and efficient model calibration.

It is then shown in Chapter 3 that under the linearized covariance structure it is possible to *define* a Heston hybrid model with a multi-factor Gaussian short-rate for which approximations are not required. As such, this hybrid model, by definition, is affine. For hybrids, with Gaussian short-rate processes for the interest rates, it is shown that the forward measure is favorable for determining the ChF and model simulation.

In order to handle hybrid payoffs sensitive to so-called *leverage* effects present in equity *and* interest rate markets we propose, in Chapter 4, a novel hybrid model in which the interest rates model is improved, and driven by the displaced-diffusion stochastic volatility Libor Market Model. We show that although the model has an involved structure it is still possible to derive the ChF, by a number of linearizations and measure changes.

Finally, in Chapter 5, models for multiple interest rate markets are considered. Due to the existence of long-dated foreign exchange-exotic products, like the so-called *Power-Reverse Dual-Currency*, we develop improved stochastic volatility foreign exchange models in which correlated stochastic interest rates are considered. We put particular emphasis on model calibration of FX options across different maturities and strikes.

Pricing modern contracts involving multiple asset classes requires well-developed pricing models by quantitative analysts. In this thesis we propose a number of hybrid models which can be used for pricing the corresponding hybrid derivatives. For the models developed we describe efficient model calibration and discuss efficient simulation with Monte Carlo techniques. We have also tested the models by pricing a number of hybrid products under extreme parameter settings.

Samenvatting (Dutch Summary)

Waarderen van langlopende financiële derivaten met hybride modellen voor aandelen- en valutakoersen.

Lech A. Grzelak

Als de financiële wereld zich in een crisis bevindt, dalen aandeelprijzen en keren investeerders zich van de markt af om hun verliezen te beperken. Centrale banken verlagen dan hun rente om de economie te stimuleren. Dit kan ertoe leiden dat aandeelprijzen stijgen, omdat het voor investeerders minder aantrekkelijk wordt om geld op de bank te houden. Uit dit voorbeeld blijkt dat fluctuaties in de rente effect kunnen hebben op het gedrag van aandelenmarkten. Dit effect wordt meegenomen in de hybride modellen die momenteel ontwikkeld worden.

Het modelleren van financiële derivaten begint meestal met het specificeren van een systeem van stochastische differentiaalvergelijkingen (SDVs), die corresponderen met toestandsvariabelen als aandeelprijs, rente, valutakoers en volatiliteit. Door correlaties te specificeren tussen de verschillende SDVs kan een hybride model gecreëerd worden, dat dan gebruikt kan worden om financiële derivaten op portefeuilles met meerdere productklassen te waarderen. Zelfs als voor ieder van de SDVs een gesloten formule kan worden afgeleid is het nog lastig om de producten efficiënt te waarderen als de correlaties ongelijk zijn aan nul.

Voor een hybride model is een analytische formule meestal niet beschikbaar en daarom worden numerieke methoden, zoals Monte Carlo simulatie (MC) of het discretiseren van de bijbehorende partiële differentiaalvergelijking (PDV), gebruikt voor waarderingen. Snelheid van berekening is een cruciaal punt voor het waarderen van Europese derivaten, vooral voor de calibratie van de onderliggende SDVs. Sommige theoretisch veelbelovende SDV-modellen worden in de praktijk niet gebruikt vanwege het gebrek aan rekensnelheid. De afgelopen 10 jaar is het Heston model met determinische rente uitgegroeid tot één van de referentiemodellen voor het waarderen van aandeelderivaten. De aanname in het Heston model dat de rente deterministisch is, heeft geen invloed op de prijs van aandeelproducten met een korte looptijd. Echter, voor wisselkoersen of aandeel-rente hybride producten met een lange looptijd, kan deze aanname onnauwkeurig zijn.

In dit proefschrift presenteren we een methode om deze producten te modelleren, gebaseerd op het Heston model dat wordt uitgebreid met een stochastisch rentemodel. Met de ontwikkelde modellen kunnen op een zeer efficiënte wijze eenvoudige derivaten worden gewaardeerd. Benaderingen van dit uitgebreide Heston hybride model, zodat de benaderende modellen in de klasse van affiene diffusieprocessen vallen, worden in dit proefschrift uitvoerig beschreven. Voor deze affiene processen is de karakteristieke functie (KF) beschikbaar. Het bestaan van een dergelijke functie zorgt ervoor dat het model op een efficiënte wijze naar liquide Europese derivaten gecalibreerd kan worden.

Het is een uitdaging om een realistisch model te definiëren waarvoor de KF bepaald kan worden, en dat een *implied volatility skew en smile*, geobserveerd in aandelen-, valutakoersen en rentemarkten, produceert en tevens de link legt, door middel van correlatie, tussen de verschillende productklassen. Het startpunt van dit proefschrift is het stochastische volatiliteitsmodel van Schöbel-Zhu, dat uitgebreid is met een Gaussisch model voor de rente. Dit wordt besproken in Hoofdstuk 1. Met dit model kunnen we, met een volledige correlatie matrix, op een efficiënte manier aandeel-rente hybride producten waarderen.

Hoewel dit model analytisch traceerbaar is, en er een semi-analytische formule voor de KF afgeleid kan worden, moeten de modelconcepten verder verbeterd worden. In de overige hoofdstukken van dit proefschrift worden gegeneraliseerde hybride modellen beschouwd. Het stochastische volatiliteitsmodel van Schöbel-Zhu wordt vervangen door het Heston model, dat een gevarieërdere volatiliteitsstructuur bevat. Dit wordt beschreven in Hoofdstuk 2. In dit model volgt het variantieproces een niet-centrale chi-kwadraat verdeling. Het belangrijkste probleem dat opgelost dient te worden, is dat van een niet-affiene covariantiestructuur. Dit kan, zoals wordt besproken in Hoofdstuk 2, worden opgelost door middel van linearisatie. Twee benaderingsmethoden worden voorgesteld. Beide resulteren in een zeer nauwkeurige en efficiënte modelcalibratie.

In Hoofdstuk 3 wordt aangetoond dat het mogelijk is om met een gelineariseerde covariantiestructuur een Heston hybride model met een multi-factor Gaussische korte-termijn-rente te definiëren, waarvoor geen additionele benaderingen vereist zijn. Daarom is dit hybride model per definitie een affien proces. Voor hybride modellen met een Gaussische korte-termijn-rentestructuur wordt aangetoond dat de *forward measure* (de voorwaartse maat) de voorkeur geniet voor het bepalen van de KF en de modelsimulatie.

Om hybride producten, die gevoelig zijn voor het zogenoemde hefboomeffect dat geobserveerd wordt in de aandelen- en rentemarkt, te kunnen waarderen, wordt in Hoofdstuk 4 een nieuw hybride model geïntroduceerd, waarin de stochastische rente verbeterd is en aangedreven wordt door het verplaatste diffusie stochastische volatiliteit Libor Markt Model. We tonen aan dat, hoewel het model een complexe structuur heeft, het toch mogelijk is om de KF af te leiden door middel van een aantal linearisaties en veranderingen van de maat.

Tot slot worden in Hoofdstuk 5 wisselkoersmodellen met meerdere valutakoersen behandeld. Vanwege het bestaan van lange-termijn exotische valutaproducten, zoals de *Power-Reverse Dual-Currency*, ontwikkelen we verbeterde valutakoersmodellen, waarin gecorreleerde rentes toegestaan zijn. We leggen extra nadruk op de modelcalibratie van opties op wisselkoersen voor verschillende uitoefenprijzen en looptijden.

Voor het waarderen van moderne financiële contracten, waarin meerdere productklassen aanwezig zijn, bij financiële instellingen zijn geavanceerde modellen nodig. In dit proefschrift stellen we een aantal hybride modellen voor, die gebruikt kunnen worden om deze contracten te waarderen. Voor de ontwikkelde modellen beschrijven we de efficiënte modelcalibratie en bespreken we simulatie met Monte Carlo technieken. De hybride modellen zijn ook getest door een aantal producten onder extreme parameterkeuzes te waarderen.

Contents

List of Symbols

Ω	Sample space
$\mathcal{F}$	σ-algebra
$\mathbb{P}$	Probability measure
$\mathbb{Q}$	Risk-neutral probability measure
$\mathbb{E}^{\mathcal{A}}(\cdot\|\mathcal{F}(t))$	Expectation operator given the information at time t with respect to the probability measure $\mathcal{A}$
$\mathbf{X}(t)$	State vector
$\Lambda_{\mathbb{Q}}^{T}(t)$	Radon-Nikodym derivative at time t
$S(t)$	Asset price at time t
$y(t)$	Spot Foreign Exchange expressed in units of domestic currency
$B(t)$	Money-savings account at time t
$M_i(t)$	Money-savings account at time t in the i'th market
$r(t)$	Instantaneous short-term rate of interest at time t
$r_i(t)$	Inst. short-term rate of interest at time t in the i'th market
$v(t)$	Inst. variance at time t
$V(t)$	Inst. variance at time t for the H-LMM model
$\sigma(t)$	Inst. volatility at time t
t	Calendar time
T	Maturity time (final trading date)
τ	Time to maturity
K	Strike price
$\mathrm{d}W_x^N(t)$	Brownian motion in process x under the measure N
$P(t,T)$	Zero-coupon bond paying €1 at time T at time t
$f(t,T)$	Inst. forward rate with maturity time T at time t
δ_{s_i}	Time interval $s_{i+1}-s_i$ for time $s_{i+1}>s_i$
$V(t,x)$	Value of the European call option at time t determined by x
$\Pi(t,T)$	Value of an exotic contract with maturity T at time t
$\Gamma_n^{b_1,b_2}$	n^{th} expansion coefficient for the COS method

N_c	Number of expansion terms in the COS method
N'	Number of integration terms in the SZHW hybrid model
Δ	Coefficient in the H1-HW hybrid model
$\Omega(t)$	Time-dependent determinist function in the H1-HW hybrid model
$\bar{\Omega}$	Constant parameter in the dynamics for the approximation of the Heston hybrid model
$\Omega_1(t)$	Time-dependent deterministic function in the AH-Gn++ model
$\widetilde{D}$	The integration domain $\widetilde{\Omega} = [b_1, b_2]$ for the COS method
Δ_{G}	Hedging parameter, called "Delta"
Γ_{G}	Hedging parameter, called "Gamma"
$\mathbf{\Sigma}$	Instantaneous covariance matrix
$\mathbf{\Sigma}_{(i,j)}$	Element (i, j) of the instantaneous covariance matrix $\mathbf{\Sigma}$
$\widetilde{\mu}(u, \tau)$	Complex-valued function, for the SZHW model, with the Fourier argument u and time to maturity τ
$V_{\mathrm{call}}(T_i, K_j)$	Theoretical model price of a call option with maturity time T_i and strike K_j
$\hat{V}_{\mathrm{call}}(T_i, K_j)$	Market price of a call option with maturity time T_i and strike K_j
$\Lambda(t)$	Time-dependent function approximating the expectation of the square-root process $v(t)$
$\widetilde{\Lambda}(t)$	Time-dependent function approximating $\Lambda(t)$
$\rho_{x,y}$	Instantaneous correlation between processes x and y
$\phi(u, x(t), t, T)$	Discounted characteristic function for process $x(t)$ at time t over time domain $[t, T]$
$\phi(u, x(t), \tau)$	Discounted characteristic function for process $x(t)$ at time t over time domain $[t, t + \tau]$
$\phi^T(u, x^T(t), \tau)$	The T-forward characteristic function for process $x^T(t)$ at time t over time domain $[t, t + \tau]$
$L(t, T_i, T_j)$	Libor rate at time t over the time period $[T_i, T_j]$
$\mathbf{L}(t)$	Lower triangular Cholesky matrix
$\mathbf{C}$	Correlation matrix
δ	Monte Carlo step size
$\Upsilon(u, t, T)$	Time-dependent function for the SZHW hybrid model
β_k	Displacing parameter in the Libor Market Model
ω_n	Weighting function for the COS method
$\mathrm{Re}(\cdot)$	Real part of the argument $(\cdot)$
SSE	Sum Squared Error
$\Gamma(a, z)$	Gamma function
$\mathcal{T}$	Tenor structure in the Libor Market Model
τ_k	A tenor defined as a time between two dates T_k and T_{k-1} i.e.: $\tau_k = T_k - T_{k-1}$
Ξ	Girsanov kernel
Φ	The cumulative distribution function of the standard normal variable

CHAPTER 1

Introduction

> The most valuable commodity I know of is information.
>
> *Gordon Gekko ("Wall Street")*

1.1 Motivation and thesis organization

When the financial sector is in crisis, stocks go down and investors escape from the market to reduce their losses. Central banks then decrease interest rates in order to increase cash flow: this may lead to an increase in stock values, since it becomes less attractive for investors to keep their money in bank accounts. It is clear, therefore, that movements in the interest rate market can influence the behavior of stock prices. This is taken into account in the so-called *hybrid* models currently being developed.

The hybrid contracts from the financial industry are based on products from different asset classes, like stock, interest rate and commodities. Since these products have different expected returns and risk levels they can be often designed to provide capital or income protection, diversification for portfolios and customized solutions for both institutional and retail markets.

Proper construction of a new hybrid product may give reduced risk and an expected return greater than that of the least risky asset. A simple example is a portfolio containing a stock with a high risk and return and a bond with a low risk and return. If one introduces an equity component into a pure bond portfolio the expected return will increase. If the percentage of the equity in the portfolio is increased, it eventually starts to dominate the structure and the risk may increase with a higher impact for a low or negative correlation.

Advanced hybrid models can be expressed by a system of stochastic differential equations (SDEs), for example for stock, volatility and interest rate, with a full correlation matrix. Such an SDE system typically contains many parameters that should be determined by calibration with financial market data. This task is challenging: European options need to be priced repeatedly within a calibration procedure, which should therefore be done extremely fast and efficiently.

At a major financial institution like a bank, one can distinguish a number of tasks that must be performed in order to price a new financial derivative product. First, the new product is defined, as the market asks for it. If this is a derivative product, then there are underlyings, modelled by stochastic differential equations (SDEs). Each asset class has different characteristics, leading to different types of SDEs. To achieve a reasonable model that is related to the present market, one calibrates the SDEs by means of European options. These products also form the basis for the hedge strategies used by the banks to reduce the risk associated with selling the new product. Once the asset price model is determined, the new derivative product is modelled accordingly. The product of interest is then priced by means of a Monte Carlo simulation for the integral formulation of the problem, or by numerical approximation of a partial differential equation.

The choice of numerical pricing method is thus based on whether one is aiming for the model calibration, in which speed of a pricing method is essential, or for the pricing of the new contract, for which robustness of the numerical method is of highest importance. Fourier-based option pricing methods are computationally fast but it is a challenge to employ them for the hybrid models mentioned above. They work whenever the characteristic function of the asset price process, i.e., the Fourier transform of the probability density function, is available.

Although hybrid models can relatively easily be defined, real use of these models is only guaranteed when they provide a satisfactory fit to market implied volatility structures and when it is possible to set a non-zero correlation structure among the processes from the different asset classes. Furthermore, highly efficient pricing of fundamental contracts needs to be available for model calibration. In this dissertation we propose models which satisfy these requirements.

This dissertation is organized as follows.

In Chapter 1 we introduce the affine diffusion framework which constitutes the fundament for the models developed. We then present the extended stochastic volatility equity model of Schöbel-Zhu [100] with stochastic interest rates of Hull-White [56]. The model is used for pricing a number of typical equity-interest rates products which are sensitive to the correlations between underlying asset classes. This chapter contains essentially the contents of the article [50].

In Chapter 2 two approximations for the non-affine Heston-Hull-White and Heston-Cox-Ross-Ingersoll hybrid models are proposed. We find that, in order to obtain an affine approximation of the Heston hybrids, it is sufficient to linearize the non-affine terms in the covariance matrix. The approximations give rise to efficient determination of the corresponding characteristic functions. Chapter 2 contains essentially the contents of the article [48].

In Chapter 3 an affine variant of the Heston-multi-factor Gaussian interest rate model is defined. For the model, denoted by AH-Gn++, we also discuss an efficient Monte Carlo simulation scheme and an effective way for calculating the Greeks of plain vanilla options. By measure change the equity forward prices are determined and the model dimensionality can be reduced. This chapter contains essentially the contents of the article [49].

In Chapter 4 the Heston hybrid model with the interest rate driven by the displaced-diffusion stochastic volatility Libor Market Model is derived. This *new* model enables pricing hybrid products that are also sensitive to interest rate smile/skew effects. By a number of linearizations the model can be used for pricing the equity plain vanilla options. This chapter contains essentially the contents of the article [46].

In Chapter 5 hybrid models developed in the context of Foreign Exchange are discussed. The models under consideration incorporate correlated interest rate processes driven either by short-rate models or by Market Models. The resulting pricing formulas form the basis for calibration strategies. This chapter contains essentially the contents of the article [47].

In Chapter 6 conclusions are presented, as well as an outlook for future research.

1.2 Affine Diffusion processes

The affine diffusion (AD) class refers to a fixed probability space $(\Omega, \mathcal{F}, \mathbb{Q})$ and a Markovian n-dimensional affine process $\mathbf{X}(t)$ in some space $D \subset \mathbb{R}^n$. The stochastic model of interest, without jumps, can be expressed by the following stochastic differential form:

$$\mathrm{d}\mathbf{X}(t) = \mu(\mathbf{X}(t))\mathrm{d}t + \sigma(\mathbf{X}(t))\mathrm{d}\widetilde{\mathbf{W}}(t),$$

where $\widetilde{\mathbf{W}}(t)$ is a $\mathcal{F}(t)$-standard column vector of independent Brownian motion in $\mathbb{R}^n$, $\mu(\mathbf{X}(t)) : D \to \mathbb{R}^n$, $\sigma(\mathbf{X}(t)) : D \to \mathbb{R}^{n\times n}$. Moreover, for processes in the AD class it is assumed that drift $\mu(\mathbf{X}(t))$, covariance $\sigma(\mathbf{X}(t))\sigma(\mathbf{X}(t))^{\mathrm{T}}$ and interest rate component $r(\mathbf{X}(t))$ are of the affine form, i.e.

$$\mu(\mathbf{X}(t)) = a_0 + a_1\mathbf{X}(t), \text{ for any } (a_0, a_1) \in \mathbb{R}^n \times \mathbb{R}^{n\times n}, \tag{1.1}$$

$$(\sigma(\mathbf{X}(t))\sigma(\mathbf{X}(t))^{\mathrm{T}})_{i,j} = (c_0)_{ij} + (c_1)_{ij}^{\mathrm{T}}\mathbf{X}(t), \text{ with } (c_0, c_1) \in \mathbb{R}^{n\times n} \times \mathbb{R}^{n\times n\times n}, \tag{1.2}$$

$$r(\mathbf{X}(t)) = r_0 + r_1^{\mathrm{T}}\mathbf{X}(t), \text{ for } (r_0, r_1) \in \mathbb{R} \times \mathbb{R}^n. \tag{1.3}$$

Then, it can be shown that for a state vector, $\mathbf{X}(t)$, the discounted characteristic function (ChF) is of the following form:

$$\phi(\mathbf{u}, \mathbf{X}(t), t, T) = \mathbb{E}^{\mathbb{Q}}\left(\mathrm{e}^{-\int_t^T r(s)\mathrm{d}s + i\mathbf{u}^{\mathrm{T}}\mathbf{X}(T)} \middle| \mathcal{F}(t)\right) = \mathrm{e}^{A(\mathbf{u},\tau)+\mathbf{B}^{\mathrm{T}}(\mathbf{u},\tau)\mathbf{X}(t)},$$

where the expectation is taken under the risk-neutral measure, $\mathbb{Q}$, and T indicates maturity time. For a time lag, $\tau := T - t$, the coefficients $A(\mathbf{u}, \tau)$ and $\mathbf{B}^{\mathrm{T}}(\mathbf{u}, \tau)$ have to satisfy certain complex-valued ordinary differential equations (ODEs) (see work of Duffie-Pan-Singleton [28] for details):

$$\begin{cases} \dfrac{\mathrm{d}}{\mathrm{d}\tau}A(\mathbf{u}, \tau) = & -r_0 + \mathbf{B}^{\mathrm{T}}(\mathbf{u}, \tau)a_0 + & \dfrac{1}{2}\mathbf{B}^{\mathrm{T}}(\mathbf{u}, \tau)c_0\mathbf{B}(\mathbf{u}, \tau), \\ \dfrac{\mathrm{d}}{\mathrm{d}\tau}\mathbf{B}(\mathbf{u}, \tau) = & -r_1 + a_1^{\mathrm{T}}\mathbf{B}(\mathbf{u}, \tau) + & \dfrac{1}{2}\mathbf{B}^{\mathrm{T}}(\mathbf{u}, \tau)c_1\mathbf{B}(\mathbf{u}, \tau). \end{cases} \tag{1.4}$$

The dimension of the (complex valued) ODEs for $\mathbf{B}(\mathbf{u},\tau)$ corresponds to the dimension of the state vector, $\mathbf{X}(t)$. Typically, multi-factor models provide a better fit to the observed market data than one-factor models. However, as the dimension of SDE system increases, the ODEs to be solved to get the ChF become increasingly complicated. If an analytic solution to the ODEs cannot be obtained, one can apply well-known numerical ODE techniques instead. This may require computational effort, which essentially makes the model problematic for practical calibration. Therefore, an objective is also to define hybrid SDE models for which an analytic solution to most of the ODEs appearing can be obtained.

1.2.1 Affine Diffusion equity models

Based on a geometric Brownian motion model for asset prices and under general equilibrium assumptions, Black and Scholes [16] derived their famous partial differential equation for option prices in 1973. Empirical studies of financial time series have, however, revealed that the normality assumption for asset prices in the Black-Scholes theory cannot capture heavy tails and asymmetries present in log-returns in practice [97]. The empirical densities are usually highly peaked compared to the normal density. Therefore, a number of alternative asset models have appeared.

A major step, away from the assumption of constant volatility in asset pricing, was made by Hull and White [55], Stein and Stein [104], Heston [54], Schöbel and Zhu [100], who defined the volatility as a diffusion process. In general, under risk-free measure $\mathbb{Q}$, a model with diffusive volatility structure can be presented as:

$$\begin{cases} \mathrm{d}S(t)/S(t) = & r\mathrm{d}t + a(t,v(t))\mathrm{d}W_x(t), \\ \mathrm{d}v(t) = & b(t,v(t))\mathrm{d}t + c(t,v(t))\mathrm{d}W_v(t), \end{cases} \tag{1.5}$$

with constant interest rate r, correlation $\mathrm{d}W_x(t)\mathrm{d}W_v(t) = \rho_{x,v}\mathrm{d}t$ and $|\rho_{x,v}| < 1$. Depending on the functions $a(t,v(t))$, $b(t,v(t))$ and $c(t,v(t))$ a number of stochastic volatility models has been defined.

By using a Black-Scholes replication argument for determining the option prices, $V(t,S(t),v(t))$, we are able to determine the following partial differential equation based on (1.5) (see Gatheral [40] for details):

$$\begin{aligned} rV \quad = \quad & \frac{\partial V}{\partial t} + rS\frac{\partial V}{\partial S} + b(t,v)\frac{\partial V}{\partial v} + \frac{1}{2}c^2(t,v)\frac{\partial^2 V}{\partial v^2} + \frac{1}{2}a^2(t,v)S^2\frac{\partial^2 V}{\partial S^2} \\ & + \rho_{x,v}a(t,v)c(t,v)S\frac{\partial^2 V}{\partial S \partial v}. \end{aligned} \tag{1.6}$$

The prices of financial derivatives can be determined by solving PDE (1.6) with respect to a final condition that defines the payoff of the instrument at time T.

In the literature a number of methods for solving the PDE are available but we are particulary interested in the Feynman-Kac formula given in the theorem below.

Theorem 1.2.1 (Feynman-Kac theorem)**.** *The partial differential equation*

$$0 = \frac{\partial V}{\partial t} + \mu(t,x)\frac{\partial V}{\partial x} + \frac{1}{2}\sigma^2(t,x)\frac{\partial^2 V}{\partial x^2} - r(t,x)V,$$

with terminal condition $H(T,x)$ has as its solution:

$$V(t,x) = \mathbb{E}\left(\mathrm{e}^{-\int_t^T r(s,X(s))\mathrm{d}s} H(T,X(T))\middle|\mathcal{F}(t)\right),$$

where the expectation is taken with respect to the process X, defined by:

$$\mathrm{d}X(t) = \mu(t,X(t))\mathrm{d}t + \sigma(t,X(t))\mathrm{d}W(t),$$

Proof. The proof can be found in [85]. ■

As we see, by the Feynman-Kac theorem we can move from the problem of solving a PDE to evaluating an expectation of a discounted payoff. In the book by Pelsser [90] a comprehensive discussion is provided.

Two of the most popular models in (1.5), (1.6) are the stochastic volatility model of Heston [54] with $a(t,v(t)) = \sqrt{v(t)}$, $b(t,v(t)) = \kappa(\bar{v} - v(t))$ and $c(t,v(t)) = \gamma\sqrt{v(t)}$ and the one by Schöbel-Zhu [100] with $a(t,v(t)) = v(t)$, $b(t,v(t)) = \kappa(\bar{v} - v(t))$ and $c(t,v(t)) = \gamma$, with constant parameters κ,γ and $\bar{v}$. Under the log-transformation i.e.: $x(t) = \log S(t)$, both models belong to the class of affine diffusion models, so that pricing of simple financial products can be done very efficiently.

Stochastic volatility has improved the accuracy of pricing derivatives under heavy-tailed return distributions significantly. Although these stochastic volatility models have become popular for derivative pricing and hedging, see, for example, [37], financial engineers have also developed other complex exotic products, that require additionally the modelling of a stochastic interest rate component. A derivative pricing tool in which all these features are explicitly included may have the potential of generating even more accurate option prices for hybrid products.

In the next subsection we discuss the short-rate models that will be used as an extension of a stochastic volatility equity framework.

1.2.2 Affine interest rate models

A first attempt to relax the assumption of deterministic interest rates is to model the rates by a stochastic instantaneous spot-rate process $r(t)$. An instantaneous short-rate is defined as the interest rate one earns on a riskless investment over an infinitesimal period of time (typically denoted by $\mathrm{d}t$) [90]. Among many, the most successful short-rate models (due to their simple, affine structure) are the models developed by Vašiček [108], Cox-Ingersoll-Ross [25] and Hull and White [56], the latter two are extensions of the Vašiček model.

We will describe the main properties of the Hull-White model in more detail.

The Hull-White model

We consider the Hull-White [56], single-factor, no-arbitrage yield curve model in which the short-term interest rate is driven by an extended Ornstein-Uhlenbeck (OU) mean reverting process,

$$\mathrm{d}r(t) = \lambda\left(\theta(t) - r(t)\right)\mathrm{d}t + \eta \mathrm{d}W_r(t), \quad r(0) = r_0 > 0, \tag{1.7}$$

where $\theta(t) > 0, t \in \mathbb{R}^+$ is a time-dependent drift term, used to fit theoretical bond prices to the yield curve observed in the market and $W_r(t)$ is a Brownian motion under risk-free measure $\mathbb{Q}$. Parameter η determines the overall level of volatility and the reversion rate parameter λ defines the relative volatilities. A high value of λ causes short-term rate movements to damp out quickly, so that the long-term volatility is reduced.

We present the derivation for the discounted characteristic function (ChF) of the interest rate process. Integrating Equation (1.7), gives, for $t \geq 0$,

$$r(t) = r_0 \mathrm{e}^{-\lambda t} + \lambda \int_0^t \theta(s)\mathrm{e}^{-\lambda(t-s)}\mathrm{d}s + \eta \int_0^t \mathrm{e}^{-\lambda(t-s)}\mathrm{d}W_r(s).$$

It is easy to show that $r(t)$ is normally distributed with

$$\mathbb{E}^{\mathbb{Q}}\left(r(t)|\mathcal{F}(0)\right) = r_0 \mathrm{e}^{-\lambda t} + \lambda \int_0^t \theta(s)\mathrm{e}^{-\lambda(t-s)}\mathrm{d}s,$$

and

$$\mathbb{V}\mathrm{ar}^{\mathbb{Q}}\left(r(t)|\mathcal{F}(0)\right) = \frac{\eta^2}{2\lambda}\left(1 - \mathrm{e}^{-2\lambda t}\right).$$

Moreover, it is known that for $\theta(t)$ constant, i.e., $\theta(t) \equiv \theta$,

$$\lim_{t\to\infty} \mathbb{E}^{\mathbb{Q}}\left(r(t)|\mathcal{F}(0)\right) = \theta.$$

This means that for large t the first moment of the process converges to the mean reverting level θ.

In order to simplify the derivations to follow we use the following proposition (see Arnold [10], Oksendal [85], Pelsser [90]).

Proposition 1.2.2 (Hull-White decomposition)**.** *The Hull-White stochastic interest rate process (1.7) can be decomposed into* $r(t) = \widetilde{r}(t) + \psi(t)$*, where*

$$\psi(t) = r_0 \mathrm{e}^{-\lambda t} + \lambda \int_0^t \theta(s)\mathrm{e}^{-\lambda(t-s)}\mathrm{d}s,$$

and

$$\mathrm{d}\widetilde{r}(t) = -\lambda \widetilde{r}(t)\mathrm{d}t + \eta \mathrm{d}W_r(t), \textit{ with } \widetilde{r}_0 = 0.$$

Proof. The proof is straightforward by Itô's lemma. ■

An advantage of this transformation is that the stochastic process $\widetilde{r}(t)$ is now a basic OU mean reverting process, determined only by λ and η, independent of function $\psi(t)$. It is easier to analyze this model than the original Hull and White model [56].

We investigate the discounted conditional characteristic function (ChF) of spot interest rate $r(t)$,

$$\begin{aligned}\phi_{\mathrm{HW}}(u, r(t), t, T) &= \mathbb{E}^{\mathbb{Q}}\left(\mathrm{e}^{-\int_t^T r(s)\mathrm{d}s + iur(T)}|\mathcal{F}(t)\right)\\ &= \mathbb{E}^{\mathbb{Q}}\left(\mathrm{e}^{-\int_t^T \psi(s)\mathrm{d}s + iu\psi(T)} \cdot \mathrm{e}^{-\int_t^T \widetilde{r}(s)\mathrm{d}s + iu\widetilde{r}(T)}|\mathcal{F}(t)\right)\\ &= \mathrm{e}^{-\int_t^T \psi(s)\mathrm{d}s + iu\psi(T)} \cdot \phi_{\mathrm{HW}}(u, \widetilde{r}(t), t, T),\end{aligned}$$

and see that process $\widetilde{r}(t)$ is affine. Hence according to [28] the discounted ChF, $\phi_{\mathrm{HW}}(u, \widetilde{r}(t), \tau) := \phi_{\mathrm{HW}}(u, \widetilde{r}(t), t, T)$, for the affine interest rate model for $u \in \mathbb{C}$ is of the following form:

$$\phi_{\mathrm{HW}}(u, \widetilde{r}(t), \tau) = \mathbb{E}^{\mathbb{Q}}\left(\mathrm{e}^{-\int_t^T \widetilde{r}(s)\mathrm{d}s + iu\widetilde{r}(T)}|\mathcal{F}(t)\right) = \mathrm{e}^{A(u,\tau)+B(u,\tau)\widetilde{r}(t)}, \tag{1.8}$$

with $\tau = T - t$. The necessary "initial" condition accompanying (1.8) is $\phi_{\mathrm{HW}}(u, \widetilde{r}(T), 0) = \mathrm{e}^{iu\widetilde{r}(T)}$, so that $A(u, 0) = 0$ and $B(u, 0) = iu$. The solutions for $A(u, \tau)$ and $B(u, \tau)$ are provided by the following lemma:

Lemma 1.2.3 (Coefficients for discounted ChF for the Hull-White model)**.** *The functions $A(u, \tau)$ and $B(u, \tau)$ in (1.8) are given by:*

$$\begin{aligned}A(u, \tau) &= \frac{\eta^2}{2\lambda^3}\left(\lambda\tau - 2\left(1 - \mathrm{e}^{-\lambda\tau}\right) + \frac{1}{2}\left(1 - \mathrm{e}^{-2\lambda\tau}\right)\right) - iu\frac{\eta^2}{2\lambda^2}\left(1 - \mathrm{e}^{-\lambda\tau}\right)^2\\ &\quad -\frac{1}{2}u^2\frac{\eta^2}{2\lambda}\left(1 - \mathrm{e}^{-2\lambda\tau}\right),\\ B(u, \tau) &= iu\mathrm{e}^{-\lambda\tau} - \frac{1}{\lambda}\left(1 - \mathrm{e}^{-\lambda\tau}\right).\end{aligned}$$

Proof. The proof can be found in [19] pp. 75. ■

By simply taking $u = 0$, we obtain the risk-free pricing formula for a zero coupon bond $P(t, T)$:

$$\begin{aligned}\phi_{\mathrm{HW}}(0, r(t), \tau) &= \mathbb{E}^{\mathbb{Q}}\left(\mathrm{e}^{-\int_t^T r(s)\mathrm{d}s} \cdot 1|\mathcal{F}(t)\right)\\ &= \exp\left(-\int_t^T \psi(s)\mathrm{d}s + A(0, \tau) + B(0, \tau)\widetilde{r}(t)\right).\end{aligned}$$

Moreover, a zero-coupon bond can be written as the product of a deterministic factor and the bond price in an ordinary Vašiček model with zero mean, under the risk-neutral measure $\mathbb{Q}$. Recall that process $\widetilde{r}(t)$ at time $t = 0$ is equal to 0, so

$$P(0, T) = \exp\left(-\int_0^T \psi(s)\mathrm{d}s + A(0, T)\right),$$

which gives

$$\psi(T) = -\frac{\partial}{\partial T}\log P(0,T) + \frac{\partial}{\partial T}A(0,T) = f(0,T) + \frac{\eta^2}{2\lambda^2}\left(1-\mathrm{e}^{-\lambda T}\right)^2, \qquad (1.9)$$

where $f(t,T)$ is an instantaneous forward rate.

This result shows that $\psi(t)$ can be obtained from the initial forward curve, $f(0,T)$. The other time-invariant parameters, λ and η, have to be estimated using market prices of, in particular, interest rate caps and swaptions. Now from Proposition 1.2.2 we have $\theta(t) = \frac{1}{\lambda}\frac{\partial}{\partial t}\psi(t) + \psi(t)$ which reads,

$$\theta(t) \quad = \quad f(0,t) + \frac{1}{\lambda}\frac{\partial}{\partial t}f(0,t) + \frac{\eta^2}{2\lambda^2}\left(1-\mathrm{e}^{-2\lambda t}\right). \qquad (1.10)$$

Moreover, the ChF, $\phi_{\mathrm{HW}}(u, r(t), \tau)$, for the Hull-White model can be simply obtained by integration of $\psi(s)$ over the interval $[t,T]$.

Advanced interest rate models

The arbitrage-free short-rate models are standard in pricing and hedging interest rate (IR) products. When dealing with *not too complicated* products they perform very well, especially in modelling at-the-money options. Despite their simple structure, it is still a challenge to link these models with other asset classes to construct the desired hybrid models. In the first three chapters of this thesis we consider hybrids in which those short-rate models are used.

Although well-accepted by practitioners in modelling IR payoffs the assumption that instantaneous rates exist is debatable [82]. Moreover, exotic, typically callable [1], interest rate products are rather difficult to be priced accurately, especially when pricing products which are sensitive to implied volatility smiles or skews as commonly observed in the interest rate market. A more general class of models which, instead of modelling the short-rate, describes the dynamics of the forward dynamics are available. These are called *the Market Models.* The hybrid models based on this, advanced, structure will be discussed in Chapters 4 and 5.

1.3 Extended Affine Diffusion models

Since the assumptions in the standard Black-Scholes [16] model on constant volatility and constant interest rates do not find justification in reality we consider models with a more realistic setup. It was found by Bakshi in [12] that by assuming the volatility and the interest rates to be stochastic one can increase the hedging performance, especially for long-term contracts. Particular example of a structure for which the correlation between the equity and interest rates has an effect on the price is the autocallable hybrid derivative. As the investor is, for example, paying the LIBOR rate in exchange for his equity exposure, the duration of the swap is equity-dependent. This structured product is sensitive to the

[1] meaning that the product comes with early-exercise features

correlation between the interest rates and underlying equity (see, for example [86], for details).

Before we consider the improved hybrid models we derive the basic framework in which the Black-Scholes equity model is extended by an arbitrage-free Hull-White IR process.

1.3.1 Black-Scholes-Hull-White hybrid model

As a starting point we extend the standard Black-Scholes model [16] by the model of Hull-White. We call this model the Black-Scholes-Hull-White hybrid (BSHW) model. The model is often treated as a benchmark for modelling Foreign Exchange (FX) [42], inflation-indexed derivatives (Consumer-Price-Index) [64] or long-maturity options [19].

Under the risk-adjusted measure, $\mathbb{Q}$, the dynamics of the model $\mathbf{X}(t) = [S(t), r(t)]^{\mathrm{T}}$ are given by the following system of SDEs:

$$\begin{cases} \mathrm{d}S(t)/S(t) = & r(t)\mathrm{d}t + \sigma \mathrm{d}W_x(t), \quad S(0) = S_0 > 0, \\ \mathrm{d}r(t) = & \lambda(\theta(t) - r(t))\mathrm{d}t + \eta \mathrm{d}W_r(t), \quad r(0) = r_0 > 0, \end{cases}$$

where $W_x(t)$ and $W_r(t)$ are two *correlated* Brownian motions with $\mathrm{d}W_x(t)\mathrm{d}W_r(t) = \rho_{x,r}\mathrm{d}t$, and $|\rho_{x,r}| < 1$, is the instantaneous-correlation parameter between the asset price and the short-rate process. Parameters σ and η determine the volatility of equity and interest rate, respectively; $\theta(t)$ is a deterministic function (as defined in Equation (1.10)) and λ determines the speed of mean reversion.

After transforming the stock to log-coordinates, $x(t) = \log S(t)$, the model reads:

$$\begin{cases} \mathrm{d}x(t) = & (r(t) - 1/2\sigma^2)\mathrm{d}t + \sigma \mathrm{d}W_x(t), \\ \mathrm{d}r(t) = & \lambda\left(\theta(t) - r(t)\right)\mathrm{d}t + \eta \mathrm{d}W_r(t). \end{cases}$$

It is easy to see that the model satisfies the affinity conditions in (1.1),(1.2) and (1.3), so that the corresponding characteristic function $\phi_{\mathrm{BSHW}}(u, x(t), t, T)$ can easily be derived. For the state vector $\mathbf{X}(t) = [x(t), r(t)]^{\mathrm{T}}$ the discounted characteristic function is given by,

$$\begin{aligned} \phi_{\mathrm{BSHW}}(\mathbf{u}, \mathbf{X}(t), t, T) &= \mathbb{E}^{\mathbb{Q}}\left(\mathrm{e}^{-\int_t^T r(s)\mathrm{d}s + i\mathbf{u}^{\mathrm{T}}\mathbf{X}(T)}|\mathcal{F}(t)\right) \\ &= \mathrm{e}^{A(\mathbf{u},\tau) + \mathbf{B}^{\mathrm{T}}(\mathbf{u},\tau)\mathbf{X}(t)}. \end{aligned}$$

With $\mathbf{u} = [u, 0]^{\mathrm{T}}$ and $\tau := T - t$ it reads:

$$\phi_{\mathrm{BSHW}}(u, x(t), t, T) = \exp\left(A(u,\tau) + B(u,\tau)x(t) + C(u,\tau)r(t)\right),$$

with the final condition $\phi_{\text{BSHW}}(u, x(T), T, T) = \mathrm{e}^{iux(T)}$, and the complex-valued functions $A(u,\tau)$, $B(u,\tau)$ and $C(u,\tau)$ satisfy the following system of ODEs:

$$\begin{aligned}
B'(u,\tau) &= 0,\\
C'(u,\tau) &= -1 + B(u,\tau) - \lambda C(u,\tau),\\
A'(u,\tau) &= \frac{1}{2}\sigma^2 B(u,\tau)(B(u,\tau)-1) + \lambda\theta(T-\tau)C(u,\tau)\\
&\quad + \frac{1}{2}\eta^2 C^2(u,\tau) + \rho_{x,r}\sigma\eta B(u,\tau)C(u,\tau),
\end{aligned}$$

with the conditions: $B(u,0) = iu$, $C(u,0) = 0$, $A(u,0) = 0$. It is easy to find the solution of the ODEs given above:

$$\begin{aligned}
B(u,\tau) &= iu,\\
C(u,\tau) &= \frac{1}{\lambda}(iu-1)(1-\mathrm{e}^{-\lambda\tau}),\\
A(u,\tau) &= \frac{1}{2}\sigma^2 iu(iu-1)\tau + \frac{\rho_{x,r}\sigma\eta}{\lambda}(iu-1)\left(\tau + \frac{1}{\lambda}\left(\mathrm{e}^{-\lambda\tau}-1\right)\right)\\
&\quad + \frac{\eta^2}{4\lambda^3}(i+u)^2\left(3 + \mathrm{e}^{-2\lambda\tau} - 4\mathrm{e}^{-\lambda\tau} - 2\lambda\tau\right) + \lambda\int_0^\tau \theta(T-s)C(u,s)\mathrm{d}s.
\end{aligned}$$

The expression for $A(u,\tau)$ contains an integral over deterministic function, $\theta(t)$, which is calibrated to the current yield. This integral can be determined analytically, which will be presented in the follow-up section.

The ChF for the BSHW model can easily be determined and Fourier inversion techniques can efficiently be used for a number of payoffs. Moreover, pricing of plain vanilla equity options can be performed analytically under the T-forward measure [19, 87], as in the standard Black-Scholes model. The concept of measure change will be discussed later in this thesis (Chapter 3) when we deal with dimension reduction for multi-factor interest rate models.

1.3.2 Extended stochastic volatility model of Schöbel-Zhu

An attempt to model the random behavior of the volatility and interest rates was presented in [11, 83] where the Heston stochastic volatility model was combined with an *independent* interest rate process.

In this section we present a stochastic volatility (SV) equity hybrid model which contains a stochastic interest rate process and a *full matrix* of correlations between the underlying Brownian motions. In particular, we add to the SV model the well-known Hull-White stochastic interest rate process [56], mentioned before.

For state vector $\mathbf{X}(t) = [S(t), r(t), \sigma(t)]^{\mathrm{T}}$ let us fix a probability space $(\Omega, \mathcal{F}, \mathbb{Q})$ and a filtration $\mathcal{F} = \{\mathcal{F}(t) : t \geq 0\}$, which satisfies the usual conditions. Furthermore, $\mathbf{X}(t)$ is assumed to be Markovian relative to $\mathcal{F}(t)$.

So, under the risk-neutral measure, $\mathbb{Q}$, we consider a three-dimensional system of stochastic differential equations, of the following form:

$$\begin{cases} \mathrm{d}S(t)/S(t) = & r(t)\mathrm{d}t + & \sigma^p(t)\mathrm{d}W_x(t), \\ \mathrm{d}r(t) = & \lambda(\theta(t) - r(t))\mathrm{d}t + & \eta\mathrm{d}W_r(t), \\ \mathrm{d}\sigma(t) = & \kappa\left(\bar{\sigma} - \sigma(t)\right)\mathrm{d}t + & \gamma\sigma^{1-p}(t)\mathrm{d}W_\sigma(t), \end{cases} \tag{1.11}$$

where p is an exponent, κ and λ control the speed of mean reversion, η represents the interest rate volatility, and $\gamma\sigma^{1-p}(t)$ determines the volatility of the $\sigma(t)$ process. Parameters $\bar{\sigma}$ and $\theta(t)$ are the long-run mean of the volatility [2] and the interest rate processes, respectively. $W_k(t)$ with $k = \{x, r, \sigma\}$ are correlated Wiener processes, also governed by an instantaneous correlation matrix:

$$\mathbf{C} := \begin{bmatrix} 1 & \rho_{x,\sigma} & \rho_{x,r} \\ \rho_{\sigma,x} & 1 & \rho_{\sigma,r} \\ \rho_{r,x} & \rho_{r,\sigma} & 1 \end{bmatrix} \mathrm{d}t. \tag{1.12}$$

The system in (1.11) for $p = \frac{1}{2}$ is the Heston-Hull-White hybrid model and, under the assumptions of non-zero correlations, will be discussed in more detail in Chapter 2. If we keep, however, $p = \frac{1}{2}$ and $r(t)$ constant, we obtain the Heston model [54],

$$\begin{cases} \mathrm{d}S(t)/S(t) = & r\mathrm{d}t + & \sqrt{\sigma(t)}\mathrm{d}W_x(t), \\ \mathrm{d}\sigma(t) = & \kappa^H\left(\bar{\sigma}^H - \sigma(t)\right)\mathrm{d}t + & \gamma^H\sqrt{\sigma(t)}\mathrm{d}W_\sigma(t), \end{cases}$$

where the variance process is of CIR-type [25].

For $p = 1$ our model is, in fact, the generalized Stein-Stein [104] model, which is also called the Schöbel-Zhu [100] model:

$$\begin{cases} \mathrm{d}S(t)/S(t) = & r\mathrm{d}t + & \sqrt{v(t)}\mathrm{d}W_x(t), \\ \mathrm{d}v(t) = & 2\kappa\left(\bar{\sigma}\sigma(t) + \dfrac{\gamma^2}{2\kappa} - v(t)\right)\mathrm{d}t + & 2\gamma\sqrt{v(t)}\mathrm{d}W_\sigma(t), \end{cases}$$

in which the squared volatility, $v(t) = \sigma^2(t)$, represents the variance of the instantaneous stock return.

It was already indicated in [54] and [100] that the plain Schöbel-Zhu model is a particular case of the original Heston model. For $\bar{\sigma} = 0$, the Schöbel-Zhu model equals the Heston model in which $\kappa^H = 2\kappa$, $\bar{\sigma}^H = \gamma^2/2\kappa$, and $\gamma^H = 2\gamma$. This relation gives a direct connection between their discounted characteristic functions (see [74]). Finally, if we set $r(t)$ constant, $p = 0$ in system of Equations (1.11), and zero correlations, the model collapses to the standard Black-Scholes model [16].

We will choose the parameters in the equations (1.11), such that we deal with the Schöbel-Zhu-Hull-White [3] (SZHW). In [39] and [24] it is was shown that the

[2] depending on parameter p, $\sigma(t)$ denotes either volatility or variance

[3] The work on the SZHW hybrid model was initiated by Pelsser [73] and resulted in a paper [106].

so-called linear-quadratic diffusion (LQD) models are equivalent to the AD models with an augmented state vector.

Now, we derive an analytic pricing formula in (semi-)closed-form for European call options under the SZHW asset pricing model with a full matrix of correlations, defined by (1.12).

The Schöbel-Zhu-Hull-White hybrid model can be expressed by the following 3D system of SDEs

$$\begin{cases} \mathrm{d}S(t)/S(t) = & r(t)\mathrm{d}t + & \sigma(t)\mathrm{d}W_x(t), \\ \mathrm{d}r(t) = & \lambda\left(\theta(t) - r(t)\right)\mathrm{d}t + & \eta \mathrm{d}W_r(t), \\ \mathrm{d}\sigma(t) = & \kappa(\bar{\sigma} - \sigma(t))\mathrm{d}t + & \gamma \mathrm{d}W_\sigma(t), \end{cases} \tag{1.13}$$

with the parameters as in Equations (1.11), for $p = 1$, and the correlations:

$$\begin{cases} \mathrm{d}W_x(t)\mathrm{d}W_\sigma(t) & = & \rho_{x,\sigma}\mathrm{d}t, \\ \mathrm{d}W_x(t)\mathrm{d}W_r(t) & = & \rho_{x,r}\mathrm{d}t, \\ \mathrm{d}W_r(t)\mathrm{d}W_\sigma(t) & = & \rho_{r,\sigma}\mathrm{d}t. \end{cases}$$

By extending the space vector (as in [24] or [89]) with another, latent, stochastic variable, defined by

$$v(t) := \sigma^2(t),$$

and choosing $x(t) = \log S(t)$, we obtain the following 4D system of SDEs,

$$\begin{cases} \mathrm{d}x(t) = & (\widetilde{r}(t) + \psi(t) - 1/2v(t))\mathrm{d}t + & \sqrt{v(t)}\mathrm{d}W_x(t), \\ \mathrm{d}\widetilde{r}(t) = & -\lambda\widetilde{r}(t)\mathrm{d}t + & \eta\mathrm{d}W_r(t), \\ \mathrm{d}v(t) = & \left(-2v(t)\kappa + 2\kappa\bar{\sigma}\sigma(t) + \gamma^2\right)\mathrm{d}t + & 2\gamma\sqrt{v(t)}\mathrm{d}W_\sigma(t), \\ \mathrm{d}\sigma(t) = & \kappa(\bar{\sigma} - \sigma(t))\mathrm{d}t + & \gamma\mathrm{d}W_\sigma(t), \end{cases} \tag{1.14}$$

where we also used $r(t) = \widetilde{r}(t) + \psi(t)$, as in Subsection 1.2.2. Note that $\theta(t)$ is now included in $\psi(t)$. We see that model (1.14) is indeed affine in state vector $\mathbf{X}(t) = [x(t), \widetilde{r}(t), v(t), \sigma(t)]^{\mathrm{T}}$. By the extension of the vector space we have obtained an affine model which enables us to apply the results from [28]. In order to simplify the calculations, we introduce a variable

$$x(t) := \widetilde{x}(t) + \Psi(t), \quad \text{where} \quad \Psi(t) = \int_0^t \psi(s)\mathrm{d}s,$$

and

$$\mathrm{d}\widetilde{x}(t) \quad = \quad \left(\widetilde{r}(t) - \frac{1}{2}v(t)\right)\mathrm{d}t + \sqrt{v(t)}\mathrm{d}W_x(t).$$

According to [28] the discounted ChF for $\mathbf{u} \in \mathbb{C}^4$ is of the following form,

$$\begin{aligned} \phi_{\mathrm{SZHW}}(\mathbf{u}, \mathbf{X}(t), t, T) &= \mathbb{E}^{\mathbb{Q}}\left(\mathrm{e}^{-\int_t^T r(s)\mathrm{d}s}\mathrm{e}^{i\mathbf{u}^{\mathrm{T}}\mathbf{X}(T)}|\mathcal{F}(t)\right) \\ &= \mathrm{e}^{-\int_t^T \psi(s)\mathrm{d}s + i\mathbf{u}^{\mathrm{T}}[\Psi(T),\psi(T),0,0]^{\mathrm{T}}}\mathbb{E}^{\mathbb{Q}}\left(\mathrm{e}^{-\int_t^T \widetilde{r}(s)\mathrm{d}s + i\mathbf{u}^{\mathrm{T}}\mathbf{X}^*(T)}|\mathcal{F}(t)\right) \\ &= \mathrm{e}^{-\int_t^T \psi(s)\mathrm{d}s + i\mathbf{u}^{\mathrm{T}}[\Psi(T),\psi(T),0,0]^{\mathrm{T}}}\mathrm{e}^{A(\mathbf{u},\tau) + \mathbf{B}^{\mathrm{T}}(\mathbf{u},\tau)\mathbf{X}^*(t)}, \end{aligned} \tag{1.15}$$

where $\mathbf{X}^*(t) = [\widetilde{x}(t), \widetilde{r}(t), v(t), \sigma(t)]^{\mathrm{T}}$ and $\mathbf{B}(\mathbf{u},\tau) = [B(\mathbf{u},\tau), C(\mathbf{u},\tau), D(\mathbf{u},\tau), E(\mathbf{u},\tau)]^{\mathrm{T}}$. Now, we set $\mathbf{u} = [u, 0, 0, 0]^{\mathrm{T}}$, so that at time T we obtain the obvious final condition:

$$\phi_{\mathrm{SZHW}}(\mathbf{u}, \mathbf{X}^*(T), T, T) = \mathbb{E}^{\mathbb{Q}}\left(\mathrm{e}^{i\mathbf{u}^{\mathrm{T}}\mathbf{X}^*(T)}|\mathcal{F}(T)\right) = \mathrm{e}^{i\mathbf{u}^{\mathrm{T}}\mathbf{X}^*(T)} = \mathrm{e}^{iu\widetilde{x}(T)},$$

(as the price at time T is known). This condition for $\tau = 0$ gives $B(u,0) = iu$, $A(u,0) = 0$, $C(u,0) = 0$, $D(u,0) = 0$, $E(u,0) = 0$. The following lemmas define the ODEs, from (1.4), and detail their solution.

Lemma 1.3.1 (Schöbel-Zhu-Hull-White ODEs)**.** *The functions $A(u,\tau)$, $B(u,\tau)$, $C(u,\tau)$, $D(u,\tau)$, $E(u,\tau)$, $u \in \mathbb{R}$, in (1.15) satisfy the following system of ODEs:*

$$\begin{aligned}
B'(u,\tau) &= 0,\\
C'(u,\tau) &= -1 + B(u,\tau) - \lambda C(u,\tau),\\
D'(u,\tau) &= 1/2B(u,\tau)(B(u,\tau)-1) + 2\left(\rho_{x,\sigma}\gamma B(u,\tau) - \kappa\right)D(u,\tau) + 2\gamma^2 D^2(u,\tau),\\
E'(u,\tau) &= \left(2\kappa\bar{\sigma}D(u,\tau) + \rho_{x,r}\eta B(u,\tau)C(u,\tau) + 2\rho_{r,\sigma}\gamma\eta C(u,\tau)D(u,\tau)\right)\\
&\quad + \left(2\gamma^2 D(u,\tau) - \kappa + \rho_{x,\sigma}\gamma B(u,\tau)\right)E(u,\tau),\\
A'(u,\tau) &= \gamma^2 D(u,\tau) + 1/2\eta^2 C^2(u,\tau) + \left[\kappa\bar{\sigma} + 1/2\gamma^2 E(u,\tau)\right.\\
&\quad \left. + \rho_{r,\sigma}\gamma\eta C(u,\tau)\right]E(u,\tau),
\end{aligned}$$

with the conditions: $B(u,0) = iu$, $C(u,0) = 0$, $D(u,0) = 0$, $E(u,0) = 0$, and $A(u,0) = 0$.

Proof. For a given state vector $\mathbf{X}^*(t) = [\widetilde{x}(t), \widetilde{r}(t), v(t), \sigma(t)]^{\mathrm{T}}$, and $\phi := \phi_{\mathrm{SZHW}}(u, \widetilde{x}(t), t, T)$ we find the system of the ODEs satisfying the following Kolmogorov backward equation:

$$\begin{aligned}
0 \quad = \quad & \frac{\partial\phi}{\partial t} + \left(\widetilde{r} - \frac{1}{2}v\right)\frac{\partial\phi}{\partial\widetilde{x}} - \lambda\widetilde{r}\frac{\partial\phi}{\partial\widetilde{r}} + \left(\gamma^2 - 2\kappa v + 2\bar{\sigma}\kappa\sigma\right)\frac{\partial\phi}{\partial v} + \kappa\left(\bar{\sigma} - \sigma\right)\frac{\partial\phi}{\partial\sigma}\\
& + \frac{1}{2}v\frac{\partial^2\phi}{\partial\widetilde{x}^2} + \frac{1}{2}\eta^2\frac{\partial^2\phi}{\partial\widetilde{r}^2} + 2v\gamma^2\frac{\partial^2\phi}{\partial v^2} + \frac{1}{2}\gamma^2\frac{\partial^2\phi}{\partial\sigma^2} + \rho_{x,r}\eta\sigma\frac{\partial^2\phi}{\partial\widetilde{x}\partial\widetilde{r}} + 2\rho_{x,\sigma}\gamma v\frac{\partial^2\phi}{\partial\widetilde{x}\partial v}\\
& + \rho_{x,\sigma}\gamma\sigma\frac{\partial^2\phi}{\partial\widetilde{x}\partial\sigma} + 2\rho_{r,\sigma}\eta\gamma\sigma\frac{\partial^2\phi}{\partial r\partial v} + \rho_{r,\sigma}\eta\gamma\frac{\partial^2\phi}{\partial r\partial\sigma} + 2\gamma^2\sigma\frac{\partial^2\phi}{\partial v\partial\sigma} - \widetilde{r}\phi, \qquad (1.16)
\end{aligned}$$

subject to terminal condition $\phi(u, \widetilde{x}(T), T, T) = \exp(iu\widetilde{x}(T))$. Since the PDE in (1.16) is affine, its solution is of the following form:

$$\begin{aligned}
\phi := \phi_{\mathrm{SZHW}}(u, \widetilde{x}(t), t, T) \quad = \quad & \exp\left(A(u,t,T) + B(u,t,T)\widetilde{x}(t) + C(u,t,T)\widetilde{r}(t)\right.\\
& \left. + D(u,t,T)v(t) + E(u,t,T)\sigma(t)\right).
\end{aligned}$$

By setting $A := A(u,t,T)$, $B := B(u,t,T)$, $C := C(u,t,T)$, $D := D(u,t,T)$ and $E := E(u,t,T)$ we find the following partial derivatives:

$$
\begin{aligned}
\frac{\partial\phi}{\partial t} &= \phi\left(\frac{\partial A}{\partial t}+\widetilde{x}\frac{\partial B}{\partial t}+\widetilde{r}\frac{\partial C}{\partial t}+v\frac{\partial D}{\partial t}+\sigma\frac{\partial E}{\partial t}\right),\\
\frac{\partial\phi}{\partial\widetilde{x}} &= B\phi,\quad \frac{\partial^2\phi}{\partial\widetilde{x}^2}=B^2\phi,\quad \frac{\partial^2\phi}{\partial\widetilde{x}\partial r}=BC\phi,\quad \frac{\partial^2\phi}{\partial\widetilde{x}\partial v}=BD\phi,\quad \frac{\partial^2\phi}{\partial\widetilde{x}\partial\sigma}=BE\phi,\\
\frac{\partial\phi}{\partial\widetilde{r}} &= C\phi,\quad \frac{\partial^2\phi}{\partial\widetilde{r}^2}=C^2\phi,\quad \frac{\partial^2\phi}{\partial\widetilde{r}\partial v}=CD\phi,\quad \frac{\partial^2\phi}{\partial\widetilde{r}\partial\sigma}=CE\phi,\\
\frac{\partial\phi}{\partial v} &= D\phi,\quad \frac{\partial^2\phi}{\partial v^2}=D^2\phi,\quad \frac{\partial^2\phi}{\partial v\partial\sigma}=DE\phi,\\
\frac{\partial\phi}{\partial\sigma} &= E\phi,\quad \frac{\partial^2\phi}{\partial\sigma^2}=E^2\phi.
\end{aligned}
$$

By substitution, PDE (1.16) becomes:

$$
\begin{aligned}
0 = {}& \frac{\partial A}{\partial t}+\widetilde{x}\frac{\partial B}{\partial t}+\widetilde{r}\frac{\partial C}{\partial t}+v\frac{\partial D}{\partial t}+\sigma\frac{\partial E}{\partial t}+\big(\widetilde{r}-\frac{1}{2}v\big)B-\lambda\widetilde{r}C+\big(\gamma^2-2\kappa v+2\bar{\sigma}\kappa\sigma\big)D\\
&+\kappa\left(\bar{\sigma}-\sigma\right)E+\frac{1}{2}vB^2+\frac{1}{2}\eta^2C^2+2v\gamma^2D^2+\frac{1}{2}\gamma^2E^2+\rho_{x,r}\eta\sigma BC+2\rho_{x,\sigma}\gamma vBD\\
&+\rho_{x,\sigma}\gamma\sigma BE+2\rho_{r,\sigma}\eta\gamma\sigma CD+\rho_{r,\sigma}\eta\gamma CE+2\gamma^2\sigma DE-\widetilde{r}.
\end{aligned}
$$

Now, for $\tau = T-t$, by collecting the terms for $\widetilde{x}$, $\widetilde{r}$, v, σ we find the set of ODEs which concludes the proof. ■

Lemma 1.3.2. *The solution to the system of ODEs, specified in Lemma 1.3.1 is given by:*

$$
\begin{aligned}
B(u,\tau) &= iu,\\
C(u,\tau) &= \frac{1}{\lambda}(iu-1)(1-\mathrm{e}^{-\lambda\tau}),\\
D(u,\tau) &= \frac{-a_1-d}{2a_2(1-g\mathrm{e}^{-d\tau})}\left(1-\mathrm{e}^{-d\tau}\right),\\
E(u,\tau) &= \mathrm{e}^{c_1\tau}\frac{1}{1-g\mathrm{e}^{-d\tau}}\left(\frac{\kappa\bar{\sigma}}{a_2}(-a_1-d)f_1(\tau)+\frac{\rho_{x,r}\eta}{\lambda}iu(iu-1)\left(f_2(\tau)+gf_3(\tau)\right)\right)\\
&\quad -\mathrm{e}^{c_1\tau}\frac{\rho_{r,\sigma}\eta\gamma}{(1-g\mathrm{e}^{-d\tau})\lambda a_2}(a_1+d)(iu-1)\left(f_4(\tau)+f_5(\tau)\right),\\
A(u,\tau) &= \frac{1}{4}\left((-a_1-d)\tau-2\log\left(\frac{1-g\mathrm{e}^{-d\tau}}{1-g}\right)\right)+f_6(\tau)+\widetilde{\mu}(u,\tau),
\end{aligned}
$$

with

$$
\widetilde{\mu}(u,\tau)=\int_0^\tau\left(\kappa\bar{\sigma}+\frac{1}{2}\gamma^2E(u,s)+\rho_{r,\sigma}\gamma\eta C(u,s)\right)E(u,s)\mathrm{d}s, \tag{1.17}
$$

where

$$\begin{aligned}
f_1(\tau) &= \frac{1}{c_1}(1-\mathrm{e}^{-c_1\tau}) + \frac{1}{c_1+d}\left(\mathrm{e}^{-(c_1+d)\tau}-1\right),\\
f_2(\tau) &= \frac{1}{c_1}(1-\mathrm{e}^{-c_1\tau}) + \frac{1}{c_1+\lambda}\left(\mathrm{e}^{-(c_1+\lambda)\tau}-1\right),\\
f_3(\tau) &= \frac{\mathrm{e}^{-(c_1+d)\tau}-1}{c_1+d} + \frac{1-\mathrm{e}^{-(c_1+d+\lambda)\tau}}{c_1+d+\lambda},\\
f_4(\tau) &= \frac{1}{c_1} - \frac{1}{c_1+d} - \frac{1}{c_1+\lambda} + \frac{1}{c_1+d+\lambda},\\
f_5(\tau) &= \mathrm{e}^{-(c_1+d+\lambda)\tau}\left(\mathrm{e}^{\lambda\tau}\left(\frac{1}{c_1+d}-\frac{\mathrm{e}^{d\tau}}{c_1}\right)+\frac{\mathrm{e}^{d\tau}}{c_1+\lambda}-\frac{1}{c_1+d+\lambda}\right),\\
f_6(\tau) &= \frac{\eta^2}{4\lambda^3}(i+u)^2\left(3+\mathrm{e}^{-2\lambda\tau}-4\mathrm{e}^{-\lambda\tau}-2\lambda\tau\right),
\end{aligned}$$

and $a_0 = -\frac{1}{2}u(i+u)$, $a_1 = 2(\rho_{x,\sigma}\gamma iu-\kappa)$, $a_2 = 2\gamma^2$, $d = \sqrt{a_1^2-4a_0a_2}$, $g = \dfrac{-a_1-d}{-a_1+d}$ *and* $c_1 = \rho_{x,\sigma}\gamma iu - \kappa - \frac{1}{2}(a_1+d)$.

Proof. In the 1D case, i.e., $\mathbf{u} = [u,0,0,0]^{\mathrm{T}}$ we start by solving the ODE for $C(u,\tau)$ (using $B(u,\tau) = iu$):

$$C'(u,\tau) + \lambda C(u,\tau) = iu - 1.$$

Standard calculations give

$$\int_0^\tau \mathrm{d}\left(\mathrm{e}^{\lambda s}C(u,s)\right) = (iu-1)\int_0^\tau \mathrm{e}^{\lambda s}\mathrm{d}s, \text{ i.e.,}$$

$$\mathrm{e}^{\lambda\tau}C(u,\tau) - \mathrm{e}^0C(u,0) = (iu-1)\left(\frac{1}{\lambda}\mathrm{e}^{\lambda\tau}-\frac{1}{\lambda}\right).$$

Using the condition, $C(u,0)=0$, gives, $C(u,\tau) = \frac{1}{\lambda}(iu-1)\left(1-\mathrm{e}^{-\lambda\tau}\right)$.

The ODE for $D(u,\tau)$ now reads:

$$D'(u,\tau) = -\frac{1}{2}u(i+u) + 2(\rho_{x,\sigma}\gamma iu-\kappa)D(u,\tau) + 2\gamma^2D^2(u,\tau).$$

In order to simplify this equation we introduce the variables $a_0 = -\frac{1}{2}u(i+u)$, $a_1 = 2(\rho_{x,\sigma}\gamma iu-\kappa)$ and $a_2 = 2\gamma^2$. The ODE can then be presented in the following form:

$$D'(u,\tau) = a_0 + a_1D(u,\tau) + a_2D^2(u,\tau). \tag{1.18}$$

Following the calculations for the Heston model in [54] the solution of (1.18) reads:

$$D(u,\tau) = \frac{-a_1-d}{2a_2(1-g\mathrm{e}^{-d\tau})}\left(1-\mathrm{e}^{-d\tau}\right),$$

with $d = \sqrt{a_1^2-4a_0a_2}$, $g = \dfrac{-a_1-d}{-a_1+d}$.

Next, we solve the ODE for $E(u,\tau)$:

$$\begin{aligned} E'(u,\tau) &= (2\kappa\bar{\sigma}D(u,\tau) + \rho_{x,r}\eta iuC(u,\tau) + 2\rho_{r,\sigma}\eta\gamma C(u,\tau)D(u,\tau)) \\ &\quad + \left(2\gamma^2 D(u,\tau) - \kappa + \rho_{x,\sigma}\gamma iu\right) E(u,\tau). \end{aligned}$$

We introduce the following functions,

$$\begin{aligned} \zeta_1(\tau) &= 2\kappa\bar{\sigma}D(u,\tau) + \rho_{x,r}\eta iuC(u,\tau) + 2\rho_{r,\sigma}\eta\gamma C(u,\tau)D(u,\tau), \\ \xi_1(\tau) &= 2\gamma^2 D(u,\tau) - \kappa + \rho_{x,\sigma}\gamma iu. \end{aligned}$$

This leads to the following ODE:

$$E'(u,\tau) - \xi_1(\tau)E(u,\tau) = \zeta_1(\tau),$$

whose solution follows from,

$$\frac{\mathrm{d}}{\mathrm{d}\tau}\left(\exp\left(-\int_0^\tau \xi_1(s)\mathrm{d}s\right)E(u,\tau)\right) = \zeta_1(\tau)\exp\left(-\int_0^\tau \xi_1(s)\mathrm{d}s\right),$$

or

$$\exp\left(-\int_0^\tau \xi_1(s)\mathrm{d}s\right)E(u,\tau) = \int_0^\tau \zeta_1(s)\exp\left(-\int_0^s \xi_1(k)\mathrm{d}k\right)\mathrm{d}s.$$

So, finally, we need to calculate

$$E(u,\tau) = \exp\left(\int_0^\tau \xi_1(s)\mathrm{d}s\right)\int_0^\tau \zeta_1(s)\exp\left(-\int_0^s \xi_1(k)\mathrm{d}k\right)\mathrm{d}s,$$

with $E(u,0)=0$.

For this, we start with the integral for $\xi_1(k)$:

$$\begin{aligned} \int_0^s \xi_1(k)\mathrm{d}k &= (\rho_{x,\sigma}\gamma iu - \kappa)\,s + 2\gamma^2\int_0^s D(u,k)\mathrm{d}k \\ &= c_1 s - \log\left(\frac{1-g\mathrm{e}^{-ds}}{1-g}\right), \end{aligned}$$

with $c_1 = \left(\rho_{x,\sigma}\gamma iu - \kappa - \frac{1}{2}(a_1+d)\right)$. Next, we need to calculate the exponent of the integral of $\xi_1(k)$:

$$\begin{aligned} \exp\left(-\int_0^s \xi_1(k)\mathrm{d}k\right) &= \exp\left(-c_1 s + \log\left(\frac{1-g\mathrm{e}^{-ds}}{1-g}\right)\right) \\ &= \frac{1-g\mathrm{e}^{-ds}}{1-g}\mathrm{e}^{-c_1 s}, \end{aligned}$$

and we can include $\zeta_1(t)$ in the integral:

$$\begin{aligned} \int_0^\tau \zeta_1(s)\mathrm{e}^{-\int_0^s \xi_1(k)\mathrm{d}k}\mathrm{d}s &= 2\kappa\bar{\sigma}\int_0^\tau D\frac{1-g\mathrm{e}^{-ds}}{(1-g)\mathrm{e}^{c_1 s}}\mathrm{d}s + \rho_{x,r}\eta iu\int_0^\tau C\frac{1-g\mathrm{e}^{-ds}}{(1-g)\mathrm{e}^{c_1 s}}\mathrm{d}s \\ &\quad + 2\rho_{r,\sigma}\eta\gamma\int_0^\tau CD\frac{1-g\mathrm{e}^{-ds}}{(1-g)\mathrm{e}^{c_1 s}}\mathrm{d}s, \end{aligned}$$

where we used the notation $D := D(u,s)$ and $C := C(u,s)$. This integral is split into three parts. The first part can be solved analytically:

$$\begin{aligned} 2\kappa\bar{\sigma}\int_0^\tau D(u,s)\frac{1-g\mathrm{e}^{-ds}}{1-g}\mathrm{e}^{-c_1 s}\mathrm{d}s &= 2\kappa\bar{\sigma}\int_0^\tau \frac{(-a_1-d)}{2a_2}\frac{\left(1-\mathrm{e}^{-ds}\right)}{1-g}\mathrm{e}^{-c_1 s}\mathrm{d}s \\ &= \kappa\bar{\sigma}\frac{(-a_1-d)}{a_2(1-g)}f_1(\tau), \end{aligned}$$

where

$$f_1(\tau) = \frac{1}{c_1}(1-\mathrm{e}^{-c_1\tau}) + \frac{1}{c_1+d}\left(\mathrm{e}^{-(c_1+d)\tau}-1\right). \tag{1.19}$$

The second integral can be solved analytically as well:

$$\begin{aligned} \rho_{x,r}\eta iu\int_0^\tau C\frac{1-g\mathrm{e}^{-ds}}{(1-g)\mathrm{e}^{c_1 s}}\mathrm{d}s &= \frac{\rho_{x,r}\eta iu(iu-1)}{\lambda(1-g)}\int_0^\tau \left(1-\mathrm{e}^{-\lambda s}\right)\left(1-g\mathrm{e}^{-ds}\right)\mathrm{e}^{-c_1 s}\mathrm{d}s \\ &= \frac{\rho_{x,r}\eta iu(iu-1)}{\lambda(1-g)}\left(f_2(\tau)+gf_3(\tau)\right), \end{aligned}$$

with $C := C(u,s)$ and

$$f_2(\tau) = \frac{1}{c_1}(1-\mathrm{e}^{-c_1\tau}) + \frac{1}{c_1+\lambda}\left(\mathrm{e}^{-(c_1+\lambda)\tau}-1\right), \tag{1.20}$$

$$f_3(\tau) = \frac{\mathrm{e}^{-(c_1+d)\tau}-1}{c_1+d} + \frac{1-\mathrm{e}^{-(c_1+d+\lambda)\tau}}{c_1+d+\lambda}, \tag{1.21}$$

and the third part reads:

$$2\rho_{r,\sigma}\eta\gamma\int_0^\tau CD\frac{1-g\mathrm{e}^{-ds}}{(1-g)\mathrm{e}^{c_1 s}}\mathrm{d}s = -\frac{\rho_{r,\sigma}\eta\gamma(a_1+d)(iu-1)}{\lambda a_2(1-g)}\left(f_4(\tau)+f_5(\tau)\right),$$

with $C := C(u,s)$, $D := D(u,s)$ and

$$f_4(\tau) = \frac{1}{c_1} - \frac{1}{c_1+d} - \frac{1}{c_1+\lambda} + \frac{1}{c_1+d+\lambda}, \tag{1.22}$$

$$f_5(\tau) = \mathrm{e}^{-(c_1+d+\lambda)\tau}\left(\mathrm{e}^{\lambda\tau}\left(\frac{1}{c_1+d}-\frac{\mathrm{e}^{d\tau}}{c_1}\right)+\frac{\mathrm{e}^{d\tau}}{c_1+\lambda}-\frac{1}{c_1+d+\lambda}\right). \tag{1.23}$$

So finally we have:

$$\begin{aligned} E(u,\tau) = {}& \mathrm{e}^{c_1\tau}\frac{1}{1-g\mathrm{e}^{-d\tau}}\left(\frac{\kappa\bar{\sigma}}{a_2}(-a_1-d)f_1(\tau)+\frac{\rho_{x,r}\eta}{\lambda}iu(iu-1)\left(f_2(\tau)+gf_3(\tau)\right)\right) \\ & -\mathrm{e}^{c_1\tau}\frac{\rho_{r,\sigma}\eta\gamma}{(1-g\mathrm{e}^{-d\tau})\lambda a_2}(a_1+d)(iu-1)\left(f_4(\tau)+f_5(\tau)\right), \end{aligned}$$

with functions $f_1(\tau)$ in (1.19), $f_2(\tau)$ in (1.20), $f_3(\tau)$ in (1.21), $f_4(\tau)$ in (1.22) and $f_5(\tau)$ in (1.23). Now, we solve the ODE for $A(u,\tau)$:

$$A'(u,\tau) = \underbrace{\gamma^2 D(u,\tau)+\frac{1}{2}\eta^2C^2(u,\tau)}_{A_1(u,\tau)} + \underbrace{\left(\kappa\bar{\sigma}+\frac{1}{2}\gamma^2E(u,\tau)+\rho_{r,\sigma}\gamma\eta C(u,\tau)\right)E(u,\tau)}_{A_2(u,\tau)},$$

with solution:

$$A(u,\tau) = A(u,0) + \int_0^\tau A_1(u,s)\mathrm{d}s + \int_0^\tau A_2(u,s)\mathrm{d}s,$$

with $A(u,0) = 0$. In order to find $A(u,\tau)$ we have to evaluate the integrals of $A_1(u,\tau)$ and $A_2(u,t)$. Integral $A_2(u,\tau)$ involves a hyper-geometric function (called the ${}_2F_1$ function or simply Gaussian function), which is computed numerically here. For integral $A_1(u,\tau)$ we have the following solution:

$$\int_0^\tau A_1(u,s)\mathrm{d}s = \frac{1}{4}\left((-a_1 - d)\tau - 2\log\left(\frac{1 - g\mathrm{e}^{-d\tau}}{1-g}\right)\right) + f_6(\tau),$$

with

$$f_6(\tau) = \frac{\eta^2}{4\lambda^3}(i+u)^2\left(3 + \mathrm{e}^{-2\lambda\tau} - 4\mathrm{e}^{-\lambda\tau} - 2\lambda\tau\right). \tag{1.24}$$

Since in the integral of $A_1(u,\tau)$ a complex-valued logarithm appears, it should be treated with some care. According to [74], an easy way to avoid any errors due to complex-valued discontinuities is to apply numerical integration. It turns out that the other formulations give rise to discontinuities which may cause inaccuracies. ■

Now, since we have found expressions for the coefficients $A(u,\tau)$ and $\mathbf{B}^{\mathrm{T}}(u,\tau)$ we return to Equation (1.15) and derive a representation in which the term structure is included. It is known that the price of a zero-coupon bond can be obtained from the characteristic function by taking $t = 0$ and $\mathbf{u} = [0,0,0,0]^{\mathrm{T}}$. So,

$$\phi_{\mathrm{SZHW}}(0, x(t), \tau) = \exp\left(-\int_0^T \psi(s)\mathrm{d}s\right)\cdot \phi_{\mathrm{SZHW}}(0, \widetilde{x}(t), \tau).$$

Since $\widetilde{r}(0) = 0$ and $v(0) = \sigma^2(0)$ we find,

$$P(0,T) = \exp\Big(A(0,\tau) + B(0,\tau)x(0) + D(0,\tau)\sigma^2(0) + E(0,\tau)\sigma(0) - \int_0^T \psi(s)\mathrm{d}s\Big),$$

with the final conditions at $u = 0$: $B(0,T) = 0,\ D(0,T) = 0,\ E(0,T) = 0$ and

$$A(0,T) = \frac{1}{2}\eta^2\int_0^T C^2(0,s)\mathrm{d}s = \frac{\eta^2}{4\lambda^3}\left(1 + 2\lambda T - \left(\mathrm{e}^{-\lambda T} - 2\right)^2\right).$$

We thus find,

$$P(0,T) = \exp\left(-\int_0^T \psi(s)\mathrm{d}s + A(0,T)\right).$$

By combining the results from the previous lemmas, we can prove the following lemma.

Lemma 1.3.3. *For $t=0$, in the Schöbel-Zhu-Hull-White model, the discounted characteristic function, $\phi_{SZHW}(u,x(0),0,T)$ for $\log S(t)$, is given by*

$$\phi_{SZHW}(u,x(0),0,T)=\exp(\widetilde{A}(u,\tau)+B(u,\tau)x(0)+D(u,\tau)\sigma^2(0)+E(u,\tau)\sigma(0)),$$

where $B(u,\tau)$, $C(u,\tau)$, $D(u,\tau)$, $E(u,\tau)$ and $A(u,\tau)$ are given in Lemma 1.3.2, and

$$\widetilde{A}(u,\tau)=A(u,\tau)+(iu-1)\int_0^T\psi(s)\mathrm{d}s=A(u,\tau)+(iu-1)\Upsilon(u,0,T), \quad (1.25)$$

with

$$\Upsilon(u,0,T)=\left\{\log\left(\frac{1}{P(0,T)}\right)+\frac{\eta^2}{2\lambda^2}\left(\tau+\frac{2}{\lambda}\left(\mathrm{e}^{-\lambda T}-1\right)-\frac{1}{2\lambda}\left(\mathrm{e}^{-2\lambda T}-1\right)\right)\right\}. \quad (1.26)$$

Proof. For $\mathbf{u}=[u,0,0,0]^{\mathrm{T}}$ Equation (1.15) reads:

$$\begin{aligned}\phi_{\mathrm{SZHW}}(u,x(0),0,T) &= \exp\left(-\int_0^T\psi(s)\mathrm{d}s+iu\int_0^T\psi(s)\mathrm{d}s\right)\phi_{\mathrm{SZHW}}(u,\widetilde{x}(0),0,T)\\ &= \exp\left((iu-1)\int_0^T\psi(s)\mathrm{d}s\right)\exp\left(A(u,\tau)+\mathbf{B}^{\mathrm{T}}(u,\tau)\mathbf{X}^*(0)\right),\end{aligned}$$

with $\mathbf{B}(u,\tau)=[B(u,\tau),C(u,\tau),D(u,\tau),E(u,\tau)]^{\mathrm{T}}$ and $\mathbf{X}^*(0)=[\widetilde{x}(0),\widetilde{r}(0),\sigma^2(0),\sigma(0)]^{\mathrm{T}}$.

We set

$$\widetilde{A}(u,\tau)=(iu-1)\int_0^T\psi(s)\mathrm{d}s+A(u,\tau), \quad (1.27)$$

with function $\psi(t)$ for the Hull-White model determined in (1.9): $\psi(t)=f(0,t)+\frac{\eta^2}{2\lambda^2}\left(1-\mathrm{e}^{-\lambda t}\right)^2$. Since $f(0,T)=-\frac{\partial}{\partial T}\log P(0,T)$ the integral in (1.27) reads

$$\int_0^T\psi(s)\mathrm{d}s = -\int_0^T\mathrm{d}\log P(0,s)+\frac{\eta^2}{2\lambda^2}\int_0^T\left(1-\mathrm{e}^{-\lambda s}\right)^2\mathrm{d}s.$$

After simplifications the proof is finished. ∎

Numerical integration for the SZHW hybrid model

Lemma 1.3.2 indicates that many terms in the ChF for the SZHW hybrid model can be obtained analytically, except the $\widetilde{\mu}(u,\tau)$-term (1.17), which requires numerical integration of the hyper-geometric function ${}_2F_1$ [76]. For a given partitioning

$$0=s_1\leq s_2\leq\ldots s_{N'-1}\leq s_{N'}=\tau,$$

we calculate the integral approximation of (1.17):

$$\widetilde{\mu}(u,\tau) \approx \sum_{i=0}^{N'-1} \left(\kappa\bar{\sigma} + \frac{1}{2}\gamma^2 E(u,s_i) + \rho_{r,\sigma}\eta\gamma C(u,s_i) \right) E(u,s_i)\delta_{s_i}, \tag{1.28}$$

with $\delta_{s_i} = s_{i+1} - s_i$ and the functions $C(u,s_i)$ and $E(u,s_i)$ as in Lemma 1.3.2. In Table 1.1 we present the numerical convergence results for two basic quadrature rules for one particular (representative) example of (1.28). It shows that both integration routines – the composite Trapezoidal and the composite Simpson rule – converge very satisfactory with only a small number of grid points, N'. Convergence with the Trapezoidal rule is of second-order, and with Simpson's rule of fourth-order, as expected. Simpson's rule is superior in terms of the ratio between time and absolute error. We therefore continue, in sections to follow, with the Simpson rule, setting $N' = 2^6$.

Table 1.1: *CPU time, absolute error, and the convergence rate for different numbers of integration points N' for evaluating function $\widetilde{\mu}(u,\tau)$. The time to maturity is set to $\tau = 1$ and $u = 5$ and the remaining parameters for the model are $\lambda = 0.5$, $\kappa = 1$, $\eta = 0.1$, $\bar{\sigma} = 0.3$, $\gamma = 0.5$, $\rho_{x,\sigma} = -50\%$, $\rho_{x,r} = 30\%$, $\rho_{r,\sigma} = -90\%$, $r_0 = 0.05$ and $\sigma_0 = 0.256$.*

$(N' = 2^{n'})$	Trapezoidal rule		Simpson's rule	
n'	time (sec)	|error|	time (sec)	|error|
2	1.5e-4	1.5e-4	1.5e-4	7.3e-6
4	2.6e-4	6.0e-6	2.7e-4	2.3e-8
6	3.4e-4	3.4e-7	3.5e-4	1.3e-10
8	6.6e-4	2.1e-8	6.7e-4	6.0e-13

1.4 Pricing, hedging and calibration

1.4.1 European options

The pricing of plain vanilla European options is commonly done in the Fourier domain when the ChF of the logarithm of the stock price is available.

In [32] a highly efficient pricing method was developed based on the Fourier-cosine expansion of the density function, and called COS method. The COS algorithm relies heavily on the availability of the characteristic function of the price process, which is guaranteed if we stay within the AD class, see Duffie-Pan-Singleton [28], Lee [70] and Lewis [71]. This method can, like the Carr-Madan method [23], compute the option prices for a whole strip of strike prices K_i, $i = 1, \ldots, N_k$ in one computation. The COS method can achieve an exponential convergence rate for European, Bermudan and barrier options for Lévy models whose probability density function is in $\mathbb{C}^\infty[b_1, b_2]$, with non-zero derivatives [32].

Here, we extend the COS method and include a stochastic interest rate process. We start the description of the COS pricing method with the general risk-neutral pricing formula:

$$\begin{aligned} V(t,S(t)) &= \mathbb{E}^{\mathbb{Q}}\left(\mathrm{e}^{-\int_t^T r(s)\mathrm{d}s} V(T,S(T))|\mathcal{F}(t)\right) \\ &= \mathbb{E}^{\mathbb{Q}}\left(\mathrm{e}^{Z(T)} V(T,\mathrm{e}^{x(T)})|\mathcal{F}(t)\right), \end{aligned} \tag{1.29}$$

where $Z(T) = -\int_t^T r(s)\mathrm{d}s$. The price of the claim $V(t,S(t))$ can be therefore expressed as:

$$V(t,S(t)) = \int_{\mathbb{R}} V(T,\mathrm{e}^x)\left(\int_{\mathbb{R}} \mathrm{e}^z f_{Z,X}(z,x)\mathrm{d}z\right)\mathrm{d}x = \int_{\mathbb{R}} V(T,\mathrm{e}^x)\hat{f}(x)\mathrm{d}x,$$

with $\hat{f}(x) = \int_{\mathbb{R}} \mathrm{e}^z f_{Z,X}(z,x)\mathrm{d}z$

As we assume a fast decay of the density function, the following approximation can be made,

$$V(t,S(t)) \approx \int_{\widetilde{D}} V(T,\mathrm{e}^x)\hat{f}(x)\mathrm{d}x, \tag{1.30}$$

where: $\widetilde{D} = [b_1, b_2]$, and $|\widetilde{D}| = b_2 - b_1$, $b_2 > b_1$. The discounted ChF is now given by:

$$\phi(\mathbf{u}, \mathbf{X}(t), t, T) = \mathbb{E}^{\mathbb{Q}}\left(\mathrm{e}^{-\int_t^T r(s)\mathrm{d}s + i\mathbf{u}^{\mathrm{T}}\mathbf{X}(T)}|\mathcal{F}(t)\right),$$

which, for $\tau = T - t$, $\mathbf{u} = [u, 0, \ldots, 0]^{\mathrm{T}}$ and $\mathbf{X}(t) = [S(t), r(t), \ldots]^{\mathrm{T}}$, reads

$$\phi(u, x(t), t, T) = \iint_{\mathbb{R}} \mathrm{e}^{z+iux} f_{Z,X}(z,x)\mathrm{d}z\mathrm{d}x = \int_{\mathbb{R}} \mathrm{e}^{iux}\hat{f}(x)\mathrm{d}x. \tag{1.31}$$

Note that the integration in (1.31) represents simply the Fourier transform of $\hat{f}(x)$, which can be approximated on a bounded domain $\widetilde{D}$,

$$\phi(u, x(t), t, T) := \phi(u, x(t), \tau) \approx \int_{\widetilde{D}} \mathrm{e}^{iux}\hat{f}(x)\mathrm{d}x =: \tilde{\phi}(u, x(t), \tau). \tag{1.32}$$

Since we are interested in the pricing of claims of the form (1.30), we link $\hat{f}(x)$ to its ChF, via the following result:

Result 1.4.1. For a given bounded domain $\widetilde{D} = [b_1, b_2]$, and N_c the number of terms in the expansion, the probability density function $\hat{f}(x)$ given by (1.30) can be approximated by,

$$\hat{f}(x) \approx \sum_{n=0}^{N_c} \frac{2\omega_n}{b_2 - b_1} \mathrm{Re}\left\{\tilde{\phi}\left(kn, x(t), \tau\right)\mathrm{e}^{-iknb_1}\right\}\cos(kn(y - b_1)),$$

with Re denoting taking the real part of the argument in brackets; $\tilde{\phi}(u, x(t), \tau)$ is the corresponding ChF, $\omega_0 = 1/2$, $\omega_n = 1$, $n \in \mathbb{N}^+$ and $k = \pi/(b_2 - b_1)$.

For a proof and for error analysis regarding the different approximations we refer to the original paper on the COS method [32].

Using the result above, we replace the probability density function $\hat{f}(x)$ in (1.30), as follows

$$\begin{aligned} V(t,S(t)) &\approx \int_{\widetilde{D}} V(T,y) \sum_{n=0}^{N_c} \theta_n \cos\left(n\pi \frac{(y-b_1)}{b_2-b_1}\right) \mathrm{d}y \\ &= \sum_{n=0}^{N_c} \omega_n \Re\left(\tilde{\phi}\left(kn, x(t), \tau\right) \mathrm{e}^{-iknb_1}\right) \Gamma_n^{b_1,b_2}, \end{aligned} \tag{1.33}$$

where $\theta_n = \frac{2\omega_n}{b_2-b_1} \mathrm{Re}\left\{\tilde{\phi}\left(kn, x(t), \tau\right) \mathrm{e}^{-iknb_1}\right\}$ and the coefficients $\Gamma_n^{b_1,b_2}$ are known analytically for European options, see [32] for details.

We note that, depending on the payoff, the $\Gamma_n^{b_1,b_2}$ in (1.33) change, but a closed-form expression is available for the most common payoffs. As the hybrid products will be calibrated to plain vanilla options, we provide the gamma coefficients for the European call options:

Result 1.4.2. The $\Gamma_n^{b_1,b_2}$ in (1.33) for pricing a call option defined by:

$$V(T,y) = \max\left(K(\mathrm{e}^y - 1), 0\right),$$

with $y = \log\left(\frac{S}{K}\right)$ for a given strike K, are given by

$$\Gamma_n^{b_1,b_2} = \frac{2K}{b_2-b_1}\left(\psi_n - \chi_n\right), \tag{1.34}$$

where

$$\chi_n = \frac{1}{1+(kn)^2}\left(\cos(n\pi)\mathrm{e}^{b_2} - \cos(-b_1 kn) + kn\sin(n\pi)\mathrm{e}^{b_2} - kn\sin(-b_1 kn)\right),$$

and

$$\psi_n = \begin{cases} \dfrac{b_2-b_1}{n\pi}\left(\sin(n\pi) - \sin\left(-b_1 kn\right)\right) & \text{for} \quad n \neq 0, \\ b_2 & \text{for} \quad n = 0. \end{cases}$$

Proof. The proof is straightforward by calculating the integral in (1.33) with the transformed payoff function $V(T,y)$. ∎

Since the coefficients $\Gamma_n^{b_1,b_2}$ are available in closed-form, the expression in (1.33) can easily be computed. The availability of such a pricing formula is particularly useful in a calibration procedure, in which the parameters of the stochastic processes need to be approximated. In practice, option pricing models are calibrated to a number of call option prices observed in the market. It is therefore necessary for such a procedure to be highly efficient and a (semi-)closed-form for an option pricing formula is desirable. The COS method's accuracy is related to the size of the integration domain, $\widetilde{D}$. If the domain is chosen too small, we expect a significant loss of accuracy. On the other hand if the domain is too wide, a large number of terms in the Fourier expansion, N_c, has to be used for satisfactory accuracy. In [32] the truncation range was defined in terms of the moments of $\log\left(\frac{S(t)}{K}\right)$ of the form:

$$b_{1,2} = \mu_1 \pm \jmath\sqrt{\mu_2 + \sqrt{\mu_4}}, \tag{1.35}$$

with the minus sign for b_1; and the plus sign for b_2, the μ_i are the corresponding $\imath$-th moments, and $\jmath$ is an appropriate constant. In our work, with the moments not directly available, we apply a simplified approximation for the integration range, and use:

$$b_{1,2} = 0 \pm \jmath\sqrt{\tau}, \tag{1.36}$$

with τ, the time to maturity. As in [32], we fix $\jmath = 8$ in (1.36).

The Greeks

When using the SZHW hybrid model the impact of the correlation effect between different asset classes on the hedging costs is particularly interesting. Since the SZHW ChF is available we can determine the Greeks. Their expression is also related to the ChF.

In the previous section we have found that the ChF for the SZHW hybrid model, for $t = 0$, can be expressed as:

$$\phi_{\text{SZHW}}(u, x(0), 0, T) = \exp(\widetilde{A}(u,\tau) + iux(0) + D(u,\tau)\sigma^2(0) + E(u,\tau)\sigma(0)).$$

The payoff sensitivity to a particular parameter, Θ, can be expressed as:

$$\frac{\partial}{\partial\Theta}V(t, S(t)) \quad = \quad \sum_{n=0}^{N_c}\omega_n\Gamma_n^{b_1,b_2}\Re\left(\mathrm{e}^{-iknb_1}\frac{\partial}{\partial\Theta}\phi_{\text{SZHW}}\left(kn, x(0), 0, T\right)\right),$$

where k, $\Gamma_n^{b_1,b_2}$ are ω_n is defined as in (1.33) and (1.34).

As we see, the calculation of the Greeks, when the ChF is available, is straightforward and only requires the differentiation of the ChF.

In the next subsection we use the SZHW model in calibration and pricing of exotics.

1.4.2 Calibration of the SZHW hybrid model

In this section we examine the Schöbel-Zhu-Hull-White hybrid model and compare its performance to the plain Heston model (without stochastic interest rates). We use financial market data to estimate the model parameters and discuss the effect of the correlation between the equity and interest rate on the estimated parameters. For this purpose we have chosen the CAC40 call option implied volatilities of 17.10.2007. We perform the calibration of the models in two stages. Firstly of all, we calibrate the parameters for the interest rate process by using caplets and swaptions. Secondly, the remaining parameters, for the underlying asset, the volatility and the correlations, are calibrated to plain vanilla option market prices. Standard procedures for the Hull-White calibration are employed [19]. Tables 1.2 and 1.3 present the estimated parameters and the associated squared sum errors (SSE) defined as,

$$\mathrm{SSE} = \sum_{i=1}^{n}\sum_{j=1}^{m}\Big(V_{\mathrm{call}}\left(T_i, K_j\right) - \hat{V}_{\mathrm{call}}\left(T_i, K_j\right)\Big)^2,$$

where $\hat{V}_{\mathrm{call}}(T_i, K_j)$ and $V_{\mathrm{call}}\left(T_i, K_j\right)$ are the market and the model prices, respectively, T_i is the ith maturity time and K_j is the jth strike. We have 32 strikes, ($m = 32$), and 20 time points ($n = 20$).

Table 1.3 shows the calibration results for the Heston and the Schöbel-Zhu-Hull-White models. Both models are reasonably well calibrated with approximately the same error. We have used a two-level calibration routine: a global search algorithm (simulated annealing) combined with a local search (Nelder-Mead) algorithm. In order to reduce parameter risk we prescribe the speed of mean reversion of the volatility process, $\kappa = 0.5$, and we have performed the calculation for a number of correlations, $\rho_{x,r}$. For the hybrid model considered some patterns in the calibrated parameters can be observed (see Table 1.3). For the SZHW model two parameters, $\bar{\sigma}$ and σ_0, are not affected by changing the correlation $\rho_{x,r}$. For the SZHW model we find $\bar{\sigma} \approx 0.2$, $\sigma_0 \approx 0.1$. Another pattern we observe is that parameter γ decreases from 0.08 to 0.02. The reverse effect is observed for positive correlation $\rho_{x,r}$. The correlation $\rho_{x,\sigma}$ between stock $S(t)$ and the volatility $\sigma(t)$ decreases from -31% to -99% for $\rho_{x,r}$ varying from -70% to -10% and increases from -72% to -38% for $\rho_{x,r}$ from 10% to 70%. Correlation $\rho_{r,\sigma}$ does not show any regularity.

In the next section we use the calibration results and check the impact of the correlation between the equity and interest rate on the prices of exotic derivative products.

For the pricing of exotic derivatives, Monte Carlo methods are commonly used, especially for products for which a closed-form pricing formula is not available.

In the Heston-type models discretization techniques like the Euler-Maruyama or Milstein schemes (see, for example, [101]) in a Monte Carlo technique may sometimes give a negative or imaginary variance. This is not acceptable. In the literature, improved techniques to perform a simulation of the AD processes have been developed, see [3, 20]. An analysis of the possible ways to overcome the negative variance problem can be found in [75].

Those schemes however are not applicable for the SZHW model. In the case of the SZHW hybrid model the volatility, by the model construction, *can* become negative. It is easy to see that the volatility, $\sigma(t)$, in the SZHW model is normally distributed, i.e.:

$$\sigma(t) \sim \mathcal{N}\big(\sigma_0 \mathrm{e}^{-\kappa t} + \bar{\sigma}(1-\mathrm{e}^{-\kappa t}),\ \frac{\gamma^2}{2\kappa}\left(1-\mathrm{e}^{-2\kappa t}\right)\big). \tag{1.37}$$

From (1.37) the probability of the volatility to become negative increases if vol-vol parameter, γ, is significantly larger than the mean reversion parameter κ. This effect is more pronounced when $\sigma_0 \to \bar{\sigma}$ and $\bar{\sigma} \to 0$.

Table 1.2: *Parameters estimated from the market data (Hull-White model), r_0 according to Proposition 1.2.2 and (1.9) is assumed to be the earliest forward rate, i.e.: $r_0 \approx f(0,\epsilon)$ for $\epsilon \to 0$. The interest rate term structure $\theta(t)$ was found via Equation (1.10).*

model	r_0	λ	η	SSE
Hull-White	0.01733	1.12	0.001	1e-3

Table 1.3: *Calibration results for the Schöbel-Zhu-Hull-White and the Heston models defined in (1.13). The experiment was done with a priori defined speed of reversion for the volatility $\kappa = 0.5$, and correlation $\rho_{x,r}$ for the SZHW model. In the simulation for the Heston model a constant interest rate of $r = 0.0327$ was chosen.*

model	$\rho_{x,r}$	$\bar{\sigma}$	γ	$\rho_{x,\sigma}$	$\rho_{r,\sigma}$	σ_0	SSE
SZHW	-70%	0.1929	0.0787	-31.16%	40.00%	0.1000	9.5e-3
	-50%	0.2000	0.0539	-39.67%	11.90%	0.0990	9.1e-3
	-30%	0.2030	0.0400	-56.99%	32.38%	0.1000	9.0e-3
	-10%	0.2049	0.0189	-98.88%	31.73%	0.1002	9.2e-3
	10%	0.2039	0.0315	-71.67%	6.34%	0.0998	9.2e-3
	30%	0.2029	0.0376	-60.39%	24.07%	0.1001	9.0e-3
	50%	0.2018	0.0429	-53.35%	25.05%	0.0980	9.0e-3
	70%	0.1981	0.0576	-38.22%	-7.76%	0.0990	9.2e-3
Heston	–	0.0770	0.3500	-66.22%	–	0.0107	7.8e-3

1.5 Pricing exotics

Here we describe some typical hybrid derivative products.

Hybrid products are financial contracts that combine different market sectors, assets and instruments. A financial innovation is regarded as useful, if it creates benefits to one of the parties involved in the contract. These benefits can be lower costs of capital for the issuer or higher returns and lower risk for the investor. New financial products are introduced in response to some market imperfection with respect to financing, investing, positioning or hedging. Hybrid products arise from the need of an investor to benefit from profits in different market sectors. Contracts can be based on the best performing sector, for example, with a guarantee that an investment cannot decrease significantly in value.

We evaluate the price differences between classical models and the hybrid model. For this purpose we consider several hybrid products, treated in subsequent subsections. The pricing is done using a Monte Carlo method.

1.5.1 A diversification product (performance basket)

Hybrid products that an investor may use in strategic trading are so-called diversification products. These products, also known as *performance baskets*, are based on sets of assets with different expected returns and risk levels. Proper construction of such products may give reduced risk compared to any single asset, and an expected return that is greater than that of the least risky asset [59]. A simple example is a portfolio with two assets: a stock with a high risk and high return and a bond with a low risk and low return. If one introduces an equity component in a pure bond portfolio the expected return will increase. However, because of a non-perfect correlation between these two assets also a risk reduction is expected. If the percentage of the equity in the portfolio is increased, it eventually starts to dominate the structure and the risk may increase with a higher impact for a low or negative correlation [59]. An example is a financial product, defined in the following way:

$$\Pi(t=0,T) = \mathbb{E}^{\mathbb{Q}}\left\{\frac{1}{B(T)}\max\left(0, \omega\cdot\frac{S(T)}{S_0} + (1-\omega)\cdot\frac{P(T,T_1)}{P(0,T_1)}\right)\big|\mathcal{F}(0)\right\}, \quad (1.38)$$

where $S(t)$ is the underlying asset at time T, $P(t,T)$ is the zero-coupon bond, ω represents a percentage ratio and $B(T)$ stands for the money-savings account with $\mathrm{d}B(t) = r(t)B(t)\mathrm{d}t$. Figure 1.1 shows the pricing results for the model discussed.

The product pricing for different correlations $\rho_{x,r}$ is performed with the Monte Carlo method and the remaining parameters calibrated from the market data. For $\omega \in [0\%, 100\%]$ the max disappears from the payoff and only a sum of discounted expectations remains. The figure shows that the positive correlation between the products in the basket significantly increases the contract value, while negative correlation has a reversed effect. The absolute difference between the models increases with percentage ω.

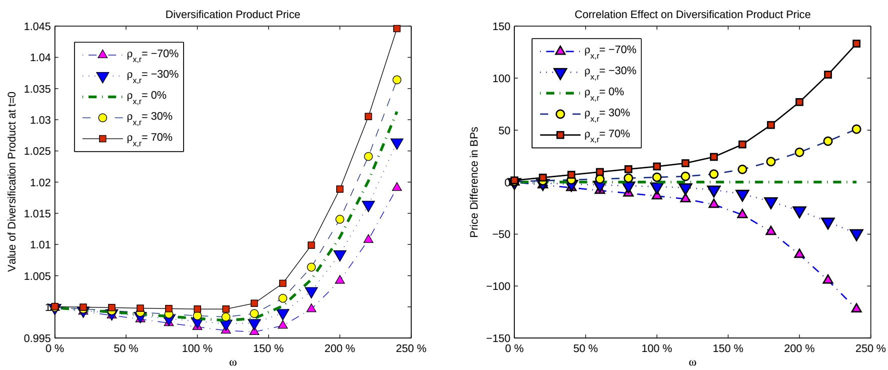

Figure 1.1: *LEFT: Pricing of a diversification hybrid product under different correlations $\rho_{x,r}$. The simulations performed with $T = 9$ and $T_1 = 10$. The remaining parameters are as in Table 1.3. RIGHT: Diversification product price differences with respect to the model with $\rho_{x,r} = 0\%$ expressed in Basis Points (BPs) for different correlations $\rho_{x,r}$.*

1.5.2 Strategic investment hybrid (best-of-strategy)

Suppose that an investor believes that if the price of a certain commodity, $S^1(t)$, goes up, then the equity markets under-perform relative to the interest rate yields, whereas, if $S^1(t)$ drops down, the equity markets over-perform relative to the interest rate [59]. If price of $S^1(t)$ is high, the market may expect an increase of the inflation and hence of the interest rates and low $S^1(t)$ price could have the opposite effect. In order to include such a feature in a hybrid product we define a contract in which an investor is allowed to buy a weighted performance coupon depending on the performance of another underlying. Such a product can be defined as follows,

$$\Pi(t=0,T) \quad = \quad \mathbb{E}^{\mathbb{Q}}\left(\mathrm{e}^{-\int_0^T r(s)\mathrm{d}s}\cdot\Pi(T,T)|\mathcal{F}(0)\right), \text{ with} \tag{1.39}$$

$$\begin{aligned}\Pi(T,T) \quad &= \quad \max\left(0,\omega\cdot\frac{L_0}{L(T)}+(1-\omega)\frac{S(T)}{S(0)}\right)\mathbf{1}_{S^1(T)>S^1(0)} \\ &\quad +\max\left(0,(1-\omega)\frac{L_0}{L(T)}+\omega\cdot\frac{S(T)}{S(0)}\right)\mathbf{1}_{S^1(T)<S^1(0)},\end{aligned} \tag{1.40}$$

where $\omega \geq 0\%$ is a weighting factor related to a percentage, $L(T)=\sum_{i=1}^{M}P(T,t_i)$ with $t_1 = T$ is the T-value of projected liabilities for certain time t_M.

Figure 1.2 shows the prices obtained from Monte Carlo simulation of the contract at time $t_0 = 0$ for maturity $T = t_1 = 3$ and time horizon $t_M = 12$ with one year spacing. Since we did not model the second underlying process, $S^1(t)$; we assume that $S^1(T) > S^1(0)$. We see that for $\omega \in [0\%, 100\%]$ the max over the sum of performances disappears and the hybrid can be relatively easily priced, i.e., separately for both underlyings ($L_0/L(t)$ and $S(t)/S(0)$). The difference between the model prices for different correlations $\rho_{x,r}$ becomes more pronounced for higher ω. The simulations performed for $\rho_{x,r} = -70\%$ and $\rho_{x,r} = 70\%$ show that for different correlations the differences in prices are significant. The figure shows that for $\omega < 150\%$ the prices, for different correlations, of the SZHW model are relatively close. The value for $\omega = 0\%$ corresponds to the case that only the stock is traded, so correlation effects are not present.

1.5.3 Cliquet options

Cliquet options are very popular in the world of equity derivatives [109]. The contracts are constructed to give a protection against downside risk combined with a significant upside potential. A cliquet option can be interpreted as a series of forward-starting European options, for which the total premium is determined in advance. The payout of each option can either be paid at the final maturity date, or at the end of a *reset* period. One of the cliquet-type structures is a *Globally Floored Cliquet* with the following payoff:

$$\Pi(t_0=0,T)=\mathbb{E}^{\mathbb{Q}}\left\{\frac{1}{B(T)}\max\left(\sum_{i=1}^{M}\min\left(A_{t_i},\mathrm{LocalCap}\right),\mathrm{MinCoupon}\right)\Big|\mathcal{F}(0)\right\}. \tag{1.41}$$

Where $B(T)$ is as in (1.38) and

$$A_{t_i}=\max\left(\mathrm{LocalFloor},\frac{S(t_i)}{S(t_{i-1})}-1\right), \text{ where } t_i = i\frac{T}{M},$$

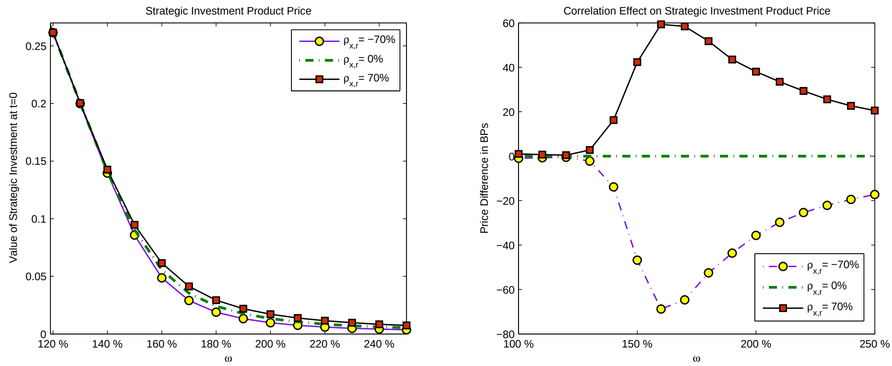

Figure 1.2: *LEFT: Discounted payoff of the strategic investment hybrid priced with the SZHW hybrid model in dependence of ω. The payoff value is calculated for different correlation $\rho_{x,r}$. Monte Carlo simulation was performed with 100.000 paths and $100T$ time-steps. RIGHT: Strategic investment product price differences with respect to the model with $\rho_{x,r} = 0\%$ expressed in Basis Points (BPs) for different correlations $\rho_{x,r}$.*

with maturity T. M indicates the number of reset periods. The term A_{t_i} can be recognized as an ATM forward-starting option, which is driven by a forward skew. It has been shown in [40] that the cliquet structures are significantly underpriced under a local volatility model for which the forward skews are basically too flat.

Since the forward prices are not known a-priori, we derive the values from the so-called *forward* characteristic function. If we define $\mathbf{X}(t)$ as the state vector at time t then the forward characteristic function, ϕ_{F}, with $t < t^* < T$ can be found as

$$
\begin{aligned}
\phi_{\mathrm{F}}(\mathbf{u}, \mathbf{X}(t), t^*, T) =& \mathbb{E}^{\mathbb{Q}} \left(\mathrm{e}^{-\int_t^T r(s)\mathrm{d}s} \mathrm{e}^{i\mathbf{u}^{\mathrm{T}}(\mathbf{X}(T)-\mathbf{X}(t^*))} | \mathcal{F}(t) \right) \\
=& \mathbb{E}^{\mathbb{Q}} \left(\mathrm{e}^{-\int_t^{t^*} r(s)\mathrm{d}s - i\mathbf{u}^{\mathrm{T}}\mathbf{X}(t^*)} \phi\left(\mathbf{u}, \mathbf{X}(t^*), t^*, T\right) | \mathcal{F}(t) \right) \\
=& \mathrm{e}^{A(\mathbf{u},t^*,T)} \mathbb{E}^{\mathbb{Q}} \left(\mathrm{e}^{-\int_t^{t^*} r(s)\mathrm{d}s - i\mathbf{u}^{\mathrm{T}}\mathbf{X}(t^*) + \mathbf{B}^{\mathrm{T}}(\mathbf{u},t^*,T)\mathbf{X}(t^*)} | \mathcal{F}(t) \right).
\end{aligned}
\tag{1.42}
$$

Figure 1.3 shows the performance of the model applied to the pricing of the cliquet option defined in (1.41). We choose here $T = 3$, $\mathrm{LocalCap} = 0.01$, $\mathrm{LocalFloor} = -0.01$ and $M = 36$ (the contract measures the monthly performance). For large values of the MinCoupon the values of the hybrid under consideration are identical, which is expected since a large MinCoupon dominates the max operator in (1.41) and the expectation becomes simply the price of a zero-coupon bond at time $t = 0$ multiplied by the deterministic MinCoupon. Figure 1.3 shows the pricing results for five correlations $\rho_{x,r} = \{-70\%, -30\%, 0\%, 30\%, 70\%\}$. We find a significant effect of the correlations between stock and the interest rate on cliquet prices.

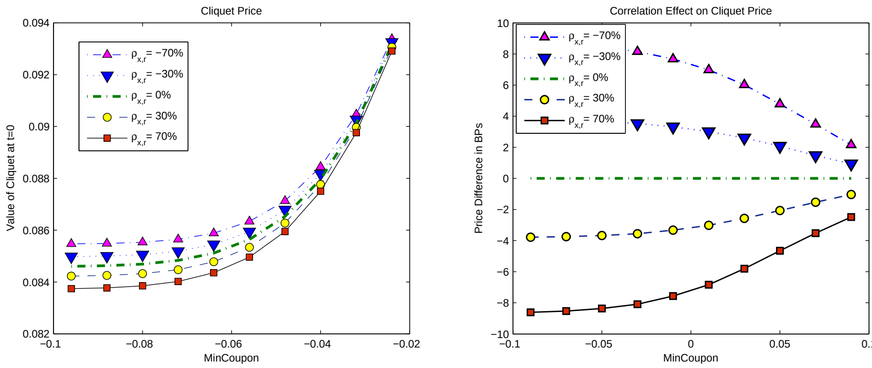

Figure 1.3: *LEFT: Pricing a cliquet product under the SZHW hybrid model. Figure presents the price of a globally floored cliquet as a function of MinCoupon given by (1.41) for* $T = 3$ *years and* $M = 36$*. The remaining parameters are as in Table 1.3. RIGHT: Cliquet price differences with respect to the model with* $\rho_{x,r} = 0\%$ *expressed in Basis Points (BPs) for different correlations* $\rho_{x,r}$*.*

1.6 Conclusion

In this, introductory, chapter we have presented an extension of the Schöbel-Zhu stochastic volatility model by the Hull-White interest rate process and priced a number of structured hybrid derivative products.

The aim is to define hybrid stochastic processes which belong to the class of affine diffusion models, as this may give efficient calibration of the model. We have shown that the Schöbel-Zhu-Hull-White model belongs to the category of affine diffusion processes. Restrictions regarding the choice of correlation structure between the different Wiener processes appearing need not be made.

Due to the resulting semi-closed form of the Schöbel-Zhu-Hull-White characteristic function we were able to calibrate in an efficient way by means of the Fourier cosine expansion pricing technique, adapted to the stochastic interest rate case.

It has been shown, by numerical experiments for different hybrid products, that the correlations between different asset classes have an impact on the derivative price.

Although the SZHW hybrid model due to a semi-closed-form characteristic function is attractive it also has its limits. The main limitation is its volatility structure i.e.: the model assumes the volatility to be normally distributed. Therefore it can not model a reflecting barrier at 0, nor deal with the absolute volatility $|\sigma(t)|$ (see [110] for discussion).

In order to determine the ChF for the extended version of the Schöbel-Zhu hybrid model the following integral needs to be determined numerically:

$$\widetilde{\mu}(\mathbf{u},\tau) = \int_0^\tau \left(\kappa\bar{\sigma} + \frac{1}{2}\gamma^2 E(\mathbf{u},s) + \rho_{r,\sigma}\gamma\eta C(\mathbf{u},s)\right) E(\mathbf{u},s)\mathrm{d}s.$$

This integration, although simple, needs to be done for each Fourier argument "$\mathbf{u}$". Depending on the pricing algorithm, the number of Fourier arguments can vary from 200, in the case of the exponentially converging COS method, to more than 4096 in FFT-based pricing algorithms. We conclude that the efficiency of pricing with the ChF for the SZHW is heavily dependent on the pricing algorithm.

Another restriction of the model is its interest rate structure which is assumed to be driven by a single factor short-rate model. Although such models are well-accepted by practitioners for pricing basic interest rate derivatives, it is a significant restriction when pricing structured hybrid products that are sensitive to the skew or smile in the interest rate market.

CHAPTER 2

On the Heston Model with Short-Rate Interest Rates

A businessman is a hybrid of a dancer and a calculator.

Paul Valery

2.1 Introduction

In this chapter we focus our attention on a hybrid extension of the stochastic volatility model of Heston [54]. This hybrid model combines two correlated asset classes: equity and interest rate. We consider an *approximation* of the full-scale model so that the model fits in the class of affine diffusion processes (AD), as in Duffie, Pan and Singleton [28]. For processes within this class a closed-form solution of the characteristic function exists.

Zhu in [112] has presented a hybrid model which could model the skew pattern for equity and included a stochastic (but uncorrelated) interest rate process. Generalizations were then presented by Giese [43] and Andreasen [6], where the Heston [54] stochastic volatility model was used, combined with an indirectly correlated interest rate process. Correlation was modeled by including additional terms in the SDEs (this approach is discussed in some detail in Section 2.3.1).

In Chapter 1, we have discussed the stochastic volatility model of Schöbel-Zhu [100] and its extension by a stochastic interest rate [50, 106]. A full matrix of correlations was directly imposed on the driving Brownian motions. The model was in the class of AD processes, but since the SZHW model is based on a Vašiček-type process [108] for the stochastic volatility, the volatilities can become negative.

A different approach to modelling equity-interest rate hybrids was presented by Benhamou *et al.* [13], extending the local volatility framework of Dupire [31] and Derman, Kani [27] and incorporating stochastic interest rates. Those models, although attractive from the calibration point of view, suffer from flattening volatilities in the case of forward-starting options. Local volatility models are not covered in this thesis.

In this chapter we investigate the Heston-Hull-White, and the Heston-Cox-Ingersoll-Ross hybrid models and propose approximations so that we can obtain their characteristic functions. The framework presented is relatively easy to understand and implement. It is inspired by the techniques of Giese and Andreasen in [43, 6]. Our approximations do not require any preliminary calculations of expectations like the Markovian projection methods [7, 8]. The option pricing method benefits greatly from the speed of characteristic function evaluations resulting from the model approximations.

The interest rate models studied here cannot generate *interest rate* implied volatility rate smiles or skews. They can therefore mainly be used for long-term equity options, and for "not too complicated" equity-interest rates hybrid products.

This chapter is organized as follows. In Section 2.2 we discuss the full-scale Heston hybrid models with stochastic interest rate processes. Section 2.3 presents a deterministic approximation of the Heston-Hull-White hybrid model, together with the corresponding characteristic function, and Section 2.4 gives the characteristic function based on another approximation of that hybrid model. Section 2.5 is dedicated to a numerical experiment where we discuss the differences between the hybrid models of Heston and the Schöbel-Zhu, and in Section 2.6 we compare the performance of our approximations with the Markovian projection method studied by Antonov *et al.* in [7, 8]. In Section 2.7 the calibration based on the approximations of the full-scale hybrid models is performed. In Appendix 2.A the Heston-Cox-Ingersoll-Ross model is discussed.

2.2 Heston hybrid models with stochastic interest rate

With state vector $\mathbf{X}(t) = [S(t), v(t)]^{\mathrm{T}}$, under the risk-neutral pricing measure, the Heston stochastic volatility model [54], which is our point-of-departure here, is specified by the following system of SDEs:

$$\begin{cases} \mathrm{d}S(t)/S(t) = & r\mathrm{d}t + & \sqrt{v(t)}\mathrm{d}W_x(t), & S(0) > 0, \\ \mathrm{d}v(t) = & \kappa(\bar{v} - v(t))\mathrm{d}t + & \gamma\sqrt{v(t)}\mathrm{d}W_v(t), & v(0) > 0, \end{cases} \tag{2.1}$$

with $r > 0$ a constant interest rate, correlation $\mathrm{d}W_x(t)\mathrm{d}W_v(t) = \rho_{x,v}\mathrm{d}t$, and $|\rho_{x,v}| < 1$. The variance process, $v(t)$, of the stock, $S(t)$, is a mean reverting square-root process, in which $\kappa > 0$ determines the speed of adjustment of the volatility towards its theoretical mean $\bar{v} > 0$, and $\gamma > 0$ is the second-order volatility, i.e., the volatility of the variance.

As already indicated in [54], the model given in (2.1) is not in the class of affine processes, whereas under the log-transform for the stock, $x(t) = \log S(t)$, it is. Then, the discounted ChF is given by:

$$\phi_{\mathrm{H}}(u, x(t), \tau) = \exp\left(A(u,\tau) + B(u,\tau)x(t) + C(u,\tau)v(t)\right), \tag{2.2}$$

where the functions $A(u,\tau)$, $B(u,\tau)$ and $C(u,\tau)$ are known in closed-form (see [54]).

The ChF is explicit, but its inverse also has to be found for pricing purposes. Because of the form of the ChF, we cannot get its inverse analytically and a numerical method for integration has to be used, see, for example, [23, 32, 70, 72] for Fourier methods.

2.2.1 Full-scale hybrid models

A constant interest rate, r, may be insufficient for pricing interest rate sensitive products. Therefore, we extend our state vector with an additional stochastic quantity, i.e.: $\mathbf{X}(t) = [S(t), v(t), r(t)]^{\mathrm{T}}$. This model corresponds to a *stochastic volatility equity hybrid model with a stochastic interest rate* process, $r(t)$. In particular, we add to the Heston model the Hull-White (HW) interest rate [56], or the square-root Cox-Ingersoll-Ross [25] (CIR) process. The extended model can be presented in the following way:

$$\begin{cases} \mathrm{d}S(t)/S(t) = & r(t)\mathrm{d}t + & \sqrt{v(t)}\mathrm{d}W_x(t), & S(0) > 0, \\ \mathrm{d}v(t) = & \kappa(\bar{v} - v(t))\mathrm{d}t + & \gamma\sqrt{v(t)}\mathrm{d}W_v(t), & v(0) > 0, \\ \mathrm{d}r(t) = & \lambda(\theta(t) - r(t))\mathrm{d}t + & \eta r^p(t)\mathrm{d}W_r(t), & r(0) > 0, \end{cases} \tag{2.3}$$

where exponent $p = 0$ in (2.3) represents the Heston-Hull-White (HHW) model and for $p = \frac{1}{2}$ it becomes the Heston-Cox-Ingersoll-Ross (HCIR) model. For both models the correlations are given by $\mathrm{d}W_x(t)\mathrm{d}W_v(t) = \rho_{x,v}\mathrm{d}t$, $\mathrm{d}W_x(t)\mathrm{d}W_r(t) = \rho_{x,r}\mathrm{d}t$, $\mathrm{d}W_v(t)\mathrm{d}W_r(t) = \rho_{v,r}\mathrm{d}t$, and κ, γ and $\bar{v}$ are as in (2.1), $\lambda > 0$ determines the speed of mean reversion for the interest rate process; $\theta(t)$, as described in Chapter 1, is the interest rate term-structure and η controls the volatility of the interest rate. We note that the interest rate process in (2.3) for $p = \frac{1}{2}$ is of the same form as the variance process $v(t)$.

System (2.3) is not in the affine form, not even with $x(t) = \log S(t)$. In particular, the symmetric instantaneous covariance matrix is given by:

$$\sigma(\mathbf{X}(t))\sigma(\mathbf{X}(t))^{\mathrm{T}} = \begin{bmatrix} v(t) & \rho_{x,v}\gamma v(t) & \rho_{x,r}\eta r^p(t)\sqrt{v(t)} \\ * & \gamma^2 v(t) & \rho_{r,v}\gamma\eta r^p(t)\sqrt{v(t)} \\ * & * & \eta^2 r^{2p}(t) \end{bmatrix}_{(3\times 3)}. \tag{2.4}$$

Setting the correlation $\rho_{r,v}$ to zero would still not make the system affine. Matrix (2.4) is of the linear form with respect to state vector $[x(t) = \log S(t), v(t), r(t)]^{\mathrm{T}}$, if two correlations, $\rho_{r,v}$ and $\rho_{x,r}$, are set to zero [1]. Models with two correlations equal to zero are covered in [83].

Since for pricing equity-interest rate products a non-zero correlation between stock and interest rate is crucial (see, for example, [59]), alternative approximations to the Heston hybrid models need to be formulated, so that correlations can be imposed. Variants are discussed in the sections to follow. These approximate

[1] where we assume positive parameters

models are evaluated with the help of the Cholesky decomposition of a correlation matrix.

We can decompose a given symmetric correlation matrix, $\mathbf{C}$, denoted by

$$\mathbf{C} = \begin{bmatrix} 1 & \rho_1 & \rho_2 \\ * & 1 & \rho_3 \\ * & * & 1 \end{bmatrix}, \tag{2.5}$$

as $\mathbf{C} = \mathbf{L}\mathbf{L}^{\mathrm{T}}$, where $\mathbf{L}$ is a lower triangular matrix with:

$$\mathbf{L} = \begin{bmatrix} 1 & 0 & 0 \\ \rho_1 & \sqrt{1-\rho_1^2} & 0 \\ \rho_2 & \frac{\rho_3-\rho_2\rho_1}{\sqrt{1-\rho_1^2}} & \sqrt{1-\rho_2^2-\left(\frac{\rho_3-\rho_2\rho_1}{\sqrt{1-\rho_1^2}}\right)^2} \end{bmatrix}. \tag{2.6}$$

We then rewrite the system of SDEs in terms of the independent Brownian motions, $\mathrm{d}\widetilde{\mathbf{W}}(t) = [\mathrm{d}\widetilde{W}_r(t), \mathrm{d}\widetilde{W}_v(t), \mathrm{d}\widetilde{W}_x(t)]^{\mathrm{T}}$, with the help of the lower triangular matrix $\mathbf{L}$.

Since our main objective is to derive a closed-form ChF with a non-zero correlation between the equity process, $S(t)$, and the interest rate, $r(t)$, we first assume that the Brownian motions for the interest rate $r(t)$ and the variance $v(t)$ are not correlated (the case of a full correlation structure is discussed in Section 2.3.3).

By exchanging the order of the state variables $\mathbf{X}(t) = [S(t), v(t), r(t)]^{\mathrm{T}}$ to $\mathbf{X}^*(t) = [r(t), v(t), S(t)]^{\mathrm{T}}$, the HHW and HCIR models in (2.3) have $\rho_1 \equiv \rho_{r,v} = 0$, $\rho_2 \equiv \rho_{x,r} \neq 0$ and $\rho_3 \equiv \rho_{x,v} \neq 0$ in (2.5) and read:

$$\begin{bmatrix} \mathrm{d}r(t) \\ \mathrm{d}v(t) \\ \frac{\mathrm{d}S(t)}{S(t)} \end{bmatrix} = \begin{bmatrix} \lambda(\theta(t)-r(t)) \\ \kappa(\bar{v}-v(t)) \\ r(t) \end{bmatrix} \mathrm{d}t + \sigma(\mathbf{X}^*(t)) \begin{bmatrix} \mathrm{d}\widetilde{W}_r(t) \\ \mathrm{d}\widetilde{W}_v(t) \\ \mathrm{d}\widetilde{W}_x(t) \end{bmatrix}, \tag{2.7}$$

with

$$\sigma(\mathbf{X}^*(t)) = \begin{bmatrix} \eta r^p(t) & 0 & 0 \\ 0 & \gamma\sqrt{v(t)} & 0 \\ \rho_{x,r}\sqrt{v(t)} & \rho_{x,v}\sqrt{v(t)} & \sqrt{1-\rho_{x,v}^2-\rho_{x,r}^2}\sqrt{v(t)} \end{bmatrix}.$$

2.2.2 Reformulated Heston hybrid models

In the previous section we have seen that for the HHW and HCIR models with a full matrix of correlations given in (2.3), the affinity relations (see Chapter 1) are not satisfied, so that the ChF cannot be obtained by standard techniques.

In order to obtain a well-defined Heston hybrid model with an *indirectly imposed correlation*, $\rho_{x,r}$, we propose the following system of SDEs:

$$\mathrm{d}S(t)/S(t) = r(t)\mathrm{d}t + \sqrt{v(t)}\mathrm{d}W_x(t) + \Omega(t)r^p(t)\mathrm{d}W_r(t) + \Delta\sqrt{v(t)}\mathrm{d}W_v(t), \tag{2.8}$$

with

$$\begin{aligned} \mathrm{d}v(t) &= \kappa(\bar{v} - v(t))\mathrm{d}t + \gamma\sqrt{v(t)}\mathrm{d}W_v(t), \quad v(0) > 0, \\ \mathrm{d}r(t) &= \lambda(\theta(t) - r(t))\mathrm{d}t + \eta r^p(t)\mathrm{d}W_r(t), \quad r(0) > 0, \end{aligned} \tag{2.9}$$

where

$$\mathrm{d}W_x(t)\mathrm{d}W_v(t) = \hat{\rho}_{x,v}\mathrm{d}t, \quad \mathrm{d}W_x(t)\mathrm{d}W_r(t) = 0, \quad \mathrm{d}W_v(t)\mathrm{d}W_r(t) = 0. \tag{2.10}$$

Here $p = 0$ for HHW and $p = \frac{1}{2}$ for HCIR. We have included a function [2], $\Omega(t)$, and a constant parameter, Δ. Note that we assume independence between the instantaneous short-rate, $r(t)$, and the variance process $v(t)$, i.e., $\hat{\rho}_{r,v} = 0$.

By exchanging the order of the state variables, to $\mathbf{X}^*(t) = [r(t), v(t), S(t)]^{\mathrm{T}}$, system (2.8) is given, in terms of the independent Brownian motions, by:

$$\begin{bmatrix} \mathrm{d}r(t) \\ \mathrm{d}v(t) \\ \dfrac{\mathrm{d}S(t)}{S(t)} \end{bmatrix} = \begin{bmatrix} \lambda(\theta(t) - r(t)) \\ \kappa(\bar{v} - v(t)) \\ r(t) \end{bmatrix} \mathrm{d}t + \hat{\sigma}(\mathbf{X}^*(t)) \begin{bmatrix} \mathrm{d}\widetilde{W}_r(t) \\ \mathrm{d}\widetilde{W}_v(t) \\ \mathrm{d}\widetilde{W}_x(t) \end{bmatrix}, \tag{2.11}$$

with

$$\hat{\sigma}(\mathbf{X}^*(t)) = \begin{bmatrix} \eta r^p(t) & 0 & 0 \\ 0 & \gamma\sqrt{v(t)} & 0 \\ \Omega(t) r^p(t) & \sqrt{v(t)}\,(\hat{\rho}_{x,v} + \Delta) & \sqrt{v(t)}\sqrt{1 - \hat{\rho}^2_{x,v}} \end{bmatrix}.$$

In the following lemma we show that the model (2.8) is equivalent to the full-scale HHW model in (2.3), with a non-zero correlation $\rho_{x,r}$.

Lemma 2.2.1. *Model (2.8) satisfies the system in (2.3) with non-zero correlation, $\rho_{x,r}$, for:*

$$\Omega(t) = \rho_{x,r}\frac{\sqrt{v(t)}}{r^p(t)}, \quad \hat{\rho}^2_{x,v} = \rho^2_{x,v} + \rho^2_{x,r}, \quad \Delta = \rho_{x,v} - \hat{\rho}_{x,v}, \tag{2.12}$$

where correlation $\hat{\rho}_{x,v}$ is as in model (2.8) and $\rho_{x,v}$ as in model (2.3).

Proof. We presented the two models (2.3) and (2.8) in terms of the independent Brownian motions, (2.7) and (2.11), respectively. By matching the appropriate coefficients in (2.7) and (2.11), we find that the following relations should hold:

$$\begin{cases} \Omega(t) r^p(t) S(t) = \rho_{x,r}\sqrt{v(t)}S(t), \\ \sqrt{1 - \hat{\rho}^2_{x,v}}\sqrt{v(t)}S(t) = \sqrt{1 - \rho^2_{x,v} - \rho^2_{x,r}}\sqrt{v(t)}S(t), \\ (\hat{\rho}_{x,v} + \Delta)\sqrt{v(t)}S(t) = \rho_{x,v}\sqrt{v(t)}S(t). \end{cases} \tag{2.13}$$

By simplifying (2.13) the proof is finished. ∎

If results (2.12) were directly included in the main system (2.8) the affinity property of the system would be lost. So, in order to satisfy the affinity constraints, *approximations* need to be introduced.

[2] this under certain conditions can also be stochastic

2.2.3 Log-transform

Before going into the details of the approximations of the HHW and HCIR models let us first find the dynamics for the log-transform of the reformulated Heston hybrid models. By applying Itô's lemma, model (2.8) in log-equity space, $x(t) = \log S(t)$, with a constant parameter, Δ, and a function $\Omega(t)$, is given by:

$$\begin{aligned} \mathrm{d}x(t) &= \left[r(t) - \frac{1}{2}\left(\Omega^2(t)r^{2p}(t) + v(t)\left(1+\Delta^2+2\hat{\rho}_{x,v}\Delta\right)\right)\right]\mathrm{d}t + \sqrt{v(t)}\mathrm{d}W_x(t) \\ & \quad +\Omega(t)r^p(t)\mathrm{d}W_r(t) + \Delta\sqrt{v(t)}\mathrm{d}W_v(t). \end{aligned}$$

Because of (2.12) the dynamics read:

$$\mathrm{d}x(t) = \left(r(t) - \frac{1}{2}v(t)\right)\mathrm{d}t + \sqrt{v(t)}\mathrm{d}W_x(t) + \Omega(t)r^p(t)\mathrm{d}W_r(t) + \Delta\sqrt{v(t)}\mathrm{d}W_v(t).$$

For a given state vector $\mathbf{X}^*(t) = [r(t), v(t), x(t)]^{\mathrm{T}}$, the symmetric instantaneous covariance matrix is given by:

$$\mathbf{\Sigma} := \begin{bmatrix} \eta^2 r^{2p}(t) & 0 & \eta\Omega(t)r^{2p}(t) \\ * & \gamma^2 v(t) & \gamma v(t)\left(\hat{\rho}_{x,v}+\Delta\right) \\ * & * & \Omega^2(t)r^{2p}(t) + v(t)\left(1+\Delta^2+2\hat{\rho}_{x,v}\Delta\right) \end{bmatrix}. \tag{2.14}$$

As we consider two cases for parameter $p = \{0, 1/2\}$, the affinity issue appears in only one term of matrix (2.14), namely, in element $(1,3)$:

$$\mathbf{\Sigma}_{(1,3)} = \eta\Omega(t)r^{2p}(t) = \eta\rho_{x,r}\sqrt{v(t)}r^p(t) = \begin{cases} \eta\rho_{x,r}\sqrt{v(t)}, & \text{for HHW}, \\ \eta\rho_{x,r}\sqrt{v(t)}\sqrt{r(t)}, & \text{for HCIR}. \end{cases} \tag{2.15}$$

Although term $\mathbf{\Sigma}_{(3,3)}$ does not appear to be of the affine form, by (2.12), it equals $\mathbf{\Sigma}_{(3,3)} = v(t)$, and therefore it is linear in the state variables.

Remark. We see that, in order to make either the HHW or the HCIR model affine, one does not necessarily need to approximate function $\Omega(t)$, but only the non-affine terms in the corresponding instantaneous covariance matrix [3]. By approximation of the non-affine covariance term, $\mathbf{\Sigma}_{(1,3)}$, the corresponding pricing PDE also changes. The Kolmogorov backward equation for the log-stock price (see, for example, [85]) is now given by:

$$\begin{aligned} 0 &= \frac{\partial\phi}{\partial t} + \left(r - \frac{1}{2}v\right)\frac{\partial\phi}{\partial x} + \kappa(\bar{v}-v)\frac{\partial\phi}{\partial v} + \lambda(\theta(t)-r)\frac{\partial\phi}{\partial r} + \frac{1}{2}v\frac{\partial^2\phi}{\partial x^2} \\ &+ \frac{1}{2}\gamma^2 v\frac{\partial^2\phi}{\partial v^2} + \frac{1}{2}\eta^2 r^{2p}\frac{\partial^2\phi}{\partial r^2} + \rho_{x,v}\gamma v\frac{\partial^2\phi}{\partial x\partial v} + \mathbf{\Sigma}_{(1,3)}\frac{\partial^2\phi}{\partial x\partial r} - r\phi, \end{aligned} \tag{2.16}$$

subject to terminal condition $\phi(u, x(T), T, T) = \exp\left(iux(T)\right)$.

The derivations in Section 2.2.3 show that system (2.8) is nothing but a *reformulation* of the original HHW system under the conditions in (2.12). It is therefore sufficient to linearize the non-affine terms in the covariance matrix to determine an affine approximation of the full-scale model. In the sections to follow we discuss two possible approximations for $\mathbf{\Sigma}_{(1,3)}$.

[3] The drifts and the interest rate are already in the affine form.

2.3 Deterministic approximation for hybrid models

In order to linearize the Heston hybrid model we provide in Subsection 2.3.1 a first approximation for the expressions in (2.15). The corresponding ChF is derived in Subsection 2.3.2.

2.3.1 Deterministic approach, the H1-HW model

The first approach to finding an approximation for the term $\mathbf{\Sigma}_{(1,3)} = \eta\rho_{x,r}\sqrt{v(t)}r^p(t)$ in matrix (2.14) is to replace it by its expectation, i.e.:

$$\mathbf{\Sigma}_{(1,3)} \approx \eta\rho_{x,r}\mathbb{E}\left(r^p(t)\sqrt{v(t)}\right) \stackrel{\perp\!\!\!\perp}{=} \eta\rho_{x,r}\mathbb{E}(r^p(t))\mathbb{E}(\sqrt{v(t)}), \tag{2.17}$$

assuming independence between $r(t)$ and $v(t)$.

The approximation for $\mathbf{\Sigma}_{(1,3)}$ in (2.17) consists of two expectations: one with respect to $\sqrt{v(t)}$ and another with respect to $r^p(t)$. $\mathbb{E}(r^p(t)) = 1$ for $p = 0$, and it is $\mathbb{E}(\sqrt{r(t)})$ for $p = 1/2$. Since the processes for $v(t)$ and $r(t)$ are then of the same type, the approximations are analogous. By taking the expectations of the stochastic variables, the model becomes of the affine form, so that we can obtain the corresponding ChF.

In Lemma 2.3.1 the closed-form expressions for the expectation and the variance of $\sqrt{v(t)}$ (a CIR-type process) are presented.

Lemma 2.3.1 (Expectation and variance for CIR-type process)**.** *For a given time $t > 0$ the expectation and variance of $\sqrt{v(t)}$, where $v(t)$ is a CIR-type process (2.1), are given by:*

$$\mathbb{E}(\sqrt{v(t)}) = \sqrt{2c(t)}\mathrm{e}^{-\lambda(t)/2}\sum_{k=0}^{\infty}\frac{1}{k!}\left(\lambda(t)/2\right)^k\frac{\Gamma\left(\frac{1+d}{2}+k\right)}{\Gamma(\frac{d}{2}+k)}, \tag{2.18}$$

and

$$\mathbb{V}\mathrm{ar}\left(\sqrt{v(t)}\right) = c(t)(d+\lambda(t)) - 2c(t)\mathrm{e}^{-\lambda(t)}\left(\sum_{k=0}^{\infty}\frac{1}{k!}\left(\lambda(t)/2\right)^k\frac{\Gamma\left(\frac{1+d}{2}+k\right)}{\Gamma\left(\frac{d}{2}+k\right)}\right)^2, \tag{2.19}$$

where

$$c(t) = \frac{1}{4\kappa}\gamma^2(1-\mathrm{e}^{-\kappa t}), \quad d = \frac{4\kappa\bar{v}}{\gamma^2}, \quad \lambda(t) = \frac{4\kappa v(0)\mathrm{e}^{-\kappa t}}{\gamma^2(1-\mathrm{e}^{-\kappa t})}, \tag{2.20}$$

with $\Gamma(k)$ being the gamma function defined by:

$$\Gamma(k) = \int_0^{\infty} t^{k-1}\mathrm{e}^{-t}\mathrm{d}t.$$

Proof. It is shown in [25, 20], that, for a given time $t > 0$, $v(t)$ is distributed as $c(t)$ times a non-central chi-square random variable, $\chi^2(d, \lambda(t))$, with d the "degrees of freedom" parameter and non-centrality parameter $\lambda(t)$, i.e.:

$$v(t) \sim c(t)\chi^2\left(d, \lambda(t)\right), \quad t > 0, \tag{2.21}$$

with

$$c(t) = \frac{1}{4\kappa}\gamma^2(1-\mathrm{e}^{-\kappa t}), \quad d = \frac{4\kappa\bar{v}}{\gamma^2}, \quad \lambda(t) = \frac{4\kappa v(0)\mathrm{e}^{-\kappa t}}{\gamma^2(1-\mathrm{e}^{-\kappa t})}. \tag{2.22}$$

So, the corresponding cumulative distribution function (CDF) can be expressed as:

$$F_{v(t)}(x) = \mathbb{P}(v(t) \leq x) = \mathbb{P}\left(\chi^2\left(d, \lambda(t)\right) \leq x/c(t)\right) = F_{\chi^2(d,\lambda(t))}\left(x/c(t)\right), \tag{2.23}$$

where:

$$F_{\chi^2(d,\lambda(t))}(y) = \sum_{k=0}^{\infty} \exp\left(-\frac{\lambda(t)}{2}\right) \frac{\left(\frac{\lambda(t)}{2}\right)^k}{k!} \frac{\Gamma\left(k+\frac{d}{2}, \frac{y}{2}\right)}{\Gamma\left(k+\frac{d}{2}\right)}, \tag{2.24}$$

with

$$\Gamma(a,z) = \int_0^z t^{a-1}\mathrm{e}^{-t}\mathrm{d}t, \quad \Gamma(z) = \int_0^\infty t^{z-1}\mathrm{e}^{-t}\mathrm{d}t.$$

Further, the corresponding density function (see for example [81]) reads:

$$f_{\chi^2(d,\lambda(t))}(y) = \frac{1}{2}\mathrm{e}^{-\frac{1}{2}(y+\lambda(t))} \left(\frac{y}{\lambda(t)}\right)^{\frac{1}{2}\left(\frac{d}{2}-1\right)} \mathcal{B}_{\frac{d}{2}-1}(\sqrt{\lambda(t)y}),$$

with

$$\mathcal{B}_a(z) = \left(\frac{z}{2}\right)^a \sum_{k=0}^{\infty} \frac{\left(\frac{1}{4}z^2\right)^k}{k!\Gamma(a+k+1)},$$

which is a modified Bessel function of the first kind (see for example [1, 45]).

The density for $v(t)$ can now be expressed as:

$$f_{v(t)}(x) \stackrel{\text{def}}{=} \frac{\mathrm{d}}{\mathrm{d}x}F_{v(t)}(x) = \frac{\mathrm{d}}{\mathrm{d}x}F_{\chi^2(d,\lambda(t))}(x/c(t)) = \frac{1}{c(t)}f_{\chi^2(d,\lambda(t))}\left(x/c(t)\right).$$

First of all, by [30] we have that:

$$\begin{aligned} \mathbb{E}(\sqrt{v(t)}|v(0)) \quad &:= \quad \int_0^\infty \frac{\sqrt{x}}{c(t)} f_{\chi^2(d,\lambda(t))}\left(\frac{x}{c(t)}\right)\mathrm{d}x \\ &= \quad \sqrt{2c(t)}\frac{\Gamma\left(\frac{1+d}{2}\right)}{\Gamma\left(\frac{d}{2}\right)} {}_1F_1\left(-\frac{1}{2}, \frac{d}{2}, -\frac{\lambda(t)}{2}\right), \end{aligned} \tag{2.25}$$

where ${}_1F_1(a;b;z)$ is a confluent hyper-geometric function, which is also known as Kummer's function [69] of the first kind, given by:

$${}_1F_1(a;b;z) = \sum_{k=0}^{\infty} \frac{(a)_k}{(b)_k}\frac{z^k}{k!}, \tag{2.26}$$

with $(a)_k$ and $(b)_k$ being Pochhammer symbols of the form:

$$(a)_k = \frac{\Gamma(a+k)}{\Gamma(a)} = a(a+1)\cdot\dots\cdot(a+k-1). \tag{2.27}$$

Now, using the principle of Kummer (see [68] pp.42) we find:

$$ {}_1F_1\left(-\frac{1}{2},\frac{d}{2},-\frac{\lambda(t)}{2}\right)=\mathrm{e}^{-\lambda(t)/2}{}_1F_1\left(\frac{1+d}{2},\frac{d}{2},\frac{\lambda(t)}{2}\right) \tag{2.28} $$

Therefore, by (2.26) and (2.28), Equation (2.25) reads:

$$ \begin{aligned} \mathbb{E}(\sqrt{v(t)}|v(0)) &= \sqrt{2c(t)}\mathrm{e}^{-\lambda(t)/2}\frac{\Gamma\left(\frac{1+d}{2}\right)}{\Gamma\left(\frac{d}{2}\right)}{}_1F_1\left(\frac{1+d}{2},\frac{d}{2},\frac{\lambda(t)}{2}\right) \\ &= \sqrt{2c(t)}\mathrm{e}^{-\lambda(t)/2}\sum_{k=0}^{\infty}\frac{1}{k!}\left(\lambda(t)/2\right)^k\frac{\Gamma\left(\frac{1+d}{2}+k\right)}{\Gamma\left(\frac{d}{2}+k\right)}, \end{aligned} $$

which concludes the proof for the expectation.

By using the properties of the non-central chi-square distribution the mean and variance of process $v(t)$ are known explicitly:

$$ \begin{aligned} \mathbb{E}(v(t)|v(0)) &= c(t)(d+\lambda(t)), \\ \mathbb{V}\mathrm{ar}(v(t)|v(0)) &= c^2(t)(2d+4\lambda(t)). \end{aligned} \tag{2.29} $$

This combined with results for $\mathbb{E}(\sqrt{v(t)})$ completes the proof. ■

The analytic expression for the expectation, either of $\sqrt{v(t)}$ or $\sqrt{r(t)}$ in (2.17), is involved and requires rather expensive numerical operations.

In the next subsection we provide details of its approximation.

The approximations for the expectation $\mathbb{E}(\sqrt{v(t)})$

In order to find a first-order approximation we can apply the so-called *delta method* (see, for example [2, 84]), which states that a function $\varphi(X)$ can be approximated by a first-order Taylor expansion at $\mathbb{E}(X)$, for a given random variable, X, with expectation, $\mathbb{E}(X)$, and variance, $\mathbb{V}\mathrm{ar}(X)$, assuming that for $\varphi(X)$ its first derivative with respect to X exists and is sufficiently smooth.

Result 2.3.2. The expectation, $\mathbb{E}(\sqrt{v(t)})$, with stochastic process $v(t)$ given by Equation (2.3), can be approximated by:

$$ \mathbb{E}(\sqrt{v(t)})\approx\sqrt{c(t)(\lambda(t)-1)+c(t)d+\frac{c(t)d}{2(d+\lambda(t))}}=:\Lambda(t), \tag{2.30} $$

with $c(t)$, d and $\lambda(t)$ given in Lemma 2.3.1, and κ, $\bar{v}$, γ and $v(0)$ are the parameters given in Equation (2.3) [4]

In order to find the approximation in Result 2.3.2 we can use the delta method as follows. Assuming function φ to be sufficiently smooth and the first two moments of X to exist, we obtain by first-order Taylor expansion:

$$ \varphi(X)\approx\varphi(\mathbb{E}X)+(X-\mathbb{E}X)\frac{\partial\varphi}{\partial X}(\mathbb{E}X). \tag{2.31} $$

[4] In the next subsection we will discuss under which conditions the expression under the square-root in (2.30) is non-negative.

Since the variance of $\varphi(X)$ can be then approximated by the variance of the right-hand side of (2.31) we have:

$$\begin{aligned}\mathbb{V}\mathrm{ar}(\varphi(X)) &\approx \mathbb{V}\mathrm{ar}\left(\varphi(\mathbb{E}X)+(X-\mathbb{E}X)\frac{\partial\varphi}{\partial X}(\mathbb{E}X)\right)\\ &= \left(\frac{\partial\varphi}{\partial X}(\mathbb{E}X)\right)^2\mathbb{V}\mathrm{ar}X. \qquad (2.32)\end{aligned}$$

By using this result for function $\varphi(v(t))=\sqrt{v(t)}$, we find

$$\mathbb{V}\mathrm{ar}(\sqrt{v(t)}) \approx \left(\frac{1}{2}\frac{1}{\sqrt{\mathbb{E}(v(t))}}\right)^2 \mathbb{V}\mathrm{ar}(v(t)) = \frac{1}{4}\frac{\mathbb{V}\mathrm{ar}(v(t))}{\mathbb{E}(v(t))}. \qquad (2.33)$$

However, from the definition of the variance we also have:

$$\mathbb{V}\mathrm{ar}(\sqrt{v(t)}) = \mathbb{E}(v(t)) - \left(\mathbb{E}(\sqrt{v(t)})\right)^2. \qquad (2.34)$$

and by combining Equations (2.33) and (2.34) we obtain the following approximation:

$$\mathbb{E}(\sqrt{v(t)}) \approx \sqrt{\mathbb{E}(v(t)) - \frac{1}{4}\frac{\mathbb{V}\mathrm{ar}(v(t))}{\mathbb{E}(v(t))}}. \qquad (2.35)$$

Since $v(t)$ is a square-root process, as in (2.8), we have

$$v(t) = v(0)\mathrm{e}^{-\kappa t} + \bar{v}(1-\mathrm{e}^{-\kappa t}) + \gamma\int_0^t \mathrm{e}^{\kappa(s-t)}\sqrt{v(s)}\mathrm{d}W_v(s). \qquad (2.36)$$

The expectation reads $\mathbb{E}(v(t)) = c(t)(d+\lambda(t))$, and for the variance we get, $\mathbb{V}\mathrm{ar}(v(t)) = c^2(t)(2d+4\lambda(t))$, with $c(t)$, d and $\lambda(t)$ given in (2.20).

Now, by substituting these expressions in (2.35), the result is confirmed.

Since Result 2.3.2 provides an explicit approximation for $\mathbf{\Sigma}_{(1,3)}$ in (2.17) in terms of a deterministic function for $\mathbb{E}(\sqrt{v(t)})$, we are, in principle, able to derive the corresponding ChF.

Limits of the approximation for $\mathbb{E}(\sqrt{v(t)})$

We show here for which parameters the expression under the square root in approximation (2.30), i.e.,

$$\Lambda(t) = \sqrt{c(t)(\lambda(t)-1) + c(t)d + \frac{c(t)d}{2(d+\lambda(t))}}, \qquad (2.37)$$

is non-negative.

Consider the following inequality:

$$c(t)(\lambda(t)-1) + c(t)d + \frac{c(t)d}{2(d+\lambda(t))} \geq 0. \qquad (2.38)$$

Division by $c(t) > 0$ gives:

$$\frac{2\left(\lambda(t)+d\right)\left(d+\lambda(t)\right)+d}{2(d+\lambda(t))} \quad \geq \quad 1. \tag{2.39}$$

So,

$$2\left(\lambda(t)+d\right)^2 - 2(\lambda(t)+d) + d \geq 0. \tag{2.40}$$

By setting $y = \lambda(t)+d$ we find $2y^2 - 2y + d \geq 0$. The parabola is non-negative for the discriminant $4 - 4\cdot 2\cdot d \leq 0$, so that the expression in (2.37) is non-negative for $d \geq \frac{1}{2}$ (i.e., $2d \geq 1$). With $d = 4\kappa\bar{v}/\gamma^2$ we can compare the inequality obtained to the Feller condition. If the Feller condition is satisfied, the expression under the square-root is certainly well-defined. If $8\kappa\bar{v}/\gamma^2 \geq 1$ but the Feller condition is not satisfied, the approximation is also valid. If the expression under the square-root in (2.37) becomes negative, we suggest using the closed-form formula in Lemma 2.3.1 instead.

Remark. We assume that the first-order linear terms in (2.31) in the Taylor expansion give an accurate representation. However, this may not work satisfactory for "flat" density functions, like those from a uniform distribution. In order to increase the accuracy, higher-order terms can be included in the expansion [2]. More discussion on the conditions for the delta method to perform well can be found in [84].

The approximation for $\mathbb{E}(\sqrt{v(t)})$ in (2.30) is still non-trivial, and may cause difficulties when deriving the corresponding characteristic functions. In order to find the coefficients of the ChF, a routine for numerically solving the corresponding ODEs has to be incorporated. Numerical integration, however, slows down the option pricing engine, and would make the SDE model less attractive. As we aim to find a closed-form expression for the ChF, we simplify $\Lambda(t)$ in (2.30). Expectation $\mathbb{E}(\sqrt{v(t)})$ can be further approximated by a function of the following form:

$$\mathbb{E}(\sqrt{v(t)}) \approx a + b\mathrm{e}^{-ct} =: \widetilde{\Lambda}(t), \tag{2.41}$$

with a, b and c constants. Appropriate values for a, b and c in (2.41) can be obtained via an optimization problem of the form, $\min_{a,b,c}\int_0^T \big(\Lambda(t) - \widetilde{\Lambda}(t)\big)\mathrm{d}t$.

We propose here, instead of a numerical approximation for these coefficients, a simple analytic expression in Result 2.3.3:

Result 2.3.3. By matching the functions $\Lambda(t)$ and $\widetilde{\Lambda}(t)$ for $t \to +\infty$, $t \to 0$ and $t = 1$, we find:

$$\begin{aligned}
\lim_{t\to+\infty}\Lambda(t) = & \sqrt{\bar{v} - \frac{\gamma^2}{8\kappa}} = & a = & \lim_{t\to+\infty}\widetilde{\Lambda}(t),\\
\lim_{t\to 0}\Lambda(t) = & \sqrt{v(0)} = & a+b = & \lim_{t\to 0}\widetilde{\Lambda}(t),\\
\lim_{t\to 1}\Lambda(t) = & \Lambda(1) = & a+b\mathrm{e}^{-c} = & \lim_{t\to 1}\widetilde{\Lambda}(t).
\end{aligned} \tag{2.42}$$

The values a, b and c can now be estimated by:

$$a = \sqrt{\bar{v} - \frac{\gamma^2}{8\kappa}}, \quad b = \sqrt{v(0)} - a, \quad c = -\log\left(b^{-1}(\Lambda(1) - a)\right), \tag{2.43}$$

where $\Lambda(t)$ is given by (2.30).

The approximation given in Result 2.3.3 may give difficulties for $\bar{v} < \gamma^2/8\kappa$ in Equation (2.43) (the expression under the square root then becomes negative). We recognize that this expression is well-defined as the expression under the square-root in the function $\Lambda(t)$ in Result 2.3.2 is positive.

In order to measure the quality of approximation (2.43) to $\mathbb{E}(\sqrt{v(t)})$ in (2.18), we perform a numerical experiment (see the results in Figure 2.1). For randomly chosen sets of parameters the approximation (2.43) resembles $\mathbb{E}(\sqrt{v(t)})$ in (2.18) very well.

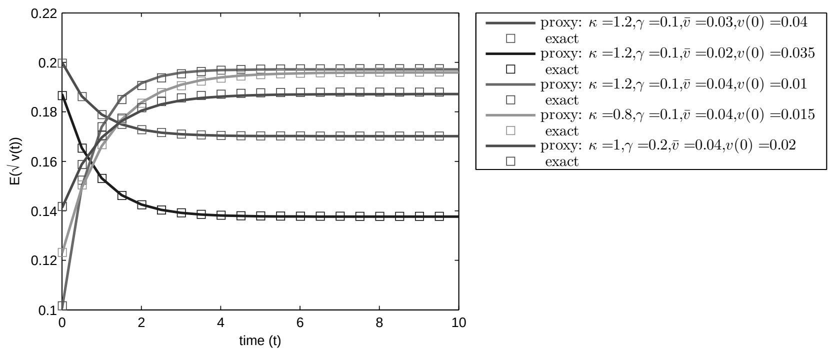

Figure 2.1: *The quality of the approximation $\mathbb{E}(\sqrt{v(t)}) \approx a + b\mathrm{e}^{-ct}$ (continuous line) versus the exact solution given in Equation (2.18) (squares) for 5 random κ, γ, $\bar{v}$ and $v(0)$.*

We call the resulting model the H1-HW model (Heston-Hull-White model-1).

The case $\Delta = 0$ and $\Omega(t) \equiv$ const.

With $\Delta = 0$ in the systems (2.8) and (2.11), the model resembles the one in [43, 6]. There, a constant parameter $\bar{\Omega} = \Omega(t)$ was prescribed, and an instantaneous correlation was *indirectly* imposed.

The following lemma, however, shows that this model with $\Delta = 0$ resembles the full-scale HHW and HCIR models only for correlation $\rho_{x,r} = 0$.

Lemma 2.3.4. *The hybrid models (2.8) with $\Delta = 0$ are full-scale HHW and HCIR models, in the sense of system (2.3), only if the instantaneous correlation between the stock and the interest rate processes in system (2.3) equals zero, i.e., $\rho_{x,r} = 0$.*

Proof. The proof is analogous to the proof of Lemma 2.2.1. We see from the equalities in (2.12) that system (2.7) resembles system (2.11) with $\Delta = 0$, only if:

$$\bar{\Omega} = \rho_{x,r}\frac{\sqrt{v(t)}}{r^p(t)}, \quad \hat{\rho}_{x,v} = \rho_{x,v}, \quad \hat{\rho}^2_{x,v} = \rho^2_{x,v} + \rho^2_{x,r}. \tag{2.44}$$

The equations (2.44) hold only for $\rho_{x,r} = 0$. So, the models with $\Delta = 0$ are not full-scale HHW and HCIR models with a non-zero correlation $\rho_{x,r}$. ■

Although the model with $\Delta = 0$ is not a properly defined Heston hybrid model, one can still proceed with the analysis. Parameter $\bar{\Omega}$ was derived based on the following equality, see [43], using the definition of the instantaneous correlation,

$$\hat{\rho}_{x,r} = \frac{\mathbb{E}\left(\mathrm{d}S(t)\mathrm{d}r(t)\right) - \mathbb{E}(\mathrm{d}S(t))\mathbb{E}(\mathrm{d}r(t))}{\sqrt{v(t)S^2(t)\ \mathrm{d}t + \bar{\Omega}^2r^{2p}(t)S^2(t)\ \mathrm{d}t}\sqrt{\eta^2r^{2p}(t)\ \mathrm{d}t}} = \frac{\bar{\Omega}r^p(t)}{\sqrt{v(t)+\bar{\Omega}^2r^{2p}(t)}}. \tag{2.45}$$

To deal with the affinity issue a constant approximation for $\bar{\Omega}$ was proposed, given by:

$$\bar{\Omega} \approx \frac{\hat{\rho}_{x,r}}{\sqrt{1-\hat{\rho}^2_{x,r}}}\mathbb{E}\left(\frac{1}{T}\int_0^T v(t)\mathrm{d}t\right)^{\frac{1}{2}} \Big/ \mathbb{E}\left(\frac{1}{T}\int_0^T r(t)\mathrm{d}t\right)^{p}. \tag{2.46}$$

By choosing $\bar{\Omega} = 0$ the model collapses to the well-known Heston-Hull-White model ($p = 0$) or Heston-CIR model ($p = \frac{1}{2}$) with zero correlation $\rho_{x,r}$.

The assumptions of constant $\bar{\Omega}$ and $\Delta = 0$ also have an impact on the corresponding pricing PDE. With the Feynman-Kac theorem the corresponding PDE is given by:

$$\begin{aligned} 0 = {} & \frac{\partial\phi}{\partial t} + \left[r - \frac{1}{2}\left(v + r^{2p}\bar{\Omega}^2\right)\right]\frac{\partial\phi}{\partial x} + \kappa(\bar{v}-v)\frac{\partial\phi}{\partial v} + \lambda(\theta(t)-r)\frac{\partial\phi}{\partial r} + \frac{1}{2}\gamma^2 v\frac{\partial^2\phi}{\partial v^2} \\ & + \frac{1}{2}\left(v + r^{2p}\bar{\Omega}^2\right)\frac{\partial^2\phi}{\partial x^2} + \frac{1}{2}\eta^2 r^{2p}\frac{\partial^2\phi}{\partial r^2} + \hat{\rho}_{x,v}\gamma v\frac{\partial^2\phi}{\partial x\partial v} + \eta\bar{\Omega}r^{2p}\frac{\partial^2\phi}{\partial x\partial r} - r\phi, \end{aligned} \tag{2.47}$$

with the same terminal condition as for (2.16). The assumption of constant $\bar{\Omega}$ and $\Delta = 0$ gives rise to additional terms in the convection and diffusion parts of PDE (2.47).

By means of a numerical experiment, we check the accuracy of the model with $\Delta = 0$ and determine whether the model approximates the full-scale HHW hybrid model sufficiently well.

We consider here the following set of parameters: $S(0) = 1$, $\kappa = 2$, $v(0) = \bar{v} = 0.05$, $\gamma = 0.1$, $\lambda = 1.2$, $r(0) = \theta = 0.05$, $\eta = 0.01$ and correlation $\rho_{x,v} = -40\%$. In the simulation we choose two different values for correlation $\rho_{x,r} = \{30\%, 50\%\}$.

We compare the following three models: The full-scale HHW model (with Monte Carlo simulation), the model with $\Delta = 0$ and our approximation for $\mathbf{\Sigma}_{(1,3)}$ in (2.16) with the projection according to Equation (2.17).

In Figure 2.2 the implied volatilities obtained are compared. The model with $\Delta = 0$ in (2.47) does not provide a satisfactory fit to the full-scale HHW

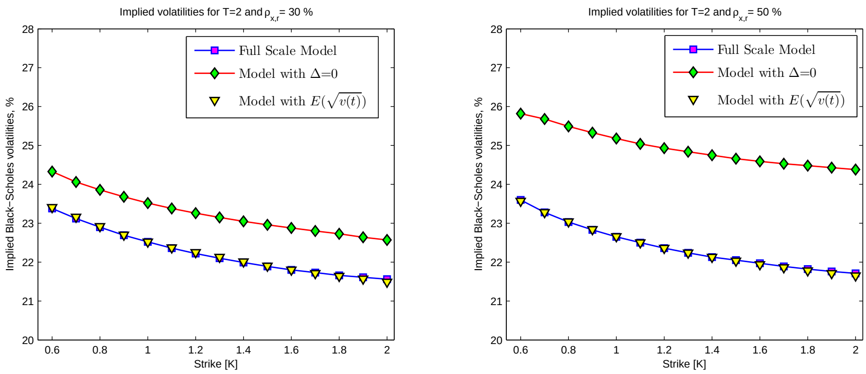

Figure 2.2: *The implied Black-Scholes volatilities for the full-scale Heston model and two approximations: the deterministic approach (model (2.16) with (2.17)), and the model with* $\Delta = 0$ *(model (2.47)).*

model, whereas the implied volatilities obtained with the deterministic hybrid approximation compare very well (they essentially overlap) with the full-scale reference results, see Figure 2.2. The *volatility compensator* Δ, as defined in Lemma 2.2.1, cannot be neglected when approximating the full-scale HHW model, as was stated in Lemma 2.3.4.

2.3.2 Characteristic function for the H1-HW model

We derive the ChF for the approximation H1-HW to the Heston-Hull-White hybrid model, given in (2.16). For $p = 0$, the non-affine term, $\mathbf{\Sigma}_{(1,3)}$, in matrix (2.16) equals $\mathbf{\Sigma}_{(1,3)} = \eta\rho_{x,r}\sqrt{v(t)}$ and will be approximated by $\mathbf{\Sigma}_{(1,3)} \approx \eta\rho_{x,r}\mathbb{E}(\sqrt{v(t)})$.

We assume here that the term-structure for the interest rate $\theta(t)$ is constant, $\theta(t) = \theta$. A generalization for this has already been discussed in Chapter 1.

According to [28], the discounted ChF for the H1-HW model is of the following form:

$$\phi_{\text{H1-HW}}(u, x(t), \tau) = \exp\left(A(u,\tau) + B(u,\tau)x(t) + C(u,\tau)r(t) + D(u,\tau)v(t)\right), \tag{2.48}$$

with final conditions $A(u,0) = 0$, $B(u,0) = iu$, $C(u,0) = 0$, and $D(u,0) = 0$, and $\tau := T - t$.

The ChF for the H1-HW model can be derived in closed-form, with the help of the following lemmas:

Lemma 2.3.5 (The ODEs related to the H1-HW model)**.** *The functions* $B(u,\tau) =: B(\tau)$, $C(u,\tau) =: C(\tau)$, $D(u,\tau) =: D(\tau)$ *and* $A(u,\tau) =: A(\tau)$ *for* $u \in \mathbb{C}$ *and* $\tau \geq 0$ *in (2.48) for the H1-HW model satisfy the following system of*

ODEs:

$$\begin{aligned}
B'(\tau) &= 0, \quad B(u,0) = iu, \\
C'(\tau) &= -1 - \lambda C(\tau) + B(\tau), \quad C(u,0) = 0, \\
D'(\tau) &= B(\tau)(B(\tau)-1)/2 + (\gamma\rho_{x,v}B(\tau) - \kappa)\,D(\tau) + \gamma^2 D^2(\tau)/2, \quad D(u,0) = 0, \\
A'(\tau) &= \lambda\theta C(\tau) + \kappa\bar{v}D(\tau) + \eta^2 C^2(\tau)/2 + \eta\rho_{x,r}\mathbb{E}(\sqrt{v(t)})B(\tau)C(\tau), \quad A(u,0) = 0,
\end{aligned}$$

with $\tau = T - t$, *and where* κ, λ, θ *and* η, $\rho_{x,r}$ *and* $\rho_{x,v}$ *correspond to the parameters in the HHW model (2.3).*

Proof. For a given state vector $X(t) = [x(t), r(t), v(t)]^{\mathrm{T}}$, and $\phi := \phi(u, X(t), t, T)$ we find the system of the ODEs satisfying the following pricing PDE:

$$\begin{aligned}
0 = \frac{\partial\phi}{\partial t} &+ \left(r - \frac{1}{2}v\right)\frac{\partial\phi}{\partial x} + \kappa(\bar{v} - v)\frac{\partial\phi}{\partial v} + \lambda(\theta(t) - r)\frac{\partial\phi}{\partial r} + \frac{1}{2}v\frac{\partial^2\phi}{\partial x^2} \\
&+ \frac{1}{2}\gamma^2 v\frac{\partial^2\phi}{\partial v^2} + \frac{1}{2}\eta^2\frac{\partial^2\phi}{\partial r^2} + \rho_{x,v}\gamma v\frac{\partial^2\phi}{\partial x\partial v} + \eta\rho_{x,r}\mathbb{E}(\sqrt{v(t)})\frac{\partial^2\phi}{\partial x\partial r} - r\phi, \quad (2.49)
\end{aligned}$$

subject to terminal condition $\phi(u, x(T), T, T) = \exp(iux(T))$.

Since the PDE in (2.49) is affine, its solution is of the following form:

$$\phi(u, x(t), t, T) = \exp\big(A(u,t,T) + B(u,t,T)x(t) + C(u,t,T)r(t) + D(u,t,T)v(t)\big).$$

By setting $A := A(u,t,T)$, $B := B(u,t,T)$, $C := C(u,t,T)$ and $D := D(u,t,T)$ we find the following partial derivatives:

$$\begin{aligned}
\frac{\partial\phi}{\partial t} &= \phi\left(\frac{\partial A}{\partial t} + x(t)\frac{\partial B}{\partial t} + r(t)\frac{\partial C}{\partial t} + v(t)\frac{\partial D}{\partial t}\right), && (2.50) \\
\frac{\partial\phi}{\partial x} &= B\phi, \quad \frac{\partial^2\phi}{\partial x^2} = B^2\phi, \quad \frac{\partial^2\phi}{\partial x\partial v} = BD\phi, \quad \frac{\partial^2\phi}{\partial x\partial r} = BC\phi, && (2.51) \\
\frac{\partial\phi}{\partial r} &= C\phi, \quad \frac{\partial^2\phi}{\partial r^2} = C^2\phi, && (2.52) \\
\frac{\partial\phi}{\partial v} &= D\phi, \quad \frac{\partial^2\phi}{\partial v^2} = D^2\phi. && (2.53)
\end{aligned}$$

By substitution, PDE (2.49) reads:

$$\begin{aligned}
0 &= \frac{\partial A}{\partial t} + x\frac{\partial B}{\partial t} + r\frac{\partial C}{\partial t} + v\frac{\partial D}{\partial t} + \left(r - \frac{1}{2}v\right)B + \kappa(\bar{v} - v)D + \lambda(\theta(t) - r)C \\
&+ \frac{1}{2}vB^2 + \frac{1}{2}\gamma^2 vD^2 + \frac{1}{2}\eta^2 C^2 + \rho_{x,v}\gamma vBD + \eta\rho_{x,r}\mathbb{E}(\sqrt{v(t)})BC - r. \quad (2.54)
\end{aligned}$$

Now, by collecting the terms for $x(t)$, $r(t)$ and $v(t)$ we find the following set of ODEs:

$$\begin{aligned}
\frac{\partial B}{\partial t} &= 0,\\
\frac{\partial C}{\partial t} &= -B + \lambda C + 1,\\
\frac{\partial D}{\partial t} &= \frac{1}{2}B + \kappa D - \frac{1}{2}\gamma^2 D^2 - \rho_{x,v}\gamma BD - \frac{1}{2}B^2,\\
\frac{\partial A}{\partial t} &= -\kappa\bar{v}D - \lambda\theta C - \frac{1}{2}\eta^2 C^2 - \rho_{x,r}\eta\mathbb{E}(\sqrt{v(t)})BC.
\end{aligned}$$

By setting $\tau = T - t$ the proof is finished. ■

The following lemma gives the closed-form solution for the functions $B(u,\tau)$, $C(u,\tau)$, $D(u,\tau)$ and $A(u,\tau)$ in (2.48).

Lemma 2.3.6 (Characteristic function for the H1-HW model)**.** *The solution of the ODE system in Lemma 2.3.5 is given by:*

$$\begin{aligned}
B(u,\tau) &= iu, && (2.55)\\
C(u,\tau) &= (iu-1)\lambda^{-1}(1-\mathrm{e}^{-\lambda\tau}), && (2.56)\\
D(u,\tau) &= \frac{1-\mathrm{e}^{-D_1\tau}}{\gamma^2\left(1-g\mathrm{e}^{-D_1\tau}\right)}\left(\kappa - \gamma\rho_{x,v}iu - D_1\right), && (2.57)\\
A(u,\tau) &= \lambda\theta I_1(\tau) + \kappa\bar{v}I_2(\tau) + \frac{1}{2}\eta^2 I_3(\tau) + \eta\rho_{x,r}I_4(\tau), && (2.58)
\end{aligned}$$

with $D_1 = \sqrt{(\gamma\rho_{x,v}iu-\kappa)^2 - \gamma^2 iu(iu-1)}$, *and where* $g = \dfrac{\kappa - \gamma\rho_{x,v}iu - D_1}{\kappa - \gamma\rho_{x,v}iu + D_1}$, κ, θ, λ, *and* γ *are as in (2.9).*

The integrals $I_1(\tau)$, $I_2(\tau)$, *and* $I_3(\tau)$ *admit an analytic solution, and* $I_4(\tau)$ *a semi-analytic solution:*

$$\begin{aligned}
I_1(\tau) &= \frac{1}{\lambda}(iu-1)\left(\tau + \frac{1}{\lambda}(\mathrm{e}^{-\lambda\tau}-1)\right),\\
I_2(\tau) &= \frac{\tau}{\gamma^2}\left(\kappa - \gamma\rho_{x,v}iu - D_1\right) - \frac{2}{\gamma^2}\log\left(\frac{1-g\mathrm{e}^{-D_1\tau}}{1-g}\right),\\
I_3(\tau) &= \frac{1}{2\lambda^3}(i+u)^2\left(3+\mathrm{e}^{-2\lambda\tau} - 4\mathrm{e}^{-\lambda\tau} - 2\lambda\tau\right),\\
I_4(\tau) &= iu\int_0^\tau \mathbb{E}(\sqrt{v(T-s)})C(u,s)\mathrm{d}s\\
&= -\frac{1}{\lambda}(iu+u^2)\int_0^\tau \mathbb{E}(\sqrt{v(T-s)})\left(1-\mathrm{e}^{-\lambda s}\right)\mathrm{d}s.
\end{aligned}$$

Proof. Obviously, due to the final condition, $B(u,0) = iu$, we have $B(u,\tau) = iu$. For the second ODE, multiplying both sides by $\mathrm{e}^{\lambda\tau}$, we get:

$$\frac{\mathrm{d}}{\mathrm{d}\tau}\left(\mathrm{e}^{\lambda\tau}C(u,\tau)\right) = (iu-1)\mathrm{e}^{\lambda\tau}, \tag{2.59}$$

by integrating both sides and using the condition, $C(u,0)=0$, we find

$$C(u,\tau)=(iu-1)\lambda^{-1}\left(1-\mathrm{e}^{-\lambda\tau}\right).$$

By setting $a=-\frac{1}{2}(u^2+iu)$, $b=\gamma\rho_{x,v}iu-\kappa$, and $c=\frac{1}{2}\gamma^2$, the ODEs for $D(u,\tau)$ and $I_2(\tau)$ are given by the following Riccati equation:

$$\frac{\mathrm{d}}{\mathrm{d}\tau}D(u,\tau) = a+bD(u,\tau)+cD^2(u,\tau), \quad D(u,0)=0, \tag{2.60}$$

$$I_2(\tau) = \kappa\bar{v}\int_0^\tau D(u,s)\mathrm{d}s. \tag{2.61}$$

Equations (2.60) and (2.61) are of the same form as those in [54]. Their solutions are given by:

$$D(u,\tau) = \frac{-b-D_1}{2c(1-G\mathrm{e}^{-D_1\tau})}(1-\mathrm{e}^{-D_1\tau}), \tag{2.62}$$

$$I_2(\tau) = \frac{1}{2c}\left((-b-D_1)\tau-2\log\left(\frac{1-G\mathrm{e}^{-D_1\tau}}{1-G}\right)\right), \tag{2.63}$$

with $D_1=\sqrt{b^2-4ac}$, $G=\dfrac{-b-D_1}{-b+D_1}$.

The evaluation of the integrals $I_1(\tau)$, $I_3(\tau)$ and $I_4(\tau)$ is straightforward. The proof is finished by the corresponding substitutions. ■

Note that by taking $\mathbb{E}(\sqrt{v(T-s)})\approx a+b\mathrm{e}^{-c(T-s)}$, with a, b and c as given in (2.41) we obtain a closed-form expression:

$$\begin{aligned} I_4(\tau) \;=\; & -\frac{1}{\lambda}(iu+u^2)\left[\frac{b}{c}\left(\mathrm{e}^{-ct}-\mathrm{e}^{-cT}\right)+a\tau+\frac{a}{\lambda}\left(\mathrm{e}^{-\lambda\tau}-1\right)\right. \\ & \left.+\frac{b}{c-\lambda}\mathrm{e}^{-cT}\left(1-e^{-\tau(\lambda-c)}\right)\right]. \end{aligned} \tag{2.64}$$

In the next section we present the generalization of the H1-HW model to a *full matrix of non-zero correlations* between the processes.

2.3.3 Hybrid model with full matrix of correlations

Similar to the approximation of the non-affine terms in the instantaneous covariance matrix of the Heston hybrid model presented in Section 2.3.1, we discuss here the inclusion of the additional correlation, $\rho_{r,v}$, between the interest rate, $r(t)$, and the stochastic variance, $v(t)$. For the state vector $\mathbf{X}(t)=[x(t),v(t),r(t)]^{\mathrm{T}}$ the model has the following symmetric instantaneous covariance matrix:

$$\mathbf{\Sigma}:=\sigma(\mathbf{X}(t))\sigma(\mathbf{X}(t))^{\mathrm{T}}=\begin{bmatrix} v(t) & \rho_{x,v}\gamma v(t) & \rho_{x,r}\eta\sqrt{v(t)} \\ * & \gamma^2 v(t) & \rho_{r,v}\gamma\eta\sqrt{v(t)} \\ * & * & \eta^2 \end{bmatrix}_{(3\times 3)}. \tag{2.65}$$

The affinity issue arises in two terms of matrix (2.65), namely, in elements $(1,3)$ and $(2,3)$:

$$\mathbf{\Sigma}_{(1,3)} = \rho_{x,r}\eta\sqrt{v(t)}, \quad \mathbf{\Sigma}_{(2,3)} = \rho_{r,v}\gamma\eta\sqrt{v(t)}.$$

For completeness, we also present the associated Kolmogorov backward equation, which is now given by:

$$\begin{aligned} 0 &= \frac{\partial\phi}{\partial t} + \left(r - \frac{1}{2}v\right)\frac{\partial\phi}{\partial x} + \kappa(\bar{v} - v)\frac{\partial\phi}{\partial v} + \lambda(\theta(t) - r)\frac{\partial\phi}{\partial r} + \frac{1}{2}v\frac{\partial^2\phi}{\partial x^2} + \frac{1}{2}\gamma^2 v\frac{\partial^2\phi}{\partial v^2} \\ &+ \frac{1}{2}\eta^2\frac{\partial^2\phi}{\partial r^2} + \rho_{x,v}\gamma v\frac{\partial^2\phi}{\partial x\partial v} + \mathbf{\Sigma}_{(1,3)}\frac{\partial^2\phi}{\partial x\partial r} + \mathbf{\Sigma}_{(2,3)}\frac{\partial^2\phi}{\partial r\partial v} - r\phi, \end{aligned} \tag{2.66}$$

with terminal condition equal to:

$$\phi(u, x(T), T, T) = \exp(iux(T)).$$

With $\rho_{r,v} = 0$ the approximating Heston-Hull-White model with a full matrix of correlations collapses to the setup in Section 2.3.1.

As before, we can use the deterministic approximations $\mathbf{\Sigma}_{(1,3)} \approx \rho_{x,r}\eta\mathbb{E}(\sqrt{v(t)})$ and $\mathbf{\Sigma}_{(2,3)} \approx \rho_{r,v}\gamma\eta\mathbb{E}(\sqrt{v(t)})$ for which Result 2.3.3 can be used.

The representations of the Heston-Hull-White model in (2.8) and the model in (2.3) with $\rho_{r,v} \neq 0$ for $p = 0$ are closely related. The lemma below specifies the relation in terms of the coefficients of the corresponding ChF.

Lemma 2.3.7 (The ChF for the approximating Heston-Hull-White model with a full matrix of correlations)**.** *The discounted ChF for the model is of the following form:*

$$\phi(u, x(t), \tau) = \exp\left(\hat{A}(u,\tau) + \hat{B}(u,\tau)x(t) + \hat{C}(u,\tau)r(t) + \hat{D}(u,\tau)v(t)\right),$$

with the functions $\hat{A}(u,\tau)$, $\hat{B}(u,\tau)$, $\hat{C}(u,\tau)$ and $\hat{D}(u,\tau)$ given by:

$$\hat{B}(u,\tau) = B(u,\tau), \quad \hat{C}(u,\tau) = C(u,\tau), \quad \hat{D}(u,\tau) = D(u,\tau), \tag{2.67}$$

with $B(u,\tau)$ in (2.55), $C(u,\tau)$ in (2.56) and $D(u,\tau)$ given in (2.57). For $\hat{A}(u,\tau)$ we have:

$$\hat{A}(u,\tau) = A(u,\tau) + \rho_{r,v}\gamma\eta\int_0^\tau \mathbb{E}(\sqrt{v(T-s)})\hat{C}(u,s)\hat{D}(u,s)\mathrm{d}s, \tag{2.68}$$

where $A(u,\tau)$ is given in (2.58).

Proof. The proof is very similar to the proof of Lemma 2.3.6. ■

The accuracy of the HHW approximations with a full matrix of correlations will be discussed in Section 2.6.

2.4 Stochastic approximation for hybrid models

In Section 2.3 a first approach to approximate the non-affine elements in the instantaneous covariance matrix was presented. Here, we model those elements by stochastic processes, and call the resulting approximate model H2-HW (Heston-Hull-White model-2).

2.4.1 Stochastic approach, the H2-HW model

In the result below an approximation for finite time t and a non-zero centrality parameter is presented.

Result 2.4.1 (Normal approximation for $\sqrt{v(t)}$, for $0 < t < \infty$)**.** For any time, $t < \infty$, the square root of $v(t)$ in (2.8) can be approximated by

$$\sqrt{v(t)} \approx \mathcal{N}\left(\sqrt{c(t)(\lambda(t)-1) + c(t)d + \frac{c(t)d}{2(d+\lambda(t))}}, c(t) - \frac{c(t)d}{2(d+\lambda(t))}\right), \quad (2.69)$$

with $c(t)$, d and $\lambda(t)$ from (2.20). Moreover, for a fixed value of x in the cumulative distribution function $F_{\sqrt{v(t)}}(x)$, and a fixed value for parameter d, the error is of order $\mathcal{O}(\lambda^2(t))$ for $\lambda(t) \to 0$ and $\mathcal{O}(\lambda(t)^{-\frac{1}{2}})$ for $\lambda(t) \to \infty$.

To show the validity of the approximations presented above, we follow Patnaik in [88] who found that an accurate approximation for the non-central chi-square distribution, $\chi^2_d(\lambda(t))$, can be obtained by an approximation with a centralized chi-square distribution, i.e.:

$$\chi^2(d, \lambda(t)) \approx a(t)\chi^2(f(t)), \quad (2.70)$$

with $a(t)$ and $f(t)$ in (2.70) chosen so that the first two moments match, i.e.:

$$a(t) = \frac{d + 2\lambda(t)}{d + \lambda(t)}, \quad f(t) = d + \frac{\lambda^2(t)}{d + 2\lambda(t)}. \quad (2.71)$$

It was shown in [25, 21] that, for a given time $t > 0$, $v(t)$ is distributed as $c(t)$ times a non-central chi-square random variable, $\chi^2(d, \lambda(t))$, with degrees of freedom parameter d and non-centrality parameter $\lambda(t)$, i.e.: $v(t) = c(t)\chi^2\left(d, \lambda(t)\right),\ t > 0$. By combining this with (2.70) we have:

$$\sqrt{v(t)} \approx \sqrt{c(t)}\sqrt{a(t)\chi^2(f(t))}. \quad (2.72)$$

Now, we use a result by Fisher [35] that for a given central chi-square random variable, $\chi^2(d)$, the expression $\sqrt{2\chi^2(d)}$ is approximately normally distributed with mean $\sqrt{2d-1}$ and unit variance, i.e.:

$$F_{\chi^2(d)}(x) \approx \Phi\left(\sqrt{2x} - \sqrt{2d-1}\right), \quad (2.73)$$

which implies:

$$\sqrt{v(t)} \approx \mathcal{N}\left(\sqrt{\left(f(t) - \frac{1}{2}\right)c(t)a(t)}, \frac{1}{2}c(t)a(t)\right). \quad (2.74)$$

The order of this approximation can be found in [65].

Remark. Also in [88] it was indicated that the normal approximation resembles the non-central chi-square distribution very well for either a large number of degrees of freedom, d, or a large non-centrality $\lambda(t)$. For $t \to 0$, the non-centrality parameter, $\lambda(t)$, tends to infinity. Therefore, accurate approximations are expected.

In the case of long maturities, the non-centrality parameter converges to 0, which may give an inaccurate approximation. In this case, satisfactory results depend on the size of the degrees of freedom parameter d. It is clear that d in (2.20) is directly related to the Feller condition. In practical applications, however, $2\kappa\bar{v}$ is often smaller than γ^2. In the numerical experiments to follow we will study the impact of violating the Feller condition.

In Result 2.4.1 we have shown that $\sqrt{v(t)}$ can be approximated well by a normally distributed random variable. As the application of Itô's lemma to find the dynamics for $\sqrt{v(t)}$ is not allowed (the square-root process is not twice differentiable at the origin [60]), we construct a stochastic process, $\xi(t)$, so that *equality in distribution* holds, i.e.: $\xi(t) \overset{\mathrm{d}}{\approx} \sqrt{v(t)}$. Since a normal random variable is completely described by its first two moments, we need to ensure that $\mathbb{E}(\xi(t)) = \mathbb{E}(\sqrt{v(t)})$ and $\mathbb{V}\mathrm{ar}(\xi(t)) = \mathbb{V}\mathrm{ar}(\sqrt{v(t)})$. For this purpose we propose the following dynamics:

$$\mathrm{d}\xi(t) = \mu^{\xi}(t)\mathrm{d}t + \psi^{\xi}(t)\mathrm{d}W_v(t), \;\; \xi(0) = \sqrt{v(0)}, \tag{2.75}$$

with some deterministic, time-dependent functions $\mu^{\xi}(t)$, and $\psi^{\xi}(t)$, determined so that the first two moments match. By moment-matching the unknown functions $\mu^{\xi}(t)$ and $\psi^{\xi}(t)$ in (2.75) read:

$$\mu^{\xi}(t) = \frac{\mathrm{d}}{\mathrm{d}t}\mathbb{E}(\sqrt{v(t)}), \quad \psi^{\xi}(t) = \sqrt{\frac{\mathrm{d}}{\mathrm{d}t}\mathbb{V}\mathrm{ar}(\sqrt{v(t)})}. \tag{2.76}$$

Using the results from Lemma 2.3.1, the expectation, $\mathbb{E}(\sqrt{v(t)})$, and the variance, $\mathbb{V}\mathrm{ar}(\sqrt{v(t)})$, can be derived:

$$\begin{aligned} \mu^{\xi}(t) &= \frac{1}{2\sqrt{2}}\frac{\Gamma\left(\frac{1+d}{2}\right)}{\sqrt{c(t)}}\left({}_1\widetilde{F}_1\left(-\frac{1}{2},\frac{d}{2},-\frac{\lambda(t)}{2}\right)\frac{1}{2}\gamma^2\mathrm{e}^{-\kappa t}\right.\\ &\quad \left.+\,{}_1\widetilde{F}_1\left(\frac{1}{2},\frac{2+d}{2},-\frac{\lambda(t)}{2}\right)\frac{v(0)\kappa}{1-\mathrm{e}^{\kappa t}}\right),\\ \psi^{\xi}(t) &= \left(\kappa(\bar{v}-v(0))\mathrm{e}^{-\kappa t} - 2\mathbb{E}(\sqrt{v(t)})\,\mu^{\xi}(t)\right)^{\frac{1}{2}}. \end{aligned} \tag{2.77}$$

Here, $\mathbb{E}(\sqrt{v(t)})$ and d, $c(t)$ and $\lambda(t)$ are as in (2.18) and the regularized hypergeometric function ${}_1\widetilde{F}_1(a;b;z) =: {}_1F_1(a;b;z)/\Gamma(b)$.

The expressions for $\mu^{\xi}(t)$ and $\psi^{\xi}(t)$ in (2.77) are exact. However, since those expressions are not cheap to compute one can find suitable approximations based on the results in Result 2.3.2, which are however not guaranteed to be well-defined for all sets of parameters.

Since the approximate hybrid models are to be used for the calibration to European-style options (with one terminal payment) we do not need path-wise equality between processes $\xi(t)$ and $\sqrt{v(t)}$, only *equality in terminal distribution* is needed.

Remark. In Section 2.4.1 we projected $\sqrt{v(t)}$ onto a normal process, $\xi(t)$. As it is common with approximations by normal processes (a non-negative random variable is projected onto another variable $\in \mathbb{R}$), this approximation comes with an error (as we indicated in Result 2.4.1). During stress-testing, examples of which are presented in Section 2.4.3 and in Section 2.6, we did not encounter any problems with this approximation. Typically, the stochastic approximation is somewhat more accurate than the deterministic approach (which is not based on a normal approximation) [5].

2.4.2 Characteristic function for the H2-HW model

We now use the (stochastic) approximation for the term $\mathbf{\Sigma}_{(1,3)}$, with the process $\mathrm{d}\xi(t)$ given by (2.75), and the time-dependent functions $\mu^{\xi}(t)$ and $\psi^{\xi}(t)$ as in (2.77).

This approximation gives rise to an extension of the 3D space variable $\mathbf{X}(t) = [S(t), v(t), r(t)]^{\mathrm{T}}$ to a 4D space $\widetilde{\mathbf{X}}(t) = [S(t), v(t), r(t), \xi(t)]^{\mathrm{T}}$, with the following system of SDEs:

$$\begin{cases} \mathrm{d}S(t)/S(t) = & r(t)\mathrm{d}t + \sqrt{v(t)}\mathrm{d}W_x(t), \;\; S(0) > 0, \\ \mathrm{d}v(t) = & \kappa(\bar{v} - v(t))\mathrm{d}t + \gamma\sqrt{v(t)}\mathrm{d}W_v(t), \;\; v(0) > 0, \\ \mathrm{d}r(t) = & \lambda(\theta(t) - r(t))\mathrm{d}t + \eta\mathrm{d}W_r(t), \;\; r(0) > 0, \\ \mathrm{d}\xi(t) = & \mu^{\xi}(t)\mathrm{d}t + \psi^{\xi}(t)\mathrm{d}W_v(t), \;\; \xi(0) = \sqrt{v(0)}, \end{cases} \tag{2.78}$$

where

$$\begin{cases} \mathrm{d}W_x(t)\mathrm{d}W_v(t) &= \rho_{x,v}\mathrm{d}t, \\ \mathrm{d}W_x(t)\mathrm{d}W_r(t) &= \rho_{x,r}\mathrm{d}t, \\ \mathrm{d}W_v(t)\mathrm{d}W_r(t) &= 0, \end{cases} \tag{2.79}$$

with $\sqrt{v(t)} \approx \xi(t)$ and $\mu^{\xi}(t)$, $\psi^{\xi}(t)$ as defined in (2.77).

By taking the log-transform, $x(t) = \log S(t)$, in the model above all the drift terms are linear, and the symmetric instantaneous covariance matrix, with $\xi(t) \approx \sqrt{v(t)}$, is given by:

$$\widetilde{\mathbf{\Sigma}} = \begin{bmatrix} v(t) & \gamma\rho_{x,v}v(t) & \rho_{x,r}\eta\xi(t) & \rho_{x,v}\psi^{\xi}(t)\xi(t) \\ * & \gamma^2 v(t) & 0 & \gamma\psi^{\xi}(t)\xi(t) \\ * & * & \eta^2 & 0 \\ * & * & * & \left(\psi^{\xi}(t)\right)^2 \end{bmatrix}, \tag{2.80}$$

which, since $\psi^{\xi}(t)$ is a deterministic time-dependent function, is now affine.

[5] The method by Antonov from [7, 8] is also not based on normal approximations.

Since the system of SDEs (2.78) is affine, we derive the corresponding ChF:

$$\begin{aligned}\phi_{\text{H2-HW}}(u,x(t),\tau) &= \exp\Big(A(u,\tau)+B(u,\tau)x(t)+C(u,\tau)r(t).\\ &\quad +D(u,\tau)v(t)+E(u,\tau)\xi(t)\Big), \end{aligned} \tag{2.81}$$

with terminal conditions $\phi_{\text{H2-HW}}(u,x(T),0)=\exp(iux(T))$ and $\xi(t)\approx\sqrt{v(t)}$.

The functions $A(u,\tau)$, $B(u,\tau)$, $C(u,\tau)$, $D(u,\tau)$ and $E(u,\tau)$ satisfy the complex-valued ODEs given by the following lemma.

Lemma 2.4.2 (The ODEs related to the H2-HW model)**.** *The functions $B(u,\tau)=:B(\tau)$, $C(u,\tau):=C(\tau)$, $D(u,\tau)=:D(\tau)$, $E(u,\tau)=:E(\tau)$ and $A(u,\tau)=:A(\tau)$ for $u\in\mathbb{C}$ and $\tau=T-t>0$ in (2.81), satisfy:*

$$\begin{aligned}
B'(\tau) &= 0,\\
C'(\tau) &= -1+B(\tau)-\lambda C(\tau),\\
D'(\tau) &= \left(B(\tau)-1\right)B(\tau)/2+\left(\gamma\rho_{x,v}B(\tau)-\kappa\right)D(\tau)+\gamma^2D^2(\tau)/2,\\
E'(\tau) &= \rho_{x,r}\eta B(\tau)C(\tau)+\psi^{\xi}(t)\rho_{x,v}B(\tau)E(\tau)+\gamma\psi^{\xi}(t)D(\tau)E(\tau),\\
A'(\tau) &= \kappa\bar{v}D(\tau)+\lambda\theta C(\tau)+\mu^{\xi}(t)E(\tau)+\eta^2C^2(\tau)/2+\left(\psi^{\xi}(t)\right)^2E^2(\tau)/2,
\end{aligned}$$

with final conditions: $B(u,0)=iu$, $C(u,0)=0$, $D(u,0)=0$, $E(u,0)=0$, $A(u,0)=0$, and functions $\mu^{\xi}(t)$, $\psi^{\xi}(t)$ as given in (2.77).

Proof. The proof is very similar to the proof of Lemma 2.3.5. ∎

Solutions to the ODEs for $B(u,\tau)$, $C(u,\tau)$ and $D(u,\tau)$ can be found in Lemma 2.3.6 where the deterministic linearization was applied.

Note that the remaining two functions, $E(u,\tau)$ and $A(u,\tau)$, contain the rather complicated functions $\mu^{\xi}(t)$ and $\psi^{\xi}(t)$. We leave these equations to be solved numerically by a basic ODE routine.

2.4.3 Numerical experiment

Here we check the performance of the deterministic (Section 2.3.2) and the stochastic (Section 2.4.2) approximations to the full-scale HHW model, in terms of differences in implied volatilities. The HHW benchmark prices were obtained by Monte Carlo simulation, performed as in [3].

In Table 2.1 we present the errors for the Black-Scholes implied volatilities, $\epsilon(\rho_{x,r})$, for different correlations between the stock, $S(t)$, and the short-rate, $r(t)$, and different strikes. We show results for a maturity of ten years, $\tau=10$, and for parameters that do not satisfy the Feller condition [6].

Both approximations give very similar, highly accurate, results for low values of the correlation, $\rho_{x,r}$. This is different for high values of $\rho_{x,r}$. The deterministic

[6]For short maturities, $\tau<10$, and for model parameters for which the Feller condition is satisfied, we did not find any significant differences between the two approximations and the full-scale model.

approach generates somewhat more bias for high strikes, whereas the stochastic approach is essentially bias-free. The errors presented in Table 2.1 depend on the size of the volatility parameter of the interest rate process, η. For very low volatility, the two approximations provide a similar level of accuracy. As the volatility of the short-rate process increases, a higher accuracy is expected for the stochastic approximation.

The performance of the methods developed is also presented in Section 2.6, where our schemes are compared to the Markovian projection method [8]. Calibration results will be presented in Section 2.7.

Table 2.1: *The implied volatilities and errors for the deterministic approximation (Approx 1) from (2.16) with approximation (2.18) and the stochastic approximation (Approx 2) from Section 2.4.1 of the HHW model compared to the Monte Carlo simulation performed with 20T steps and 100.000 paths. The error is defined as the difference between reference implied volatilities and the approximations. The parameters were chosen as* $T = 10$, $\kappa = 0.3$, $\gamma = 0.6$, $v(0) = \bar{v} = 0.05$, $\lambda = 0.01$, $r(0) = \theta = 0.02$, $\eta = 0.01$, $S(0) = 100$ *and the correlations* $\rho_{x,v} = -30\%$ *and* $\rho_{x,r} \in \{20\%, 60\%\}$. *Numbers in brackets indicate standard deviations.*

$\rho_{x,r}$	Strike	Monte Carlo imp.vol. [%]	Approx 1	Approx 2	err.1	err.2
	40 %	26.26 (0.22)	25.87	25.99	0.39 %	0.27 %
	80 %	20.07 (0.22)	20.03	20.02	0.04 %	0.05 %
20%	100 %	18.43 (0.24)	18.55	18.36	-0.12 %	0.07 %
	120 %	17.51 (0.20)	17.74	17.42	-0.23 %	0.09 %
	180 %	17.40 (0.22)	17.55	17.36	-0.15 %	0.04 %
	40 %	26.27 (0.14)	26.21	26.61	0.06 %	-0.34 %
	80 %	20.59 (0.11)	21.00	20.91	-0.41 %	-0.32 %
60%	100 %	19.11 (0.10)	19.84	19.22	-0.72 %	-0.10 %
	120 %	18.31 (0.10)	19.21	18.18	-0.90 %	0.13 %
	180 %	18.25 (0.11)	18.92	18.34	-0.67 %	-0.09 %

2.5 Comparison with Schöbel-Zhu model

Here, we look closer at the H1-HW model and compare it to the Schöbel-Zhu model with Gaussian interest rates (presented in Chapter 1). For both models the interest rate process $r(t)$ is identical, driven by a correlated, normally distributed, short-rate model, so that we only need to focus on the differences between the volatility processes.

The volatility in the Schöbel-Zhu model is driven by a normally distributed Ornstein-Uhlenbeck-type process $\sigma(t)$, whereas in the Heston model the volatility is driven by $\sqrt{v(t)}$ with $v(t)$ distributed as $c(t)$ times a non-central chi-square random variable, $\chi^2(d, \lambda(t))$, as discussed in Subsection 2.4.1.

We determine under which conditions the two volatility processes, for the Schöbel-Zhu, $\sigma(t)$, and for the Heston model, $\sqrt{v(t)}$, coincide. In other words: we determine under which conditions $\sqrt{v(t)}$ is approximately a normal distribution (as $\sigma(t)$ in the Schöbel-Zhu model is normally distributed).

In Result 2.4.1 we have found that for any time, $t < \infty$ the square root of the variance process $v(t)$ in (2.8) can be approximated by:

$$\sqrt{v(t)} \approx \mathcal{N}\left(\Lambda(t), c(t) - \frac{c(t)d}{2(d+\lambda(t))}\right), \tag{2.82}$$

with $c(t)$, d and $\lambda(t)$ from (2.20) and $\Lambda(t)$ from (2.30).

As already indicated in the remark in Section 2.4.1 the normal approximation (2.82) is a satisfactory approximation for either a large number of degrees of freedom, d, or a large non-centrality parameter $\lambda(t)$. A large number of degrees of freedom, $d \gg 0$, implies that $4\kappa\bar{v} \gg \gamma^2$, which is closely related to the Feller condition, $2\kappa\bar{v} > \gamma^2$. The Heston model thus has a similar volatility structure as the Schöbel-Zhu model when the Feller condition is satisfied.

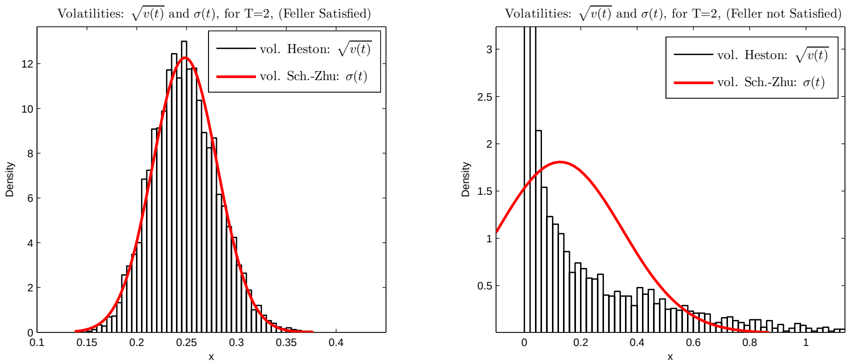

Figure 2.3: *Histogram for* $\sqrt{v(t)}$ *(the Heston model) and density for* $\sigma(t)$ *(the Schöbel-Zhu model); Maturity* $T = 2$. *LEFT: Feller condition satisfied* $\kappa = 1.2$, $v(0) = \bar{v} = 0.0625$, $\gamma = 0.1$*; RIGHT: The Feller condition violated* $\kappa = 0.25$, $v(0) = \bar{v} = 0.0625$, $\gamma = 0.625$ *as in [7].*

Figure 2.3 confirms this observation. The volatilities for the Heston and Schöbel-Zhu models differ significantly when the Feller condition does not hold as the volatility in the Heston model gives rise to much heavier tails than those in the Schöbel-Zhu model. This may have an effect when calibrating the models to the market data with significant implied volatility smile or skew.

Here we examine both models and check their performance when calibration to real market data. The Schöbel-Zhu-Hull-White and the H1-HW models (i.e. affine Heston with Hull-White short-rate process) are calibrated to implied volatilities from the S&P500 (27/09/2010) with spot price at 1145.88. For both models the correlation between the stock and interest rates, $\rho_{x,r}$, is set to $+30\%$.

The calibration results, presented in Table 2.2, confirm that the H1-HW model is more *flexible* than the Schöbel-Zhu-Hull-White model. The difference is pronounced for large strikes at which the error for the affine Heston hybrid model is up to 20 times lower than for the Schöbel-Zhu-Hull-White hybrid model.

When comparing the new, H1-HW hybrid model, to the extended Schöbel-Zhu model, we find that both models require an additional integration in the

Table 2.2: *Calibration results for the Schöbel-Zhu hybrid model (SZHW) and the H1-HW hybrid.*

T	Strike	Market	SZHW	H1-HW	err.(SZHW)	err.(H1-HW)
T=6m	40%	57.61	54.02	57.05	3.59 %	-0.56 %
	80%	31.38	34.33	33.22	-2.95 %	1.84 %
	100%	22.95	25.21	21.57	-2.26 %	-1.38 %
	120%	15.9	18.80	16.38	-2.90 %	0.48 %
	180%	24.54	22.60	24.40	1.94 %	-0.14 %
T=1y	40%	48.53	47.01	48.21	1.52 %	0.32 %
	80%	30.37	31.69	31.07	-1.32 %	-0.70 %
	100%	24.49	24.97	24.28	-0.48 %	0.21 %
	120%	19.23	19.09	19.14	0.14 %	0.09 %
	180%	18.42	18.28	18.40	0.14 %	0.02 %
T=5y	40%	41.30	40.00	41.20	1.30 %	0.10 %
	80%	31.12	31.88	31.38	-0.76 %	-0.26 %
	100%	27.83	28.75	27.86	-0.92 %	-0.03 %
	120%	25.13	25.93	24.91	-0.80 %	0.22 %
	180%	19.28	18.57	19.32	0.71 %	-0.04 %
T=10y	40%	36.76	36.15	36.75	0.61 %	0.01 %
	80%	31.04	31.25	31.08	-0.21 %	-0.04 %
	100%	29.18	29.47	29.18	-0.29 %	0.00 %
	120%	27.66	27.93	27.62	-0.27 %	0.04 %
	180%	24.34	24.15	24.35	0.19 %	-0.01 %

ChF calculation. The integration in the H1-HW model is independent of the complex plane arguments, which means that this additional integration, in the case of the H1-HW model, needs to be performed only once, while in the case of the SZHW model the number of additional integrals depends on the number of Fourier space arguments.

2.6 Comparison to Markov Projection method

In this section we compare our results to the Markovian projection (MP) method [8]. We check the results of three different approximation schemes: The MP method, Approx 1, i.e. the approximation with $\sqrt{v(t)} \approx \mathbb{E}(\sqrt{v(t)})$ (Section 2.3.1), and Approx 2, i.e. the method with $\sqrt{v(t)} \approx \mathcal{N}(\cdot)$ (Section 2.4.1).

In the experiment, taken directly from [7], we price an equity option with continuous dividend. The model parameters for the HHW model are given by $\kappa = 0.25$, $\bar{v} = v(0) = 0.0625$, $\gamma = 0.625$, $\lambda = 0.05$, $\eta = 0.01$, a zero-coupon bond is given by $P(0,T) = \mathrm{e}^{-0.05T}$, and a continuous dividend of 2%. The full matrix of correlations, as in [7], is given by:

$$C = \begin{bmatrix} 1 & \rho_{x,v} & \rho_{x,r} \\ \rho_{x,v} & 1 & \rho_{v,r} \\ \rho_{x,r} & \rho_{v,r} & 1 \end{bmatrix} = \begin{bmatrix} 100\% & -40\% & 30\% \\ -40\% & 100\% & 15\% \\ 30\% & 15\% & 100\% \end{bmatrix}. \tag{2.83}$$

The Monte Carlo reference for the implied volatilities, the corresponding standard deviations, and the results for the MP method are all taken from [7].

In order to incorporate a continuous dividend in the equity model one can model foreign exchange (FX), in which the volatility of the foreign interest rates is set to zero. In such a setup, the forward, $F(t)$, is defined as:

$$F(t) = S(t)\frac{P_f(t,T)}{P_d(t,T)}, \quad \text{and} \quad F(0) = S(0)\frac{\mathrm{e}^{-0.02T}}{\mathrm{e}^{-0.05T}},$$

where $P_f(t,T)$ and $P_d(t,T)$ are the foreign and domestic zero-coupon bonds, respectively, paying €1 at the maturity T. By switching from the spot risk-neutral measure, $\mathbb{Q}$, to the $T-$forward measure, $\mathbb{Q}^T$, discounting will be decoupled from taking the expectation, i.e.:

$$\mathbb{E}^{\mathbb{Q}}\left(\frac{1}{B(T)}\max(S(T)-K,0)|\mathcal{F}(0)\right) = P_d(0,T)\mathbb{E}^T\left(\max(F(T)-K,0)|\mathcal{F}(0)\right).$$

Moreover, the forward, $F(t)$, is a martingale with dynamics given by:

$$\begin{aligned} \mathrm{d}F(t)/F(t) &= \sqrt{v(t)}\mathrm{d}W_x^T(t) - \eta B_r(t,T)\mathrm{d}W_r^T(t), \\ \mathrm{d}v(t) &= \left(\kappa(\bar{v}-v(t)) + \gamma\rho_{v,r}\eta B_r(t,T)\sqrt{v(t)}\right)\mathrm{d}t + \gamma\sqrt{v(t)}\mathrm{d}W_v^T(t), \end{aligned} \tag{2.84}$$

where $B_r(t,T) = \frac{1}{\lambda}\left(\mathrm{e}^{-\lambda(T-t)}-1\right)$, and the full correlation structure given in (2.83).

Under the log-transform, $x(t) = \log F(t)$, the Kolmogorov backward partial differential equation reads:

$$\begin{aligned} -\frac{\partial\phi}{\partial t} &= \kappa(\bar{v}-v)\frac{\partial\phi}{\partial v} + \left(\frac{1}{2}v - \rho_{x,r}\eta B_r(t,T)\sqrt{v} - \frac{1}{2}\eta^2 B_r^2(t,T)\right)\left(\frac{\partial^2\phi}{\partial x^2} - \frac{\partial\phi}{\partial x}\right) \\ &+ \left(\rho_{x,v}\gamma v - \rho_{v,r}\gamma\eta\sqrt{v}B_r(t,T)\right)\frac{\partial^2\phi}{\partial x\partial v} + \frac{1}{2}\gamma^2 v\frac{\partial^2\phi}{\partial v^2} + \rho_{v,r}\gamma\eta\sqrt{v}\frac{\partial\phi}{\partial v}, \end{aligned} \tag{2.85}$$

with the final condition $\phi(u, x(T), T, T) = \mathrm{e}^{iux(T)}$.

We linearize PDE (2.85) in two ways: By the deterministic approach described in Section 2.3.1 and Section 2.3.3, and by the stochastic approach as in Section 2.4.1. Both approximations result in affine approximations of PDE (2.85) [7].

The results of the experiments performed, presented in Table 2.3, show a highly satisfactory accuracy of the HHW approximations introduced in this chapter. When comparing to the MP method, we see that the MP method is more accurate for low strike values, whereas our proxies perform favorably for larger strike values, especially when large maturities are considered.

In Figure 2.4 the error results for $T = 10$ are presented. In this experiment, the stochastic approximation, Approx 2, performed somewhat better than the deterministic approach, Approx 1.

In the case of the deterministic approach, pricing of European options is done in a split-second (the corresponding ChF is analytic when the Feller condition is

[7] Since the moments of the square-root process under the $T-$forward measure are difficult to find, we first project $\sqrt{v(t)}$ on a normal process, under measure $\mathbb{Q}$, and then change measures.

Table 2.3: *The error for the deterministic (Approx 1) and stochastic approximation (Approx 2) of the HHW model compared to the MP method. The Markovian projection and Monte Carlo results with the corresponding standard deviations were taken from [3]. The error is defined as the difference between the reference implied volatilities and the approximation.*

T	Strike	imp.vol.	MP	Approx 1	Approx 2	err.MP	err.1	err.2
	86.07	24.45	24.49	24.48	24.48	-0.04 %	-0.03 %	-0.03 %
	92.77	22.25	22.27	22.27	22.25	-0.02 %	-0.02 %	0.00 %
1y	100.00	20.36	20.32	20.35	20.30	0.04 %	0.01 %	0.06 %
	107.79	19.42	19.34	19.38	19.34	0.08 %	0.04 %	0.08 %
	116.18	19.67	19.64	19.62	19.64	0.03 %	0.05 %	0.03 %
	77.12	22.61	22.65	22.61	22.63	-0.04 %	0.00 %	-0.02 %
	87.82	20.05	20.05	20.09	20.06	0.00 %	-0.04 %	-0.01 %
3y	100.00	17.95	17.91	18.09	17.90	0.04 %	-0.14 %	0.05 %
	113.87	17.23	17.14	17.32	17.15	0.09 %	-0.09 %	0.08 %
	129.67	18.02	17.92	17.93	18.00	0.10 %	0.09 %	0.02 %
	71.50	21.89	21.94	21.90	21.95	-0.05 %	-0.01 %	-0.06 %
	84.56	19.43	19.45	19.52	19.48	-0.02 %	-0.09 %	-0.05 %
5y	100.00	17.49	17.44	17.71	17.45	0.05 %	-0.22 %	0.04 %
	118.26	16.83	16.72	17.01	16.76	0.11 %	-0.18 %	0.07 %
	139.85	17.55	17.42	17.49	17.57	0.13 %	0.06 %	-0.02 %
	62.23	21.55	21.61	21.57	21.68	-0.06 %	-0.02 %	-0.13 %
	78.89	19.52	19.51	19.67	19.61	0.01 %	-0.15 %	-0.09 %
10y	100.00	18.01	17.91	18.31	17.97	0.10 %	-0.30 %	-0.04 %
	126.77	17.41	17.22	17.67	17.30	0.19 %	-0.26 %	0.11 %
	160.70	17.75	17.51	17.79	17.78	0.24 %	-0.04 %	-0.03 %
	51.13	22.28	22.32	22.37	22.47	-0.04 %	-0.09 %	-0.19 %
	71.50	20.91	20.86	21.14	21.03	0.05 %	-0.23 %	-0.12 %
20y	100.00	19.94	19.77	20.27	19.91	0.17 %	-0.33 %	0.03 %
	139.85	19.44	19.16	19.77	19.32	0.28 %	-0.33 %	0.12 %
	195.58	19.40	19.05	19.63	19.39	0.35 %	-0.23 %	0.01 %

satisfied; one integration step is required otherwise). In the case of the stochastic approach a numerical routine for solving the ODEs is employed. This however can also be done highly efficiently, as it is presented in Appendix in Table 2.7.

2.7 Calibration of the Heston hybrid models

Here, we evaluate the performance of the approximations H1-HW and H2-HW for the HHW hybrid model in a calibration setting.

Reference call option prices, based on synthetic data representative for the skew and smile patterns observed in real-life applications are used. For all models the simulation was performed with an a-priori defined speed of mean reversion for the variance process, $\kappa = 0.3$ (which is set small on purpose). The calibration is here performed with constant correlation, $\rho_{x,r} = 20\%$. In practice, this correlation can be obtained from historical data, as the correlations between different asset classes cannot be easily implied from the market [17].

The calibration procedure is performed in two stages. First, the parameters for the short-rate process are determined (independent of the equity part). In

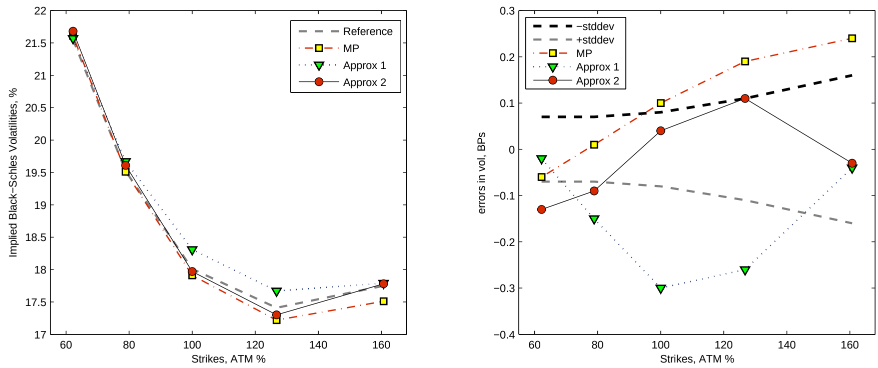

Figure 2.4: *LEFT: Implied volatilities for a maturity of 10 years. RIGHT: The error for the different approximations. (MP stands for Markovian Projection, Approx 1 is the deterministic approach, and Approx 2 corresponds to the approximation with* $\sqrt{v(t)} \approx \mathcal{N}(\cdot)$*.)*

the second stage, the calibrated $r(t)$ is included in the Heston model, and the remaining parameters are determined. The parameters for the interest rate part are found to be $\lambda_{\text{HW}} = 0.501$, $\eta_{\text{HW}} = 0.005$ and $r(0) = 0.04$.

We also perform, as a benchmark, the calibration of the pure Heston model with constant interest rate, see Table 2.4. SSE stands for the "sum-squared error". We calibrate the models for different maturities, τ.

Table 2.4: *Calibration results for the Heston stochastic volatility model with deterministic interest rate. The mean reversion parameter is* $\kappa = 0.3$.

model	γ	$\bar{v}$	$\rho_{x,v}$	$v(0)$	r	**SSE**
Heston ($\tau = 0.5$)	0.5992	0.0823	-58.32%	0.0407	0.04	4.9063E-4
Heston ($\tau = 10$)	0.6019	0.0828	-48.49%	0.0411	0.04	1.2182E-4

In Table 2.5 the calibration results for the HHW approximations, H1-HW and H2-HW, are presented. For both models a highly satisfactory fit is obtained, with a slightly better performance of the stochastic approximation H2-HW. For $\rho_{x,r} = 20\%$ the calibration procedure gives roughly the same sets of parameters for both models. When comparing the calibration results for HHW with those for the pure Heston model, we see that the inclusion of stochastic interest rates in the model results in a lower vol-vol parameter, γ, and a more negative correlation, $\rho_{x,v}$. The lower value of parameter γ can be explained by the additional volatility which comes from the interest rate process.

In Figure 2.5 the corresponding implied volatilities, for the full-scale model, for a short and long maturity time ($\tau = 0.5y$ and $\tau = 10y$) are presented. The left-hand sides of the figure present the implied volatilities and their errors for H1-HW and H2-HW. The related implied volatilities of the full-scale HHW model,

Table 2.5: *Calibration results for the H1-HW model from Section 2.3.2, and the H2-HW model from Section 2.4.2, with $\kappa = 0.3$, and correlation $\rho_{x,r} = 20\%$.*

model	τ	γ	$\bar{v}$	$\rho_{x,v}$	$v(0)$	**SSE**
H1-HW	$\tau = 0.5$	0.5840	0.0822	-60.06%	0.0407	4.4581E-4
	$\tau = 10$	0.4921	0.0826	-61.50%	0.0418	3.2912E-4
H2-HW	$\tau = 0.5$	0.5879	0.0930	-60.10%	0.0398	4.9677E-4
	$\tau = 10$	0.4884	0.0820	-60.72%	0.0421	8.5934E-5

with the parameters from H1-HW and H2-HW, are shown in the right-hand side of the figure.

Both hybrid models perform very well. For long maturities a higher accuracy for the hybrid models compared to the plain Heston model can be observed.

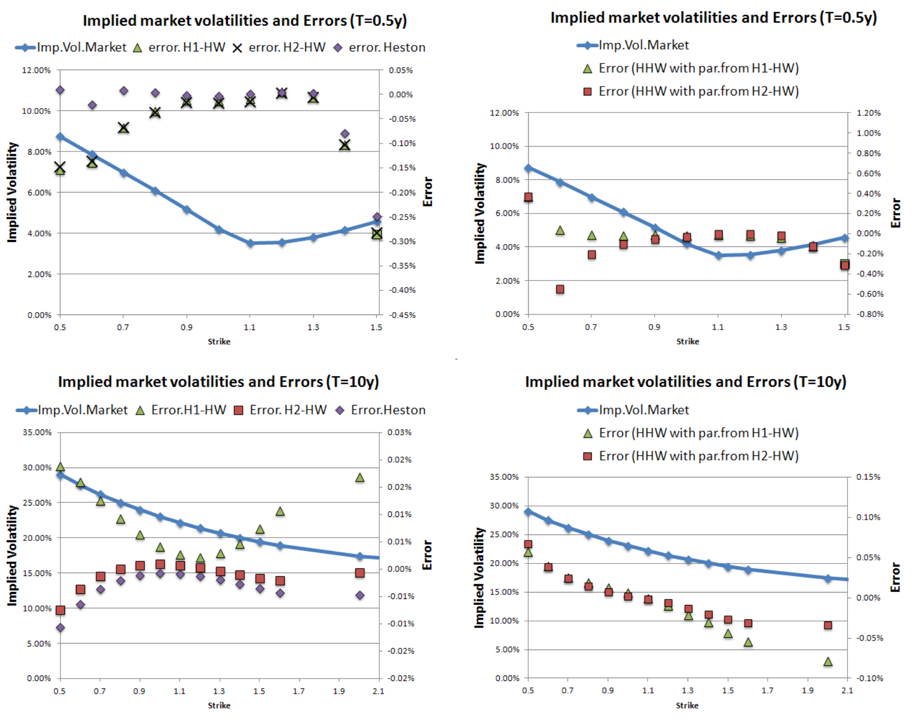

Figure 2.5: *For $\tau = 0.5$ and $\tau = 10$, $\rho_{x,r} = 20\%$, the implied Black-Scholes volatilities for Heston hybrid models are compared to the pure Heston model and a reference implied volatility curve. The left-hand graphs present the implied volatilities and errors for H1-HW and H2-HW. The implied volatilities for the full-scale HHW model, with the parameters from H1-HW and H2-HW are in the right-hand figures.*

2.8 Conclusion

The main goal of this chapter was to present approximations of the extended Heston stochastic volatility equity model with stochastic interest rates. We have focused our attention on the Heston-Hull-White model.

By approximations of the non-affine terms in the corresponding instantaneous covariance matrix, we placed the approximate hybrid model in the framework of affine diffusion processes. The approximations in the models have been validated by comparing the implied volatilities to the full-scale hybrid models.

The deterministic and the stochastic approaches for approximating the instantaneous covariance matrix of the hybrid model provide satisfactory approximations for prices for European options.

2.A Appendix: Heston-Cox-Ingersoll-Ross hybrid model

We also present the ChF for a Heston-Cox-Ingersoll-Ross hybrid model, $p = 1/2$ in (2.3), which is more involved than the Hull-White based hybrid models. In the Heston-CIR model the non-affine term is given in (2.15). Again we use two approximations to obtain the ChF. In the first model, H1-CIR, we use the deterministic setup and for the second model, H2-CIR, we determine the stochastic approximation.

Characteristic function for the H1-CIR model

The dynamics for the stock, $S(t)$, in the Heston-CIR model read:

$$\begin{cases} \mathrm{d}S(t)/S(t) = & r(t)\mathrm{d}t + & \sqrt{v(t)}\mathrm{d}W_x(t), & S(0) > 0 \\ \mathrm{d}v(t) = & \kappa(\bar{v} - v(t))\mathrm{d}t + & \gamma\sqrt{v(t)}\mathrm{d}W_v(t), & v(0) > 0, \\ \mathrm{d}r(t) = & \lambda(\theta(t) - r(t))\mathrm{d}t + & \eta\sqrt{r(t)}\mathrm{d}W_r(t), & r(0) > 0, \end{cases} \tag{A-1}$$

with $\mathrm{d}W_x(t)\mathrm{d}W_v(t) = \rho_{x,v}\mathrm{d}t$, $\mathrm{d}W_x(t)\mathrm{d}W_r(t) = \rho_{x,r}\mathrm{d}t$ and $\mathrm{d}W_v(t)\mathrm{d}W_r(t) = 0$.

Here, we assume that the non-affine term in the pricing PDE (2.16), $\mathbf{\Sigma}_{(1,3)}$, in (2.15) can be approximated, as:

$$\mathbf{\Sigma}_{(1,3)} \approx \eta\rho_{x,r}\mathbb{E}\left(\sqrt{r(t)}\sqrt{v(t)}\right) \stackrel{\perp\!\!\!\perp}{=} \eta\rho_{x,r}\mathbb{E}(\sqrt{r(t)})\mathbb{E}(\sqrt{v(t)}). \tag{A-2}$$

Since the processes involved are of the same type, the expectations in (A-2) can be determined as presented in Section 2.3.1. For the log-stock, $x(t) = \log S(t)$, the ChF and the corresponding Riccati ODEs are defined as below:

$$\phi_{\text{H1-CIR}}(u, x(t), \tau) = \exp\left(A(u,\tau) + B(u,\tau)x(t) + C(u,\tau)r(t) + D(u,\tau)v(t)\right), \tag{A-3}$$

Lemma 2.A.1 (The ODEs related to the H1-CIR model)**.** *The functions* $B(u,\tau) =: B(\tau)$*,* $C(u,\tau) =: C(\tau)$*,* $D(u,\tau) =: D(\tau)$ *and* $A(u,\tau) =: A(\tau)$ *for*

$u \in \mathbb{C}$ and $\tau > 0$ in (A-3) satisfy:

$$\begin{aligned}
B'(\tau) &= 0, \quad B(u,0) = iu, \\
C'(\tau) &= -1 + B(\tau) - \lambda C(\tau) + \eta^2 C^2(\tau)/2, \quad C(u,0) = 0, \\
D'(\tau) &= (B(\tau) - 1)\, B(\tau)/2 + (\gamma \rho_{x,v} B(\tau) - \kappa)\, D(\tau) + \gamma^2 D^2(\tau)/2, \quad D(u,0) = 0, \\
A'(\tau) &= \kappa \bar{v} D(\tau) + \lambda \theta C(\tau) + \eta \rho_{x,r} \mathbb{E}(\sqrt{v(t)}) \mathbb{E}(\sqrt{r(t)}) B(\tau) C(\tau), \quad A(u,0) = 0.
\end{aligned}$$

with $\tau = T - t$, $\mathbb{E}(\sqrt{v(t)})$ and $\mathbb{E}(\sqrt{r(t)})$ from Lemma 2.3.1.

Proof. The proof is very similar to the proof in Lemma 2.3.5. ∎

Lemma 2.A.2 (Solutions for the ChF coefficients of the H1-CIR model)**.** *The solutions for the ODEs for $B(u,\tau)$, $C(u,\tau)$, $D(u,\tau)$ and $A(u,\tau)$, defined in Lemma 2.A.1, are given by:*

$$B(u,\tau) = iu, \tag{A-4}$$

$$C(u,\tau) = \frac{1 - \mathrm{e}^{-D_1 \tau}}{\eta^2 \left(1 - G_1 \mathrm{e}^{-D_1 \tau}\right)} \left(\lambda - D_1\right), \tag{A-5}$$

$$D(u,\tau) = \frac{1 - \mathrm{e}^{-D_2 \tau}}{\gamma^2 \left(1 - G_2 \mathrm{e}^{-D_2 \tau}\right)} \left(\kappa - \gamma \rho_{x,v} iu - D_2\right), \tag{A-6}$$

and

$$\begin{aligned}
A(u,\tau) = \int_0^\tau \Big(& \kappa \bar{v} D(u,s) + \lambda \theta C(u,s) \\
& + \rho_{x,r} \eta iu \mathbb{E}(\sqrt{v(T-s)}) \mathbb{E}(\sqrt{r(T-s)}) C(u,s) \Big)\, \mathrm{d}s,
\end{aligned} \tag{A-7}$$

with $D_1 = \sqrt{\lambda^2 + 2\eta^2(1 - iu)}$, $D_2 = \sqrt{(\gamma \rho_{x,v} iu - \kappa)^2 - (iu - 1) iu \gamma^2}$, $G_1 = \dfrac{\lambda - D_1}{\lambda + D_1}$ and $G_2 = \dfrac{\kappa - \gamma \rho_{x,v} iu - D_2}{\kappa - \gamma \rho_{x,v} iu + D_2}$.

Proof. The proof is very similar to the proof in Lemma 2.3.6. ∎

The integral for $A(u,\tau)$ in Lemma 2.A.2 can be determined analytically only for constant approximations of the two expectations involved.

Characteristic function for the H2-CIR model

As before, we aim to find an approximation of the instantaneous covariance matrix for which the affinity of the approximation model is obtained, but now with the stochastic approximation.

$\mathbf{\Sigma}_{(1,3)}$ now consists of two stochastic components, $\sqrt{v(t)}$ and $\sqrt{r(t)}$. We approximate both and obtain:

$$\mathbf{\Sigma}_{(1,3)} \approx \widetilde{\mathbf{\Sigma}}_{(1,3)} = \rho_{x,r} \eta \xi(t) R(t), \quad R(t) \approx \sqrt{r(t)}, \quad \xi(t) \approx \sqrt{v(t)}. \tag{A-8}$$

This form, based on the product of two random variables, is not affine. To linearize (A-8) we need to specify the joint dynamics, $\mathrm{d}(\sqrt{v(t)}\sqrt{r(t)})$. If we assume that the dynamics for $\mathrm{d}(\sqrt{v(t)})$ and $\mathrm{d}(\sqrt{r(t)})$ can be approximated by normally distributed processes, we find, by Itô's lemma, that the dynamics of $z(t) = \xi(t)R(t)$ are given by:

$$\mathrm{d}z(t) = \left(\mu^R(t)\xi(t) + \mu^\xi(t)R(t)\right)\mathrm{d}t + \psi^\xi(t)R(t)\mathrm{d}W_v(t) + \psi^R(t)\xi(t)\mathrm{d}W_r(t). \quad \text{(A-9)}$$

With three additional variables, $\xi(t)$, $R(t)$ and $z(t)$, the state vector $\mathbf{X}(t)$, with log-stock process $x(t) = \log S(t)$ is expanded to $\mathbf{X}(t) = [x(t), v(t), r(t), \xi(t), R(t), z(t)]^{\mathrm{T}}$, with the following corresponding system of SDEs:

$$\begin{cases} \mathrm{d}x(t) = & (r(t) - 1/2v(t))\,\mathrm{d}t + & \sqrt{v(t)}\mathrm{d}W_x(t), & x(0) = \log(S(0)), \\ \mathrm{d}v(t) = & \kappa(\bar{v} - v(t))\mathrm{d}t + & \gamma\sqrt{v(t)}\mathrm{d}W_v(t), & v(0) > 0, \\ \mathrm{d}r(t) = & \lambda(\theta(t) - r(t))\mathrm{d}t + & \eta\sqrt{r(t)}\mathrm{d}W_r(t), & r(0) > 0, \end{cases} \quad \text{(A-10)}$$

with the linearizing variables $\xi(t)$, $R(t)$ and $z(t)$ given by:

$$\begin{aligned} \mathrm{d}\xi(t) = &\ \mu^\xi(t)\mathrm{d}t + \psi^\xi(t)\mathrm{d}W_v(t), \quad \xi(0) = \sqrt{v(0)}, \\ \mathrm{d}R(t) = &\ \mu^R(t)\mathrm{d}t + \psi^R(t)\mathrm{d}W_r(t), \quad R(0) = \sqrt{r(0)}, \end{aligned} \quad \text{(A-11)}$$

and

$$\mathrm{d}z(t) = \left(\mu^R(t)\xi(t) + \mu^\xi(t)R(t)\right)\mathrm{d}t + \psi^\xi(t)\sqrt{r(t)}\mathrm{d}W_v(t) + \psi^R(t)\sqrt{v(t)}\mathrm{d}W_r(t), \quad \text{(A-12)}$$

with $z(0) = \sqrt{r(0)}\sqrt{v(0)}$, $\xi(t) \approx \sqrt{v(t)}$, $R(t) \approx \sqrt{r(t)}$, $z(t) \approx \sqrt{v(t)}\sqrt{r(t)}$ and the other parameters as in (2.3). Since $\psi^\xi(t)$ and $\psi^R(t)$ are deterministic time-dependent functions, the approximate H2-CIR model is now affine and we can derive the corresponding ChF:

$$\begin{aligned} \phi_{\text{H2-CIR}}(u, x(t), \tau) = \exp\Big(&A(u,\tau) + B(u,\tau)x(t) + C(u,\tau)r(t) + D(u,\tau)v(t) \\ &+ E(u,\tau)\xi(t) + F(u,\tau)R(t) + G(u,\tau)z(t)\Big), \end{aligned} \quad \text{(A-13)}$$

with $\xi(t) = \sqrt{v(t)}$, $R(t) = \sqrt{r(t)}$, $z(t) = \sqrt{v(t)}\sqrt{r(t)}$, and where the functions $A(u,\tau)$, $B(u,\tau)$, $C(u,\tau)$, $D(u,\tau)$, $E(u,\tau)$, $F(u,\tau)$ and $G(u,\tau)$ satisfy the ODEs given by the following lemma.

Lemma 2.A.3 (The ODEs related to the H2-CIR model)**.** *The functions $B(u,\tau) =: B(\tau)$, $C(u,\tau) =: C(\tau)$, $D(u,\tau) =: D(\tau)$, $E(u,\tau) =: E(\tau)$, $F(u,\tau) =: F(\tau)$, $G(u,\tau) =: G(\tau)$ and $A(u,\tau) =: A(\tau)$ for $u \in \mathbb{C}$ and $\tau > 0$ in (A-13),* *satisfy:*

$$\begin{aligned}
B'(\tau) &= 0, \\
C'(\tau) &= -1 + B(\tau) - \lambda C(\tau) + \eta^2 C^2(\tau)/2 + (\psi^\xi(t))^2 G^2(\tau)/2, \\
F'(\tau) &= \mu^\xi(t) G(\tau) + \psi^R(t)\eta C(\tau) G(\tau) + (\psi^\xi(t))^2 E(\tau) G(\tau), \\
G'(\tau) &= \eta\rho_{x,r} B(\tau) C(\tau) + \rho_{x,v}\psi^\xi(t) B(\tau) G(\tau) + \gamma\psi^\xi(t) D(\tau) G(\tau) \\
&\quad + \eta\psi^R(t) C(\tau) G(\tau), \\
A'(\tau) &= \kappa\bar{v} D(\tau) + \lambda\theta C(\tau) + \mu^\xi(t) E(\tau) + \mu^R(t) F(\tau) + (\psi^\xi(t))^2 E^2(\tau)/2 \\
&\quad + (\psi^R(\tau))^2 F^2(\tau)/2,
\end{aligned}$$

and

$$\begin{aligned}
D'(\tau) &= B(\tau)\left(B(\tau) - 1\right)/2 - \kappa D(\tau) + \gamma\rho_{x,v} B(\tau) D(\tau) + \gamma^2 D^2(\tau)/2 \\
&\quad + \rho_{x,r}\psi^R(t) B(\tau) G(\tau) + (\psi^R(t))^2 G^2(t)/2, \\
E'(\tau) &= \mu^R(t) G(\tau) + \psi^\xi(t)\rho_{x,v} B(\tau) E(\tau) + \gamma\psi^\xi(t) D(\tau) E(\tau) \\
&\quad + \rho_{x,r}\psi^R(t) B(\tau) F(\tau) + (\psi^R(t))^2 F(\tau) G(\tau),
\end{aligned}$$

with the final conditions: $B(u,0) = iu$, $C(u,0) = 0$, $D(u,0) = 0$, $E(u,0) = 0$, $F(u,0) = 0$, $G(u,0) = 0$ *and* $A(u,0) = 0$. *Parameters* $\mu^\xi(t)$, $\mu^R(t)$, $\psi^\xi(t)$, $\psi^R(t)$ *are specified in (2.77), and the remaining parameters are in (A-10).*

It is difficult to solve the system of the ODEs given in Lemma 2.A.3 analytically. To find the solution we have used an explicit Runge-Kutta method [36, 66], *ode45* from the MATLAB package. Numerical results are presented in the next subsection.

The extension of the H2-CIR model to the case of a full matrix of correlations is a trivial exercise.

Numerical experiment

We compare the performance of the approximations H1-CIR and H2-CIR with the full-scale HCIR model. As in the case of the HHW models, we have set here $T = 10$, and the model parameters are chosen so that the Feller condition does not hold. The results, presented in Table 2.6, are very satisfactory. Both approximation models, H1-CIR and H2-CIR, provide an error, $\epsilon(\rho_{x,r})$, for a call option within the confidence bounds. For higher correlation $\rho_{x,r}$ the error grows, but it is still small.

We also present the time needed for obtaining the vanilla option prices, with the characteristic functions H2-HW (Section 2.4.2) and H2-CIR (Section 2.A) based on the numerical solution of the system of Riccati ODEs. Table 2.7 shows that, although the ODEs in Lemma 2.A.3 need to be solved numerically, the time for obtaining European option prices by the COS pricing method [32] is often less than 0.1 seconds. The pricing of the options by means of the COS method, a method based on Fourier cosine series expansions, was performed with a fixed number of 250 terms, which guaranteed highly accurate option prices (up to machine precision).

Table 2.6: *The implied volatilities and errors for the deterministic approximation (Approx 1) from (2.16) with approximation (2.18) and the stochastic approximation (Approx 2) from Section 2.4.1 of the HCIR model compared to the Monte Carlo simulation performed with 20T steps and 100.000 paths. The error is defined as the difference between the reference implied volatilities and the approximation. The parameters were chosen as follows:* $\kappa = 0.3$, $\gamma = 0.6$, $v(0) = \bar{v} = 0.05$, $\lambda = 0.01$, $r(0) = \theta = 0.02$, $\eta = 0.01$, $S(0) = 100$ *and the correlations* $\rho_{x,v} = -30\%$ *and* $\rho_{x,r} \in \{20\%, 60\%\}$. *Numbers in brackets indicate standard deviations.*

$\rho_{x,r}$	Strike	Monte Carlo imp.vol. [%]	Approx 1	Approx 2	err.1	err.2
	40 %	25.66 (0.17)	25.68	25.74	-0.02 %	-0.08 %
	80 %	19.17 (0.15)	19.21	19.25	-0.04 %	-0.08 %
20%	100 %	17.10 (0.18)	17.19	17.09	-0.09 %	-0.01 %
	120 %	15.77 (0.17)	15.90	15.85	-0.14 %	-0.08 %
	180 %	15.84 (0.18)	15.90	15.86	-0.06 %	-0.02 %
	40 %	24.95 (0.14)	25.72	25.79	-0.77 %	-0.84 %
	80 %	18.93 (0.12)	19.32	19.32	-0.39 %	-0.39 %
60%	100 %	16.92 (0.13)	17.37	17.08	-0.44 %	-0.15 %
	120 %	15.60 (0.13)	16.17	15.93	-0.57 %	-0.32 %
	180 %	15.57 (0.14)	16.10	15.98	-0.53 %	-0.41 %

The tolerance for the ODE solves, by *ode45* from MATLAB, is varied in the experiments shown in the table.

Table 2.7: *Time in seconds for pricing a call option based on an explicit Runge-Kutta method combined with the COS method.*

Model	Accuracy	Maturity				
		$\tau = 0.5$	$\tau = 1$	$\tau = 2$	$\tau = 5$	$\tau = 10$
H2-HW	10^{-2}	4.37e-2	4.80e-2	6.41e-2	7.49e-2	8.10e-2
	10^{-5}	5.32e-2	5.82e-2	8.05e-2	9.74e-2	1.21e-1
H2-CIR	10^{-2}	7.78e-2	7.80e-2	8.38e-2	8.48e-2	8.90e-2
	10^{-5}	8.33e-2	8.97e-2	1.05e-1	1.34e-1	1.62e-1

2.B Appendix: The error analysis in the context of the SZHW hybrid model

When linearizing the full-scale Heston-Hull-White model, as it was presented in Section 2.3, some error is generated. As an exact solution for the HHW model is not available it is difficult to assess this error analytically.

In this section we therefore analyze the projections employed in the Heston hybrid model in the *context of the SZHW model* which, as shown in Section 2.5, under certain conditions is *closely related* [8] to the Heston hybrid model. Moreover, error analysis under the SZHW model is easier since, for the full-scale model, the ChF is available.

[8] in terms of generated implied volatilities

The pricing PDE for the SZHW hybrid model is given (see Lemma 1.3.1) by:

$$\begin{aligned}
0 &= \frac{\partial\phi}{\partial t}+\left(\widetilde{r}-\frac{1}{2}v\right)\frac{\partial\phi}{\partial\widetilde{x}}-\lambda\widetilde{r}\frac{\partial\phi}{\partial\widetilde{r}}+\left(\gamma^2-2\kappa v+2\bar{\sigma}\kappa\sigma\right)\frac{\partial\phi}{\partial v}+\kappa\left(\bar{\sigma}-\sigma\right)\frac{\partial\phi}{\partial\sigma}\\
&\quad+\frac{1}{2}v\frac{\partial^2\phi}{\partial\widetilde{x}^2}+\frac{1}{2}\eta^2\frac{\partial^2\phi}{\partial\widetilde{r}^2}+2v\gamma^2\frac{\partial^2\phi}{\partial v^2}+\frac{1}{2}\gamma^2\frac{\partial^2\phi}{\partial\sigma^2}+\rho_{x,r}\eta\sigma\frac{\partial^2\phi}{\partial\widetilde{x}\partial\widetilde{r}}+2\rho_{x,\sigma}\gamma v\frac{\partial^2\phi}{\partial\widetilde{x}\partial v}\\
&\quad+\rho_{x,\sigma}\gamma\sigma\frac{\partial^2\phi}{\partial\widetilde{x}\partial\sigma}+2\rho_{r,\sigma}\eta\gamma\sigma\frac{\partial^2\phi}{\partial r\partial v}+\rho_{r,\sigma}\eta\gamma\frac{\partial^2\phi}{\partial r\partial\sigma}+2\gamma^2\sigma\frac{\partial^2\phi}{\partial v\partial\sigma}-\widetilde{r}\phi, \quad\text{(A-14)}
\end{aligned}$$

with terminal conditions given in Equation (1.16).

As presented in Chapter 1, PDE (A-14) is affine, i.e. linear in its state variables, so the ChF is known in closed form.

However, we can apply the linearizing procedure also here, as in the case of the H1-HW model, and project the terms in front of the cross derivative between the log-stock, $x(t)$, and the interest rate, $r(t)$ [9], i.e.:

$$\rho_{x,r}\eta\sigma(t)\frac{\partial^2\phi}{\partial\widetilde{x}\partial\widetilde{r}}\approx\rho_{x,r}\eta\mathbb{E}(\sigma(t))\frac{\partial^2\phi}{\partial\widetilde{x}\partial\widetilde{r}}. \quad\text{(A-15)}$$

We call the approximation with modified covariance structure, as in (A-15), the SZHW-1 model. Both models, the SZHW in (A-14) and the SZHW-1 with (A-15), belong to the class of affine diffusions.

The expectation $\mathbb{E}(\sigma(t))$ in (A-15), with $\sigma(t)$ as in (1.14), is known analytically (see Chapter 1) and it is given by:

$$\mathbb{E}(\sigma(t)|\mathcal{F}(0))=\sigma_0\mathrm{e}^{-\kappa t}+\bar{\sigma}\left(1-\mathrm{e}^{-\kappa t}\right). \quad\text{(A-16)}$$

As the ChF for the SZHW model is of the following form:

$$\begin{aligned}
\phi(u,\widetilde{x}(t),\tau) &= \exp\big(A(u,\tau)+B(u,\tau)\widetilde{x}(t)+C(u,\tau)\widetilde{r}(t)\\
&\quad+D(u,\tau)v(t)+E(u,\tau)\sigma(t)\big), \quad\text{(A-17)}
\end{aligned}$$

with the functions $A(u,\tau)$, $B(u,\tau)$, $C(u,\tau)$, $D(u,\tau)$ and $E(u,\tau)$ given in Lemma 1.3.2 the projection in (A-15) in the SZHW-1 model will result in a similar ChF, as presented in the following lemma.

Lemma 2.B.1 (Characteristic function for the SZHW-1 model)**.** *The ChF for the SZHW-1 model is given by:*

$$\begin{aligned}
\phi_1(u,\widetilde{x}(t),\tau) &= \exp\big(A_1(u,\tau)+B(u,\tau)\widetilde{x}(t)+C(u,\tau)\widetilde{r}(t)\\
&\quad+D(u,\tau)v(t)+E_1(u,\tau)\sigma(t)\big), \quad\text{(A-18)}
\end{aligned}$$

with the functions $B(u,\tau)$, $C(u,\tau)$ and $D(u,\tau)$ as for the SZHW model in Lemma 1.3.2 and the functions $A_1(u,\tau)$ and $E_1(u,\tau)$ given by:

$$E_1(u,\tau) = E(u,\tau)+\rho_{x,r}\eta\varepsilon_1(u,\tau), \quad\text{(A-19)}$$

[9] indicated by the color in Equation (A-14)

where

$$\varepsilon_1(u,\tau) = \frac{\mathrm{e}^{c_1\tau}}{\lambda(1-g\mathrm{e}^{-d\tau})}(i+u)u\Big(f_2(\tau)+gf_3(\tau)\Big), \tag{A-20}$$

and $E(u,\tau)$, c_1, d, g, $f_2(\tau)$ and $f_3(\tau)$ from Lemma 1.3.2. Function $A_1(u,\tau)$ is given by:

$$\begin{aligned} A_1(u,\tau) &= A(u,\tau) + \rho_{x,r}\eta iu\int_0^\tau C(u,\tau)\mathbb{E}(\sigma(\tau-s))\mathrm{d}s \\ &= A(u,\tau) + \rho_{x,r}\eta\varepsilon_2(u,\tau), \end{aligned} \tag{A-21}$$

with

$$\begin{aligned} \varepsilon_2(u,\tau) &= \frac{(i+u)u\mathrm{e}^{-\kappa\tau}}{\kappa\lambda^2(\lambda-\kappa)}\Big[\lambda^2(\sigma_0-\bar{\sigma}) + \kappa\mathrm{e}^{(\kappa-\lambda)\tau}(\bar{\sigma}\kappa-\lambda\sigma_0) \\ &\quad + \mathrm{e}^{\kappa\tau}(\kappa-\lambda)(\lambda\sigma_0-\bar{\sigma}(\kappa+\lambda)+\bar{\sigma}\kappa\lambda\tau)\Big], \end{aligned} \tag{A-22}$$

and $A(u,\tau)$ for the SZHW model given in Lemma 1.3.2.

Proof. The only difference between the SZHW and the SZHW-1 pricing PDEs is in the cross term in (A-15). Similarly to the SZHW model it can be easily shown that the model corresponding ODEs are of the following form:

$$\begin{aligned} &B'(u,\tau) = 0, \\ &C'(u,\tau) = -1 + B(u,\tau) - \lambda C(u,\tau), \\ &D'(u,\tau) = 1/2B(u,\tau)(B(u,\tau)-1) + 2\left(\rho_{x,\sigma}\gamma B(u,\tau)-\kappa\right)D(u,\tau) + 2\gamma^2D^2(u,\tau), \\ &E_1'(u,\tau) = 2\left(\kappa\bar{\sigma}+\rho_{r,\sigma}\gamma\eta C(u,\tau)\right)D(u,\tau) + \left(2\gamma^2D(u,\tau)-\kappa+\rho_{x,\sigma}\gamma B(u,\tau)\right)E_1(u,\tau), \\ &A_1'(u,\tau) = 1/2\eta^2C^2(u,\tau) + \Big[\kappa\bar{\sigma}+1/2\gamma^2E_1(u,\tau)+\rho_{r,\sigma}\gamma\eta C(u,\tau)\Big]E_1(u,\tau) \\ &\qquad\quad + \gamma^2D(u,\tau) + \rho_{x,r}\eta B(u,\tau)C(u,\tau)\mathbb{E}(\sigma(t)), \end{aligned}$$

with the conditions: $B(u,0)=iu$, $C(u,0)=0$, $D(u,0)=0$, $E_1(u,0)=0$, and $A_1(u,0)=0$. We notice that the ODEs for $B(u,\tau)$, $C(u,\tau)$ and $D(u,\tau)$ are of the same form as in the case of the SZHW model. The remaining two ODEs, for $E_1(u,\tau)$ and for $A_1(u,\tau)$, differ only in one term, i.e.: in the SZHW model in the ODE for $E(u,\tau)$ the term $\rho_{x,r}\eta B(u,\tau)C(u,\tau)$ is replaced by $\rho_{x,r}\eta B(u,\tau)C(u,\tau)\mathbb{E}(\sigma(t))$ in the ODE for $A_1(u,\tau)$.

By integrating the ODEs, in a similar manner as in the SZHW model in Lemma 1.3.2, the proof is finished. ■

Now, we investigate the error when pricing the European options. We asses the error defined as the absolute difference between the European option prices. For determined ChF, the European-style option prices are available by using the

COS method. In this case the absolute error reads:

$$\begin{aligned}\text{error} &= \Big|\sum_{n=0}^{N_c}\omega_n\Re\left(\mathrm{e}^{-iknb_1}\left(\tilde{\phi}\left(kn,\widetilde{x}(t),\tau\right)-\tilde{\phi}_1\left(kn,\widetilde{x}(t),\tau\right)\right)\right)\Gamma_n^{b_1,b_2}\Big|\\ &\leq \sum_{n=0}^{N_c}\omega_n\Big|\Gamma_n^{b_1,b_2}\Big|\cdot\Big|\Re\left(\mathrm{e}^{-iknb_1}\left(\tilde{\phi}\left(kn,\widetilde{x}(t),\tau\right)-\tilde{\phi}_1\left(kn,\widetilde{x}(t),\tau\right)\right)\right)\Big|,\end{aligned}$$

with ω_n and $\Gamma_n^{b_1,b_2}$, b_1 and N_c given in Chapter 1 and $\widetilde{\phi}.(kn,\widetilde{x}(t),\tau)$ as in (1.32).

Now, we use the fact that for a complex number $z=a+ib$ it follows that: $|\Re(z)|\leq\Re|z|=|z|$, so that the error can be bounded from above by:

$$\begin{aligned}\text{error} &\leq \sum_{n=0}^{N_c}\omega_n\Big|\Gamma_n^{b_1,b_2}\Big|\cdot\Big|\mathrm{e}^{-iknb_1}\left(\tilde{\phi}\left(kn,\widetilde{x}(t),\tau\right)-\tilde{\phi}_1\left(kn,\widetilde{x}(t),\tau\right)\right)\Big|\\ &= \sum_{n=0}^{N_c}\omega_n\Big|\Gamma_n^{b_1,b_2}\Big|\cdot\Big|\mathrm{e}^{-iknb_1}\Big|\cdot\Big|\tilde{\phi}\left(kn,\widetilde{x}(t),\tau\right)-\tilde{\phi}_1\left(kn,\widetilde{x}(t),\tau\right)\Big|.\end{aligned}$$

As indicated in Lemma 2.B.1 the characteristic functions are related by:

$$\tilde{\phi}_1\left(kn,\widetilde{x}(t),\tau\right) = \tilde{\phi}\left(kn,\widetilde{x}(t),\tau\right)\mathrm{e}^{\rho_{x,r}\eta\varepsilon_1(kn,\tau)\sigma_0+\rho_{x,r}\eta\varepsilon_2(kn,\tau)}, \quad \text{(A-23)}$$

so that the upper bound reads:

$$\text{error} \leq \sum_{n=0}^{N_c}\omega_n\Big|\Gamma_n^{b_1,b_2}\Big|\cdot\Big|\mathrm{e}^{-iknb_1}\Big|\cdot\Big|\tilde{\phi}\left(kn,\widetilde{x}(t),\tau\right)\left(1-\mathrm{e}^{\rho_{x,r}\eta\varepsilon_1(kn,\tau)\sigma_0+\rho_{x,r}\eta\varepsilon_2(kn,\tau)}\right)\Big|,$$

which can be expressed as:

$$\begin{aligned}\text{error} &\leq \sum_{n=0}^{N_c}\omega_n\Big|\Gamma_n^{b_1,b_2}\Big|\cdot\Big|\mathrm{e}^{-iknb_1}\Big|\cdot\Big|\tilde{\phi}\left(kn,\widetilde{x}(t),\tau\right)\Big|\cdot\Big|1-\mathrm{e}^{\rho_{x,r}\eta(\varepsilon_1(kn,\tau)\sigma_0+\varepsilon_2(kn,\tau))}\Big|\\ &= \sum_{n=0}^{N_c}\omega_n\Big|\Gamma_n^{b_1,b_2}\Big|\cdot\Big|\tilde{\phi}\left(kn,\widetilde{x}(t),\tau\right)\Big|\cdot\Big|1-\mathrm{e}^{\rho_{x,r}\eta(\varepsilon_1(kn,\tau)\sigma_0-\varepsilon_2(kn,\tau))}\Big|\\ &\leq \sum_{n=0}^{N_c}\omega_n\Big|\Gamma_n^{b_1,b_2}\Big|\cdot\Big|1-\mathrm{e}^{\rho_{x,r}\eta(\varepsilon_1(kn,\tau)\sigma_0-\varepsilon_2(kn,\tau))}\Big|.\end{aligned}$$

By a first-order Taylor expansion we find:

$$\begin{aligned}\Big|1-\mathrm{e}^{\varepsilon_1(kn,\tau)\sigma_0-\varepsilon_2(kn,\tau)}\Big| &\approx \Big|\rho_{x,r}\eta\left(\varepsilon_1(kn,\tau)\sigma_0-\varepsilon_2(kn,\tau)\right)\Big|\\ &= \eta\Big|\rho_{x,r}\Big|\cdot\Big|\varepsilon_1(kn,\tau)\sigma_0-\varepsilon_2(kn,\tau)\Big| =: \hat{\epsilon}, \text{(A-24)}\end{aligned}$$

as $\eta>0$ and $\rho_{x,r}\in[-1,1]$.

Since the expressions for $\varepsilon_1(kn,\tau)$ and $\varepsilon_2(kn,\tau)$ are of rather complicated form we consider the case $\lambda \to 0$ and $\kappa \to 0$ which implies:

$$\lim_{\lambda,\kappa\to 0} \varepsilon_1(kn,\tau) = \frac{1}{\gamma^2}\left[\tau\sqrt{kn(i+kn)\gamma^2}\tanh\left(\tau\sqrt{kn(i+kn)\gamma^2}\right) + -1 + \operatorname{sech}\left(\tau\sqrt{kn(kn+i)\gamma^2}\right)\right] =: \hat{\varepsilon}_1, \tag{A-25}$$

$$\lim_{\lambda,\kappa\to 0} \varepsilon_2(kn,\tau) = -\frac{1}{2}kn(kn+i)\sigma_0\tau^2. \tag{A-26}$$

In the limit for $\kappa,\lambda \to 0$ function $\varepsilon_1(kn,\tau)$ does not depend on σ_0, so that we can express $\hat{\epsilon}$ from (A-24), for $\sigma_0 > 0$, as:

$$\begin{aligned}\lim_{\lambda,\kappa\to 0} \hat{\epsilon} &= \eta\left|\rho_{x,r}\right| \cdot \lim_{\lambda,\kappa\to 0}\left|\varepsilon_1(kn,\tau)\sigma_0 - \varepsilon_2(kn,\tau)\right| \\ &= \eta\sigma_0\left|\rho_{x,r}\right| \cdot \left|\hat{\varepsilon}_1 + \frac{1}{2}kn(kn+i)\tau^2\right|.\end{aligned} \tag{A-27}$$

We see that for a given volatility parameter, γ, and maturity, τ, the limit in the first-order approximation for the upper bound of the error increases with the magnitude of interest rate volatility parameter, η, the volatility level, σ_0, and the correlation between equity and interest rate, $\rho_{x,r}$. The absolute error also is time dependent.

As we have seen earlier, when comparing the H1-HW model with the full-scale HHW model in Table 2.3, the experiments showed that the approximating H1-HW model generated a somewhat smaller bias for very low and very large strikes. We check here whether the same phenomena is present when dealing with the SZHW model and its approximating variant. In Figure 2.6 the numerical results, for long-maturity time, show a similar *error pattern* as in the case of the Heston-hybrid model presented in Table 2.3.

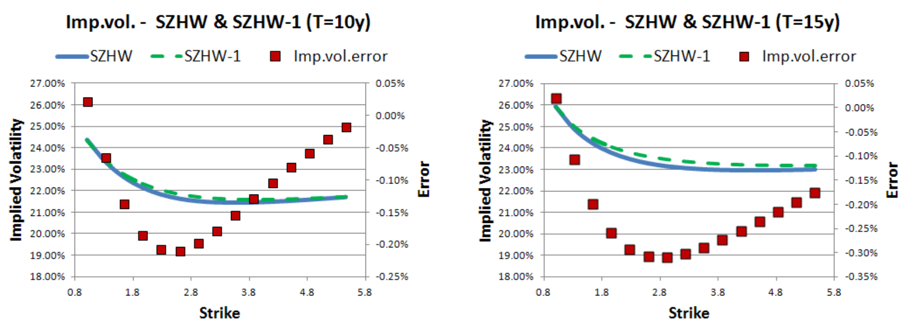

Figure 2.6: *Implied volatilities for the SZHW and the SZHW-1 models with* $P(0,t) = \mathrm{e}^{-0.06t}$, $\kappa = 0.1$, $\bar{\sigma} = 0.2$, $\gamma = 0.06$, $\lambda = 0.01$, $\eta = 0.01$, $\rho_{x,\sigma} = -40\%$, $\rho_{x,r} = 30\%$, $\rho_{r,\sigma} = 10\%$ *and* $\sigma_0 = \bar{\sigma}$. *LEFT: The results for* $\tau = 10y$. *RIGHT: The results for* $\tau = 15y$.

In Figure 2.7 the densities for both models under the same sets of parameters are presented. The figures show that the agreement between the models *in the* *tails* of the distribution is very good. However, some discrepancies are present around *the mean*.

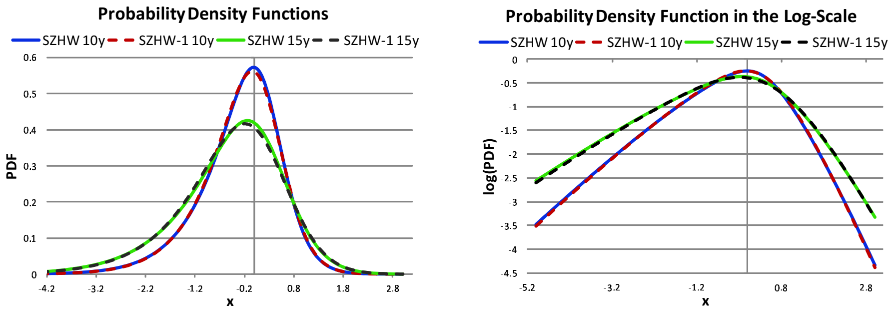

Figure 2.7: *LEFT: densities for the SZHW and the SZHW-1 model. RIGHT: log-transformed densities for both models. For both experiments the parameters are as chosen in Figure 2.6.*

CHAPTER 3

The Affine Heston Model with Correlated Multi-Factor Interest Rates

> But it ain't about how hard you hit; it's about how hard you can get hit, and keep moving forward... It's how much you can take, and keep moving forward. That's how winning is done.
>
> *Rocky Balboa ("Rocky V")*

3.1 Introduction

In this chapter we present a hybrid model in which the equity part is again driven by the Heston model [54], but for the short-rate process a Gaussian *multi-factor* model [57] is taken with a non-zero correlation between the different asset classes. The model introduced here is defined in such a way that it belongs to the affine diffusion framework for which the corresponding characteristic function can be determined. This facilitates the use of Fourier-based algorithms [23, 32], for efficient pricing of plain vanilla contracts. Additionally, Monte Carlo simulation can be performed by a straightforward generalization of the scheme developed by Andersen in [3]. By defining the affine hybrid Heston model under the *forward measure*, we can price several financial derivative products (like American options [33]) in a similar way as under the plain Heston model.

The interest rates are driven by multi-factor Gaussian rates [57]. This model provides a rich pattern for the term structure movements and recovers a *humped* volatility structure observed in the market. The hybrid model under consideration can be used for hybrid payoffs which have a limited sensitivity to the interest rate smile.

For the model proposed also the Greeks for plain vanilla options can be efficiently determined and used for hedging. When hedging hybrid products, exposed to different sources of risks coming from equity or interest rate, it is crucial to choose an appropriate set of hedging instruments. Particularly, correlation risk needs to be taken into account here. As it is difficult to find a *pure* correlation product in the market which can be used for hedging, one may consider, similarly as for hedging of jump processes (as presented in [52]), a mean-variance hedging strategy based on a portfolio of stocks, options and interest rate instruments, like caplets and swaptions.

In Section 3.2 we define the Heston-Gaussian two-factor hybrid model and discuss the affinity issue. In the follow-up section, which is the core of this chapter, we propose an affine version of this hybrid model. We derive the model under the T-forward measure and provide the corresponding characteristic function. In the same section we describe the derivation of the Greeks as well as Monte Carlo simulation; we also discuss properties like a positive-definite covariance matrix. Section 3.4 is dedicated to numerical experiments where we check the hybrid model performance for pricing a hybrid product.

3.2 Hybrid with multi-factor short-rate process

3.2.1 Model under the spot measure

Suppose we have given two asset classes defined by the vectors $\mathbf{X}^{\bar{n}\times 1}(t)$, $\bar{n} \in \mathbb{N}^+$ for the equity and for the interest rates $\mathbf{R}^{\bar{m}\times 1}(t)$, $\bar{m} \in \mathbb{N}^+$. One can take high-dimensional processes involving stochastic volatility, and define the following system of governing stochastic differential equations (SDEs):

$$\begin{cases} \mathrm{d}\mathbf{R}(t) = & a(\mathbf{R}(t))\mathrm{d}t + & b(\mathbf{R}(t))\mathrm{d}\mathbf{W}_{\mathbf{R}}(t), \\ \mathrm{d}\mathbf{X}(t) = & c(\mathbf{X}(t), \mathbf{R}(t))\mathrm{d}t + & d(\mathbf{X}(t))\mathrm{d}\mathbf{W}_{\mathbf{X}}(t), \\ \mathbf{Z}(t)\mathbf{Z}^{\mathrm{T}}(t) = & \mathbf{C}_{\mathbf{H}}\mathrm{d}t, & \end{cases} \tag{3.1}$$

where $\mathbf{H}(t) = [\mathbf{R}(t), \mathbf{X}(t)]^{\mathrm{T}}$, $\mathbf{Z}(t) = [\mathrm{d}\mathbf{W}_{\mathbf{R}}(t), \mathrm{d}\mathbf{W}_{\mathbf{X}}(t)]^{\mathrm{T}}$, $\mathbf{C}_{\mathbf{H}}$ is a $(\bar{n}+\bar{m})\times(\bar{n}+\bar{m})$ matrix which represents the instantaneous correlation between the Brownian motions. The noises $\mathrm{d}\mathbf{W}_{\cdot}(t)$ are assumed to be multi-dimensional, and correlation within the asset classes is allowed, i.e., $\mathbf{C}_{\mathbf{R}} = (\mathrm{d}\mathbf{W}_{\mathbf{R}}(t))(\mathrm{d}\mathbf{W}_{\mathbf{R}}(t))^{\mathrm{T}}$, $\mathbf{C}_{\mathbf{X}} = (\mathrm{d}\mathbf{W}_{\mathbf{X}}(t))(\mathrm{d}\mathbf{W}_{\mathbf{X}}(t))^{\mathrm{T}}$, as well as correlations between these classes.

Since the Heston model in [54] is sufficient for explaining the smile-shaped implied volatilities in equity, we take this model as the benchmark for the equity part. In particular, the model for the state vector $\mathbf{X}(t) = [x(t) = \log S(t), v(t)]^{\mathrm{T}}$ is described by the following system of SDEs:

$$\begin{cases} \mathrm{d}x(t) = & (r(t) - 1/2v(t))\,\mathrm{d}t + & \sqrt{v(t)}\mathrm{d}W_x(t), & S(0) > 0, \\ \mathrm{d}v(t) = & \kappa\,(\bar{v} - v(t))\,\mathrm{d}t + & \gamma\sqrt{v(t)}\mathrm{d}W_v(t), & v(0) > 0, \end{cases} \tag{3.2}$$

with $\mathrm{d}W_x(t)\mathrm{d}W_v(t) = \rho_{x,v}\mathrm{d}t$, the speed of mean reversion $\kappa > 0$; $\bar{v} > 0$ is the long-term mean of the stochastic variance process $v(t)$, and $\gamma > 0$ specifies the volatility of the variance process. Note that the term $1/2v(t)$ in the $x(t)$-process results from Itô's lemma when deriving the dynamics for $\log S(t)$.

For the interest rate process we consider here the Gaussian multi-factor short-rate model (Gn++) [19], also known as a multi-factor Hull-White model [57]. The model, for a given state vector $\mathbf{R}(t) = [r(t), \zeta_1(t), \dots, \zeta_{n-1}(t)]^{\mathrm{T}}$, is defined by the following system of SDEs:

$$\begin{cases} \mathrm{d}r(t) = & (\theta(t) + \sum_{k=1}^{n-1} \zeta_k(t) - \beta r(t))\mathrm{d}t + \quad \eta \mathrm{d}W_r(t), \quad r(0) > 0, \\ \mathrm{d}\zeta_k(t) = & \qquad\qquad -\lambda_k \zeta_k(t)\mathrm{d}t + \quad \varsigma_k \mathrm{d}W_{\zeta_k}(t), \quad \zeta_k(0) = 0, \end{cases} \tag{3.3}$$

where

$$\mathrm{d}W_r(t)\mathrm{d}W_{\zeta_k}(t) = \rho_{r,\zeta_k}\mathrm{d}t, \ k = 1, \dots, n-1, \quad \mathrm{d}W_{\zeta_i}(t)\mathrm{d}W_{\zeta_j}(t) = \rho_{\zeta_i,\zeta_j}\mathrm{d}t, \ \ i \neq j,$$

with $\beta > 0$, $\lambda_k > 0$ the mean reversion parameters; $\eta > 0$ and parameters ς_k determine the volatility magnitude of the interest rate. In the system above, coefficient $\theta(t) > 0$, $t \in \mathbb{R}^+$, stands again for the long-term interest rate (which is usually calibrated to the current yield curve).

The Gn++ model provides a satisfactory fit to at-the-money humped structures of the volatility of the instantaneous forward rates. Moreover, the easy construction of the model (based on a multivariate normal distribution) provides closed-form solutions for caps and swaptions, enabling fast calibration. On the other hand, since the model is assumed to be normal, the interest rates can become negative. This however is known and is taken care of in practical applications (see for example [96]).

By taking the equity model $\mathbf{X}(t)$ as introduced in (3.2) and the interest rate part $\mathbf{R}(t)$ from (3.3), a hybrid model $\mathbf{H}(t) = [\mathbf{R}(t), \mathbf{X}(t)]^{\mathrm{T}} = [r(t), \zeta_1(t), \dots, \zeta_{n-1}(t), v(t), x(t)]^{\mathrm{T}}$ can be defined with the following instantaneous correlation structure:

$$\mathbf{C_H} := \left[\begin{array}{cccc|cc} 1 & \rho_{r,\zeta_1} & \dots & \rho_{r,\zeta_{n-1}} & 0 & \rho_{x,r} \\ \rho_{r,\zeta_1} & 1 & \dots & \rho_{\zeta_1,\zeta_{n-1}} & 0 & \rho_{x,\zeta_1} \\ \vdots & \vdots & \ddots & \vdots & \vdots & \vdots \\ \rho_{r,\zeta_{n-1}} & \rho_{\zeta_{n-1},\zeta_1} & \dots & 1 & 0 & \rho_{x,\zeta_{n-1}} \\ \hline 0 & 0 & \dots & 0 & 1 & \rho_{x,v} \\ \rho_{x,r} & \rho_{x,\zeta_1} & \dots & \rho_{x,\zeta_{n-1}} & \rho_{x,v} & 1 \end{array}\right]. \tag{3.4}$$

Model $\mathbf{H}(t)$ is the *Heston-Gaussian n-factor hybrid model* (H-Gn++). Note that the equity and the interest rate asset classes are linked by correlations in the right-upper and left-lower diagonal blocks of matrix $\mathbf{C_H}$. Our main objective is the preservation of the correlation, $\rho_{x,r}$, between the log-equity and the interest rate.

As it is nontrivial to hedge equity-interest rate hybrids by liquidly traded standard instruments (see [17] for details), and as the correlations between different asset classes cannot be easily implied from the market, historical estimates are often used. However, as soon as hybrid product prices become available, one can use the additional correlations (degrees of freedom) to enhance the hybrid model performance.

Assuming $V := V(t, \mathbf{H}(t))$ to represent the value of a European claim, we can derive the corresponding pricing partial differential equation (PDE) [40] with the help of the arbitrage-free pricing theorem and the use of Itô's formula:

$$
\begin{aligned}
0 = {} & (r - 1/2v)\frac{\partial V}{\partial x} + \kappa\left(\bar{v} - v\right)\frac{\partial V}{\partial v} + \Big(\theta(t) + \sum_{k=1}^{n-1}\zeta_k - \beta r\Big)\frac{\partial V}{\partial r} - \sum_{k=1}^{n-1}\lambda_k\zeta_k\frac{\partial V}{\partial \zeta_k} - rV \\
& + \frac{1}{2}v\frac{\partial^2 V}{\partial x^2} + \frac{1}{2}\gamma^2 v\frac{\partial^2 V}{\partial v^2} + \frac{1}{2}\eta^2\frac{\partial^2 V}{\partial r^2} + \frac{1}{2}\sum_{k=1}^{n-1}\varsigma_k^2\frac{\partial^2 V}{\partial \zeta_k} + \rho_{x,v}\gamma v\frac{\partial^2 V}{\partial x\partial v} + \rho_{x,r}\eta\sqrt{v}\frac{\partial^2 V}{\partial x\partial r} \\
& + \sqrt{v}\sum_{k=1}^{n-1}\rho_{x,\zeta_k}\varsigma_k\frac{\partial^2 V}{\partial x\partial \zeta_k} + \sum_{k-1}^{n-1}\rho_{r,\zeta_k}\varsigma_k\eta\frac{\partial^2 V}{\partial r\partial \zeta_k} + \frac{\partial V}{\partial t} + \sum_{k=1}^{n-2}\sum_{j=k+1}^{n-1}\rho_{\zeta_k,\zeta_j}\varsigma_k\varsigma_j\frac{\partial^2 V}{\partial \zeta_k\partial \zeta_j},
\end{aligned}
\tag{3.5}
$$

with specific boundary and final conditions (for details on boundary conditions for similar problems, see, for example, [29] pp.241).

Covariance structure

The solution of the (n+2)D convection-diffusion-reaction PDE in (3.5) can be approximated by means of standard numerical techniques, like finite differences (see for example [80]). This may however cost substantial CPU time for the model evaluation. An alternative is to use the Feynman-Kac theorem (see Chapter 1) and reformulate the problem as an integral equation related to the discounted expected payoff.

Let us take the following state vector $\mathbf{H} = [r(t), \zeta_1(t), \ldots, \zeta_{n-1}(t), v(t), x(t)]^{\mathrm{T}}$, and determine the associated (symmetric) instantaneous covariance matrix $\mathbf{\Sigma_H}$ of hybrid model (3.1) with (3.2) and (3.3):

$$
\mathbf{\Sigma_H} := \left[\begin{array}{ccc|cc}
\eta^2 & \ldots & \rho_{r,\zeta_{n-1}}\eta\varsigma_{n-1} & 0 & \rho_{x,r}\eta\sqrt{v} \\
\vdots & \ddots & \vdots & \vdots & \vdots \\
\rho_{r,\zeta_{n-1}}\eta\varsigma_{n-1} & \ldots & \varsigma_{n-1}^2 & 0 & \rho_{x,\zeta_{n-1}}\varsigma_{n-1}\sqrt{v} \\
\hline
0 & \ldots & 0 & \gamma^2 v & \rho_{x,v}\gamma v \\
\rho_{x,r}\eta\sqrt{v} & \ldots & \rho_{x,\zeta_{n-1}}\varsigma_{n-1}\sqrt{v} & \rho_{x,v}\gamma v & v
\end{array}\right].
\tag{3.6}
$$

For the H-Gn++ hybrid model the instantaneous covariance matrix in (3.6) is not affine in all terms of the right-upper block. In order to stay in the affine class with non-zero correlations between the assets, *approximations* should be introduced.

In order to *define* an alternative model which is affine, it appears necessary to relate the instantaneous covariance matrix in (3.6) to the corresponding stochastic differential equations. This can be done by expressing the model in terms of the independent Brownian motions, $\mathrm{d}\widetilde{\mathbf{W}}(t) = [\mathrm{d}\widetilde{W}_r(t), \mathrm{d}\widetilde{W}_{\zeta_1}(t), \ldots, \mathrm{d}\widetilde{W}_{\zeta_{n-1}}(t), \mathrm{d}\widetilde{W}_v(t), \mathrm{d}\widetilde{W}_x(t)]^{\mathrm{T}}$. For a state vector $\mathbf{H}(t) = [r(t), \zeta_1(t), \ldots, \zeta_{n-1}(t), v(t), x(t)]^{\mathrm{T}}$, the model can be rewritten, in terms of independent Brownian motions as:

$$\mathrm{d}\mathbf{H}(t) = \mu(\mathbf{H}(t))\mathrm{d}t + \mathbf{A}(t)\mathbf{U}\mathrm{d}\widetilde{\mathbf{W}}(t), \tag{3.7}$$

where $\mu(\mathbf{H}(t))$ represents the drift for system $\mathrm{d}\mathbf{H}(t)$ and $\mathbf{U}$ is the Cholesky lower triangular matrix so that $\mathbf{C}_{\mathbf{H}} = \mathbf{U}\mathbf{U}^{\mathrm{T}}$ for matrix $\mathbf{C}_{\mathbf{H}}$ in (3.4) and matrix $\mathbf{A}(t)$ is given by:

$$\mathbf{A}(t) = \left[\begin{array}{cccc|cc} \eta & 0 & \dots & 0 & 0 & 0 \\ 0 & \varsigma_1 & \dots & 0 & 0 & 0 \\ \vdots & \vdots & \ddots & \vdots & \vdots & \vdots \\ 0 & 0 & \dots & \varsigma_{n-1} & 0 & 0 \\ \hline 0 & 0 & \dots & 0 & \gamma\sqrt{v(t)} & 0 \\ 0 & 0 & \dots & 0 & 0 & \sqrt{v(t)} \end{array}\right]. \tag{3.8}$$

Equivalently, model (3.7) can be expressed as:

$$\mathrm{d}\mathbf{H}(t) = \mu(\mathbf{H}(t))\mathrm{d}t + \mathbf{L}(t)\mathrm{d}\widetilde{\mathbf{W}}(t), \tag{3.9}$$

with

$$\mathbf{L}(t)\mathbf{L}(t)^{\mathrm{T}} = \mathbf{\Sigma}_{\mathbf{H}}, \tag{3.10}$$

and $\mathbf{\Sigma}_{\mathbf{H}}$ the instantaneous covariance matrix in (3.6).

The model representation of (3.9) is favorable compared to (3.7) since we have a direct relation between the covariance matrix (3.6) and the SDEs.

3.2.2 Zero-coupon bonds under multi-factor Gaussian model

In the sections to follow we reduce the dimension of the pricing problem by an appropriate measure change, and *define an affine version* of the multi-factor hybrid model.

In order to derive the multi-factor hybrid model under the forward measure the corresponding zero-coupon bond needs to be determined first.

Under the risk-neutral measure, $\mathbb{Q}$, we consider the n-factor interest rate model in (3.3), with a full correlation matrix with $\rho_{r,\zeta_i} \neq 0$, and $\rho_{\zeta_i,\zeta_j} \neq 0$ for $i, j = \{1, \dots, n-1\}$, $i \neq j$.

This model is affine in all state variables, so we can derive the corresponding characteristic function (see [28]) for $r(T)$:

$$\begin{aligned} \phi_{\mathrm{Gn++}}(u, r(t), \tau) &= \mathbb{E}^{\mathbb{Q}}\left(\mathrm{e}^{-\int_t^T r(s)\mathrm{d}s}\mathrm{e}^{iur(T)}\middle|\mathcal{F}(t)\right) \\ &= \exp\left(A(u,\tau) + B(u,\tau)r(t) + \sum_{k=1}^{n-1} C_k(u,\tau)\zeta_k(t)\right), \end{aligned} \tag{3.11}$$

with final condition $\phi_{\mathrm{Gn++}}(u, r(T), 0) = \mathrm{e}^{iur(T)}$, where conventionally $\tau = T - t$. The functions $A(u, \tau)$, $B(u, \tau)$ and $C_k(u, \tau)$ are known explicitly and are given by the set of Riccati-type ODEs:

$$
\begin{aligned}
B'(u,\tau) &= -1-\beta B(u,\tau),\\
C_k'(u,\tau) &= B(u,\tau)-\lambda_k C_k(u,\tau), \qquad\qquad (3.12)\\
A'(u,\tau) &= \theta(t)B(u,\tau)+\frac{1}{2}\eta^2B^2(u,\tau)+\eta\sum_{k=1}^{n-1}\rho_{r,\zeta_k}\varsigma_k B(u,\tau)C(u,\tau)\\
&\quad+\frac{1}{2}\sum_{i=1}^{n-1}\sum_{j=1}^{n-1}\rho_{\zeta_i,\zeta_j}\varsigma_i\varsigma_j C_i(u,\tau)C_j(u,\tau),
\end{aligned}
$$

with terminal conditions $B(u,0)=iu$, $C_k(u,0)=0$ and $A(u,0)=0$. These ODEs can be solved analytically. By setting $u=0$ in (3.11) the zero-coupon bond price is obtained, i.e.:

$$
P(t,T)\overset{\text{def}}{=}\mathbb{E}^{\mathbb{Q}}\left(\mathrm{e}^{-\int_t^T r(s)\mathrm{d}s}\big|\mathcal{F}(t)\right)=\exp\left(A(t,T)+B(t,T)r(t)+\sum_{k=1}^{n-1}C_k(t,T)\zeta_k(t)\right), \tag{3.13}
$$

where

$$
A(t,T):=A(0,\tau),\quad B(t,T):=B(0,\tau),\quad C_k(t,T):=C_k(0,\tau). \tag{3.14}
$$

By applying Itô's lemma to Equation (3.13), the zero-coupon bond dynamics under the $\mathbb{Q}$ measure read:

$$
\frac{\mathrm{d}P(t,T)}{P(t,T)} = r(t)\mathrm{d}t+\eta B(t,T)\mathrm{d}W_r(t)+\sum_{k=1}^{n-1}\varsigma_k C_k(t,T)\mathrm{d}W_{\zeta_k}(t), \tag{3.15}
$$

where the functions $B(t,T)$ and $C_k(t,T)$ satisfy the ODEs (3.12) via (3.14). Their solution reads:

$$
B(t,T) = \frac{1}{\beta}\left(\mathrm{e}^{-\beta(T-t)}-1\right), \tag{3.16}
$$

$$
C_k(t,T) = \frac{1}{\beta(\lambda_k-\beta)}\mathrm{e}^{-\beta(T-t)}-\frac{1}{\lambda_k(\lambda_k-\beta)}\mathrm{e}^{-\lambda_k(T-t)}-\frac{1}{\lambda_k\beta}, \tag{3.17}
$$

with

$$
C_k(t,T)=\frac{1}{\beta^2}\left(\mathrm{e}^{-\beta(T-t)}(1+\beta(T-t))-1\right),\quad \text{for}\quad \lambda_k\to\beta,
$$

and $k=\{1,\ldots,n-1\}$.

The dynamics for the zero-coupon bond are important when switching measures in the hybrid model.

3.3 The Affine Heston-Gn++ model (AH-Gn++)

In this section, which is the main part of this chapter, we define *the affine hybrid Heston-Gn++ model*. Since the model proposed is, by its structure, similar to the Heston-multi-factor-Gaussian model (denoted by H-Gn++) we abbreviated the model by "AH-Gn++" here, which stands for "affine version of the H-Gn++ model". Note that we define the AH-Gn++ model as a new model here, not as an approximation only for calibration.

For convenience, we start with $n = 2$. The AH-G2++ model with the state vector $\mathbf{H}(t) = [r(t), \zeta(t), v(t), S(t)]^{\mathrm{T}}$ under the risk-neutral measure $\mathbb{Q}$, is given by the following system of SDEs:

$$\begin{bmatrix} \mathrm{d}r(t) \\ \mathrm{d}\zeta(t) \\ \mathrm{d}v(t) \\ \mathrm{d}S(t)/S(t) \end{bmatrix} = \begin{bmatrix} \theta(t) + \zeta(t) - \beta r(t), \\ -\lambda\zeta(t) \\ \kappa(\bar{v} - v(t)) \\ r(t) \end{bmatrix} \mathrm{d}t + \mathbf{L}(t) \begin{bmatrix} \mathrm{d}\widetilde{W}_r(t) \\ \mathrm{d}\widetilde{W}_\zeta(t) \\ \mathrm{d}\widetilde{W}_v(t) \\ \mathrm{d}\widetilde{W}_x(t) \end{bmatrix}, \tag{3.18}$$

where

$$\mathbf{L}(t)\mathbf{L}(t)^{\mathrm{T}} = \left[\begin{array}{cc|cc} \eta^2 & \rho_{r,\zeta}\eta\varsigma & 0 & \rho_{x,r}\eta\alpha(t) \\ \rho_{r,\zeta}\varsigma\eta & \varsigma^2 & 0 & \rho_{x,\zeta}\varsigma\alpha(t) \\ \hline 0 & 0 & \gamma^2 v & \rho_{x,v}\gamma v \\ \rho_{x,r}\eta\alpha(t) & \rho_{x,\zeta}\varsigma\alpha(t) & \rho_{x,v}\gamma v & v \end{array}\right] =: \mathbf{\Sigma_H}. \tag{3.19}$$

Here, the function $\alpha(t)$ in (3.19) is a deterministic function depending on time t (whereas in the case of the full-scale H-G2++ model $\alpha(t) = \sqrt{v(t)}$). With a deterministic function $\alpha(t)$, matrix $\mathbf{\Sigma_H}$ in (3.19) does not contain any non-affine elements, so that the AH-G2++ model belongs to the class of affine processes and we have the characteristic function.

Application of the Cholesky decomposition to matrix $\mathbf{\Sigma_H}$ in (3.19) gives for matrix $\mathbf{L}(t)$:

$$\mathbf{L}(t) = \begin{bmatrix} \eta & 0 & 0 & 0 \\ \varsigma\mathbf{U}_{2,1} & \varsigma\mathbf{U}_{2,2} & 0 & 0 \\ 0 & 0 & \gamma\sqrt{v(t)} & 0 \\ \alpha(t)\mathbf{U}_{4,1} & \alpha(t)\mathbf{U}_{4,2} & \mathbf{U}_{4,3}\sqrt{v(t)} & \sqrt{v(t)(1-\mathbf{U}_{4,3}^2) - \alpha^2(t)\left(\mathbf{U}_{4,1}^2 + \mathbf{U}_{4,2}^2\right)} \end{bmatrix}, \tag{3.20}$$

where $\mathbf{U}$ is the lower triangular Cholesky matrix obtained from the correlation matrix, with values for $\mathbf{U}_{i,j}$ given by:

$$\begin{cases} \mathbf{U}_{2,1} = \rho_{r,\zeta}, \quad \mathbf{U}_{4,1} = \rho_{x,r}, \quad \mathbf{U}_{4,3} = \rho_{x,v}, \\ \mathbf{U}_{2,2} = \sqrt{1-\rho_{r,\zeta}^2}, \quad \mathbf{U}_{4,2} = (\rho_{x,\zeta} - \rho_{x,r}\rho_{r,\zeta}) \big/ \sqrt{1-\rho_{r,\zeta}^2}. \end{cases} \tag{3.21}$$

The correlation structure between equity and interest rate in the AH-G2++ model in (3.18) with (3.19) is dependent on the function $\alpha(t)$. If we set, for example, $\alpha(t) \equiv 0$, independence between the asset classes is imposed. Our main objective is to choose a function $\alpha(t)$ such that the AH-G2++ model stays affine and that it resembles the full-scale H-G2++ model.

3.3.1 The function $\alpha(t)$

In this section we determine function $\alpha(t)$ in (3.19) for the AH-Gn++ model. In the H-Gn++ model each of the non-affine terms contains the term $\sqrt{v(t)}$, where

$v(t)$ is the square-root process defined in (3.18) with dynamics:

$$\mathrm{d}v(t) = \kappa(\bar{v} - v(t))\mathrm{d}t + \gamma\sqrt{v(t)}\mathrm{d}\widetilde{W}_v(t),$$

(with all the parameters specified in (3.2)). Since function $\alpha(t)$ is related to the $\sqrt{v(t)}$-term in the H-Gn++ model, a natural definition for $\alpha(t)$ in the AH-Gn++ model appears to be:

$$\alpha(t) := \mathbb{E}(\sqrt{v(t)}),$$

where variance process $v(t)$ is of square-Bessel CIR-type [25].

The process is guaranteed to be positive if the Feller condition [34] for $v(t)$, i.e., $2\kappa\bar{v} \geq \gamma^2$, is satisfied.

Since function $\alpha(t)$ is defined as an approximation of $\sqrt{v(t)}$ it is given by:

$$\alpha(t) := \mathbb{E}(\sqrt{v(t)}) = \sqrt{2c(t)}\mathrm{e}^{-\lambda(t)/2}\sum_{k=0}^{\infty}\frac{1}{k!}\left(\lambda(t)/2\right)^k \frac{\Gamma\left(\frac{1+d}{2}+k\right)}{\Gamma(\frac{d}{2}+k)}, \tag{3.22}$$

where $c(t)$, d and $\lambda(t)$ are defined in (2.22). Detailed derivations of this expectation can be found in Chapter 2.

3.3.2 The affine hybrid model under measure change

Here we move the model from the spot measure, generated by the money-savings account, $M(t)$, to the *forward measure* where the numéraire is the zero-coupon bond, $P(t,T)$. As indicated in [82], the forward is defined as,

$$F(t) = \frac{S(t)}{P(t,T)} = \frac{\mathrm{e}^{x(t)}}{P(t,T)}, \tag{3.23}$$

where $F(t)$ represents the forward, $S(t)$ stands for stock, $x(t)$ is log-stock defined in (3.2) and $P(t,T)$ as defined in (3.15) represents the value of the zero-coupon bond paying €1 at maturity T.

Under the AH-G2++ hybrid model the stock dynamics $\mathrm{d}S(t)$, in terms of the independent Brownian motions, are given by:

$$\begin{aligned}\frac{\mathrm{d}S(t)}{S(t)} &= r(t)\mathrm{d}t + \psi_1(t)\mathrm{d}\widetilde{W}_r(t) + \psi_2(t)\mathrm{d}\widetilde{W}_\zeta(t) + \psi_3(t)\sqrt{v(t)}\mathrm{d}\widetilde{W}_v(t)\\ &\quad + \sqrt{v(t)\psi_4(t) + \psi_5(t)}\mathrm{d}\widetilde{W}_x(t),\end{aligned} \tag{3.24}$$

with $\psi_1(t) = \mathbf{U}_{4,1}\alpha(t)$, $\psi_2(t) = \mathbf{U}_{4,2}\alpha(t)$, $\psi_3(t) = \mathbf{U}_{4,3}$, $\psi_4(t) = 1 - \mathbf{U}_{4,3}^2$ and $\psi_5(t) = -\alpha^2(t)\left(\mathbf{U}_{4,1}^2 + \mathbf{U}_{4,2}^2\right)$ where $\mathbf{U}_{i,j}$ is defined by (3.21) and $\alpha(t) := \mathbb{E}(\sqrt{v(t)})$.

The zero-coupon bond, $P(t,T)$ in (3.15), in terms of independent Brownian motions, is defined as:

$$\begin{aligned}\frac{\mathrm{d}P(t,T)}{P(t,T)} &= r(t)\mathrm{d}t + \left(\eta B(t,T) + \rho_{r,\zeta}\varsigma C(t,T)\right)\mathrm{d}\widetilde{W}_r(t)\\ &\quad + \varsigma C(t,T)\sqrt{1-\rho_{r,\zeta}^2}\mathrm{d}\widetilde{W}_\zeta(t),\end{aligned}$$

with $B(t,T)$ in (3.16) and $C(t,T)$ in (3.17). By switching from the risk-neutral measure, $\mathbb{Q}$, to the T-forward measure, $\mathbb{Q}^T$, the discounting will be *decoupled* from taking the expectation, i.e.:

$$V(t,F(t)) = P(t,T)\mathbb{E}^T\left(\max\left(F(T)-K,0\right)|\mathcal{F}(t)\right).$$

In order to determine the dynamics for $F(t)$ in (3.23), we apply Itô's formula:

$$\begin{aligned}\frac{\mathrm{d}F(t)}{F(t)} &= \left(\varsigma^2C^2 + B\eta(B\eta-\psi_1(t)) + \varsigma C\left(2\rho_{r,\zeta}\eta B - \rho_{r,\zeta}\psi_1(t) - \sqrt{1-\rho_{r,\zeta}^2}\psi_2(t)\right)\right)\mathrm{d}t\\ &+\hat{\psi}_1(t)\mathrm{d}\widetilde{W}_r(t) + \hat{\psi}_2(t)\mathrm{d}\widetilde{W}_\zeta(t) + \psi_3(t)\sqrt{v(t)}\mathrm{d}\widetilde{W}_v(t) + \sqrt{v(t)\psi_4(t)+\psi_5(t)}\mathrm{d}\widetilde{W}_x(t),\end{aligned}$$

with $\hat{\psi}_1(t) := \psi_1(t) - (\rho_{r,\zeta}\varsigma C + \eta B)$, $\hat{\psi}_2(t) := \psi_2(t) - \varsigma C\sqrt{1-\rho_{r,\zeta}^2}$ and, for the sake of notation, we have set $B := B(t,T)$ and $C := C(t,T)$.

Forward $F(t)$ is a martingale under the T-forward measure, i.e.,

$$\mathbb{E}^T(F(T)|\mathcal{F}(t)) = F(t),$$

and the corresponding Brownian motions under the T-forward measure, $\mathrm{d}\widetilde{W}_x^T(t)$, $\mathrm{d}\widetilde{W}_v^T(t)$, $\mathrm{d}\widetilde{W}_r^T(t)$ and $\mathrm{d}\widetilde{W}_\zeta^T(t)$, need to be determined.

A change of measure from the spot to the T-forward measure requires a change of numéraire from the money-savings account, $M(t)$, to the zero-coupon bond, $P(t,T)$. In the model we assumed non-zero correlations between interest rates and equity, and all the processes within each asset class, which implies that all processes, except the variance, will change their dynamics by changing the measure.

Before we determine the dynamics under the changed numéraire let us recall two important theorems:

Theorem 3.3.1 (Radon-Nikodym derivative)**.** *Let $\mathbb{Q}^N$ be the equivalent martingale measure with respect to numéraire $N(t)$. Let $\mathbb{Q}^M$ be the equivalent martingale measure with respect to numéraire $M(t)$. The Radon-Nikodym derivative that allows us to change equivalent martingale measure $\mathbb{Q}^M$ into $\mathbb{Q}^N$ is given by:*

$$\Lambda_M^N(t) := \left.\frac{\mathrm{d}\mathbb{Q}^N}{\mathrm{d}\mathbb{Q}^M}\right|_{\mathcal{F}(t)} = \frac{N(t)}{N(0)}\frac{M(0)}{M(t)}.$$

Proof. The proof can be found in [41]. ■

Theorem 3.3.2 (Girsanov theorem)**.** *For any stochastic process $y(t)$ for which*

$$\int_0^t y^2(s)\mathrm{d}s < \infty,$$

with probability one, we define the Radon-Nikodym derivative

$$\Lambda_{\mathbb{Q}}^*(t) = \left.\frac{\mathrm{d}\mathbb{Q}^*}{\mathrm{d}\mathbb{Q}}\right|_{\mathcal{F}(t)},$$

given by:

$$\Lambda^*_{\mathbb{Q}}(t) = \exp\left(\int_0^t y(s)\mathrm{d}W^{\mathbb{Q}}(s) - \frac{1}{2}\int_0^t y^2(s)\mathrm{d}s\right),$$

where $W^{\mathbb{Q}}(t)$ is a Brownian motion under the measure $\mathbb{Q}$. Under the measure $\mathbb{Q}^*$ the process

$$\mathrm{d}W^*(t) = \mathrm{d}W^{\mathbb{Q}}(t) - y(t)\mathrm{d}t,$$

is also a Brownian motion.

The lemma below provides us with the model dynamics under the T-forward measure, $\mathbb{Q}^T$.

Lemma 3.3.3 (The AH-G2++ model dynamics under the $\mathbb{Q}^T$-measure)**.** *Under the T-forward measure, the AH-G2++ model is described by the following dynamics:*

$$\begin{aligned} \frac{\mathrm{d}F(t)}{F(t)} &= \hat{\psi}_1(t)\mathrm{d}\widetilde{W}^T_r(t) + \hat{\psi}_2(t)\mathrm{d}\widetilde{W}^T_\zeta(t) + \psi_3(t)\sqrt{v(t)}\mathrm{d}\widetilde{W}^T_v(t) \qquad (3.25)\\ &\quad + \sqrt{v(t)\psi_4(t) + \psi_5(t)}\mathrm{d}\widetilde{W}^T_x(t), \qquad (3.26)\\ \mathrm{d}v(t) &= \kappa(\bar{v} - v(t))\mathrm{d}t + \gamma\sqrt{v(t)}\mathrm{d}\widetilde{W}^T_v(t), \end{aligned}$$

where $\hat{\psi}_1(t) = \psi_1(t) - (\rho_{r,\zeta}\varsigma C(t,T) + \eta B(t,T))$, $\hat{\psi}_2(t) = \psi_2(t) - \varsigma C(t,T)\sqrt{1-\rho^2_{r,\zeta}}$ and $\psi_i(t)$, $i = \{1,\ldots,5\}$ as in (3.24) with

$$\begin{aligned} \mathrm{d}r(t) &= \left(\hat{\theta}(t) + \zeta(t) - \beta r(t)\right)\mathrm{d}t + \eta\mathrm{d}\widetilde{W}^T_r(t),\\ \mathrm{d}\zeta(t) &= \left(-\lambda\zeta(t) + \varsigma\eta\rho_{r,\zeta}B(t,T) + \varsigma^2 C(t,T)\right)\mathrm{d}t + \varsigma\rho_{r,\zeta}\mathrm{d}\widetilde{W}^T_r(t)\\ &\quad + \varsigma\sqrt{1-\rho^2_{r,\zeta}}\mathrm{d}\widetilde{W}^T_\zeta(t), \end{aligned}$$

with $\hat{\theta}(t) = \theta(t) + \eta^2 B(t,T) + \rho_{r,\zeta}\eta\varsigma C(t,T)$, with a correlation matrix given in (3.4), and with $B(t,T)$, $C(t,T)$ in (3.16) and (3.17).

Since the interest rates are Gaussian, and in the corresponding SDEs the diffusion parts are independent of the state variables, the dimension of the underlying pricing problem is reduced under the T-forward measure (as the forward, $F(t)$, and the variance process, $v(t)$, do not contain $r(t)$ or $\zeta(t)$).

Proof. For a given state vector, $\mathrm{d}\mathbf{H}(t) = [\mathrm{d}r(t), \mathrm{d}\zeta(t), \mathrm{d}v(t), \mathrm{d}F(t)/F(t)]^{\mathrm{T}}$, we express the model in terms of the independent Brownian motions as:

$$\mathrm{d}\mathbf{H}(t) = \mu(\mathbf{H}(t))\mathrm{d}t + \mathbf{L}(t)\mathrm{d}\widetilde{\mathbf{W}}(t), \qquad (3.27)$$

where $\mu(\mathbf{H}(t))$ represents the drift for system $\mathrm{d}\mathbf{H}(t)$ and $\mathbf{L}(t)$ is defined in (3.20). Now, we determine the Radon-Nikodym derivative [41], $\Lambda^T_{\mathbb{Q}}(t)$,:

$$\Lambda^T_{\mathbb{Q}}(t) = \left.\frac{\mathrm{d}\mathbb{Q}^T}{\mathrm{d}\mathbb{Q}}\right|_{\mathcal{F}(t)} = \frac{P(t,T)M(0)}{P(0,T)M(t)}, \qquad (3.28)$$

where $P(t,T)$ is a zero-coupon bond as defined in (3.15) and $M(t)$ is the money-savings account. By calculating the Itô derivative of Equation (3.28) we get:

$$\frac{\mathrm{d}\Lambda_{\mathbb{Q}}^T(t)}{\Lambda_{\mathbb{Q}}^T(t)} = \eta B(t,T)\mathrm{d}W_r(t) + \varsigma C(t,T)\mathrm{d}W_\zeta(t),$$

which, in terms of the independent Brownian motions, is given by:

$$\begin{aligned}\frac{\mathrm{d}\Lambda_{\mathbb{Q}}^T(t)}{\Lambda_{\mathbb{Q}}^T(t)} &= \eta B(t,T)\mathrm{d}\widetilde{W}_r(t) + \varsigma C(t,T)\left(\rho_{r,\zeta}\mathrm{d}\widetilde{W}_r(t) + \sqrt{1-\rho_{r,\zeta}^2}\mathrm{d}\widetilde{W}_\zeta(t)\right)\\ &= \Big(\eta B(t,T) + \rho_{r,\zeta}\varsigma C(t,T)\Big)\mathrm{d}\widetilde{W}_r(t) + \varsigma C(t,T)\sqrt{1-\rho_{r,\zeta}^2}\mathrm{d}\widetilde{W}_\zeta(t).\end{aligned}$$

The representation above shows the *Girsanov kernel* which describes the transition from $\mathbb{Q}$ to $\mathbb{Q}^T$, i.e.,

$$\mathrm{d}\widetilde{\mathbf{W}}^T(t) = \Xi(t)\mathrm{d}t + \mathrm{d}\widetilde{\mathbf{W}}(t).$$

So,

$$\mathrm{d}\widetilde{\mathbf{W}}(t) := \begin{bmatrix}\mathrm{d}\widetilde{W}_r(t)\\ \mathrm{d}\widetilde{W}_\zeta(t)\\ \mathrm{d}\widetilde{W}_v(t)\\ \mathrm{d}\widetilde{W}_x(t)\end{bmatrix} = \begin{bmatrix}\mathrm{d}\widetilde{W}_r^T(t)\\ \mathrm{d}\widetilde{W}_\zeta^T(t)\\ \mathrm{d}\widetilde{W}_v^T(t)\\ \mathrm{d}\widetilde{W}_x^T(t)\end{bmatrix} + \begin{bmatrix}\eta B(t,T) + \rho_{r,\zeta}\varsigma C(t,T)\\ \varsigma C(t,T)\sqrt{1-\rho_{r,\zeta}^2}\\ 0\\ 0\end{bmatrix}\mathrm{d}t. \tag{3.29}$$

Now, by substitution of $\mathrm{d}\widetilde{\mathbf{W}}(t)$ from (3.29) in (3.27) and appropriate substitutions the proof of Lemma 3.3.3 is finalized. ■

3.3.3 The log-transform and the characteristic function

Under the log-transform, $x^T(t) := \log F(t)$, we obtain the following model dynamics:

$$\begin{aligned}\mathrm{d}x^T(t) = & -\frac{1}{2}\left(\hat{\psi}_1^2(t) + \hat{\psi}_2^2(t) + \psi_5(t) + v(t)\left(\psi_3^2(t) + \psi_4(t)\right)\right)\mathrm{d}t + \hat{\psi}_1(t)\mathrm{d}\widetilde{W}_r^T(t)\\ & + \hat{\psi}_2(t)\mathrm{d}\widetilde{W}_\zeta^T(t) + \psi_3(t)\sqrt{v(t)}\mathrm{d}\widetilde{W}_v^T(t) + \sqrt{v(t)\psi_4(t) + \psi_5(t)}\mathrm{d}\widetilde{W}_x^T(t), \qquad (3.30)\\ \mathrm{d}v(t) = & \ \kappa(\bar{v} - v(t))\mathrm{d}t + \gamma\sqrt{v(t)}\mathrm{d}\widetilde{W}_v^T(t), \qquad (3.31)\end{aligned}$$

with independent Brownian motions, $\mathrm{d}\widetilde{W}_r^T(t)$, $\mathrm{d}\widetilde{W}_\zeta^T(t)$, $\mathrm{d}\widetilde{W}_v^T(t)$ and $\mathrm{d}\widetilde{W}_x^T(t)$. The remaining parameters are as in (3.18). With the closed-form expressions for $\hat{\psi}_1(t)$, $\hat{\psi}_2(t)$, $\psi_3(t)$, $\psi_4(t)$ and $\psi_5(t)$:

$$\begin{aligned}\hat{\psi}_1(t) &= \mathbf{U}_{4,1}\mathbb{E}(\sqrt{v(t)}) - (\rho_{r,\zeta}\varsigma C(t,T) + \eta B(t,T)),\\ \hat{\psi}_2(t) &= \mathbf{U}_{4,2}\mathbb{E}(\sqrt{v(t)}) - \varsigma C(t,T)\sqrt{1-\rho_{r,\zeta}^2},\\ \psi_3(t) &= \mathbf{U}_{4,3},\\ \psi_4(t) &= 1 - \mathbf{U}_{4,3}^2,\\ \psi_5(t) &= -\mathbb{E}^2(\sqrt{v(t)})\left(\mathbf{U}_{4,1}^2 + \mathbf{U}_{4,2}^2\right),\end{aligned}$$

and $\mathbf{U}$ the Cholesky matrix in (3.21), the dynamics in (3.30) can be simplified:

$$\begin{aligned}\mathrm{d}x^T(t) &= \frac{1}{2}\left(\chi(t,T)-v(t)\right)\mathrm{d}t+\hat{\psi}_1(t)\mathrm{d}\widetilde{W}_r^T(t)+\hat{\psi}_2(t)\mathrm{d}\widetilde{W}_\zeta^T(t)+\psi_3(t)\sqrt{v(t)}\mathrm{d}\widetilde{W}_v^T(t)\\ &\quad+\sqrt{v(t)\psi_4(t)+\psi_5(t)}\mathrm{d}\widetilde{W}_x^T(t),\end{aligned}$$

with:

$$\begin{aligned}\chi(t,T) &= -\varsigma^2C^2(t,T)-\eta^2B^2(t,T)-2\rho_{r,\zeta}\varsigma\eta B(t,T)C(t,T)\\ &\quad+2\mathbb{E}(\sqrt{v(t)})\Big(\rho_{x,r}\eta B(t,T)+\rho_{x,\zeta}\varsigma C(t,T)\Big).\end{aligned}\tag{3.32}$$

For the log-forward, $x^T(t)$, the Fokker-Planck equation for $V := V(t,\mathbf{H}(t))$ with $\mathbf{H}(t)=[x^T(t),v(t)]^{\mathrm{T}}$ is given by:

$$\begin{aligned}-\frac{\partial V}{\partial t} &= \kappa(\bar{v}-v)\frac{\partial V}{\partial v}+\frac{1}{2}\left(v-\chi(t,T)\right)\left(\frac{\partial^2 V}{\partial x^2}-\frac{\partial V}{\partial x}\right)\\ &\quad+\frac{1}{2}\gamma^2 v\frac{\partial^2 V}{\partial v^2}+\rho_{x,v}\gamma v\frac{\partial^2 V}{\partial x\partial v},\end{aligned}\tag{3.33}$$

with the deterministic, time-dependent function $\chi(t,T)$ in (3.32).

For the affine model, with $\tau=T-t$, the forward characteristic function is of the following form:

$$\phi^T(u,x^T(t),\tau)=\mathbb{E}^T\left(\mathrm{e}^{iux^T(T)}|\mathcal{F}(t)\right)=\mathrm{e}^{\hat{A}(u,\tau)+\hat{B}(u,\tau)x^T(t)+\hat{C}(u,\tau)v(t)},\tag{3.34}$$

with terminal condition $\phi^T(u,x^T(T),0)=\mathrm{e}^{iux^T(T)}$. Functions $\hat{A}(u,\tau)$, $\hat{B}(u,\tau)$ and $\hat{C}(u,\tau)$ satisfy, using $\hat{\mathbf{B}}(u,\tau)=[\hat{B}(u,\tau),\hat{C}(u,\tau)]^{\mathrm{T}}$, the following Riccati ordinary differential equations:

$$\begin{aligned}\hat{B}'(\tau) &= 0,\\ \hat{C}'(\tau) &= 1/2(\hat{B}^2(\tau)-\hat{B}(\tau))+(\rho_{x,v}\gamma\hat{B}(\tau)-\kappa)\hat{C}(\tau)+1/2\gamma^2\hat{C}^2(\tau),\\ \hat{A}'(\tau) &= \kappa\bar{v}\hat{C}(\tau)-1/2\chi(t,T)(\hat{B}^2(\tau)-\hat{B}(\tau)),\end{aligned}$$

with $\chi(t,T)$ in (3.32), $\hat{B}(0)=iu$, $\hat{C}(0)=0$ and $\hat{A}(0)=0$. The ODEs are of *Heston-type*, so that the solution is given in closed-form as $\hat{B}(u,\tau)=iu$,

$$\hat{C}(u,\tau)=\frac{1-\mathrm{e}^{-d_1\tau}}{\gamma^2\left(1-g\mathrm{e}^{-d_1\tau}\right)}\left(\kappa-\rho_{x,v}\gamma iu-d_1\right),\tag{3.35}$$

and for $\hat{A}(u,\tau)$ we find:

$$\begin{aligned}\hat{A}(u,\tau) &= \frac{\kappa\bar{v}}{\gamma^2}\left[\left(\kappa-\rho_{x,v}\gamma iu-d_1\right)\tau-2\log\left(\frac{1-g\mathrm{e}^{-d_1\tau}}{1-g}\right)\right]\\ &\quad+\frac{1}{2}(u^2+iu)\int_0^\tau\chi(T-s,T)\mathrm{d}s,\end{aligned}\tag{3.36}$$

with $d_1 = \sqrt{(\rho_{x,v}\gamma iu - \kappa)^2 + \gamma^2(u^2+iu)}$, and $g = \frac{-\rho_{x,v}\gamma iu + \kappa - d_1}{-\rho_{x,v}\gamma iu + \kappa + d_1}$, and $\chi(t,T)$ defined in (3.32).

The integral in (3.36) of the deterministic function $\chi(t,T)$ can be calculated explicitly. This integral does not contain the Fourier argument "u" which implies that for pricing a whole strip of strikes, one computation suffices. This is an advantage compared to other hybrid models, like the Schöbel-Zhu-Hull-White model, where each argument, u, requires the calculation of an integral.

Remark (Extension to an n-factor affine model). In Section 3.3.2 we have shown that switching between the measures, from the spot to the forward, reduces the complexity of the corresponding PDE for the forward price, $F(t)$, considerably. By taking Gaussian interest rates the forward dynamics $\mathrm{d}F(t)$ do not depend on interest rate variables, as only volatility coefficients from the interest rate processes are present. The generalization from a two-factor interest rate model to an n-factor model does therefore not complicate the pricing problem- it is merely a change of coefficients.

It is easy to deduce that under the AH-Gn++ model the Fokker-Planck equation for $V(t) := V(t,\mathbf{H}(t))$ with $\mathbf{H}(t) = [x^T(t), v(t)]^{\mathrm{T}}$ is given by:

$$\begin{aligned} -\frac{\partial V}{\partial t} &= \kappa(\bar{v}-v)\frac{\partial V}{\partial v} + \frac{1}{2}\left(v - \hat{\chi}(t,T)\right)\left(\frac{\partial^2 V}{\partial x^2} - \frac{\partial V}{\partial x}\right) \\ &\quad + \frac{1}{2}\gamma^2 v\frac{\partial^2 V}{\partial v^2} + \rho_{x,v}\gamma v\frac{\partial^2 V}{\partial x \partial v}, \end{aligned} \tag{3.37}$$

with function $\hat{\chi}(t,T)$ given by:

$$\begin{aligned} \hat{\chi}(t,T) = &-\sum_{i=1}^{n-1}\sum_{j=1}^{n-1}\rho_{\zeta_i,\zeta_j}\varsigma_i\varsigma_j C_i(t,T)C_j(t,T) - 2\eta B(t,T)\sum_{k=1}^{n-1}\rho_{r,\zeta_k}\varsigma_k C_k(t,T) \\ &-\eta^2 B^2(t,T) + 2\mathbb{E}(\sqrt{v(t)})\Big(\rho_{x,r}\eta B(t,T) + \sum_{k=1}^{n-1}\rho_{x,\zeta_k}\varsigma_k C_k(t,T)\Big), \end{aligned} \tag{3.38}$$

with $B(t,T)$ and $C_k(t,T)$ defined in (3.16) and (3.17), expectation $\mathbb{E}(\sqrt{v(t)})$ from Equation (3.22) and all the parameters as defined in (3.2) and (3.3).

Since the PDE structure in (3.37) of the AH-Gn++ model is the same as for the AH-G2++ model in (3.5), the results from Section 3.3.3 can directly be used (only the function $\chi(t,T)$ in (3.36) needs to be replaced by $\hat{\chi}(t,T)$ from (3.38)).

Positive definiteness of the covariance matrix $\mathbf{\Sigma_H}$

When performing a simulation of a model, either by a Monte Carlo method or by finite-differences for the associated PDE, the corresponding covariance matrix needs to be defined properly.

Since $\mathbf{L}(t)$ in the AH-G2++ model is obtained from the Cholesky decomposition of the covariance matrix, $\mathbf{L}(t)\mathbf{L}(t)^{\mathrm{T}} = \mathbf{\Sigma_H}$, we need to determine under which conditions matrix $\mathbf{\Sigma_H}$ is positive-definite.

Positive definiteness of the covariance matrix is necessary for performing a Monte Carlo simulation.

Since we deal with a 2×2 covariance matrix (by the change of measure the number of state variables was reduced from four to two), we use Sylvester's criterion to determine whether the covariance matrix is positive-definite. For 2×2-matrix the criterion states that a Hermitian matrix is positive-definite if the upper left element of matrix $\mathbf{\Sigma_H}$ and matrix $\mathbf{\Sigma_H}$ itself have positive determinants.

The covariance matrix $\mathbf{\Sigma_H}$ is given by:

$$\mathbf{\Sigma_H} = \frac{1}{2}\begin{bmatrix} (v(t) - \chi(t,T)) & \rho_{x,v}\gamma v(t) \\ \rho_{x,v}\gamma v(t) & \gamma^2 v(t) \end{bmatrix},$$

with $\chi(t,T)$ in (3.32).

We check when $v(t) > \chi(t,T)$. Since we deal with a non-negative square-root process for $v(t)$, the expression on the left-hand side is always non-negative, i.e., $v(t) \geq 0$. By (3.32) we can rewrite $\chi(t,T)$ as:

$$\begin{aligned} \chi(t,T) \quad = \quad & -\left(\varsigma C(t,T) + \rho_{r,\zeta}\eta B(t,T)\right)^2 - \eta^2 B^2(t,T)\left(1 - \rho_{r,\zeta}^2\right) \\ & +2\mathbb{E}(\sqrt{v(t)})\Big(\rho_{x,r}\eta B(t,T) + \rho_{x,\zeta}\varsigma C(t,T)\Big). \end{aligned}$$

Since $B(t,T) \leq 0$ and $C(t,T) \leq 0$ for any $t \leq T$ and $\lambda > 0$, $\beta > 0$, by setting $\rho_{x,r} > 0$ and $\rho_{x,\zeta} > 0$ the expression for $\chi(t,T)$ is negative guaranteeing that the condition for positive-definiteness is satisfied. In the case $\rho_{x,r} < 0$ or $\rho_{x,\zeta} < 0$, the inequality $v(t) > \chi(t,T)$ needs to be satisfied, which is typically not a problem, especially for large values of $v(t)$.

For the determinant of matrix $\mathbf{\Sigma_H}$ we find:

$$\det \mathbf{\Sigma_H} = \gamma^2 v(t)\left(v(t) - \chi(t,T)\right) - \rho_{x,v}^2\gamma^2 v^2(t) \quad > \quad 0,$$

which can be expressed as:

$$v(t)(1 - \rho_{x,v}^2) \quad > \quad \chi(t,T). \tag{3.39}$$

As before the left-hand side of Inequality (3.39) is positive for $|\rho_{x,v}| < 1$ and $v(t) > 0$ whereas $\chi(t,T)$ is negative for the conditions described before.

3.3.4 European option pricing and hedging

European option prices can be obtained highly efficiently by use of the COS pricing method from Chapter 1, which is based on the availability of the characteristic function.

From the general risk-neutral pricing formula the price of any European claim, $V(T, F(T))$, defined in terms of the underlying stock process, $F(T)$, can be written as:

$$V(t, F(t)) \approx P(t,T)\sum_{n=0}^{N_c}\omega_n \Re\left(\phi^T\left(kn, x^T(t), \tau\right)\mathrm{e}^{-iknb_1}\right)\Gamma_n^{b_1,b_2}, \tag{3.40}$$

where the coefficients $\Gamma_n^{b_1,b_2}$ are known analytically for European options, see Chapter 1 for details.

An important asset of the AH-G2++ model is the availability of the corresponding characteristic function so that we can calibrate the model fast and efficiently to plain vanilla contracts. We can also price certain exotic contracts, whose pricing can be related to the characteristic function. Moreover, Greeks can be derived easily for European contracts.

The Greeks determine the price sensitivities to changes in the underlying model parameters. We provide formulas for Delta, Δ_{G}, Gamma, Γ_{G}, and the sensitivities to the correlations, $\rho_{x,r}$, $\rho_{x,\zeta}$ and $\rho_{r,\zeta}$.

From the definition of a delta hedge we have:

$$\Delta_{\mathrm{G}} := \frac{\partial V(t,x^T(t))}{\partial S(t)} = \frac{\partial V(t,x^T(t))}{\partial F(t)}\frac{\partial F(t)}{\partial S(t)} = \frac{1}{P(t,T)}\frac{\partial V(t,x^T(t))}{\partial F(t)}.$$

With $u = kn$, the characteristic function of the AH-G2++ model reads:

$$\phi^T(kn, x^T(t), \tau) = \exp\Big(ikn\log(F(t)) + \hat{C}(kn,\tau)v(t) + \hat{A}(kn,\tau)\Big), \tag{3.41}$$

with $\hat{C}(kn,\tau)$ and $\hat{A}(kn,\tau)$ from (3.35), (3.36) and Equation (3.40), so that we have:

$$\Delta_{\mathrm{G}} \approx \frac{1}{F(t)}\sum_{n=0}^{N_c}\omega_n\Re\Big\{\phi^T\left(kn, x^T(t),\tau\right)\mathrm{e}^{-iknb_1}ikn\Big\}\Gamma_n^{b_1,b_2},$$

with $k = \pi/(b_2 - b_1)$.

For Gamma, $\Gamma_{\mathrm{G}} = \dfrac{\partial \Delta_{\mathrm{G}}}{\partial S(t)}$ we find:

$$\Gamma_{\mathrm{G}} \approx \frac{1}{P(t,T)}\frac{1}{F^2(t)}\sum_{n=0}^{N_c}\omega_n\Re\left\{\phi^T\left(kn, x^T(t),\tau\right)\mathrm{e}^{-ib_1kn}\Big((ikn)^2 - ikn\Big)\right\}\Gamma_n^{b_1,b_2}.$$

For the derivatives with respect to correlation, which we call [1] Rho(ρ), for $\rho = \{\rho_{x,r}, \rho_{x,\zeta}, \rho_{r,\zeta}\}$, we find:

$$\mathrm{Rho}(\rho) := \frac{\partial}{\partial\rho}V(t,x) \approx P(t,T)\sum_{n=0}^{N_c}\omega_n\Re\left\{\phi^T\left(kn, x^T(t),\tau\right)\mathrm{e}^{-ib_1kn}\frac{\partial}{\partial\rho}\hat{A}(kn,\tau)\right\}\Gamma_n^{b_1,b_2},$$

with $\hat{A}(kn,\tau)$ as in (3.41).

Depending on different correlations, $\rho = \{\rho_{x,r}, \rho_{x,\zeta}, \rho_{r,\zeta}\}$, we determine three partial derivatives $\frac{\partial}{\partial\rho}A(kn,\tau)$:

$$\begin{aligned}
\frac{\partial}{\partial\rho_{x,r}}\hat{A}(kn,\tau) &= \eta((kn)^2 + ikn)\int_0^\tau \mathbb{E}(\sqrt{v(T-s)})B(T-s,T)\mathrm{d}s,\\
\frac{\partial}{\partial\rho_{x,\zeta}}\hat{A}(kn,\tau) &= \varsigma((kn)^2 + ikn)\int_0^\tau \mathbb{E}(\sqrt{v(T-s)})C(T-s,T)\mathrm{d}s,\\
\frac{\partial}{\partial\rho_{r,\zeta}}\hat{A}(kn,\tau) &= -\varsigma\eta((kn)^2 + ikn)\int_0^\tau B(T-s,T)C(T-s,T)\mathrm{d}s,
\end{aligned}$$

[1] not to be confused with the derivative with respect to interest rate in a standard Black-Scholes model which is also called "rho"

with $B(t,T)$ defined in (3.16) and $C(t,T)$ in (3.17).

Here, we check the effect of correlations on the Greeks for a basic call option under the AH-G2++ model. We perform two experiments. First of all, in Figure 3.1(a), we show Δ_{G}, Γ_{G}, Rho($\rho_{x,r}$), Rho($\rho_{x,\zeta}$) and Rho($\rho_{r,\zeta}$). Secondly, in Figure 3.1(b) we vary the correlation between stock and the interest rate, $\rho_{x,r}$, and present the effect on Δ_{G}. In the experiments we consider a maturity of 15 years, $T = 15$, and a discount factor $P(0,T) = \exp(-0.06T)$ with the following set of parameters, $S(0) = 1$, $\kappa = 0.3$, $\bar{v} = 0.02$, $\gamma = 0.251$, $\beta = 0.03$, $\eta = 0.02$, $\lambda = 1.1$ and $\varsigma = 0.02$. The correlation structure is set as follows:

$$\begin{bmatrix} 1 & \rho_{x,v} & \rho_{x,r} & \rho_{x,\zeta} \\ * & 1 & 0 & 0 \\ * & * & 1 & \rho_{r,\zeta} \\ * & * & * & 1 \end{bmatrix} = \begin{bmatrix} 1 & -30\% & 20\% & 10\% \\ * & 1 & 0 & 0 \\ * & * & 1 & -90\% \\ * & * & * & 1 \end{bmatrix}.$$

The experiments indicate that when hedging these long-maturity European

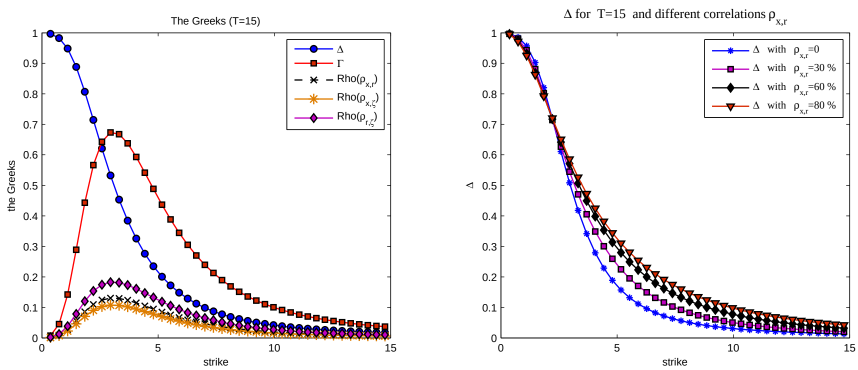

Figure 3.1: *(a) Several Greek values for a call option. (b) Effect on delta of correlation, $\rho_{x,r}$, for a call option. For $T = 15$ the forward price $F(0) \approx 2.46$.*

options, the correlation between stock and interest rates, $\rho_{x,r}$, has a significant effect on a hedge. Figure 3.1(b) also shows that if one assumes $\rho_{x,r} = 0$ and performs delta hedging, the portfolio will be under/over hedged if the correlation is non-zero in reality.

In order to explain the increase of Δ_{G} as $\rho_{x,r}$ increases, we need to look at the underlying forward price, $F(t)$. The forward dynamics, $\mathrm{d}F(t)/F(t)$, in Lemma 3.3.3 can be expressed as:

$$\frac{\mathrm{d}F(t)}{F(t)} = \sqrt{\Omega_1(t) - 2\rho_{x,r}\eta\mathbb{E}(\sqrt{v(t)})B(t,T)}\mathrm{d}W_F^T(t), \tag{3.42}$$

with

$$\begin{aligned} \Omega_1(t) &= v(t) + \varsigma^2 C^2(t,T) + \eta^2 B^2(t,T) + 2\rho_{r,\zeta}\varsigma\eta B(t,T)C(t,T) \\ &\quad -2\rho_{x,\zeta}\varsigma\mathbb{E}(\sqrt{v(t)})C(t,T), \end{aligned}$$

and *another* Brownian motion $\mathrm{d}W_F^T(t)$.

Assuming that all the parameters are constants, we analyze how the volatility term in front of $\mathrm{d}W_F(t)$ in (3.42) behaves for different correlations $\rho_{x,r}$. We find that for any set of parameters $\mathbb{E}(\sqrt{v(t)}) > 0$ and $B(t,T) \leq 0$. Therefore an increase of the correlation $\rho_{x,r}$ is directly related to an increase of the volatility of the forward. This explains the additional hedging costs presented in Figure 3.1(b) in the presence of positive correlation between stock and the interest rate. The same pattern may be observed regarding $\rho_{x,\zeta}$ and $\rho_{r,\zeta}$.

3.3.5 Efficient Monte Carlo simulation

Here, we briefly discuss an efficient Monte Carlo simulation scheme for the AH-G2++ model. We will adopt the algorithm by Andersen (see [3]), originally developed for the pure Heston stochastic volatility model.

As presented in Lemma 3.3.3 the AH-G2++ (as well as the H-G2++) model can formulated as:

$$\begin{aligned}\frac{\mathrm{d}F(t)}{F(t)} &= \hat{\psi}_1(t)\mathrm{d}\widetilde{W}_r^T(t) + \hat{\psi}_2(t)\mathrm{d}\widetilde{W}_\zeta^T(t) + \rho_{x,v}\sqrt{v(t)}\mathrm{d}\widetilde{W}_v^T(t)\\ &\quad+\sqrt{v(t)\left(1-\rho_{x,v}^2\right)+\psi_5(t)}\mathrm{d}\widetilde{W}_x^T(t),\\ \mathrm{d}v(t) &= \kappa(\bar{v}-v(t))\mathrm{d}t + \gamma\sqrt{v(t)}\mathrm{d}\widetilde{W}_v^T(t),\end{aligned}$$

with

$$\begin{aligned}\hat{\psi}_1(t) &= \mathbf{U}_{4,1}\alpha(t) - (\rho_{r,\zeta}\varsigma C(t,T) + \eta B(t,T)),\\ \hat{\psi}_2(t) &= \mathbf{U}_{4,2}\alpha(t) - \varsigma C(t,T)\sqrt{1-\rho_{r,\zeta}^2},\\ \psi_5(t) &= -\alpha^2(t)\left(\mathbf{U}_{4,1}^2 + \mathbf{U}_{4,2}^2\right),\end{aligned}$$

and $\mathbf{U}_{4,1}$, $\mathbf{U}_{4,2}$ are defined in (3.21). We have $\alpha(t) = \mathbb{E}(\sqrt{v(t)})$ for the AH-G2++ model (and $\alpha(t) = \sqrt{v(t)}$ for the H-G2++ model). Since the difference between the AH-G2++ and the H-G2++ model appears only in function $\alpha(t)$ the Monte Carlo schemes are very similar.

In both models the dynamics for the forward, $F(t)$, do not depend on the interest rate processes, $r(t)$ or $\zeta(t)$. This implies that for Monte Carlo paths for $F(t)$ only the 2D stochastic differential equations for the forward, $F(t)$, and its variance process, $v(t)$, need to be discretized.

Since the Brownian motions in the models are independent, we can perform a simplifying factorization,

$$\begin{aligned}\frac{\mathrm{d}F(t)}{F(t)} &= \sqrt{\hat{\psi}_1^2(t) + \hat{\psi}_2^2(t) + v(t)\left(1-\rho_{x,v}^2\right) + \psi_5(t)}\mathrm{d}\widetilde{W}_F^T(t) + \rho_{x,v}\sqrt{v(t)}\mathrm{d}\widetilde{W}_v^T(t),\\ \mathrm{d}v(t) &= \kappa(\bar{v}-v(t))\mathrm{d}t + \gamma\sqrt{v(t)}\mathrm{d}\widetilde{W}_v^T(t),\end{aligned}$$

with $\mathrm{d}\widetilde{W}_F^T(t)$ independent of $\mathrm{d}\widetilde{W}_v^T(t)$.

In log-transformed coordinates, $x^T(t) = \log F(t)$, we find with Itô's lemma:

$$\mathrm{d}x^T(t) = \frac{1}{2}\left(\chi(t,T) - v(t)\right)\mathrm{d}t + \sqrt{\xi_1(t,v(t))}\mathrm{d}\widetilde{W}_F^T(t) + \rho_{x,v}\sqrt{v(t)}\mathrm{d}\widetilde{W}_v^T(t), \quad (3.43)$$

with $\xi_1(t,v(t)) = -\chi(t,T) + v(t) - \rho_{x,v}^2 v(t)$, where

$$\begin{aligned}\chi(t,T) \quad &:= \quad -\varsigma^2 C^2(t,T) - \eta^2 B^2(t,T) - 2\rho_{r,\zeta}\varsigma\eta B(t,T)C(t,T) \\ &\qquad +2\alpha(t)\Big(\rho_{x,r}\eta B(t,T) + \rho_{x,\zeta}\varsigma C(t,T)\Big),\end{aligned}$$

and $\alpha(t) = \sqrt{v(t)}$ for the H-G2++ model or $\alpha(t) = \mathbb{E}(\sqrt{v(t)})$ for the AH-G2++ model.

The variance process, $v(t)$, is independent of the interest rates processes, $r(t)$ and $\zeta(t)$. For $t > 0$, $v(t)$ is from a non-central chi-square distribution [25]. The direct sampling of $v(t)$ can be very efficiently performed with the Quadratic Exponential (QE) scheme proposed in [3].

In order to obtain a bias-free scheme (see [20]) for sampling the forward price process, it is convenient to first integrate the SDE for $v(t)$, i.e:

$$v(t+\delta) = v(t) + \int_t^{t+\delta} \kappa(\bar{v} - v(s))\mathrm{d}s + \gamma\int_t^{t+\delta}\sqrt{v(s)}\mathrm{d}\widetilde{W}_v^T(s). \quad (3.44)$$

Process $x^T(t)$ from (3.43) can be expressed in integral form as:

$$\begin{aligned}x^T(t+\delta) \quad &= \quad x^T(t) + \frac{1}{2}\int_t^{t+\delta}\left(\chi(s,T) - v(s)\right)\mathrm{d}s + \int_t^{t+\delta}\sqrt{\xi_1(s,v(s))}\mathrm{d}\widetilde{W}_F^T(s) \\ &\qquad +\rho_{x,v}\int_t^{t+\delta}\sqrt{v(s)}\mathrm{d}\widetilde{W}_v^T(s). \qquad (3.45)\end{aligned}$$

The last integral in (3.45) can easily be determined by Equation (3.44). In the discretization (3.45) we distinguish between time and stochastic-type integrals. These integrals can be handled as indicated in [3]: For a state-dependent function $f(t,v(t))$ the time integrals can be approximated by

$$\int_t^{t+\delta} f(t,v(s))\mathrm{d}s \approx \delta\Big(w_1 f(t,v(t)) + w_2 f(t+\delta, v(t+\delta))\Big),$$

with certain weights w_1 and w_2. For the stochastic integrals we have, with help of Itô's isometry,

$$\int_t^{t+\delta}\sqrt{\xi_1(s,v(s))}\mathrm{d}\widetilde{W}_F^T(s) \sim \mathcal{N}\Big(0, \int_t^{t+\delta}\xi_1(s,v(s))\mathrm{d}s\Big),$$

with $\mathcal{N}(a,b)$ indicating a normal distribution with mean a and variance b.

We note that an extension from a 2-factor interest rate process to n factors is trivial, since only the functions $\chi(s,T)$ and $\xi_1(s,v(s))$ then consist of more terms.

The scheme developed will be used in a number of experiments in the sections to follow.

3.4 Numerical experiments

In this section we focus on pricing of European options, and check the performance of the hybrid models when pricing an exotic hybrid derivative.

3.4.1 The AH-G2++ and the H-G2++ models for pricing long-term maturity options

In this experiment we check the performance of the H-G2++ model against its affine sister, the AH-G2++ model, for pricing plain vanilla options.

First of all, we generate European call prices with the H-G2++ hybrid model by a Monte Carlo simulation (from Section 3.3.5). Secondly, we compare, in terms of implied volatilities, with results from the AH-G2++ hybrid model obtained by the COS method. We consider two cases, one in which the model parameters satisfy the Feller condition for the stock and another experiment in which they do not satisfy this condition.

Experiment 3.4.1 (Feller's condition satisfied, $2\kappa\bar{v} > \gamma^2$)**.** We compare the results of the H-G2++ and AH-G2++ models. The parameters are chosen as:

$$\kappa = 0.8 \;\; \bar{v} = 0.2, \;\; \gamma = 0.2, \;\; \beta = 1.1, \;\; \eta = 0.01, \;\; \lambda = 0.8, \;\; \varsigma = 0.015,$$

and the correlation is given by:

$$\begin{bmatrix} 1 & \rho_{x,v} & \rho_{x,r} & \rho_{x,\zeta} \\ * & 1 & \rho_{v,r} & \rho_{v,\zeta} \\ * & * & 1 & \rho_{r,\zeta} \\ * & * & * & 1 \end{bmatrix} = \begin{bmatrix} 1 & -30\% & 35\% & 8\% \\ * & 1 & 0\% & 0\% \\ * & * & 1 & -40\% \\ * & * & * & 1 \end{bmatrix}.$$

The initial conditions are $S(0) = 1$ and $v(0) = \bar{v}$ with the initial yield given by $P(0,T) = \exp(-0.03T)$. With these parameters the Feller condition for the stock is satisfied. We choose four maturities $\tau = 1$, $\tau = 5$, $\tau = 10$ and $\tau = 20$. Table 3.1 shows an almost perfect correspondence between the volatilities from the Monte Carlo method (for the H-G2++ hybrid model) and the COS method (for the AH-G2++ model).

Experiment 3.4.2 (Feller's condition violated, $2\kappa\bar{v} \leq \gamma^2$)**.** In practice there are many cases in which the Feller condition is not satisfied. Therefore we check the performance of the affine hybrid model in such a setup. In this experiment we choose $\kappa = 0.4$, $\bar{v} = 0.2$ and $\gamma = 0.6$ and the remaining parameters are as in Experiment 3.4.1. The Feller condition does not hold in this case, as $0.16 \ngeq 0.36$. Therefore, the probability of hitting zero is positive. Table 3.2 shows that our tractable hybrid model, the AH-G2++, provides values close to the H-G2++ model.

These experiments, with standard parameters, show that the results of the AH-G2++ model resemble the results of the H-G2++ very well.

Remark. The AH-Gn++ and the H-Gn++ models differ only in the definition of function $\alpha(t)$ in the associated covariance matrix. This $\alpha(t)$ is multiplied either by $\rho_{x,r}\eta$ or by $\rho_{x,\zeta}\varsigma$. It is therefore evident that both models produce very similar results when either the correlations or the volatilities for the interest rates, ς,

Table 3.1: *Difference in implied volatilities between the H-G2++ (simulated with Monte Carlo) and the AH-G2++ (simulated with Fourier inversion). Numbers in brackets indicate standard deviations. The simulation was performed with Feller's condition satisfied.*

		Implied Volatility [%]		
T	Strike	H-G2++ (MC)	AH-G2++ (Fourier)	difference
1y	0.8869	44.81 (0.19)	44.79	-0.02 %
	0.9324	44.67 (0.23)	44.65	-0.02 %
	1.0305	44.40 (0.30)	44.38	-0.02 %
	1.1388	44.16 (0.38)	44.13	-0.03 %
	1.1972	44.04 (0.42)	44.01	-0.03 %
5y	0.8308	44.59 (0.11)	44.60	0.01 %
	0.9290	45.07 (0.12)	45.07	0.01 %
	1.1618	37.89 (0.15)	37.89	0.00 %
	1.4530	30.86 (0.23)	30.85	-0.01 %
	1.6248	27.52 (0.25)	27.50	-0.02 %
10y	0.8400	44.57 (0.09)	44.54	-0.02 %
	0.9839	44.44 (0.13)	44.42	-0.02 %
	1.3499	44.22 (0.25)	44.20	-0.02 %
	1.8519	44.00 (0.40)	43.99	0.02 %
	2.1692	43.90 (0.48)	43.88	0.01 %
20y	0.9316	44.55 (0.18)	44.49	-0.05 %
	1.1651	44.46 (0.22)	44.40	-0.06 %
	1.8221	44.31 (0.38)	44.24	-0.07 %
	2.8497	44.16 (0.45)	44.07	-0.08 %
	3.5638	44.08 (0.52)	44.00	-0.08 %

η, are *small*. Obviously the correlations are, by definition, bounded by 1. The volatilities for the short-rate models are on the other hand typically also of small size (values < 0.1 are often reported in the literature [19]). In the experiments to follow we check the model performance for unrealistically high volatilities to stress the proposed AH-G2++ model.

3.4.2 Pricing of a hybrid product

In this test we consider an equity-interest rate diversification hybrid product. This product is based on sets of assets with different expected returns and risk levels. The example is defined as:

$$\Pi(T_1, T) = \max\left(\hat{w}_1 S(T_1) + \hat{w}_2 P(T_1, T), 0\right), \tag{3.46}$$

where for $T_1 < T$, $S(T_1)$ is the underlying asset at time T_1, $P(T_1, T)$ is a zero-coupon bond which pays €1 at time T and $\hat{w}_1$ and $\hat{w}_2$ are weighting factors, which can be either positive (in a long position) or negative (in a short position).

The value of the contract in (3.46), at time t, under the risk-neutral measure $\mathbb{Q}$, can be expressed by:

$$\Pi(t, T) = M(t)\mathbb{E}^{\mathbb{Q}}\left(\frac{1}{M(T_1)} \max\left(\hat{w}_1 S(T_1) + \hat{w}_2 P(T_1, T), 0\right) \Big| \mathcal{F}(t)\right). \tag{3.47}$$

Table 3.2: *Difference in implied volatilities between the H-G2++ (simulated with Monte Carlo) and the AH-G2++ (simulated with Fourier inversion). Numbers in brackets indicate standard deviations. The simulation was performed with Feller's condition violated.*

	Implied Volatility [%]			
T	Strike	H-G2++ (MC)	AH-G2++ (Fourier)	difference
	0.8869	43.12 (0.15)	43.17	0.05 %
	0.9324	42.53 (0.16)	42.58	0.05 %
1y	1.0305	41.48 (0.16)	41.54	0.06 %
	1.1388	40.71 (0.20)	40.76	0.04 %
	1.1972	40.44 (0.26)	40.48	0.04 %
	0.8308	40.29 (0.08)	40.26	-0.03 %
	0.9290	39.59 (0.09)	39.54	-0.05 %
5y	1.1618	38.40 (0.13)	38.33	-0.08 %
	1.4530	37.59 (0.17)	37.48	-0.11 %
	1.6248	37.33 (0.17)	37.22	-0.11 %
	0.8400	39.82 (0.14)	39.71	-0.11 %
	0.9839	39.22 (0.17)	39.11	-0.11 %
10y	1.3499	38.17 (0.23)	38.06	-0.11 %
	1.8519	37.37 (0.35)	37.28	-0.10 %
	2.1692	37.09 (0.40)	37.01	-0.08 %
	0.9316	39.71 (0.06)	39.60	-0.11 %
	1.1651	39.24 (0.06)	39.13	-0.11 %
20y	1.8221	38.40 (0.15)	38.29	-0.11 %
	2.8497	37.73 (0.30)	37.62	-0.11 %
	3.5638	37.48 (0.41)	37.36	-0.12 %

Since the expectation in (3.47) contains a correlated stock, a zero-coupon bond, and the money-savings account this expectation is difficult to determine analytically.

However, by a change of numéraire, from the money-savings account to a zero-bond maturing at time T the expectation in (3.47) simplifies significantly.

The Radon-Nikodym derivative is known as:

$$\Lambda_{\mathbb{Q}}^{T}(T_1) = \frac{\mathrm{d}\mathbb{Q}^T}{\mathrm{d}\mathbb{Q}}\Big|_{\mathcal{F}(T_1)} = \frac{P(T_1,T)}{P(t,T)}\frac{M(t)}{M(T_1)}.$$

So, the price in (3.47) under the $T-$forward measure, $\mathbb{Q}^T$, reads:

$$\Pi(t,T) = P(t,T)\mathbb{E}^T\left(\frac{1}{P(T_1,T)}\max\left(\hat{w}_1 S(T_1) + \hat{w}_2 P(T_1,T), 0\right)\Big|\mathcal{F}(t)\right).$$

Since the forward $F(t)$ is defined as $F(t) = S(t)/P(t,T)$ the expectation above reduces to:

$$\Pi(t,T) = P(t,T)\mathbb{E}^T\left(\max\left(\hat{w}_1 F(T_1) + \hat{w}_2, 0\right)\Big|\mathcal{F}(t)\right). \tag{3.48}$$

We recognize that the expectation (3.48) is a call option on the forward with strike $K = -\hat{w}_2$ and a constant multiplier, $\hat{w}_1$ [2].

[2]The expectation (3.48) can also be written as: $\hat{w}_1\mathbb{E}^T\left(\max\left(F(T_1) + \frac{\hat{w}_2}{\hat{w}_1}, 0\right)\Big|\mathcal{F}(t)\right)$ where the ratio $\hat{w}_2/\hat{w}_1$ can be seen as a gearing factor.

Since we consider the affine Heston hybrid model, AH-G2++ here, we can simply determine the price of (3.48) by the COS method described in Chapter 1. The evaluation of such a payoff can be evaluated in a split-second.

We now perform the experiment in which we compare the performance of the H-G2++ and the AH-G2++ models for this hybrid product. For $T_1 = 5$ and $T = 8$ we choose the following set of parameters [3]: $\kappa = 0.25$, $\bar{v} = v(0) = 0.0625$, $\gamma = 0.625$, $\beta = 0.05$, $\eta = 0.03$, $\lambda = 0.4$, $\varsigma = 0.05$, $\rho_{x,v} = -30\%$ and $\rho_{r,\zeta} = -20\%$. The zero-coupon bond $P(0,T) = \exp(-0.03T)$ and $\rho_{x,r} = \rho_{x,\zeta}$. The prices for the hybrid product $\Pi(t,T)$ in (3.48) are calculated for different correlations between stock and the interest rate, $\rho_{x,r}$. For the payoff we take $\hat{w}_1 = 1$ and $\hat{w}_2 = \{-4,\dots,0\}$ and evaluate Monte Carlo prices with 100.000 paths and $10T_1$ time-steps for the H-G2++ model and by the Fourier expansion for the AH-G2++ model. The output is presented in Figure 3.2(a).

In Figure 3.2(b) the results for an extreme parameter setting are presented. In this experiment we have taken a high volatility for the interest rates $\eta = 0.25$ (whereas typically $\eta, \varsigma < 0.25$ as presented in [19]). We report that for such an extreme parameter set the AH-G2++ model provides results which agree rather well with those obtained by the H-G2++ model. This is another indication of the highly satisfactory performance of AH-G2++.

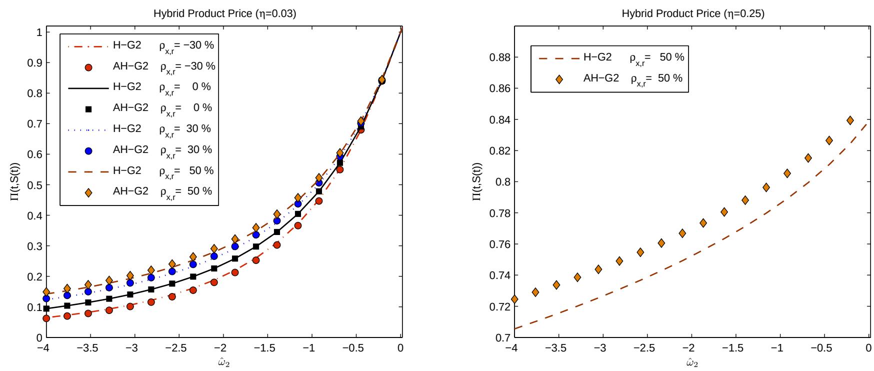

Figure 3.2: *Prices generated by the H-G2++ and the AH-G2++ models. LEFT: results for $\eta = 0.03$, RIGHT: results for $\eta = 0.25$.*

3.5 Conclusion

In this chapter we have constructed an equity-interest rate hybrid model with non-zero correlation between the asset classes. The model is defined in the class of affine diffusion processes so that we can determine a closed-form characteristic function. By defining the affine hybrid Heston model under the forward measure, we can price several financial derivative products as easily as under the plain Heston model.

[3] The stochastic volatility parameters are chosen as in [7].

For the affine Heston-Gaussian multi-factor model, AH-Gn++, we have discussed an efficient Monte Carlo simulation scheme and a way for calculating the Greeks of plain vanilla options. We have also shown that the AH-Gn++ model provides prices similar to the (non-affine) Heston-Gaussian multi-factor (H-Gn++) model and superior (as shown in Chapter 2) to Schöbel-Zhu variants if the Feller condition is violated.

CHAPTER 4

An Equity-Interest Rate Hybrid Model with Stochastic Volatility and Interest Rate Smile

When you smile, I don't know what to do
Cause I could lose everything in a minute or two
And it seems like the end of the world...
When you smile

Dream Syndicate ("When you smile")

4.1 Introduction

In Chapters 2 and 3 the extension of the Heston model with stochastic interest rates was established by using short-rate processes, like Hull-White or multi-factor models. These interest rate models cannot generate implied volatility smiles or skews as commonly observed in the interest rate market. For hybrid products that are exposed to the interest rate smile, more involved models are required. In the present chapter we develop such a hybrid model.

For several years the log-normal Libor Market Model (LMM) [18, 63, 79] has established itself as a benchmark for interest-rate derivatives. Without enhancements this model is also not able to incorporate strike-dependent volatilities of fixed income derivatives, such as caps and swaptions. An important step forward in the modelling were the local volatility-type [4], and the stochastic volatility extensions [4, 5, 94], with which a model can be fitted reasonably well to market data, while the model's stability can still be guaranteed.

In the literature a number of stochastic volatility extensions of LMM have been presented, see e.g., Brigo and Mercurio [19]. The model on which our work is based is the displaced-diffusion stochastic volatility (DD-SV) model developed by Andersen and Andreasen [5]. It was Piterbarg's paper [92] which connected the time-dependent model volatilities and skews for Libor and swap rates to the market implied quantities. The concept in [92] of *effective skew* and *effective volatility* enables the calibration of the volatility smiles for a grid of swaptions.

In this chapter we develop an equity-interest rate hybrid model with equity modeled by the Heston model and the interest rate driven by the Libor Market Model, namely, by the displaced-diffusion-stochastic-volatility model (DD-SV) [5]. In practice, the equity calibration is performed with an a-priori calibrated interest rate model. Therefore a very efficient and fast model evaluation is mandatory.

By changing the measure from the risk-neutral to the forward measure, associated with the zero-coupon bond as the numéraire, the dimension of the approximating characteristic function can be significantly reduced (as it was shown in Chapter 3). This, combined with *freezing* the Libor rates and appropriate *linearizations* of the non-affine terms arising in the corresponding instantaneous covariance matrix are the key issues to efficient model evaluation. For a whole strip of strikes the approximate hybrid model developed can be evaluated for equity plain vanilla European options in just milliseconds.

We focus on the fast evaluation for the vanilla equity option prices under this hybrid process, and assume that the parameters for the interest rate model have been determined a-priori.

The chapter is set up as follows. First of all, in Section 4.2, we discuss the generalization of the Heston model and provide details about the DD-SV interest rate model. In Section 4.3 the dynamics for the equity forward model are derived and an approximation for the corresponding characteristic function is developed in Section 4.4. Numerical experiments, in which the accuracy of the approximations is checked, are presented in Section 4.5.

4.2 The equity and interest rate models

4.2.1 The Heston model and extensions

With state vector $\mathbf{X}(t) = [S(t), v(t)]^{\mathrm{T}}$, under the risk-neutral pricing measure, the Heston stochastic volatility model [54], is specified by two stochastic differential equations: the variance process, $v(t)$, and the the stock, $S(t)$ (see Chapter 2 for details).

The model, under the log-transform for the stock, $x(t) = \log S(t)$, belongs to the class of affine processes [28]. For $\tau = T - t$, the characteristic function (ChF) is therefore given by:

$$\phi_{\mathrm{H}}(u, x(t), \tau) = \exp\left(A(u,\tau) + B_x(u,\tau)x(t) + B_v(u,\tau)v(t)\right), \tag{4.1}$$

where the complex-valued functions $A(u,\tau)$, $B_x(u,\tau)$ and $B_v(u,\tau)$ are known in closed-form (see for example [54]).

The ChF is explicit, but its inverse also has to be found for pricing purposes.

Since a deterministic interest rate is not sufficient for our pricing purposes here, we relax this assumption and assume the rates to be stochastic. A first extension of the framework has been done by defining the correlated short-rate process, $r(t)$, of the following form:

$$\mathrm{d}r(t) = \mu_r(t, r(t))\mathrm{d}t + \sigma_r(t, r(t))\mathrm{d}W_r(t), \qquad r(0) > 0.$$

Depending on the functions $\mu_r(t, r(t))$, and $\sigma_r(t, r(t))$ many different interest rate models are available. Popular single factor versions include the Hull-White [56], Cox-Ingersoll-Ross [25] (both discussed in Chapters 1 and 2) or Black-Karasinski [15] models. Multi-factor models arise by extending the single-factor processes with additional sources of randomness (see Chapter 3).

In Chapter 2, in order to determine a ChF, we have proposed linear approximations for the non-affine terms in the instantaneous covariance matrix related to a short-rate based hybrid model. With such a short-rate model, however, the interest rate can only be calibrated well to at-the-money products like caps and swaptions. Those models can therefore only be used for relatively basic hybrid products, which are insensitive to the interest rate smile and skew.

When developing a more advanced hybrid model, moving away from the short-rate processes to the market models, the main difficulty is to link the discrete tenor Libor rates, $L(t, T_i, T_j)$, for $T_i < T_j$ to the continuous equity process, $S(t)$. This issue is addressed here.

In the section to follow we present the main concepts of the market models.

4.2.2 The Market model with stochastic volatility

Here, we build the basis for the LMM interest rate process in the Heston hybrid model.

For a given set of maturities $\mathcal{T} = \{T_0, T_1, T_2, \ldots, T_N\}$ with a tenor structure $\tau_k = T_k - T_{k-1}$ for $k = 1, \ldots, N$ we define $P(t, T_i)$ to be the price of a zero-coupon treasury bond maturing at time $T_i(\geq t)$, with face-value €1 and the forward Libor rate $L_k(t) := L(t, T_{k-1}, T_k)$:

$$L(t, T_{k-1}, T_k) \equiv \frac{1}{\tau_k}\left(\frac{P(t, T_{k-1})}{P(t, T_k)} - 1\right), \text{ for } t < T_{k-1}. \tag{4.2}$$

For modelling the Libor Market Model, we take the displaced-diffusion-stochastic volatility model (DD-SV) by [5]. The Libor rate $L_k(t)$ is defined under its *natural measure* by the following system of stochastic differential equations (SDEs):

$$\begin{cases} \mathrm{d}L_k(t) = & \sigma_k(t)\left(\beta_k(t)L_k(t) + (1 - \beta_k(t))L_k(0)\right)\sqrt{V(t)}\mathrm{d}W_k^k(t), \quad L_k(0) > 0, \\ \mathrm{d}V(t) = & \lambda(V(0) - V(t))\mathrm{d}t + \eta\sqrt{V(t)}\mathrm{d}W_V^k(t), \quad V(0) > 0, \end{cases} \tag{4.3}$$

with

$$\begin{cases} \mathrm{d}W_i^k(t)\mathrm{d}W_j^k(t) = & \rho_{i,j}\mathrm{d}t, \quad \text{for } i \neq j, \\ \mathrm{d}W_V^k(t)\mathrm{d}W_i^k(t) = & 0, \end{cases}$$

where $\sigma_k(t)$ determines the level of the volatility smile. Parameter $\beta_k(t)$ controls the slope of the volatility smile, and λ determines the speed of mean reversion for the variance and influences the speed at which the volatility smile flattens as the swaption expiry increases [92]. Parameter η determines the curvature of the smile. Subscript i and superscript j in $\mathrm{d}W_i^j(t)$ indicate the associated process and the corresponding measure, respectively. Throughout this chapter we assume that the DD-SV model in (4.3) is already in the *effective* parameter framework developed in [92]. This means that approximate time-homogeneous parameters are used instead of time-dependent parameters. For this reason we set $\beta_k(t) \equiv \beta_k$ and $\sigma_k(t) \equiv \sigma_k$.

An important feature, which will be shown in next section, is that in our framework it is convenient to work under the T_N-*terminal measure* associated with the last zero-coupon bond, $P(t, T_N)$.

By taking

$$\phi_k(t) = \beta_k L_k(t) + (1 - \beta_k) L_k(0), \tag{4.4}$$

under the T_N-terminal measure and for $k < N$, the Libor dynamics are given by:

$$\begin{cases} \mathrm{d}L_k(t) = & -\phi_k(t)\sigma_k V(t) \displaystyle\sum_{j=k+1}^{N} \frac{\tau_j \phi_j(t)\sigma_j}{1 + \tau_j L_j(t)} \rho_{k,j} \mathrm{d}t + \sigma_k \phi_k(t) \sqrt{V(t)} \mathrm{d}W_k^N(t), \\ \mathrm{d}V(t) = & \lambda(V(0) - V(t))\mathrm{d}t + \eta\sqrt{V(t)}\mathrm{d}W_V^N(t), \end{cases} \tag{4.5}$$

with

$$\begin{cases} \mathrm{d}W_i^N(t)\mathrm{d}W_j^N(t) = & \rho_{i,j}\mathrm{d}t, \quad \text{for } i \neq j, \\ \mathrm{d}W_k^N(t)\mathrm{d}W_V^N(t) = & 0. \end{cases}$$

In the DD-SV model in (4.3) the change of measure does not affect the drift in the process for the stochastic variance, $V(t)$. This is due to the assumption of independence between infinitesimal increments between the variance process, $V(t)$, and the Libors, $L_k(t)$. Although a generalization to a non-zero correlation is possible (see [111]), it is not strictly necessary. The model, by the displacement construction and the stochastic variance, already provides a satisfactory fit to market data.

Note that for $k = N$ the dynamics for $L(t, T_{k-1}, T_k)$ do not contain a drift term (Libor $L(t, T_{N-1}, T_N)$ is a martingale under the T_N measure).

When changing the measure for the stock process from the risk-neutral to the T_N-forward measure, one needs to find the form for the zero-coupon bond, $P(t, T_N)$. By the recursive Equation (4.2) it is easy to find the following expression for the last bond (needed in Equation (4.10) to follow):

$$P(t, T_N) = P(t, T_{m(t)}) \Big(\prod_{j=m(t)+1}^{N} (1 + \tau_j L(t, T_{j-1}, T_j)) \Big)^{-1}, \tag{4.6}$$

with $m(t) = \min(k : t \leq T_k)$ (empty products in (4.6) are defined to be equal to 1). The bond $P(t, T_N)$ in (4.6) is fully determined by the Libor rates $L_k(t)$, $k = 1, \ldots, N$ and the bond $P(t, T_{m(t)})$. Although the Libors $L_k(t)$ are defined in system (4.5) the bond $P(t, T_{m(t)})$ is not yet well-defined in the current framework.

In the following subsection we discuss possible interpolation methods for the *short-dated* bond $P(t, T_{m(t)})$.

4.2.3 Interpolations of short-dated bonds

Let us consider the discrete tenor structure $\mathcal{T}$ and the Libor rates $L_k(t)$ as defined in (4.2). As already indicated in [18, 82], the main problem with market models is that they do not provide continuous time dynamics for any bond in the tenor structure. Therefore, it is rather difficult, without additional assumptions, to define a short-rate process, $r(t)$, which can be used in combination with the Heston model for equity.

In this section we discuss how to extend the market model, so that the no-arbitrage conditions are met and the bonds $P(t, T_i)$ for $t \notin \mathcal{T}$ are well-defined.

We start with the interpolation technique introduced in [98]. In this approach a linear interpolation which produces a piecewise deterministic short-rate for $t \in (T_{m(t)-1}, T_{m(t)}]$ is used. The method is equivalent with assuming a zero volatility for all zero-coupon bonds, $P(t, T_i)$, maturing at a next (future) date in the tenor structure $\mathcal{T}$, i.e.: $t \leq T_{m(t)}$, the zero-coupon bond $P(t, T_{m(t)})$ is well-defined and arbitrage-free (see [98, 14]), if,

$$P(t, T_{m(t)}) \approx \left(1 + (T_{m(t)} - t)L(T_{m(t)-1}, T_{m(t)})\right)^{-1}, \text{ for } T_{m(t)-1} < t < T_{m(t)}. \tag{4.7}$$

Representation (4.7) satisfies the main features of the zero-coupon bond, i.e., for $t \to T_{m(t)}$ the bond $P(t, T_{m(t)}) \to 1$. Since Eq. (4.7) implies a zero volatility interpolation for the intermediate intervals, a deterministic interest rate is assumed for intermediate time points, $T_{m(t)-1} < t < T_{m(t)}$.

The assumption of a locally deterministic interest rate in short-dated bonds may however be unsatisfactory, for example, for pricing path-sensitive products in which the payment does not occur at the pre-specified dates, $T_i \in \mathcal{T}$. In such a case, one can use an interpolation which incorporates some internal volatility. An alternative, arbitrage-free interpolation for zero-coupon bonds is, for example, given by:

$$P(t, T_{m(t)}) \approx \left(1 + (T_{m(t)} - t)\psi_1(t)\right)^{-1}, \text{ for } t \leq T_{m(t)},$$

with $\psi_1(t) = \vartheta(t)L_{m(t)}(T_{m(t)-1}) + (1 - \vartheta(t))L_{m(t)+1}(t)$, and $\vartheta(t)$ is a (chosen) deterministic function which controls the level of the volatility in the short-dated bonds.

More details on interpolation approaches can be found in [98, 91, 26, 14].

Remark. When calibrating the equity-interest rate hybrid model, the interest rate part is usually calibrated to the market data, independent of the equity part. Afterwards, the calibrated interest rate model is combined with the equity component. With suitable correlations imposed, the remaining parameters are then determined. Obviously, in the last step the hybrid parameters are determined by calibration to equity option values. By assuming that the equity maturities, T_i, are defined to be the same dates as the zero-coupon bonds in the LMM, there is no need for advanced zero-coupon bond interpolations. The interpolation routines are, however, often required when pricing the hybrids themselves. The hybrid product pricing is typically performed with a short-step Monte Carlo simulation, for which the assumption of a constant short-term interest rate may not be satisfactory. Especially if the hybrid payments occur at dates that are not specified in the tenor structure $\mathcal{T}$.

4.3 The Hybrid Heston-LMM

In this section we construct the hybrid model.

As indicated in for example [77], when pricing interest rate derivatives the usual reference measure is the spot measure $\mathbb{Q}$, associated with a directly re-balanced bank account numéraire $B(t)$. When dealing with an equity-interest rate hybrid model however, after calibrating the interest rate part, one needs to price the European equity options in order to determine the unknown equity parameters. The price of a European call option is given by:

$$\Pi(t,T_N) = B(t)\mathbb{E}^{\mathbb{Q}}\left(\frac{(S(T_N)-K)^+}{B(T_N)}\big|\mathcal{F}(t)\right), \text{ with } t < T_N, \tag{4.8}$$

with K the strike, $S(T_N)$ the stock price at time T_N, filtration $\mathcal{F}(t)$ and a numéraire $B(T_N)$. Since the money-savings account, $B(T_N)$, is a stochastic quantity, the joint distribution of $1/B(T_N)$ and $S(T_N)$ is required to determine the value in (4.8). This however may be a difficult task. Obviously this issue is avoided when switching between the appropriate measures: From the risk-free measure $\mathbb{Q}$ to the forward measure associated with the zero-coupon bond maturing at the payment day, T_N, $P(t,T_N)$ (see [62]). With the Radon-Nikodym derivative we obtain:

$$\begin{aligned}\Pi(t,T_N) &= P(t,T_N)\mathbb{E}^{T_N}\left(\frac{(S(T_N)-K)^+}{P(T_N,T_N)}\big|\mathcal{F}(t)\right)\\ &= P(t,T_N)\mathbb{E}^{T_N}\left(\left(F^{T_N}(T_N)-K\right)^+\big|\mathcal{F}(t)\right), \text{with } t < T_N,\end{aligned} \tag{4.9}$$

with $F^{T_N}(t)$ the forward of the stock $S(t)$, defined as:

$$F^{T_N}(t) = \frac{S(t)}{P(t,T_N)}. \tag{4.10}$$

4.3.1 Derivation of the hybrid model

Under the T_N-forward measure we assume that the equity process is driven by the Heston stochastic volatility model, given by the following dynamics:

$$\begin{cases}\dfrac{\mathrm{d}S(t)}{S(t)} = (\dots)\mathrm{d}t + \sqrt{v(t)}\mathrm{d}W_x^N(t), & S(0)>0,\\ \mathrm{d}v(t) = \kappa(\bar{v}-v(t))\mathrm{d}t + \gamma\sqrt{v(t)}\mathrm{d}W_v^N(t), & v(0)>0.\end{cases} \tag{4.11}$$

Note that the drift in (4.11) is not yet specified.

For the interest rate model we choose the DD-SV Libor Market Model under the T_N-measure generated by the numéraire $P(t,T_N)$, given by:

$$\begin{cases} \mathrm{d}L_k(t) = & -\phi_k(t)\sigma_k V(t) \displaystyle\sum_{j=k+1}^{N} \frac{\tau_j\phi_j(t)\sigma_j}{1+\tau_j L_j(t)}\rho_{k,j}\mathrm{d}t + \sigma_k\phi_k(t)\sqrt{V(t)}\mathrm{d}W_k^N(t), \\ \mathrm{d}V(t) = & \lambda(V(0)-V(t))\mathrm{d}t + \eta\sqrt{V(t)}\mathrm{d}W_V^N(t), \end{cases} \tag{4.12}$$

with a non-zero correlation between the stock process, $S(t)$, and its variance process, $v(t)$, between the Libors, $L_i(t)$ and $L_j(t)$, for $i,j = 1\dots N,\quad i \neq j$, and between the stock $S(t)$ and Libor rates, i.e.:

$$\begin{cases} \mathrm{d}W_x^N(t)\mathrm{d}W_v^N(t) = & \rho_{x,v}\mathrm{d}t, \\ \mathrm{d}W_x^N(t)\mathrm{d}W_j^N(t) = & \rho_{x,j}\mathrm{d}t, \\ \mathrm{d}W_i^N(t)\mathrm{d}W_j^N(t) = & \rho_{i,j}\mathrm{d}t. \end{cases} \tag{4.13}$$

We assume a zero correlation between the Libors $L_i(t)$ and their variance process $V(t)$, between the Libors and the variance process for equity, $v(t)$, between the variance processes, $v(t)$ and $V(t)$, and between the stock $S(t)$ and the variance of the Libors, $V(t)$.

For the calculation of the value of the European option given in (4.9), we first need to determine the dynamics for the forward, $F^{T_N}(t)$. From Itô's lemma we get:

$$\begin{aligned} \mathrm{d}F^{T_N}(t) \quad = \quad & \frac{1}{P(t,T_N)}\mathrm{d}S(t) - \frac{S(t)}{P^2(t,T_N)}\mathrm{d}P(t,T_N) + \frac{S(t)}{P^3(t,T_N)}\left(\mathrm{d}P(t,T_N)\right)^2 \\ & - \frac{1}{P^2(t,T_N)}(\mathrm{d}S(t))(\mathrm{d}P(t,T_N)). \end{aligned}$$

Since the forward is a martingale under the T_N-measure generated by the zero-coupon bond, $P(t,T_N)$, the forward dynamics do not contain a drift term. This implies that we do not encounter any "dt"-terms in the dynamics of $\mathrm{d}F^{T_N}(t)$, i.e.:

$$\mathrm{d}F^{T_N}(t) = \frac{1}{P(t,T_N)}\mathrm{d}S(t) - \frac{S(t)}{P^2(t,T_N)}\mathrm{d}P(t,T_N). \tag{4.14}$$

Equation (4.14) shows that in order to find the dynamics for process $\mathrm{d}F^{T_N}(t)$ the dynamics for $P(t,T_N)$ also need to be determined. With the approximation introduced in Section 4.2.3, the bond $P(t,T_N)$ is given by

$$P(t,T_N) = \left(\left(1 + (T_{m(t)} - t)L_{m(t)}(T_{m(t)-1})\right) \prod_{j=m(t)+1}^{N} \left(1+\tau_j L(t,T_{j-1},T_j)\right) \right)^{-1}.$$

Before we derive the Itô dynamics for the zero-coupon bond, $P(t,T_N)$, we define, for ease of notation, the following "support variables":

$$\begin{aligned} f(t) \quad &= \quad 1 + (T_{m(t)} - t)L(T_{m(t)-1}, T_{m(t)-1}, T_{m(t)}), \\ g_j(t, L_j(t)) \quad &= \quad 1 + \tau_j L(t, T_{j-1}, T_j). \end{aligned}$$

By taking the log-transform of the bond, $\log P(t, T_N)$, we find:

$$\log P(t, T_N) = -\log(f(t)) - \sum_{j=m(t)+1}^{N} \log g_j(t, L_j(t)),$$

so that the dynamics for the log-bond read:

$$\mathrm{d}\log P(t, T_N) = -\mathrm{d}\log(f(t)) - \sum_{j=m(t)+1}^{N} \mathrm{d}\log g_j(t, L_j(t)). \tag{4.15}$$

On the other hand, by applying Itô's lemma to $\log P(t, T_N)$ we get:

$$\mathrm{d}\log P(t, T_N) = \frac{1}{P(t, T_N)}\mathrm{d}P(t, T_N) - \frac{1}{2}\left(\frac{1}{P(t, T_N)}\right)^2 (\mathrm{d}P(t, T_N))^2. \tag{4.16}$$

By neglecting the $\mathrm{d}t$-terms (as we do not encounter any "$\mathrm{d}t$"-terms in the dynamics of $\mathrm{d}F^{T_N}(t)$) and by matching Equations (4.15) and (4.16), we obtain:

$$\frac{\mathrm{d}P(t, T_N)}{P(t, T_N)} = -\sum_{j=m(t)+1}^{N} \mathrm{d}\log g_j(t, L_j(t)), \tag{4.17}$$

with the dynamics for $\mathrm{d}\log g_j(t, L_j(t))$:

$$\mathrm{d}\log g_j(t, L_j(t)) = \frac{\tau_j}{1 + \tau_j L_j(t)}\mathrm{d}L_j(t). \tag{4.18}$$

After substitution of (4.17), (4.18) and (4.12) and neglecting the $\mathrm{d}t$-terms the dynamics for the bond $P(t, T_N)$ are given by:

$$\frac{\mathrm{d}P(t, T_N)}{P(t, T_N)} = -\sum_{j=m(t)+1}^{N} \frac{\tau_j \sigma_j \phi_j(t)\sqrt{V(t)}}{1 + \tau_j L_j(t)}\mathrm{d}W_j^N(t). \tag{4.19}$$

Now, we return to the derivations for the forward, $F^{T_N}(t)$, in Equation (4.14). By Equation (4.11) these can be expressed as:

$$\frac{\mathrm{d}F^{T_N}(t)}{F^{T_N}(t)} = \sqrt{v(t)}\mathrm{d}W_x^N(t) - \frac{1}{P(t, T_N)}\mathrm{d}P(t, T_N). \tag{4.20}$$

Finally, by combining Equations (4.20) and (4.19) the dynamics for the forward $F^{T_N}(t)$ are determined:

$$\frac{\mathrm{d}F^{T_N}(t)}{F^{T_N}(t)} = \sqrt{v(t)}\mathrm{d}W_x^N(t) + \sum_{j=m(t)+1}^{N} \frac{\tau_j \sigma_j \phi_j(t)\sqrt{V(t)}}{1 + \tau_j L_j(t)}\mathrm{d}W_j^N(t). \tag{4.21}$$

Since the forward, $F^{T_N}(t)$, is a martingale under the T_N-measure (i.e., fully determined in terms of the volatility structure), the interpolation, with zero volatility, does not affect the dynamics for the forward $F^{T_N}(t)$. As indicated in [95], under the forward measure the forward price (4.21) includes components arising from the volatilities of the zero-coupon bonds that connect the spot and the forward prices.

4.4 Approximation for the hybrid model

With the stock process, $S(t)$, under the T_N-terminal measure driven by the Heston model with a stochastic, correlated variance process, $v(t)$, we obtained the dynamics in (4.21) for the forward prices, $F^{T_N}(t)$, with $\mathrm{d}W_x^N(t)\mathrm{d}W_v^N(t) = \rho_{x,v}\mathrm{d}t$, and the parameters as defined in (4.11). The Libor rates $L_i(t)$ are defined in (4.12).

We call this model the *Heston-Libor Market Model*, abbreviated by *H-LMM*, here. This is the full-scale model, which requires approximations for efficient pricing of European equity options.

The model in (4.21) is not of the affine form, as it contains terms like $\phi_j(t)/(1+\tau_i L_i(t))$. Therefore we cannot use the standard techniques from [28] to determine the ChF. The availability of a ChF is especially important for the model calibration, where fast pricing for equity plain vanilla products is essential. For this reason we *freeze* the Libor rates [44, 58, 61], i.e.:

$$L_j(t) \approx L_j(0). \tag{4.22}$$

As a consequence $\phi_j(t) \approx L_j(0)$ (with $\phi_j(t)$ in (4.4)) and the dynamics for the forward $F^{T_N}(t)$ read:

$$\frac{\mathrm{d}F^{T_N}(t)}{F^{T_N}(t)} \approx \sqrt{v(t)}\mathrm{d}W_x^N(t) + \sum_{j=m(t)+1}^{N} \frac{\tau_j \sigma_j L_j(0)\sqrt{V(t)}}{1+\tau_j L_j(0)}\mathrm{d}W_j^N(t),$$

with the correlations and the remaining processes given in (4.13). Now, we determine the log-transform of the forward $x^{T_N}(t) := \log F^{T_N}(t)$. With $\mathcal{A} = \{m(t)+1,\ldots,N\}$ and application of Itô's lemma, the dynamics for $x^{T_N}(t)$ are given by:

$$\begin{aligned}\mathrm{d}x^{T_N}(t) \quad &\approx \quad -\frac{1}{2}\Big(\sum_{j\in\mathcal{A}} \psi_j \sqrt{V(t)}\mathrm{d}W_j^N(t) + \sqrt{v(t)}\mathrm{d}W_x^N(t)\Big)^2 \\ &\qquad + \sqrt{v(t)}\mathrm{d}W_x^N(t) + \sum_{j\in\mathcal{A}} \psi_j \sqrt{V(t)}\mathrm{d}W_j^N(t),\end{aligned}$$

with

$$\psi_j = \frac{\tau_j \sigma_j L_j(0)}{1+\tau_j L_j(0)}.$$

The square of the sum in the drift can be reformulated, by

$$\Big(\sum_{j=1}^{N} x_j\Big)^2 = \sum_{j=1}^{N} x_j^2 + \sum_{\substack{i,j=1,\ldots,N\\ i\neq j}} x_i x_j, \quad \text{for } N>0.$$

By taking $x_j = \psi_j \sqrt{V(t)} \mathrm{d}W_j^N$ the dynamics can now be expressed as:

$$\mathrm{d}x^{T_N}(t) \approx -\frac{1}{2}\Big(v(t) + V(t)\Big(\sum_{j\in\mathcal{A}} \psi_j^2 + \sum_{\substack{i,j\in\mathcal{A}\\ i\neq j}} \psi_i\psi_j\rho_{i,j}\Big) + 2\sqrt{V(t)}\sqrt{v(t)}\sum_{j\in\mathcal{A}} \psi_j\rho_{x,j}\Big)\mathrm{d}t$$
$$+\sqrt{v(t)}\mathrm{d}W_x^N(t) + \sqrt{V(t)}\sum_{j\in\mathcal{A}}\psi_j \mathrm{d}W_j^N(t).$$

By setting,

$$A_1(t) := \sum_{j\in\mathcal{A}} \psi_j^2 + \sum_{\substack{i,j\in\mathcal{A}\\ i\neq j}} \psi_i\psi_j\rho_{i,j}, \quad \text{and} \quad A_2(t) := \sum_{j\in\mathcal{A}} \psi_j\rho_{x,j}, \tag{4.23}$$

we obtain

$$\begin{aligned} \mathrm{d}x^{T_N}(t) \quad &\approx \quad -\frac{1}{2}\left(v(t) + V(t)A_1(t) + 2\sqrt{V(t)}\sqrt{v(t)}A_2(t)\right)\mathrm{d}t \\ &\qquad +\sqrt{v(t)}\mathrm{d}W_x^N(t) + \sqrt{V(t)}\sum_{j\in\mathcal{A}}\psi_j\mathrm{d}W_j^N(t). \end{aligned} \tag{4.24}$$

On the other hand the *frozen* Libor dynamics are given by:

$$\mathrm{d}L_k(t) \approx -\sigma_k L_k(0)V(t)\sum_{j=k+1}^{N}\psi_j\rho_{k,j}\mathrm{d}t + \sigma_k L_k(0)\sqrt{V(t)}\mathrm{d}W_k^N(t),$$

which, by taking

$$B_1(k) = \sum_{j=k+1}^{N}\psi_j\rho_{k,j},$$

equal to

$$\mathrm{d}L_k(t) \approx -\sigma_k L_k(0)V(t)B_1(k)\mathrm{d}t + \sigma_k L_k(0)\sqrt{V(t)}\mathrm{d}W_k^N(t), \tag{4.25}$$

with the variance process $V(t)$ given in (4.12).

Here, we derive the instantaneous covariance for the stochastic model given by (4.24) and (4.25) with the variance processes in (4.11) and (4.12). Since the dynamics for the forward $F^{T_N}(t)$ contain the Libor rates, the dimension of the covariance matrix will be dependent on time t. For a given state vector $\mathbf{X}(t) = [x^{T_N}(t), v(t), L_1^N(t), L_2^N(t), \ldots, L_N^N(t), V(t)]^{\mathrm{T}}$, the covariance matrix will be of the following form:

$$\mathbf{\Sigma} = \begin{bmatrix} \mathbf{\Sigma}_{x,x} & \mathbf{\Sigma}_{x,v} & \mathbf{\Sigma}_{x,L_1} & \mathbf{\Sigma}_{x,L_2} & \cdots & \mathbf{\Sigma}_{x,L_N} & 0 \\ \mathbf{\Sigma}_{v,x} & \mathbf{\Sigma}_{v,v} & 0 & 0 & \cdots & 0 & 0 \\ \mathbf{\Sigma}_{L_1,x} & 0 & \mathbf{\Sigma}_{L_1,L_1} & \mathbf{\Sigma}_{L_1,L_2} & \cdots & \mathbf{\Sigma}_{L_1,L_N} & 0 \\ \mathbf{\Sigma}_{L_2,x} & 0 & \mathbf{\Sigma}_{L_2,L_1} & \mathbf{\Sigma}_{L_2,L_2} & \cdots & \mathbf{\Sigma}_{L_2,L_N} & 0 \\ \vdots & \vdots & \vdots & \vdots & \ddots & \vdots & \vdots \\ \mathbf{\Sigma}_{L_N,x} & 0 & \mathbf{\Sigma}_{L_N,L_1} & \mathbf{\Sigma}_{L_N,L_2} & \cdots & \mathbf{\Sigma}_{L_N,L_N} & 0 \\ 0 & 0 & 0 & 0 & \cdots & 0 & \mathbf{\Sigma}_{V,V} \end{bmatrix}\mathrm{d}t, \tag{4.26}$$

with

$$\begin{aligned}\boldsymbol{\Sigma}_{x,x} &= v(t) + V(t)A_1(t) + 2\sqrt{V(t)}\sqrt{v(t)}A_2(t),\\ \boldsymbol{\Sigma}_{L_i,L_j} &= \rho_{i,j}\sigma_i\sigma_j L_i(0)L_j(0)V(t),\\ \boldsymbol{\Sigma}_{x,L_i} &= \rho_{x,i}\sigma_i L_i(0)\sqrt{v(t)}\sqrt{V(t)} + \sigma_i L_i(0)V(t)\sum_{j\in\mathcal{A}}\psi_j\rho_{i,j},\end{aligned}$$

and

$$\boldsymbol{\Sigma}_{v,v} = \gamma^2 v(t),\quad \boldsymbol{\Sigma}_{L_i,L_i} = \sigma_i^2 L_i^2(0)V(t),\quad \boldsymbol{\Sigma}_{V,V} = \eta^2 V(t),\quad \boldsymbol{\Sigma}_{x,v} = \rho_{x,v}\gamma v(t).$$

Zeros are present in the covariance matrix due to the assumption of zero correlation for $\rho_{x,V}$, ρ_{v,L_i}, $\rho_{L_i,V}$ and $\rho_{v,V}$. The covariance matrix as well as the drift in Equation (4.24) include the non-affine terms $\sqrt{v(t)}\sqrt{V(t)}$. Therefore the resulting model is not affine and we cannot easily derive the corresponding ChF. Appropriate approximations will be introduced in the next subsection.

4.4.1 The hybrid model linearization

In order to bring the system in an affine form, approximations for the non-affine terms in the instantaneous covariance matrix (4.26) are necessary (as done in Chapter 2 for a hybrid with stochastic volatility for equity and a short-rate model for the interest rate). In the present work, we linearize these terms by projection on the first moments, as follows:

$$\begin{aligned}\sqrt{v(t)}\sqrt{V(t)} &\approx \mathbb{E}\left(\sqrt{v(t)}\sqrt{V(t)}\right)\\ &\stackrel{\perp\!\!\!\perp}{=} \mathbb{E}\left(\sqrt{v(t)}\right)\mathbb{E}\left(\sqrt{V(t)}\right) =: \hat{\alpha}(t),\end{aligned} \tag{4.27}$$

with $\perp\!\!\!\perp$ indicating independence between the processes $v(t)$ and $V(t)$. By [30] and simplifications as in [69] the closed-form expression for the expectation of the square-root of square-root process, $\mathbb{E}(\sqrt{v(t)})$, can be found [1] in Chapter 2.

4.4.2 The forward characteristic function

With the approximations introduced, the non-affine terms in the drift and in the instantaneous covariance matrix have been linearized. Therefore this approximate model is in the class of affine processes. With the approximations, under the log-transform, the forward, $x^{T_N}(t)$, is governed by the following SDE:

$$\begin{aligned}\mathrm{d}x^{T_N}(t) &= -\frac{1}{2}\left(v(t) + V(t)A_1(t) + 2\hat{\alpha}(t)A_2(t)\right)\mathrm{d}t\\ &\quad + \sqrt{v(t)}\mathrm{d}W_x^N(t) + \sqrt{V(t)}\sum_{j\in\mathcal{A}}\psi_j \mathrm{d}W_j^N(t),\end{aligned}$$

[1] The expectation for $\mathbb{E}(\sqrt{V(t)})$ is found analogously.

(with $A_1(t)$ and $A_2(t)$ as in (4.23) and $\hat{\alpha}(t)$ from (4.27)) which is of the affine form. We call this approximation to the full-scale hybrid model, the *approximate Heston-Libor Market Model*, denoted by *H1-LMM.*

Now, we derive the corresponding forward characteristic function of the model. Since the dimension of the hybrid changes over time, the number of coefficients in the corresponding characteristic function will also change. For a given time to expiry, $\tau = T_N - t$, and $\mathcal{B} = \{m(T_N - \tau) + 1, \dots, T_N\}$ the forward characteristic function for the approximate hybrid model is of the following form:

$$\begin{aligned}\phi^{T_N}(u, x^{T_N}(t), \tau) &= \exp(A(u,\tau) + B_x(u,\tau)x^{T_N}(t) + B_v(u,\tau)v(t) \\ &\quad + \sum_{j\in\mathcal{B}} B_j(u,\tau)L_j(t) + B_V(u,\tau)V(t)),\end{aligned} \tag{4.28}$$

subject to the terminal condition $\phi^{T_N}(u, \mathbf{X}(T_N), 0) = \exp(iux^{T_N}(T_N))$, which, according to Equation (4.10), equals $\phi^{T_N}(u, \mathbf{X}(T_N), 0) = \exp(iu \log S(T_N))$. The coefficients $A(u,\tau)$, $B_x(u,\tau)$, $B_v(u,\tau)$, $B_j(u,\tau)$ and $B_V(u,\tau)$ satisfy the system of ODEs in the lemma below:

Lemma 4.4.1. *The functions $B_x(u,\tau) =: B_x$, $B_v(u,\tau) =: B_v$, $B_j(u,\tau) =: B_j$, $B_V(u,\tau) =: B_V$ and $A(u,\tau) =: A$ for the forward characteristic function given in (4.28) satisfy the following ODEs:*

$$B_x'(u,\tau) = 0, \qquad B_j'(u,\tau) = 0, \ \textit{for } j \in \mathcal{A},$$

and

$$\begin{aligned}
B_v'(u,\tau) &= \frac{1}{2}B_x(B_x - 1) + (\rho_{x,v}\gamma B_x - \kappa)B_v + \frac{1}{2}\gamma^2 B_v^2, \\
B_V'(u,\tau) &= \frac{1}{2}A_1(t)B_x(B_x - 1) - \sum_{j\in\mathcal{A}} \sigma_j L_j(0) B_x B_j \sum_{k\in\mathcal{A}} \psi_k \rho_{k,j} - \lambda B_V \\
&\quad + \frac{1}{2}\sum_{j\in\mathcal{A}} \sigma_j^2 L_j^2(0) B_j^2 + \sum_{\substack{i,j\in\mathcal{A} \\ i\neq j}} \rho_{i,j}\sigma_i\sigma_j L_i(0)L_j(0)B_iB_j + \frac{1}{2}\eta^2 B_V^2, \\
A'(u,\tau) &= \hat{\alpha}(t)A_2(t)B_x(B_x - 1) + \kappa\bar{v}B_v + \lambda V(0)B_V \\
&\quad + \sum_{j\in\mathcal{A}} \rho_{x,j}\sigma_j L_j(0)\hat{\alpha}(t)B_xB_j,
\end{aligned}$$

where $\mathcal{A} = \{m(t) + 1, \dots, N\}$, $t = T_N - \tau$ with final conditions $B_x(u, 0) = iu$, $B_j(u, 0) = 0$, $B_v(u, 0) = 0$, $B_V(u, 0) = 0$ and $A(u, 0) = 0$.

Proof. For affine processes, $\mathbf{X}(t)$, the forward ChF, $\phi^{T_N}(\mathbf{u}, \mathbf{X}(t), \tau)$, is given by [28]:

$$\phi^{T_N}(\mathbf{u}, \mathbf{X}(t), \tau) = \mathbb{E}^{T_N}\left(\mathrm{e}^{i\mathbf{u}^{\mathrm{T}}\mathbf{X}(T)}\middle|\mathcal{F}(t)\right) = \mathrm{e}^{A(\mathbf{u},\tau)+\mathbf{B}^{\mathrm{T}}(\mathbf{u},\tau)\mathbf{X}(t)}, \tag{4.29}$$

with time lag, $\tau = T_N - t$. Here, the expectation is taken under the T_N-forward measure, $\mathbb{Q}^{T_N}$. The complex-valued functions $A(\mathbf{u},\tau)$ and $\mathbf{B}^{\mathrm{T}}(\mathbf{u},\tau)$ have to satisfy a system of complex-valued ODEs (see Chapter 1 for details).

Under the log-transform we find that the state vector $\mathbf{X}(t)$ has $N+3$ elements ($n = N+3$):

$$\mathbf{X}(t) = [x^{T_N}(t), v(t), L_1(t), \dots, L_N(t), V(t)]^{\mathrm{T}}.$$

With the Heston equity model (4.24) and the stochastic volatility Libor Market Model in (4.25) we set vector $\mathbf{u} = [u, 0, \dots, 0]^{\mathrm{T}}$. In order to find the functions $A(u,\tau)$ and $\mathbf{B}^{\mathrm{T}}(u,\tau)$ in (4.29) we need to determine the matrices a_1^{T}, c_0, c_1 and the vector a_0 as given in Chapter 1 (Equations (1.1), (1.2) and (1.3)). By the approximations in (4.22) and (4.27), the drifts in the Libors, $L_i(t)$, and in the forward dynamics do not contain any non-affine terms. For $\mathcal{A} = \{m(t)+1, \dots, N\}$, $t = T_N - \tau$, the non-zero elements in matrix a_1^{T} are given by:

$$\begin{aligned} a_1^{\mathrm{T}}(2,1) &= -0.5, & a_1^{\mathrm{T}}(2,2) &= -\kappa, \\ a_1^{\mathrm{T}}(N+3,1) &= -0.5A_1(t), & a_1^{\mathrm{T}}(N+3,N+3) &= -\lambda, \end{aligned}$$

with

$$a_1^{\mathrm{T}}(N+3, j+2) = -\sigma_j L_j(0) B_1(j), \text{ for } j \in \mathcal{A}.$$

To determine the matrices c_1 and c_0 we use the instantaneous covariance matrix from (4.26). For matrix c_1 the non-zero elements are given by:

$$\begin{aligned} c_1(1,1,2) &= 1, & c_1(1,1,N+3) &= A_1(t), \\ c_1(2,1,2) &= \rho_{x,v}\gamma, & c_1(1,2,2) &= \rho_{x,v}\gamma, \\ c_1(2,2,2) &= \gamma^2, & c_1(N+3,N+3,N+3) &= \eta^2, \end{aligned}$$

and

$$\begin{aligned} c_1(j+2,j+2,N+3) &= \sigma_j^2 L_j^2(0), \text{ for } j \in \mathcal{A}, \\ c_1(i+2,j+2,N+3) &= \rho_{i,j}\sigma_i\sigma_j L_i(0) L_j(0), \text{ for } i,j \in \mathcal{A},\ i \neq j, \\ c_1(1,j+2,N+3) &= \sigma_j L_j(0) \sum_{k\in\mathcal{A}} \psi_k \rho_{j,k}, \\ c_1(j+2,1,N+3) &= c_1(1,j+2,N+3). \end{aligned}$$

In essence, the first and the second index of c_1 indicate which covariance term we deal with, whereas the third term indicates which variable is defined. The unspecified matrix values are equal to zero.

For matrix c_0 and vector a_0 we get:

$$c_0(1,1) = 2\hat{\alpha}(t)A_2(t), \quad c_0(1,j+2) = c_0(j+2,1) = \rho_{x,j}\sigma_j\hat{\alpha}(t)L_j(0), \text{ for } j \in \mathcal{A}.$$

and

$$a_0(1) = -\hat{\alpha}(t)A_2(t), \quad a_0(2) = \kappa\bar{v}, \quad a_0(N+3) = \lambda V(0).$$

By substitutions and appropriate matrix multiplications in the general solution for $A(u,\tau)$ and $\mathbf{B}(u,\tau)$ like in Chapter 1 (see Equation 1.4) the proof is finished. ■

Corollary 4.4.2. *Under the T_N-forward measure the characteristic function for $x^{T_N}(t)$ in (4.28) does not contain the terms $B_j(u,\tau)$ for $j = 1, \dots, N$ and $L_j(t)$. This implies a dimension reduction for the corresponding pricing PDE.*

Lemma 4.4.1 indicates that $B_x(u,\tau) = iu$ and $B_j(u,\tau) = 0$, giving rise to a simplification of the forward ChF:

$$\phi^{T_N}(u, x^{T_N}(t), \tau) = \exp(A(u,\tau) + iux^{T_N}(t) + B_v(u,\tau)v(t) + B_V(u,\tau)V(t)), \tag{4.30}$$

with $B_v(u,\tau)$, $B_V(u,\tau)$ and $A(u,\tau)$ given by:

$$\begin{cases} B'_v(u,\tau) = & -\frac{1}{2}(u^2+iu) + (\rho_{x,v}\gamma iu - \kappa)B_v + \frac{1}{2}\gamma^2 B_v^2, \\ B'_V(u,\tau) = & -\frac{1}{2}A_1(t)(u^2+iu) - \lambda B_V + \frac{1}{2}\eta^2 B_V^2, \\ A'(u,\tau) = & -\hat{\alpha}(t)A_2(t)(u^2+iu) + \kappa\bar{v}B_v + \lambda V(0)B_V, \end{cases} \tag{4.31}$$

subject to the final conditions:

$$B_v(u,0) = 0, \quad B_V(u,0) = 0, \quad A(u,0) = 0.$$

With the help of the Feynman-Kac theorem, one can show that the forward characteristic function, $\phi^{T_N} := \phi^{T_N}(u, x^{T_N}(t), \tau)$, given in (4.30) with functions $B_v(u,\tau)$, $B_V(u,\tau)$ and $A(u,\tau)$ in (4.31) satisfies the following Kolmogorov backward equation:

$$\begin{aligned} 0 &= \frac{\partial\phi^{T_N}}{\partial t} + \frac{1}{2}\left(v + A_1(t)V + 2A_2(t)\hat{\alpha}(t)\right)\left(\frac{\partial^2\phi^{T_N}}{\partial x^2} - \frac{\partial\phi^{T_N}}{\partial x}\right) + \kappa(\bar{v} - v)\frac{\partial\phi^{T_N}}{\partial v} \\ &+ \lambda(V(0) - V)\frac{\partial\phi^{T_N}}{\partial V} + \frac{1}{2}\eta^2 V\frac{\partial^2\phi^{T_N}}{\partial V^2} + \frac{1}{2}\gamma^2 v\frac{\partial^2\phi^{T_N}}{\partial v^2} + \rho_{x,v}\gamma v\frac{\partial^2\phi^{T_N}}{\partial x\partial v}, \end{aligned} \tag{4.32}$$

subject to $\phi(u, x^{T_N}(T_N), 0) = \exp\left(iux^{T_N}(T_N)\right)$, with $\hat{\alpha}(t)$ in (4.27), and $A_1(t)$, $A_2(t)$ in (4.23).

Since $\hat{\alpha}(t)$ is a deterministic function of time, the PDE coefficients in (4.32) are all affine.

The complex-valued functions $B_v(u,\tau)$, $B_V(u,\tau)$ and $A(u,\tau)$ in Lemma 4.4.1 are of the Heston-type. For constant parameters an analytic closed-form solution is available, however, since the functions $A_1(t)$ and $A_2(t)$ are not constant but piecewise constant an alternative approach needs to be used. As indicated in [4] an analytic, but recursive, solution is also available for piecewise constant parameters. We provide the solutions in Proposition 4.4.3.

Proposition 4.4.3 (Piece-wise complex-valued functions $A(u,\tau)$, $B_v(u,\tau)$ and $B_V(u,\tau)$)**.** *For a given grid, $0 = \tau_0 < \tau_1 < \cdots < \tau_N = \tau$, and time interval, $s_j = \tau_j - \tau_{j-1}$, $j = 1,\ldots,N$, the piece-wise constant complex-valued coefficients, $B_v(u,\tau)$ and $B_V(u,\tau)$, are given by the following recursive expressions:*

$$\begin{aligned} B_v(u,\tau_j) &= B_v(u,\tau_{j-1}) + \frac{\left(\kappa - \rho_{x,v}\gamma iu - d_j^1 - \gamma^2 B_v(u,\tau_{j-1})\right)\left(1 - \mathrm{e}^{-d_j^1 s_j}\right)}{\gamma^2(1 - g_j^1\mathrm{e}^{-d_j^1 s_j})}, \\ B_V(u,\tau_j) &= B_V(u,\tau_{j-1}) + \frac{\left(\lambda - d_j^2 - \eta^2 B_V(u,\tau_{j-1})\right)\left(1 - \mathrm{e}^{-d_j^2 s_j}\right)}{\eta^2(1 - g_j^2\mathrm{e}^{-d_j^2 s_j})}, \end{aligned}$$

and,

$$\begin{aligned}
A(u,\tau_j) &= A(u,\tau_{j-1}) + \frac{\kappa\bar{v}}{\gamma^2}\left((\kappa-\rho_{x,v}\gamma iu - d_j^1)s_j - 2\log\left(\frac{1-g_j^1\mathrm{e}^{-d_j^1 s_j}}{1-g_j^1}\right)\right)\\
&\quad +\frac{\lambda V(0)}{\eta^2}\left((\lambda-d_j^2)s_j - 2\log\left(\frac{1-g_j^2\mathrm{e}^{-d_j^2 s_j}}{1-g_j^2}\right)\right)\\
&\quad -A_2(t)(u^2+iu)\int_{\tau_{j-1}}^{\tau_j}\hat{\alpha}(t)\mathrm{d}t,
\end{aligned}$$

with:

$$d_j^1 = \sqrt{(\rho_{x,v}\gamma iu-\kappa)^2+\gamma^2(iu+u^2)},\quad d_j^2=\sqrt{\lambda^2+\eta^2A_1(t)(u^2+iu)},$$
$$g_j^1 = \frac{(\kappa-\rho_{x,v}\gamma iu)-d_j^1-\gamma^2B_v(u,\tau_{j-1})}{(\kappa-\rho_{x,v}\gamma iu)+d_j^1-\gamma^2B_v(u,\tau_{j-1})},\quad g_j^2=\frac{\lambda-d_j^2-\eta^2B_V(u,\tau_{j-1})}{\lambda+d_j^2-\eta^2B_V(u,\tau_{j-1})},$$

and the final conditions $B_v(u,\tau_0)=0$, $B_V(u,\tau_0)=0$ and $A(u,\tau_0)=0$. Moreover, for $t=T_N-\tau_j$, the functions $A_1(t)$ and $A_2(t)$ are defined in (4.23) and $\hat{\alpha}(t)$ in (4.27) with the parameters κ, γ, λ, η and $\rho_{x,v}$ given in (4.11), (4.12) and (4.13).

Proof. We notice that the functions $A_1(t)$ and $A_2(t)$ are constant between the times τ_i. For simplicity, we set $\tau_0=0$, and $\tau=T-t$. Since $B_j(u,\tau)=0$, the equations which need to be solved are given by:

$$\begin{aligned}
B_v'(u,\tau) &= b_{1,0}+b_{1,1}B_v+b_{1,2}B_v^2,\\
B_V'(u,\tau) &= b_{2,0}+b_{2,1}B_V+b_{2,2}B_V^2,\\
A'(u,\tau) &= a_0B_v+a_1B_V+f(t),
\end{aligned}$$

with certain initial conditions for $B_v(u,\tau_0)$, $B_V(u,\tau_0)$ and $A(u,\tau_0)$ and coefficients:

$$\begin{aligned}
b_{1,0} &= -\frac{1}{2}(u^2+iu),\quad & b_{1,1} &= \rho_{x,v}\gamma iu-\kappa,\quad & b_{1,2} &= \frac{1}{2}\gamma^2,\\
b_{2,0} &= -\frac{1}{2}A_1(t)(u^2+iu),\quad & b_{2,1} &= -\lambda,\quad & b_{2,2} &= \frac{1}{2}\eta^2,
\end{aligned}$$

and the coefficients for $A(u,\tau)$:

$$a_0 = \kappa\bar{v},\quad a_1=\lambda V(0),\quad f(t)=-\hat{\alpha}(t)A_2(t)(u^2+iu).$$

Since $B_v(u,\tau)$ and $B_V(u,\tau)$ are not depending on $A(u,\tau)$ a closed-form solution is available (see, for example, [54, 111]). For $\tau>0$ we find:

$$\begin{aligned}
B_v(u,\tau) &= B_v(u,\tau_0)+\frac{(-b_{1,1}-d_1-2b_{1,2}B_v(u,\tau_0))}{2b_{1,2}(1-g_1\mathrm{e}^{-d_1(\tau-\tau_0)})}(1-\mathrm{e}^{-d_1(\tau-\tau_0)}),\\
B_V(u,\tau) &= B_V(u,\tau_0)+\frac{(-b_{2,1}-d_2-2b_{2,2}B_V(u,\tau_0))}{2b_{2,2}(1-g_2\mathrm{e}^{-d_2(\tau-\tau_0)})}(1-\mathrm{e}^{-d_2(\tau-\tau_0)}),
\end{aligned}$$

with:

$$\begin{aligned} d_1 &= \sqrt{b_{1,1}^2 - 4b_{1,0}b_{1,2}}, \quad & d_2 &= \sqrt{b_{2,1}^2 - 4b_{2,0}b_{2,2}}, \\ g_1 &= \frac{-b_{1,1} - d_1 - 2B_v(u,\tau_0)b_{1,2}}{-b_{1,1} + d_1 - 2B_v(u,\tau_0)b_{1,2}}, \quad & g_2 &= \frac{-b_{2,1} - d_2 - 2B_V(u,\tau_0)b_{2,2}}{-b_{2,1} + d_2 - 2B_v(u,\tau_0)b_{2,2}}, \end{aligned}$$

For $A(u,\tau)$ we have:

$$A(u,\tau) = A(u,\tau_0) + a_0 \int_0^\tau B_v(u,s)\mathrm{d}s + a_1 \int_0^\tau B_V(u,s)\mathrm{d}s + \int_0^\tau f(\tau - s)\mathrm{d}s.$$

The first two integrals can be solved analytically:

$$\begin{aligned} \int_0^\tau B_v(u,s)\mathrm{d}s &= \frac{1}{2b_{1,2}}\left((-b_{1,1}+d_1)(\tau-\tau_0) - 2\log\left(\frac{1-g_1\mathrm{e}^{-d_1(\tau-\tau_0)}}{1-g_1}\right)\right), \\ \int_0^\tau B_V(u,s)\mathrm{d}s &= \frac{1}{2b_{2,2}}\left((-b_{2,1}+d_2)(\tau-\tau_0) - 2\log\left(\frac{1-g_2\mathrm{e}^{-d_2(\tau-\tau_0)}}{1-g_2}\right)\right). \end{aligned}$$

For the last integral we have:

$$\int_0^\tau f(\tau - s)\mathrm{d}s = -(u^2 + iu)\int_0^\tau \hat{\alpha}(\tau - s)A_2(\tau - s)\mathrm{d}s.$$

Since $A_2(\tau - s)$ is constant between 0 and τ, function $A_2(\tau - s)$ can be taken outside the integral. The proof is finished by the appropriate substitutions. ■

With a characteristic function available for the log-transformed forward, $x^{T_N}(t)$, we can compute European option prices for equity maturing at the terminal time, T_N. In the case of an option maturing at a time different from the terminal time T_N (say at T_i with $i < N$), one needs to price the equity forward $F^{T_i}(t)$, and therefore an appropriate change of measure for the H-LMM model (4.21) should be applied. Since the forward $F^{T_i}(t)$ is a martingale under the T_i-forward measure, it does not contain a drift term. On the other hand, the variance process, $v(t)$, for the Heston model is neither correlated with the Libors nor with the Libor's variance process, $V(t)$. The change of measure therefore does not affect variance process $v(t)$. Now we present a proof for this statement.

Proposition 4.4.4. *The dynamics of the variance process, $v(t)$, given in (4.11) are not affected by changing the forward measure generated by numéraire $P(t,T_i)$, for $i = 1,\ldots,N$.*

Proof. Under the T_N-forward measure the model with the forward stock, $F^{T_N}(t)$ in (4.21), with the variance process, $v(t)$ in (4.11), and the Libor rates as given in (4.12), can, in terms of the independent Brownian motions, be expressed as:

$$\begin{bmatrix} \mathrm{d}L_1(t) \\ \mathrm{d}L_2(t) \\ \cdots \\ \mathrm{d}L_N(t) \\ \mathrm{d}V(t) \\ \mathrm{d}F^N(t) \\ \mathrm{d}v(t) \end{bmatrix} = \begin{bmatrix} \mu_1(t) \\ \mu_2(t) \\ \cdots \\ \mu_N(t) \\ \lambda(V(0)-V(t)) \\ \mu_N(t)=0 \\ \kappa(\bar{v}-v(t)) \end{bmatrix} \mathrm{d}t + \mathbf{A}\mathbf{L} \begin{bmatrix} \mathrm{d}\widetilde{W}_1^N(t) \\ \mathrm{d}\widetilde{W}_2^N(t) \\ \cdots \\ \mathrm{d}\widetilde{W}_N^N(t) \\ \mathrm{d}\widetilde{W}_V^N(t) \\ \mathrm{d}\widetilde{W}_x^N(t) \\ \mathrm{d}\widetilde{W}_v^N(t) \end{bmatrix},$$

with

$$\mathbf{A} = \begin{bmatrix} \sigma_1\phi_1(t)\sqrt{V(t)} & \dots & 0 & 0 & 0 & 0 \\ \vdots & \ddots & \vdots & \vdots & \vdots & \vdots \\ 0 & \dots & \sigma_N\phi_N(t)\sqrt{V(t)} & 0 & 0 & 0 \\ 0 & \dots & 0 & \eta\sqrt{V(t)} & 0 & 0 \\ \Upsilon_1(t)\sqrt{V(t)} & \dots & \Upsilon_N(t)\sqrt{V(t)} & 0 & \sqrt{v(t)} & 0 \\ 0 & \dots & 0 & 0 & 0 & \gamma\sqrt{v(t)} \end{bmatrix},$$

where $\Upsilon_j(t) = \frac{\tau_j\sigma_j\phi_j(t)\sqrt{V(t)}}{1+\tau_j L_j(t)}$ and $\mathbf{L}$ is the Cholesky lower triangular of the correlation matrix, $\mathbf{C}$, which is given by:

$$\mathbf{C} = \begin{bmatrix} 1 & \rho_{1,2} & \dots & \rho_{1,N} & 0 & \rho_{x,1} & 0 \\ \rho_{2,1} & 1 & \dots & \rho_{2,N} & 0 & \rho_{x,2} & 0 \\ \vdots & \vdots & \ddots & \vdots & \vdots & \vdots & \vdots \\ \rho_{N,1} & \rho_{N,2} & \dots & 1 & 0 & \rho_{x,N} & 0 \\ 0 & 0 & \dots & 0 & 0 & 0 & 0 \\ \rho_{x,1} & \rho_{x,2} & \dots & \rho_{x,N} & 0 & 1 & \rho_{x,v} \\ 0 & 0 & \dots & 0 & 0 & \rho_{x,v} & 1 \end{bmatrix}.$$

With $\zeta_k(t)$ the k-th row vector from matrix $\mathbf{M} = \mathbf{A}\mathbf{L}$, the Radon-Nikodym derivative, $\Lambda_N^{N-1}(t)$, is given by:

$$\Lambda_N^{N-1}(t) = \frac{\mathrm{d}\mathbb{Q}^{N-1}}{\mathrm{d}\mathbb{Q}^N}\Big|_{\mathcal{F}(t)} = \frac{P(0,T_N)}{P(0,T_{N-1})}(1+\tau_N L_N(t)).$$

From the representation above, the dynamics for the Libor $L_N(t)$ can be expressed as:

$$\mathrm{d}L_N(t) = \zeta_N(t)\mathrm{d}\widetilde{\mathbf{W}}^N(t).$$

Therefore, the dynamics for $\Lambda_{N-1}^N(t)$ read:

$$\mathrm{d}\Lambda_N^{N-1}(t) = \Lambda_N^{N-1}(t)\frac{\tau_N\zeta_N(t)}{1+\tau_N L_N(t)}\mathrm{d}\widetilde{\mathbf{W}}^N(t).$$

By the Girsanov theorem this implies that the change of measure is given by:

$$\mathrm{d}\widetilde{\mathbf{W}}^N(t) = \frac{\tau_N\zeta_N(t)^{\mathrm{T}}}{1+\tau_N L_N(t)}\mathrm{d}t + \mathrm{d}\widetilde{\mathbf{W}}^{N-1}(t). \tag{4.33}$$

We wish to find the dynamics for process $v(t)$ under the measure $\mathbb{Q}^{N-1}$. In terms of the independent Brownian motions the variance process $v(t)$ is given by:

$$\mathrm{d}v(t) = \kappa(\bar{v} - v(t))\mathrm{d}t + \zeta_{N+3}(t)\mathrm{d}\widetilde{\mathbf{W}}^N(t),$$

with

$$\zeta_{N+3}(t) = \left[\underbrace{0,\ 0,\ 0,\ldots,0}_{N+1},\ \gamma\sqrt{v(t)}\rho_{x,v},\ \gamma\sqrt{v(t)}\sqrt{1-\rho_{x,v}^2}\right].$$

By Equation (4.33) the dynamics for $v(t)$ under $\mathbb{Q}^{N-1}$ are given by:

$$\mathrm{d}v(t) = \kappa(\bar{v} - v(t))\mathrm{d}t + \zeta_{N+3}(t)\left(\frac{\tau_N \zeta_N(t)^{\mathrm{T}}}{1+\tau_N L_N(t)}\mathrm{d}t + \mathrm{d}\widetilde{\mathbf{W}}^{N-1}(t)\right).$$

Since

$$\zeta_N(t) = \left[\underbrace{\ldots,\ ,\ldots,\ ,\ldots,}_{N+1}\ 0,\ 0\right],$$

so the scalar product $\zeta_{N+3}(t)\zeta_N(t)^{\mathrm{T}} = 0$. This results in the following dynamics for the process $v(t)$ under the $\mathbb{Q}^{N-1}$ measure:

$$\mathrm{d}v(t) = \kappa(\bar{v} - v(t))\mathrm{d}t + \zeta_{N+3}(t)\mathrm{d}\widetilde{\mathbf{W}}^{N-1}(t).$$

Since for all $j = 1,\ldots,N$ the scalar product $\zeta_{N+3}(t)\zeta_j(t)^{\mathrm{T}} = 0$, changing the corresponding forward measures does not affect the drift of the variance process $v(t)$. This observation concludes the proof. ■

4.5 Numerical results

In this section several numerical experiments are presented. First of all, the accuracy of the approximate model, H1-LMM, is compared with the full-scale H-LMM model for European call option prices. Furthermore, the sensitivity to the interest rate skew for both models is checked. Finally, we use a typical equity-interest rate hybrid payoff function and compare the performance of the new H-LMM model with the Heston-Hull-White hybrid model.

4.5.1 Accuracy of the H1-LMM model

We check here the accuracy of the developed approximation H1-LMM. We compare Monte Carlo European call prices from the full-scale H-LMM model with corresponding prices obtained by the Fourier inverse algorithm [32] for the H1-LMM model. In the Monte Carlo simulation we work under one measure, the T_N-terminal measure. So, the prices for different option maturities are calculated by the following expression:

$$\Pi_{\mathrm{MC}}(t,T_N) \quad = \quad P(t,T_N)\mathbb{E}^{T_N}\left(\frac{(S_{T_i}-K)^+}{P(T_i,T_N)}\big|\mathcal{F}(t)\right),\ \text{for } i \leq N,$$

which by Equation (4.10) equals:

$$\Pi_{\mathrm{MC}}(t,T_i) \quad = \quad P(t,T_N)\mathbb{E}^{T_N}\left(\left(F^{T_N}(T_i)-\frac{K}{P(T_i,T_N)}\right)^+ \big|\mathcal{F}(t)\right),$$

with K the strike price, and the bond $P(T_i,T_N)$ is given by (4.6).

The prices calculated by the Fourier inverse algorithm are obtained by the following expression:

$$\Pi_{\mathrm{F}}(t,T_i) \quad = \quad P(t,T_i)\mathbb{E}^{T_i}\left(\left(F^{T_i}(T_i)-K\right)^+ \big|\mathcal{F}(t)\right),$$

with the ChF from Proposition 4.4.3. As mentioned, the change of measure does not affect the volatility of the Heston process. Pricing under different measures is therefore consistent.

When calibrating the plain Heston model in practice, the parameters obtained rarely satisfy the Feller condition [2], $\gamma^2 < 2\kappa\bar{v}$. In order to mimic a realistic setting, we also choose parameters that do *not* satisfy this inequality, i.e.:

$$\kappa = 1.2, \quad \bar{v} = 0.1, \quad \gamma = 0.5, \quad S(0) = 1, \quad v(0) = 0.1.$$

For the interest rate model we take:

$$\beta_k = 0.5, \quad \sigma_k = 0.25, \quad \lambda = 1, \quad V(0) = 1, \quad \eta = 0.1.$$

In the correlation matrix a number of elements need to be specified. For the correlations between the Libor rates, we set large positive values, as frequently observed in the fixed income markets (see for example [19]), $\rho_{i,j} = 98\%$, for $i,j = 1,\ldots,N, \quad i \neq j$. For the correlation between $S(t)$ and $v(t)$ we set a negative correlation, $\rho_{x,v} = -30\%$, which corresponds to the skew in the implied volatility for equity. And, finally, the correlation between the stock and the Libors, $\rho_{x,i} = 50\%$ for $i = 1,\ldots,N$. In practice this correlation would be estimated from historical data [17]. The following correlation matrix results:

$$\begin{bmatrix} 1 & \rho_{x,v} & \rho_{x,1} & \ldots & \rho_{x,N} & \rho_{x,V} \\ \rho_{v,x} & 1 & \rho_{v,1} & \ldots & \rho_{v,N} & \rho_{v,V} \\ \rho_{1,x} & \rho_{1,v} & 1 & \ldots & \rho_{1,N} & \rho_{1,V} \\ \vdots & \vdots & \vdots & \ddots & \vdots & \vdots \\ \rho_{N,x} & \rho_{N,v} & \rho_{N,1} & \ldots & 1 & \rho_{N,V} \\ \rho_{V,x} & \rho_{V,v} & \rho_{V,1} & \ldots & \rho_{V,N} & 1 \end{bmatrix} = \begin{bmatrix} 1 & -30\% & 50\% & \ldots & 50\% & 0 \\ -30\% & 1 & 0 & \ldots & 0 & 0 \\ 50\% & 0 & 1 & \ldots & 98\% & 0 \\ \vdots & \vdots & \vdots & \ddots & \vdots & \vdots \\ 50\% & 0 & 98\% & \ldots & 1 & 0 \\ 0 & 0 & 0 & \ldots & 0 & 1 \end{bmatrix}.$$

The accuracy and the associated standard deviations, in terms of prices of the European call option prices for equity (with the Monte Carlo simulation versus the Fourier inversion of the ChF), are presented in Table 4.1. In Figure 4.1 the corresponding implied volatility plots are presented. The accuracy of the approximations introduced (H1-LMM) is highly satisfactory for this experiment.

[2] If the Feller condition is satisfied this ensures that the variance process is positive.

Table 4.1: *The European equity call option prices of H1-LMM compared to H-LMM. The H-LMM Monte Carlo experiment was performed with 20.000 paths and 20 intermediate points between dates T_{i-1} and T_i, for $i = 1, \ldots, N$. The tenor structure was chosen to be $\mathcal{T} = \{T_1, \ldots, T_{10}\}$ with the terminal measure $T_N = T_{10}$. Numbers in parentheses are sample standard deviations. The simulation was repeated 10 times.*

Strike K	**European Equity Call Option Price**					
	T_2		T_5		T_{10}	
	ChF	MC	ChF	MC	ChF	MC
$K = 40\%$	0.6418	0.6424 (0.0035)	0.7017	0.7014 (0.0034)	0.7821	0.7818 (0.0081)
$K = 80\%$	0.3299	0.3316 (0.0030)	0.4638	0.4648 (0.0034)	0.6203	0.6210 (0.0082)
$K = 100\%$	0.2149	0.2167 (0.0027)	0.3730	0.3742 (0.0034)	0.5562	0.5572 (0.0083)
$K = 120\%$	0.1332	0.1345 (0.0024)	0.2993	0.3004 (0.0034)	0.5008	0.5020 (0.0083)
$K = 160\%$	0.0483	0.0486 (0.0016)	0.1933	0.1941 (0.0034)	0.4109	0.4126 (0.0082)
$K = 200\%$	0.0184	0.0184 (0.0010)	0.1268	0.1273 (0.0031)	0.3419	0.3438 (0.0080)
$K = 240\%$	0.0078	0.0076 (0.0006)	0.0850	0.0852 (0.0026)	0.2878	0.2901 (0.0079)

4.5.2 Interest rate skew

Approximation H1-LMM was based on freezing the appropriate Libor rates and on linearizations in the instantaneous covariance matrix. By freezing the Libors, i.e.: $L_k(t) \equiv L_k(0)$ we have that $\phi_k(t) = \beta_k L_k(t) + (1 - \beta_k) L_k(0) = L_k(0)$.

In the DD-SV model, parameter β_k controls the slope of the interest rate volatility smile, so by freezing the Libors to $L_k(0)$ the information about the interest rate skew is not included in the approximation H1-LMM [3].

We perform here an experiment with the full-scale model (H-LMM). By a Monte Carlo simulation, we check the influence of parameter β_k on the equity implied volatilities [16]. In Table 4.2 the equity implied volatilities for the European call option for H-LMM are presented. The experiment displays a small impact of the different β_k's on the equity implied volatilities, which implies that our approximation, H1-LMM, makes sense for various parameters β_k in the interest rate modelling in the present setting.

To explain the small effect of variation in β_k on the equity implied volatility we need to return to the equity forward equation in (4.21), i.e.:

$$\frac{\mathrm{d}F^{T_N}(t)}{F^{T_N}(t)} = \sqrt{v(t)}\mathrm{d}W_x^N(t) + \sum_{j=m(t)+1}^{N} \frac{\tau_j \sigma_j \phi_j(t) \sqrt{V(t)}}{1 + \tau_j L_j(t)} \mathrm{d}W_j^N(t).$$

The equity forward is based on two types of correlated volatilities: The equity with $\mathrm{d}W_x^N(t)$ and the interest rate with $\mathrm{d}W_j^N(t)$ for $j = 1, \ldots, N$. Since in

[3] the model remains sensitive to interest rate volatility

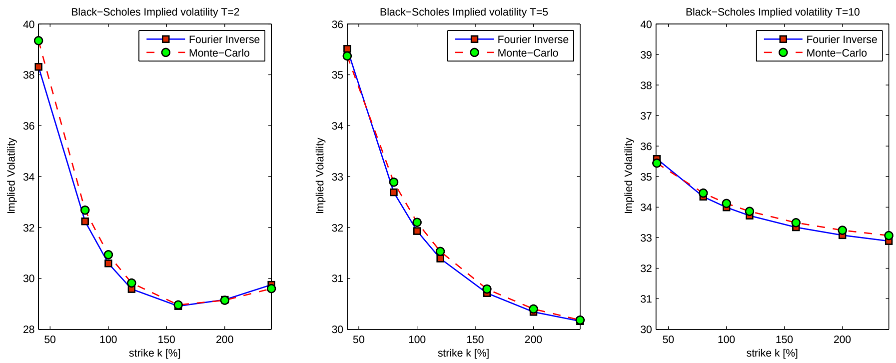

Figure 4.1: *Comparison of implied Black-Scholes volatilities for the European equity option, obtained by Fourier inversion of H1-LMM and by Monte Carlo simulation of H-LMM.*

the experiment we have chosen a realistic set of parameters (as in Section 4.5.1) with a rather large parameter $\gamma = 0.5$, the first term in the forward SDE above, $\sqrt{v(t)}\mathrm{d}W_x^N(t)$, is dominating. The other volatilities contribute in particular when large maturities are considered. The theoretical proof for this statement is rather involved, but we can simply illustrate it by setting $t = 0$. For the equity part we then have: $\sqrt{v(0)} \approx 0.3162$, and for the interest rate $\sqrt{V(0)}\sum_{j=1}^{N} \frac{\tau_j\sigma_j L_j(0)}{1+\tau_j L_j(0)} \approx 0.0122N$, where N corresponds to the number of Libors considered.

4.5.3 Pricing a hybrid product

Although the interest rate skew parameter, β_k, does not strongly influence the equity prices, it may still have an impact on the hybrid contract price. In this subsection we use H-LMM and price a typical exotic payoff.

As indicated in [59], an investor interested in structured products may look for higher expected return (higher coupons) than available from basic market instruments. By trading hybrid products she/he can also trade the correlation, for example, by including multiple assets in a structured derivatives product, and therefore the basket volatility can be reduced. This typically makes the corresponding option cheaper.

The main advantage of H-LMM lies in its capability to price hybrid products that are sensitive to an equity smile, an interest rate smile and the correlation between the assets. A hybrid payoff which contains the equity and interest rate assets is the so-called *minimum of several assets payoff*, see [59]. The contract is made for an investor willing to take some risk in one asset class in order to obtain a participation in a different asset class. If the investor wants to be involved in an n-years Constant Maturity Swap (CMS), by taking some risk in equity, this can be expressed by the following payoff:

$$\text{Payoff} = \max\left(0, \min\left(C_n(T), k\% \times \frac{S(T)}{S(t)}\right)\right),$$

Table 4.2: *The effect of the interest rate skew, controlled by β_k, on the equity implied volatilities. The Monte Carlo simulation was performed with the setup from Table 4.1. The maturity is $T_N = 10$. Values in brackets indicate implied volatility standard deviations (the experiment was repeated 10 times).*

Strike K	**Equity Implied Volatilities**		
	$\beta_k = 0$	$\beta_k = 0.5$	$\beta_k = 1$
$K = 40\%$	35.71 % (0.0290)	35.50% (0.0221)	34.60 % (0.0460)
$K = 80\%$	34.63 % (0.0109)	34.49 % (0.0086)	34.26 % (0.0175)
$K = 100\%$	34.23 % (0.0087)	34.15 % (0.0066)	33.99 % (0.0139)
$K = 120\%$	33.90 % (0.0073)	33.89 % (0.0055)	33.78 % (0.0119)
$K = 160\%$	33.40 % (0.0058)	33.53 % (0.0045)	33.47 % (0.0097)
$K = 200\%$	33.05 % (0.0052)	33.28 % (0.0041)	33.26 % (0.0088)
$K = 240\%$	32.81 % (0.0048)	33.09 % (0.0039)	33.12 % (0.0085)

with $S(t)$ being the stock price at time t and $C_n(t)$ is an n-years CMS. By setting the tenor structure $\mathcal{T} = \{1, \ldots, 10\}$, with payment date $T_N = 5$ and maturity $T_M = 10$, we obtain the following pricing equation:

$$\Pi_{\mathrm{H}}(t, T_5) = P(t, T_5)\mathbb{E}^{T_5}\left(\max\left(0, \min\left(\frac{1 - P(T_5, T_{10})}{\sum_{k=6}^{10} P(T_5, T_k)}, k\% \times \frac{S(T_5)}{S(t)}\right)\right)|\mathcal{F}(t)\right). \tag{4.34}$$

In our simulation, the bonds $P(T_i, T_j)$ are obtained from the SV-DD Libor Market Model and determined by (4.6) for $t = T_i$ and $T_N = T_j$. As a first test we check the sensitivity to the interest rate skew (by changing β and keeping the correlation $\rho_{x,i} = 0\%$, for all i) and to the correlation between the stock, $S(t)$, and the Libor rates, $L_i(t)$, by varying the correlation, $\rho_{x,i} = \{0\%, -70\%, 70\%\}$, for all i. Figure 4.2 shows the corresponding results. We see a significant impact on the hybrid prices, which suggests that plain equity models, or equity short-rate hybrid models, may lead to different prices for such hybrid products.

Insight in the added value of H-LMM can be gained by comparing the H-LMM results with, for example, the Heston-Hull-White (HHW) hybrid model. In the HHW model the equity part is driven by the Heston process, as in Equation (4.11), but the interest rate is driven by a Hull-White short-rate process given by the following SDE:

$$\mathrm{d}r(t) = \lambda(\theta(t) - r(t))\mathrm{d}t + \eta \mathrm{d}W_r(t), \text{ with } r(0) > 0,$$

with term structure $\theta(t)$, positive parameters λ, η and $\mathrm{d}W_x(t)\mathrm{d}W_r(t) = \rho_{x,r}\mathrm{d}t$.

Before performing the pricing of the hybrid product the model parameters need to be determined. The models were calibrated to data sets provided in Tables 4.3 and 4.4.

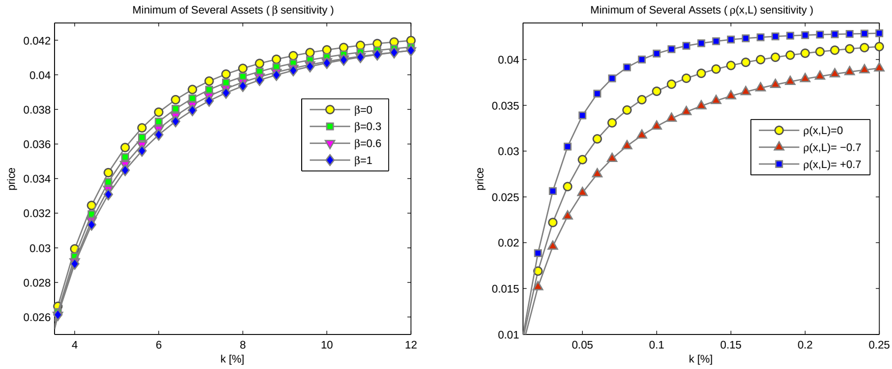

Figure 4.2: *The value for a minimum of several assets hybrid product. The prices are obtained by Monte Carlo simulation with 20.000 paths and 20 intermediate points. LEFT: Influence of* β*; RIGHT: Influence of* $\rho_{x,L}$*.*

Table 4.3: *The standardized European equity call option values for different maturities* ($T[y]$) *and strikes* ($K[\%]$)*.*

Strike K	European Equity Call Option Price						
	$T = 0.5$	$T = 1$	$T = 2$	$T = 3$	$T = 4$	$T = 5$	$T = 10$
40%	0.610	0.620	0.642	0.663	0.683	0.702	0.779
80%	0.235	0.271	0.329	0.378	0.421	0.461	0.612
100%	0.098	0.143	0.212	0.271	0.322	0.368	0.546
120%	0.030	0.067	0.131	0.190	0.244	0.293	0.489
160%	0.003	0.015	0.051	0.095	0.141	0.188	0.397
200%	0.000	0.004	0.023	0.051	0.086	0.125	0.328
240%	0.000	0.001	0.012	0.030	0.055	0.086	0.275
260%	0.000	0.001	0.009	0.024	0.045	0.073	0.253
300%	0.000	0.000	0.005	0.016	0.031	0.053	0.216

For H-LMM, the parameters from Section 4.5.1 were found. In the calibration of the HHW model, we first calibrated the Hull-White process, for which we obtained:

$$\lambda = 0.0614, \quad \eta = 0.0133, \quad r_0 = 0.05.$$

Then, with an imposed correlation between the stock and the short-rate, $\rho_{x,r} = 50\%$, the remaining parameters were found to be:

$$\kappa = 0.650, \quad \gamma = 0.469, \quad \bar{v} = 0.090, \quad \rho_{x,v} = -22.2\%, \quad v(0) = 0.114.$$

In Figure 4.3(left) the pricing results with the two hybrid models are presented. For $k > 5\%$ (with k in Equation (4.34)) a significant difference between the

Table 4.4: *The zero-coupon bonds for different maturities* T*.*

Strike	The zero-coupon bonds $P(0,T)$						
	$T = 0.5$	$T = 1$	$T = 2$	$T = 3$	$T = 4$	$T = 5$	$T = 10$
$P(0,T)$	0.9756	0.9512	0.9048	0.8607	0.8187	0.7788	0.6065

obtained prices is observed, although the two models were calibrated to the same data set.

Payoff equation (4.34) shows that, as the percentage k increases, the dominating part of the product will be the CMS rate. We conclude that the Hull-White underlying model for the short-rate indeed does not take into account the interest rate smile/skew and therefore gives different prices for a smile/skew sensitive product.

In Figure 4.3(right) the histograms of the CMS rate for both models are presented. The histograms show a significantly fatter tail in the case of the DD-SV model than one for the Hull-White short-rate model.

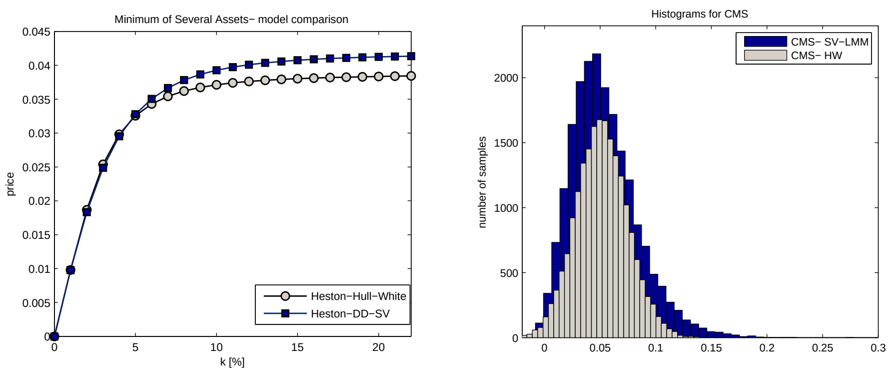

Figure 4.3: *LEFT: Hybrid prices obtained by two different hybrid models, H-LMM and HHW. The models were calibrated to the same data set; RIGHT: CMS rate for the H-LMM and the HHW models.*

4.6 Conclusion

The financial industry does not only require models that are well-defined and capture the important features in the market, but also efficient calibration of a model to market data should be feasible.

We have proposed an equity-interest rate hybrid model with stochastic volatility for stock and for the interest rates. To bring the model within the class of affine processes, we projected the non-affine terms on time-dependent functions. This approximation to the full-scale model is affine, and we have determined a closed-form forward characteristic function. By this the approximate hybrid model, H1-LMM, can be used for calibration purposes.

The main advantage of the model developed lies in its ability to price hybrid produces exposed to the interest rate smile accurately and efficiently.

CHAPTER 5

On Cross-Currency Models with Stochastic Volatility and Correlated Interest Rates

A fair exchange is no robbery.

- English 16th Century Proverbs

5.1 Introduction

Due to the existence of complex FX products, like the *Power-Reverse Dual-Currency* [103], the *Equity-CMS Chameleon* or the *Equity-Linked Range Accrual TRAN swaps* [22], that all have a long lifetime and are sensitive to smiles or skews in the market, improved models with stochastic interest rates need to be developed.

The literature on modelling foreign exchange (FX) rates is rich and many stochastic models are available. An industrial standard is a model from [38, 103], where log-normally distributed FX dynamics are assumed and Gaussian, one-factor, interest rates are used. This model gives analytic expressions for the prices of basic products for at-the-money options. Extensions on the interest rate side were presented by Schlögl in [99] or Mikkelsen in [78], where the short-rate model was replaced by a Libor Market Model framework.

A Gaussian interest rate model was also used in [93], in which a local volatility model was applied for generating the skews present in the FX market. In another paper, [67], a displaced-diffusion model for FX was combined with the interest rate Libor Market Model.

Stochastic volatility FX models have also been investigated. For example, in [107] the Schöbel-Zhu model was applied for pricing FX in combination with short-rate processes. This model leads to a semi-closed-form for the characteristic function. However, for a normally distributed volatility process it is difficult to outperform the Heston model with independent stochastic interest rates [107].

Research on the Heston dynamics in combination with *correlated* interest rates has led to some interesting models. In [6] and [43] an indirectly imposed correlation structure between Gaussian short-rates and FX was presented. The model is intuitively appealing, but it may give rise to very large model parameters [8]. An alternative model was presented in [8, 9], in which calibration formulas were developed by means of Markov projection techniques.

In this chapter we present an FX Heston-type model in which the interest rates are stochastic processes, correlated with the governing FX processes. We first discuss the Heston FX model with Gaussian interest rate (Hull-White model [56]) short-rate processes. In this model a full matrix of correlations is used.

This model, denoted by *FX-HHW* here, is a generalization of our work in Chapters 2 and 3, where we dealt with the problem of finding an affine representation of the Heston equity model with a correlated stochastic interest rate. In this chapter, we apply this technique in the world of foreign exchange.

Secondly, we extend the framework by modelling the interest rates by a market model, i.e., by the stochastic volatility displaced-diffusion Libor Market Model [5, 92]. In this hybrid model, called *FX-HLMM* here, we incorporate a non-zero correlation between the FX and the interest rates and between the rates from different currencies. Because it is not possible to obtain closed-form formulas for the associated characteristic function, we use a linearization approximation, as developed earlier, in Chapter 4.

For both models we provide details on how to include a foreign stock in the multi-currency pricing framework.

Fast model evaluation is highly desirable for FX options in practice, especially during the calibration of the hybrid model. This is the main motivation for the generalization of the linearization techniques presented earlier in this thesis to the world of foreign exchange. We will see that the resulting approximations can be used very well in the FX context.

The present chapter is organized as follows. In Section 5.2 we discuss the dynamics of FX rate under the extended Heston model by stochastic interest rates, described by short-rate processes. We provide details about some approximations in the model, and then derive the related forward characteristic function. We also discuss the model's accuracy and calibration results. Section 5.3 gives the details for the cross-currency model with interest rates driven by the market model and Section 5.4 concludes.

5.2 Multi-Currency model with short-rate interest rates

Here, we derive the model for the spot FX, $y(t)$, expressed in units of domestic currency, per unit of a foreign currency.

We start the analysis with the specification of the underlying interest rate processes, $r_d(t)$ and $r_f(t)$. At this stage we assume that the interest rate dynamics are defined via *short-rate processes*, which under their spot measures, i.e., $\mathbb{Q}-$domestic and $\mathbb{Z}-$foreign, are driven by the Hull-White [56] one-factor model:

$$\begin{aligned} \mathrm{d}r_d(t) &= \lambda_d(\theta_d(t) - r_d(t))\mathrm{d}t + \eta_d \mathrm{d}W_d^{\mathbb{Q}}(t), & (5.1)\\ \mathrm{d}r_f(t) &= \lambda_f(\theta_f(t) - r_f(t))\mathrm{d}t + \eta_f \mathrm{d}W_f^{\mathbb{Z}}(t), & (5.2)\end{aligned}$$

where $W_d^{\mathbb{Q}}(t)$ and $W_f^{\mathbb{Z}}(t)$ are Brownian motions under $\mathbb{Q}$ and $\mathbb{Z}$, respectively. Parameters λ_d, λ_f determine the speed of mean reversion to the time-dependent term structure functions $\theta_d(t)$, $\theta_f(t)$, and parameters η_d, η_f are the volatility coefficients.

These processes, under the appropriate measures, are linear in their state variables, so that for a given maturity T $(0 < t < T)$ the zero-coupon bonds (ZCB) are known to be of the following form:

$$\begin{aligned} P_d(t,T) = &\ \exp\left(A_d(t,T) + B_d(t,T)r_d(t)\right), \\ P_f(t,T) = &\ \exp\left(A_f(t,T) + B_f(t,T)r_f(t)\right), \end{aligned} \tag{5.3}$$

with $A_d(t,T)$, $A_f(t,T)$ and $B_d(t,T)$, $B_f(t,T)$ analytically known quantities (see for example Chapter 1). In the model the money market accounts are given by:

$$\mathrm{d}M_d(t) = r_d(t)M_d(t)\mathrm{d}t, \quad \text{and} \quad \mathrm{d}M_f(t) = r_f(t)M_f(t)\mathrm{d}t. \tag{5.4}$$

By using the Heath-Jarrow-Morton arbitrage-free argument, [53], the dynamics for the ZCBs, under their own measures generated by the money-savings accounts, are known and given by the following result:

Result 5.2.1 (ZCB dynamics under the risk-free measure)**.** The risk-free dynamics of the zero-coupon bonds, $P_d(t,T)$ and $P_f(t,T)$, with maturity T are given by:

$$\begin{aligned} \frac{\mathrm{d}P_d(t,T)}{P_d(t,T)} &= r_d(t)\mathrm{d}t - \left(\int_t^T \sigma_d(t,s)\mathrm{d}s\right)\mathrm{d}W_d^{\mathbb{Q}}(t), \\ \frac{\mathrm{d}P_f(t,T)}{P_f(t,T)} &= r_f(t)\mathrm{d}t - \left(\int_t^T \sigma_f(t,s)\mathrm{d}s\right)\mathrm{d}W_f^{\mathbb{Z}}(t), \end{aligned}$$

where $\sigma_d(t,T)$, $\sigma_f(t,T)$ are the volatility functions of the instantaneous forward rates $f_d(t,T)$, $f_f(t,T)$, respectively, that are given by:

$$\begin{aligned} \mathrm{d}f_d(t,T) &= \sigma_d(t,T)\int_t^T \sigma_d(t,s)\mathrm{d}s + \sigma_d(t,T)\mathrm{d}W_d^{\mathbb{Q}}(t), \\ \mathrm{d}f_f(t,T) &= \sigma_f(t,T)\int_t^T \sigma_f(t,s)\mathrm{d}s + \sigma_f(t,T)\mathrm{d}W_f^{\mathbb{Z}}(t). \end{aligned}$$

Proof. For the proof see [82]. ■

The spot-rates at time t are defined by $r_d(t) \equiv f_d(t,t)$, $r_f(t) \equiv f_f(t,t)$.

By means of the volatility structures, $\sigma_d(t,T)$, $\sigma_f(t,T)$, one can define a number of short-rate processes. In our framework the volatility functions are chosen to be $\sigma_d(t,T) = \eta_d \exp(-\lambda_d(T-t))$ and $\sigma_f(t,T) = \eta_f \exp(-\lambda_f(T-t))$. The Hull-White short-rate processes, $r_d(t)$ and $r_f(t)$ as in (5.1), (5.2), are then obtained and the term structures, $\theta_d(t)$, $\theta_f(t)$, expressed in terms of instantaneous forward rates, are also known. The choice of specific volatility determines the dynamics of the ZCBs:

$$\begin{aligned}\frac{\mathrm{d}P_d(t,T)}{P_d(t,T)} &= r_d(t)\mathrm{d}t + \eta_d B_d(t,T)\mathrm{d}W_d^{\mathbb{Q}}(t),\\ \frac{\mathrm{d}P_f(t,T)}{P_f(t,T)} &= r_f(t)\mathrm{d}t + \eta_f B_f(t,T)\mathrm{d}W_f^{\mathbb{Z}}(t),\end{aligned} \tag{5.5}$$

with $B_d(t,T)$ and $B_f(t,T)$ as in (5.3), given by:

$$B_d(t,T) = \frac{1}{\lambda_d}\left(\mathrm{e}^{-\lambda_d(T-t)} - 1\right), \quad B_f(t,T) = \frac{1}{\lambda_f}\left(\mathrm{e}^{-\lambda_f(T-t)} - 1\right). \tag{5.6}$$

For a detailed discussion on short-rate processes, we refer to the analysis of Musiela and Rutkowski in [82].

In the next subsection we define the FX hybrid model.

5.2.1 The model with correlated, Gaussian interest rates

The FX-HHW model, with all processes defined under the domestic risk-neutral measure, $\mathbb{Q}$, is of the following form:

$$\begin{aligned}\mathrm{d}y(t)/y(t) &= (r_d(t) - r_f(t))\,\mathrm{d}t + \sqrt{v(t)}\mathrm{d}W_y^{\mathbb{Q}}(t),\\ \mathrm{d}v(t) &= \kappa(\bar{v} - v(t))\mathrm{d}t + \gamma\sqrt{v(t)}\mathrm{d}W_v^{\mathbb{Q}}(t),\\ \mathrm{d}r_d(t) &= \lambda_d(\theta_d(t) - r_d(t))\mathrm{d}t + \eta_d\mathrm{d}W_d^{\mathbb{Q}}(t),\\ \mathrm{d}r_f(t) &= \left(\lambda_f(\theta_f(t) - r_f(t)) - \eta_f\rho_{y,f}\sqrt{v(t)}\right)\mathrm{d}t + \eta_f\mathrm{d}W_f^{\mathbb{Q}}(t),\end{aligned} \tag{5.7}$$

with $y(0) > 0$, $v(0) > 0$, $r_d(0) > 0$ and $r_f(0)$. Here, the parameters κ, λ_d, and λ_f determine the speed of mean reversion of the latter three processes, their long-term mean is given by $\bar{v}$, $\theta_d(t)$, $\theta_f(t)$, respectively. The volatility coefficients for the processes $r_d(t)$ and $r_f(t)$ are given by η_d and η_f and the volatility-of-variance parameter for process $v(t)$ is γ.

In the model we consider a full matrix of correlations between the Brownian motions $\mathbf{W}(t) = \left[W_y^{\mathbb{Q}}(t), W_v^{\mathbb{Q}}(t), W_d^{\mathbb{Q}}(t), W_f^{\mathbb{Q}}(t)\right]^{\mathrm{T}}$:

$$\mathrm{d}\mathbf{W}(t)(\mathrm{d}\mathbf{W}(t))^{\mathrm{T}} = \begin{pmatrix} 1 & \rho_{y,v} & \rho_{y,d} & \rho_{y,f}\\ \rho_{y,v} & 1 & \rho_{v,d} & \rho_{v,f}\\ \rho_{y,d} & \rho_{v,d} & 1 & \rho_{d,f}\\ \rho_{y,f} & \rho_{v,f} & \rho_{d,f} & 1\end{pmatrix}\mathrm{d}t. \tag{5.8}$$

Under the domestic-spot measure the drift in the short-rate process, $r_f(t)$, gives rise to an additional term, $-\eta_f\rho_{y,f}\sqrt{v(t)}$. This term ensures the existence of martingales, under the domestic spot measure, for the following prices (for more discussion, see [102]):

$$\chi_1(t) := y(t)\frac{M_f(t)}{M_d(t)} \quad \text{and} \quad \chi_2(t) := y(t)\frac{P_f(t,T)}{M_d(t)},$$

where $P_f(t,T)$ is the price foreign zero-coupon bond (5.5) and the money-savings accounts $M_d(t)$ and $M_f(t)$ are from (5.4).

To see that the processes $\chi_1(t)$ and $\chi_2(t)$ are martingales, one can apply the Itô product rule, which gives:

$$\begin{aligned} \mathrm{d}\chi_1(t)/\chi_1(t) &= \sqrt{v(t)}\mathrm{d}W_y^{\mathbb{Q}}(t), \\ \mathrm{d}\chi_2(t)\chi_2(t) &= \sqrt{v(t)}\mathrm{d}W_y^{\mathbb{Q}}(t) + \eta_f B_f(t,T)\mathrm{d}W_f^{\mathbb{Q}}(t). \end{aligned}$$

The change of dynamics of the underlying processes, from the foreign-spot to the domestic-spot measure, also influences the dynamics for the associated bonds, which, under the domestic risk-neutral measure, $\mathbb{Q}$, with the money-savings account considered as a numéraire, have the following representations

$$\frac{\mathrm{d}P_d(t,T)}{P_d(t,T)} = r_d(t)\mathrm{d}t + \eta_d B_d(t,T)\mathrm{d}W_d^{\mathbb{Q}}(t), \tag{5.9}$$

$$\frac{\mathrm{d}P_f(t,T)}{P_f(t,T)} = \left(r_f(t) - \rho_{y,f}\eta_f B_f(t,T)\sqrt{v(t)}\right)\mathrm{d}t + \eta_f B_f(t,T)\mathrm{d}W_f^{\mathbb{Q}}(t), \tag{5.10}$$

with $B_d(t,T)$ and $B_f(t,T)$ as in (5.6).

5.2.2 Pricing of FX options

In order to perform efficient calibration of the model we need to be able to price basic options on the FX rate, $V(t,\mathbf{X}(t))$, for a given state vector, $\mathbf{X}(t) = [y(t), v(t), r_d(t), r_f(t)]^{\mathrm{T}}$:

$$V(t,\mathbf{X}(t)) = \mathbb{E}^{\mathbb{Q}}\left(\frac{M_d(t)}{M_d(T)}\max(y(T)-K,0)\Big|\mathcal{F}(t)\right),$$

with

$$M_d(t) = \exp\left(\int_0^t r_d(s)\mathrm{d}s\right).$$

Now, we consider a forward price, $\hat{\Pi}(t)$, such that:

$$\mathbb{E}^{\mathbb{Q}}\left(\frac{\max(y(T)-K,0)}{M_d(T)}\Big|\mathcal{F}(t)\right) = \frac{V(t,\mathbf{X}(t))}{M_d(t)} =: \hat{\Pi}(t).$$

By Itô's lemma we have:

$$\mathrm{d}\hat{\Pi}(t) = \frac{1}{M_d(t)}\mathrm{d}V(t) - r_d(t)\frac{V(t)}{M_d(t)}\mathrm{d}t, \tag{5.11}$$

with $V(t) := V(t, \mathbf{X}(t))$. We know that $\hat{\Pi}(t)$ must be a martingale, i.e.: $\mathbb{E}(\mathrm{d}\hat{\Pi}(t)) = 0$. Including this in (5.11) gives the following *Fokker-Planck forward equation* for V:

$$\begin{aligned}
r_d V \;=\;& \frac{1}{2}\eta_f^2 \frac{\partial^2 V}{\partial r_f^2} + \rho_{d,f}\eta_d\eta_f \frac{\partial^2 V}{\partial r_d \partial r_f} + \frac{1}{2}\eta_d^2 \frac{\partial^2 V}{\partial r_d^2} + \rho_{v,f}\gamma\eta_f\sqrt{v}\frac{\partial^2 V}{\partial v \partial r_f} \\
&+\rho_{v,d}\gamma\eta_d\sqrt{v}\frac{\partial^2 V}{\partial v \partial r_d} + \frac{1}{2}\gamma^2 v \frac{\partial^2 V}{\partial v^2} + \rho_{y,f}\eta_f y\sqrt{v}\frac{\partial^2 V}{\partial y \partial r_f} + \rho_{y,d}\eta_d y\sqrt{v}\frac{\partial^2 V}{\partial y \partial r_d} \\
&+\rho_{y,v}\gamma y v \frac{\partial^2 V}{\partial y \partial v} + \frac{1}{2}y^2 v \frac{\partial^2 V}{\partial y^2} + \left(\lambda_f(\theta_f(t) - r_f) - \rho_{y,f}\eta_f\sqrt{v}\right)\frac{\partial V}{\partial r_f} \\
&+\lambda_d(\theta_d(t) - r_d)\frac{\partial V}{\partial r_d} + \kappa(\bar{v} - v)\frac{\partial V}{\partial v} + (r_d - r_f)y\frac{\partial V}{\partial y} + \frac{\partial V}{\partial t}.
\end{aligned}$$

This 4D PDE contains non-affine terms, like square-roots and products. It is therefore difficult to solve it analytically. Finding a numerical solution for this PDE is therefore rather expensive and not easily applicable for model calibration. In the next subsection we propose an *approximation* of the model, which is useful for calibration.

The FX model under the forward domestic measure

To reduce the complexity of the pricing problem, we move from the domestic spot measure, generated by the money-savings account in the domestic market, $M_d(t)$, to the domestic *forward FX measure* where the numéraire is the domestic zero-coupon bond, $P_d(t,T)$. As indicated in [82, 93], the forward is given by:

$$\mathrm{FX}^T(t) = y(t)\frac{P_f(t,T)}{P_d(t,T)}, \tag{5.12}$$

where $\mathrm{FX}^T(t)$ represents the forward exchange rate under the T-forward measure, and $y(t)$ stands for foreign exchange rate under the domestic spot measure. The superscript should *not* be confused with the transpose notation used at other places in the text.

By switching from the domestic risk-neutral measure, $\mathbb{Q}$, to the domestic T-forward measure, $\mathbb{Q}^T$, the discounting will be decoupled from taking the expectation, i.e.:

$$\Pi(t,T) = P_d(t,T)\mathbb{E}^T\left(\max\left(\mathrm{FX}^T(T) - K, 0\right)|\mathcal{F}(t)\right).$$

In order to determine the dynamics for $\mathrm{FX}^T(t)$ in (5.12), we apply Itô's formula:

$$\begin{aligned}
\mathrm{dFX}^T(t) =\;& \frac{P_f(t,T)}{P_d(t,T)}\mathrm{d}y(t) + \frac{y(t)}{P_d(t,T)}\mathrm{d}P_f(t,T) - y(t)\frac{P_f(t,T)}{P_d^2(t,T)}\mathrm{d}P_d(t,T) \\
&+y(t)\frac{P_f(t,T)}{P_d^3(t,T)}\left(\mathrm{d}P_d(t,T)\right)^2 + \frac{1}{P_d(t,T)}\left(\mathrm{d}y(t)\mathrm{d}P_f(t,T)\right) \\
&-\frac{P_f(t,T)}{P_f^2(t,T)}\left(\mathrm{d}P_d(t,T)\mathrm{d}y(t)\right) - \frac{y(t)}{P_d^2(t,T)}\mathrm{d}P_d(t,T)\mathrm{d}P_f(t,T).
\end{aligned} \tag{5.13}$$

After substitution of SDEs (5.7), (5.9) and (5.10) into (5.13), we arrive at the following FX forward dynamics:

$$\frac{\mathrm{dFX}^T(t)}{\mathrm{FX}^T(t)} = \eta_d B_d(t,T)\Big(\eta_d B_d(t,T) - \rho_{y,d}\sqrt{v(t)} - \rho_{d,f}\eta_f B_f(t,T)\Big)\mathrm{d}t \\ +\sqrt{v(t)}\mathrm{d}W_y^{\mathbb{Q}}(t) - \eta_d B_d(t,T)\mathrm{d}W_d^{\mathbb{Q}}(t) + \eta_f B_f(t,T)\mathrm{d}W_f^{\mathbb{Q}}(t).$$

Since $\mathrm{FX}^T(t)$ is a martingale under the T-forward domestic measure, i.e.,

$$P_d(t,T)\mathbb{E}^T(\mathrm{FX}^T(T)|\mathcal{F}(t)) = P_d(t,T)\mathrm{FX}^T(t) =: P_f(t,T)y(t),$$

the appropriate Brownian motions under the $T-$forward domestic measure, $\mathrm{d}W_y^T(t)$, $\mathrm{d}W_v^T(t)$, $\mathrm{d}W_d^T(t)$ and $\mathrm{d}W_f^T(t)$, need to be determined.

A change of measure from domestic-spot to domestic T-forward measure requires a change of numéraire from money-savings account, $M_d(t)$, to zero-coupon bond, $P_d(t,T)$. In the model we incorporate a full matrix of correlations, which implies that all processes will change their dynamics by changing the measure from spot to forward. Lemma 5.2.2 provides the model dynamics under the domestic T-forward measure, $\mathbb{Q}^T$.

Lemma 5.2.2 (The FX-HHW model dynamics under the $\mathbb{Q}^T$ measure)**.** *Under the T-forward domestic measure, the model in (5.7) is governed by the following dynamics:*

$$\frac{\mathrm{d}FX^T(t)}{FX^T(t)} = \sqrt{v(t)}\mathrm{d}W_y^T(t) - \eta_d B_d(t,T)\mathrm{d}W_d^T(t) + \eta_f B_f(t,T)\mathrm{d}W_f^T(t), \quad (5.14)$$

where

$$\mathrm{d}v(t) = \Big(\kappa(\bar{v} - v(t)) + \gamma\rho_{v,d}\eta_d B_d(t,T)\sqrt{v(t)}\Big)\mathrm{d}t + \gamma\sqrt{v(t)}\mathrm{d}W_v^T(t), \quad (5.15)$$

$$\mathrm{d}r_d(t) = \big(\lambda_d(\theta_d(t) - r_d(t)) + \eta_d^2 B_d(t,T)\big)\mathrm{d}t + \eta_d \mathrm{d}W_d^T(t), \quad (5.16)$$

$$\mathrm{d}r_f(t) = \Big(\lambda_f(\theta_f(t) - r_f(t)) - \eta_f\rho_{y,f}\sqrt{v(t)} + \eta_d\eta_f\rho_{d,f}B_d(t,T)\Big)\mathrm{d}t + \eta_f\mathrm{d}W_f^T(t), \quad (5.17)$$

with a full matrix of correlations given in (5.8), and with $B_d(t,T)$, $B_f(t,T)$ given by (5.6).

Proof. Since the domestic short-rate process, $r_d(t)$, is driven by one source of uncertainty (only one Brownian motion $\mathrm{d}W_d^{\mathbb{Q}}(t)$), it is convenient to change the order of the state variables, from $\mathrm{d}\mathbf{X}(t) = [\mathrm{dFX}^T(t)/\mathrm{FX}^T(t), \mathrm{d}v(t), \mathrm{d}r_d(t), \mathrm{d}r_f(t)]^{\mathrm{T}}$ to $\mathrm{d}\mathbf{X}^*(t) = [\mathrm{d}r_d(t), \mathrm{d}r_f(t), \mathrm{d}v(t), \mathrm{dFX}^T(t)/\mathrm{FX}^T(t)]^{\mathrm{T}}$ and express the model in terms of the independent Brownian motions $\mathrm{d}\widetilde{\mathbf{W}}^{\mathbb{Q}}(t) = [\mathrm{d}\widetilde{W}_d(t), \mathrm{d}\widetilde{W}_f(t), \mathrm{d}\widetilde{W}_v(t), \mathrm{d}\widetilde{W}_y(t)]^{\mathrm{T}}$, i.e.:

$$\begin{bmatrix} \mathrm{d}r_d \\ \mathrm{d}r_f \\ \mathrm{d}v \\ \dfrac{\mathrm{dFX}^T}{\mathrm{FX}^T} \end{bmatrix} = \mu(\mathbf{X}^*)\mathrm{d}t + \begin{bmatrix} \eta_d & 0 & 0 & 0 \\ 0 & \eta_f & 0 & 0 \\ 0 & 0 & \gamma\sqrt{v} & 0 \\ -\eta_d B_d & \eta_f B_f & 0 & \sqrt{v} \end{bmatrix} \mathbf{L} \begin{bmatrix} \mathrm{d}\widetilde{W}_d^{\mathbb{Q}} \\ \mathrm{d}\widetilde{W}_f^{\mathbb{Q}} \\ \mathrm{d}\widetilde{W}_v^{\mathbb{Q}} \\ \mathrm{d}\widetilde{W}_y^{\mathbb{Q}} \end{bmatrix},$$

which, equivalently, can be written as:

$$\mathrm{d}\mathbf{X}^*(t) = \mu(\mathbf{X}^*)\mathrm{d}t + \mathbf{A}\mathbf{L}\mathrm{d}\widetilde{\mathbf{W}}^{\mathbb{Q}}(t), \tag{5.18}$$

where $\mu(\mathbf{X}^*)$ represents the drift for system $\mathrm{d}\mathbf{X}^*(t)$ and $\mathbf{L}$ is the Cholesky lower-triangular matrix of the following form:

$$\mathbf{L} = \begin{bmatrix} 1 & 0 & 0 & 0 \\ \mathbf{L}_{2,1} & \mathbf{L}_{2,2} & 0 & 0 \\ \mathbf{L}_{3,1} & \mathbf{L}_{3,2} & \mathbf{L}_{3,3} & 0 \\ \mathbf{L}_{4,1} & \mathbf{L}_{4,2} & \mathbf{L}_{4,3} & \mathbf{L}_{4,4} \end{bmatrix} \stackrel{\text{def}}{=} \begin{bmatrix} 1 & 0 & 0 & 0 \\ \rho_{f,d} & \mathbf{L}_{2,2} & 0 & 0 \\ \rho_{v,d} & \mathbf{L}_{3,2} & \mathbf{L}_{3,3} & 0 \\ \rho_{y,d} & \mathbf{L}_{4,2} & \mathbf{L}_{4,3} & \mathbf{L}_{4,4} \end{bmatrix}. \tag{5.19}$$

The representation presented above seems to be favorable, since the short-rate process, $r_d(t)$, can be considered independently of the other processes.

The matrix model representation in terms of orthogonal Brownian motions results in the following dynamics for the domestic short-rate, $r_d(t)$, under measure $\mathbb{Q}$:

$$\mathrm{d}r_d(t) = \lambda_d(\theta_d(t) - r_d(t))\mathrm{d}t + \zeta_1(t)\mathrm{d}\widetilde{\mathbf{W}}^{\mathbb{Q}}(t),$$

and for the domestic ZCB:

$$\frac{\mathrm{d}P_d(t,T)}{P_d(t,T)} = r_d(t)\mathrm{d}t + B_d(t,T)\zeta_1(t)\mathrm{d}\widetilde{\mathbf{W}}^{\mathbb{Q}}(t),$$

with $\zeta_k(t)$ being the k'th row vector resulting from multiplying the matrices $\mathbf{A}$ and $\mathbf{L}$. Note, that for the 1D Hull-White short-rate processes $\zeta_1(t) = \left[\eta_d, 0, 0, 0\right]$.

Now, we derive the Radon-Nikodym derivative [41], $\Lambda_{\mathbb{Q}}^T(t)$,:

$$\Lambda_{\mathbb{Q}}^T(t) \quad = \quad \frac{\mathrm{d}\mathbb{Q}^T}{\mathrm{d}\mathbb{Q}}\Big|_{\mathcal{F}(t)} = \frac{P_d(t,T)M_d(0)}{P_d(0,T)M_d(t)}. \tag{5.20}$$

By calculating the Itô derivative of Equation (5.20) we get:

$$\frac{\mathrm{d}\Lambda_{\mathbb{Q}}^T(t)}{\Lambda_{\mathbb{Q}}^T(t)} \quad = \quad B_d(t,T)\zeta_1(t)\mathrm{d}\widetilde{\mathbf{W}}^{\mathbb{Q}}(t),$$

which implies that the Girsanov kernel for the transition from $\mathbb{Q}$ to $\mathbb{Q}^{\mathrm{T}}$ is given by $B_d(t,T)\zeta_1(t)$ which is the T-bond volatility given by $\eta_d B_d(t,T)$, i.e.:

$$\Lambda_{\mathbb{Q}}^T(t) = \exp\left(-\frac{1}{2}\int_0^t B_d^2(s,T)\zeta_1^2(s)\mathrm{d}s + \int_0^t B_d(s,T)\zeta_1(s)\mathrm{d}\widetilde{\mathbf{W}}^{\mathbb{Q}}(s)\right).$$

So,

$$\mathrm{d}\widetilde{\mathbf{W}}^T(t) = -B_d(t,T)\zeta_1^{\mathrm{T}}(t)\mathrm{d}t + \mathrm{d}\widetilde{\mathbf{W}}^{\mathbb{Q}}(t).$$

Since the vector $\zeta_1^T(t)$ is of scalar form, the Brownian motion under the T-forward measure is given by:

$$\mathrm{d}\widetilde{\mathbf{W}}^{\mathbb{Q}}(t) = \left[\mathrm{d}\widetilde{W}_d^T(t) + \eta_d B_d(t,T)\mathrm{d}t, \mathrm{d}\widetilde{W}_f^T(t), \mathrm{d}\widetilde{W}_v^T(t), \mathrm{d}\widetilde{W}_y^T(t)\right]^{\mathrm{T}}.$$

Now, from the vector representation (5.18) we get that:

$$\mathbf{L}\mathrm{d}\widetilde{\mathbf{W}}^{\mathbb{Q}} = \begin{bmatrix} \eta_d B_d \mathrm{d}t + & \mathrm{d}\widetilde{W}_d^T \\ \rho_{d,f}\eta_d B_d \mathrm{d}t + & \rho_{d,f}\mathrm{d}\widetilde{W}_d^T + \mathbf{L}_{2,2}\mathrm{d}\widetilde{W}_f^T \\ \rho_{v,d}\eta_d B_d \mathrm{d}t + & \rho_{v,d}\mathrm{d}\widetilde{W}_d^T + \mathbf{L}_{3,2}\mathrm{d}\widetilde{W}_f^T + \mathbf{L}_{3,3}\mathrm{d}\widetilde{W}_y^T \\ \rho_{y,d}\eta_d B_d \mathrm{d}t + & \rho_{y,d}\mathrm{d}\widetilde{W}_d^T + \mathbf{L}_{4,2}\mathrm{d}\widetilde{W}_f^T + \mathbf{L}_{4,3}\mathrm{d}\widetilde{W}_y^T + \mathbf{L}_{4,4}\mathrm{d}\widetilde{W}_v^T \end{bmatrix}.$$

Returning to the *dependent* Brownian motions under the T-forward measure, gives us:

$$\begin{aligned} \frac{\mathrm{dFX}^T(t)}{\mathrm{FX}^T(t)} &= \sqrt{v(t)}\mathrm{d}W_y^T(t) - \eta_d B_d(t,T)\mathrm{d}W_d^T(t) + \eta_f B_f(t,T)\mathrm{d}W_f^T(t), \\ \mathrm{d}v(t) &= \left(\kappa(\bar{v} - v(t)) + \gamma\rho_{v,d}\eta_d B_d(t,T)\sqrt{v(t)}\right)\mathrm{d}t + \gamma\sqrt{v(t)}\mathrm{d}W_v^T(t), \\ \mathrm{d}r_d(t) &= \left(\lambda_d(\theta_d(t) - r_d(t)) + \eta_d^2 B_d(t,T)\right)\mathrm{d}t + \eta_d \mathrm{d}W_d^T(t), \\ \mathrm{d}r_f(t) &= \left(\lambda_f(\theta_f(t) - r_f(t)) - \eta_f\rho_{y,f}\sqrt{v(t)} + \eta_d\eta_f\rho_{d,f}B_d(t,T)\right)\mathrm{d}t + \eta_f \mathrm{d}W_f^T(t), \end{aligned}$$

with the full matrix of correlations given in (5.8). ■

From the system in Lemma 5.2.2 we see that after moving from the domestic-spot $\mathbb{Q}$-measure to the domestic T-forward $\mathbb{Q}^T$ measure, the forward exchange rate $\mathrm{FX}^T(t)$ does not depend explicitly on the short-rate processes $r_d(t)$ or $r_f(t)$. It does not contain a drift term and only depends on $\mathrm{d}W_d^T(t)$, $\mathrm{d}W_f^T(t)$, see (5.14).

Remark. Since the sum of three correlated, normally distributed random variables, $Q = X + Y + Z$, remains normal with the mean equal to the sum of the individual means and the variance equal to

$$v_Q^2 = v_X^2 + v_Y^2 + v_Z^2 + 2\rho_{X,Y}v_X v_Y + 2\rho_{X,Z}v_X v_Z + 2\rho_{Y,Z}v_Y v_Z,$$

we can represent the forward (5.14) as:

$$\begin{aligned} \mathrm{dFX}^T/\mathrm{FX}^T &= \big(v + \eta_d^2 B_d^2 + \eta_f^2 B_f^2 - 2\rho_{y,d}\eta_d B_d\sqrt{v} \\ &\quad + 2\rho_{y,f}\eta_f B_f\sqrt{v} - 2\rho_{d,f}\eta_d\eta_f B_d B_f\big)^{\frac{1}{2}}\,\mathrm{d}W_F^T. \end{aligned} \tag{5.21}$$

Although the representation in (5.21) reduces the number of Brownian motions in the dynamics for the FX, one still needs to find the appropriate cross-terms, like $\mathrm{d}W_F^T(t)\mathrm{d}W_v^T(t)$, in order to obtain the covariance terms. For clarity we therefore prefer to stay with the standard notation.

Remark. The dynamics of the forwards, $\mathrm{FX}^T(t)$ in (5.14) or in (5.21), do not depend explicitly on the interest rate processes, $r_d(t)$ and $r_f(t)$, and are completely described by the appropriate diffusion coefficients. This suggests that the short-rate variables will not enter the pricing PDE. Note that this is only the case for models in which the diffusion coefficient for the interest rate does not depend on the level of the interest rate.

In the next section we derive the corresponding pricing PDE and provide the necessary model approximations.

5.2.3 Approximations and the forward characteristic function

As the dynamics of the forward foreign exchange, $\mathrm{FX}^T(t)$, under the domestic forward measure involve only the interest rate diffusions $\mathrm{d}W_d^T(t)$ and $\mathrm{d}W_f^T(t)$, a significant reduction of the pricing problem is achieved.

In order to find the forward ChF we take, as usual, the log-transform of the forward rate $\mathrm{FX}^T(t)$, i.e.: $x^T(t) := \log \mathrm{FX}^T(t)$, for which we obtain the following dynamics:

$$\mathrm{d}x^T(t) = \left(\zeta(t, \sqrt{v(t)}) - \frac{1}{2}v(t)\right)\mathrm{d}t + \sqrt{v(t)}\mathrm{d}W_y^T(t) - \eta_d B_d \mathrm{d}W_d^T(t) + \eta_f B_f \mathrm{d}W_f^T(t), \tag{5.22}$$

with the variance process, $v(t)$, given by:

$$\mathrm{d}v(t) = \left(\kappa(\bar{v} - v(t)) + \gamma\rho_{v,d}\eta_d B_d\sqrt{v(t)}\right)\mathrm{d}t + \gamma\sqrt{v(t)}\mathrm{d}W_v^T(t),$$

where we used the notation $B_d := B_d(t,T)$ and $B_f := B_f(t,T)$, and

$$\zeta(t, \sqrt{v(t)}) = (\rho_{y,d}\eta_d B_d - \rho_{y,f}\eta_f B_f)\sqrt{v(t)} + \rho_{d,f}\eta_d\eta_f B_d B_f - \frac{1}{2}\left(\eta_d^2 B_d^2 + \eta_f^2 B_f^2\right).$$

By applying the Feynman-Kac theorem we find the following pricing PDE:

$$\begin{aligned} -\frac{\partial \phi^T}{\partial t} &= \left(\kappa(\bar{v} - v) + \rho_{v,d}\gamma\eta_d\sqrt{v}B_d\right)\frac{\partial \phi^T}{\partial v} + \left(\frac{1}{2}v - \zeta(t,\sqrt{v})\right)\left(\frac{\partial^2\phi^T}{\partial (x^T)^2} - \frac{\partial \phi^T}{\partial x^T}\right) \\ &\quad + \left(\rho_{y,v}\gamma v - \rho_{v,d}\gamma\eta_d\sqrt{v}B_d + \rho_{v,f}\gamma\eta_f\sqrt{v}B_f\right)\frac{\partial^2\phi^T}{\partial x^T\partial v} + \frac{1}{2}\gamma^2 v\frac{\partial^2\phi^T}{\partial v^2}, \end{aligned}$$

with $B_f := B_f(t,T)$ and $B_d := B_d(t,T)$. This PDE contains non-affine $\sqrt{v}$-terms so that it is nontrivial to find its solution. In Chapter 2 two methods for linearization of these non-affine square roots of the square-root process [25] were proposed. The first method is to project the non-affine square-root terms on their first moments. This is also the approach followed here [1].

The approximation of the non-affine terms in the corresponding PDE is then done as follows. We assume:

$$\sqrt{v(t)} \approx \mathbb{E}(\sqrt{v(t)}) =: \alpha(t), \tag{5.23}$$

with the expectation of the square root of $v(t)$ determined.

Projection of the non-affine terms on their first moments allows us to derive the corresponding forward characteristic function, ϕ^T, which is then of the following form:

$$\phi^T(u, x^T(t), t, T) = \exp(A(u,\tau) + B(u,\tau)x^T(t) + C(u,\tau)v(t)),$$

[1] Since the moments of the square-root process under the T-forward measure are difficult to determine for $\sqrt{v(t)}$ we have set $\rho_{v,d} = 0$ or, in other words, the expectation is calculated under measure $\mathbb{Q}$.

where $\tau = T - t$, and the functions $A(\tau) := A(u,\tau)$, $B(\tau) := B(u,\tau)$ and $C(\tau) := C(u,\tau)$ are given by:

$$\begin{aligned}
B'(\tau) &= 0,\\
C'(\tau) &= -\kappa C(\tau) + (B^2(\tau) - B(\tau))/2 + \rho_{y,v}\gamma B(\tau)C(\tau) + \gamma^2 C^2(\tau)/2,\\
A'(\tau) &= \kappa\bar{v}C(\tau) + \rho_{v,d}\gamma\eta_d\alpha(\tau)B_d(\tau)C(\tau) - \zeta(\tau,\alpha(\tau))\left(B^2(\tau) - B(\tau)\right)\\
&\quad + \left(-\rho_{v,d}\eta_d\gamma\alpha(\tau)B_d(\tau) + \rho_{v,f}\gamma\eta_f\alpha(\tau)B_f(\tau)\right)B(\tau)C(\tau),
\end{aligned}$$

with $\alpha(t) = \mathbb{E}(\sqrt{v(t)})$, and $B_i(\tau) = \lambda_i^{-1}\left(\mathrm{e}^{-\lambda_i\tau} - 1\right)$ for $i = \{d, f\}$. The initial conditions are: $B(0) = iu$, $C(0) = 0$ and $A(0) = 0$.

With $B(\tau) = iu$, the complex-valued function $C(\tau)$ is of the Heston-type, [54], and its solution reads:

$$C(\tau) = \frac{1 - \mathrm{e}^{-d\tau}}{\gamma^2(1 - g\mathrm{e}^{-d\tau})}\left(\kappa - \rho_{y,v}\gamma iu - d\right), \tag{5.24}$$

with $d = \sqrt{(\rho_{y,v}\gamma iu - \kappa)^2 - \gamma^2 iu(iu-1)}$, $g = \dfrac{\kappa - \gamma\rho_{y,v}iu - d}{\kappa - \gamma\rho_{y,v}iu + d}$.

The parameters κ, γ, $\rho_{y,v}$ are given in (5.7).

Function $A(\tau)$ is given by:

$$\begin{aligned}
A(\tau) &= \int_0^\tau \Big(\kappa\bar{v} + \rho_{v,d}\gamma\eta_d\alpha(s)B_d(s) - \rho_{v,d}\eta_d\gamma\alpha(s)B_d(s)iu\\
&\quad + \rho_{v,f}\gamma\eta_f\alpha(s)B_f(s)iu\Big)C(s)\mathrm{d}s + (u^2 + iu)\int_0^\tau \zeta(s,\alpha(s))\mathrm{d}s,
\end{aligned}$$

with $C(s)$ in (5.24). It is most convenient to solve $A(\tau)$ *numerically* with, for example, Simpson's quadrature rule. With correlations $\rho_{v,d}$, $\rho_{v,f}$ equal to zero, a closed-form expression for $A(\tau)$ would be available (see Chapter 2 for details).

We denote the *approximation*, by means of linearization, of the full-scale FX-HHW model by *FX-HHW1*. It is clear that efficient pricing with Fourier-based methods can be done with FX-HHW1, and not with FX-HHW.

By the projection of $\sqrt{v(t)}$ on its first moment in (5.23) the corresponding PDE is affine in its coefficients, and reads:

$$\begin{aligned}
-\frac{\partial\phi^T}{\partial t} &= \left(\kappa(\bar{v} - v) + \Psi_1\right)\frac{\partial\phi^T}{\partial v} + \left(\frac{1}{2}v - \zeta(t,\alpha(t))\right)\left(\frac{\partial^2\phi^T}{\partial(x^T)^2} - \frac{\partial\phi^T}{\partial x^T}\right)\\
&\quad + \left(\rho_{y,v}\gamma v - \Psi_2\right)\frac{\partial^2\phi^T}{\partial x^T\partial v} + \frac{1}{2}\gamma^2 v\frac{\partial^2\phi^T}{\partial v^2},
\end{aligned}\tag{5.25}$$

with: $\phi^T(u, x^T(T), T, T) = \mathbb{E}^T\left(\mathrm{e}^{iux^T(T)}\middle|\mathcal{F}(T)\right) = \mathrm{e}^{iux^T(T)}$, and

$$\zeta(t,\alpha(t)) = \Psi_3 + \rho_{d,f}\eta_d\eta_f B_d(t,T)B_f(t,T) - \frac{1}{2}\left(\eta_d^2 B_d^2(t,T) + \eta_f^2 B_f^2(t,T)\right).$$

The three terms, Ψ_1, Ψ_2, and Ψ_3, in PDE (5.25) contain the function $\alpha(t)$:

$$\begin{aligned}
\Psi_1 &:= \rho_{v,d}\gamma\eta_d B_d(t,T)\alpha(t),\\
\Psi_2 &:= \left(\rho_{v,d}\gamma\eta_d B_d(t,T) - \rho_{v,f}\gamma\eta_f B_f(t,T)\right)\alpha(t),\\
\Psi_3 &:= \left(\rho_{y,d}\eta_d B_d(t,T) - \rho_{y,f}\eta_f B_f(t,T)\right)\alpha(t).
\end{aligned}$$

When solving the pricing PDE for $t \to T$, the terms $B_d(t,T)$ and $B_f(t,T)$ tend to zero, and all terms that contain the approximation vanish. The case $t \to 0$ is furthermore trivial, since $\sqrt{v(t)} \stackrel{t\to 0}{\longrightarrow} \mathbb{E}(\sqrt{v(0)})$.

Under the T-forward domestic FX measure, the projection of the non-affine terms on their first moments is expected to provide high accuracy. In Section 5.2.5 we perform a numerical experiment to validate this.

5.2.4 Pricing a foreign stock in the FX-HHW model

Here, we focus our attention on pricing a foreign stock, $S_f(t)$, in a domestic market. With this extension we can, in principle, price equity-FX-interest rate hybrid products.

With an equity smile/skew present in the market, we assume that $S_f(t)$ is given by the Heston stochastic volatility model:

$$\begin{aligned} \mathrm{d}S_f(t)/S_f(t) &= & r_f(t)\mathrm{d}t+ & \quad\sqrt{\omega(t)}\mathrm{d}W_{S_f}^{\mathbb{Z}}(t), \\ \mathrm{d}\omega(t) &= & \kappa_f(\bar{\omega}-\omega(t))\mathrm{d}t+ & \quad\gamma_f\sqrt{\omega(t)}\mathrm{d}W_{\omega}^{\mathbb{Z}}(t), \\ \mathrm{d}r_f(t) &= & \lambda_f(\theta_f(t)-r_f(t)))\mathrm{d}t+ & \quad\eta_f\mathrm{d}W_f^{\mathbb{Z}}(t), \end{aligned} \tag{5.26}$$

where $\mathbb{Z}$ indicates the foreign-spot measure and the model parameters, κ_f, γ_f, λ_f, $\theta_f(t)$ and η_f, are as before.

Before deriving the stock dynamics in domestic currency, the model has to be calibrated in the foreign market to plain vanilla options. This can be efficiently done with the help of a fast pricing formula (as introduced in Chapter 2).

With the foreign short-rate process, $r_f(t)$, established in (5.7) we need to determine the drifts for $S_f(t)$ and its variance process, $\omega(t)$, under the domestic spot measure. The foreign stock, $S_f(t)$, can be expressed in domestic currency by multiplication with the FX, $y(t)$, and by discounting with the domestic money-savings account, $M_d(t)$. Such a stock is a tradable asset, so the price $y(t)S_f(t)/M_d(t)$ (with $y(t)$ in (5.7), $S_f(t)$ from (5.26) and the domestic money-saving account $M_d(t)$ in (5.4)) needs to be a martingale.

By applying Itô's lemma to $y(t)S_f(t)/M_d(t)$, we find

$$\frac{\mathrm{d}\left(y(t)\frac{S_f(t)}{M_d(t)}\right)}{y(t)\frac{S_f(t)}{M_d(t)}} = \rho_{y,S_f}\sqrt{v(t)}\sqrt{\omega(t)}\mathrm{d}t + \sqrt{v(t)}\mathrm{d}W_y^{\mathbb{Q}}(t) + \sqrt{\omega(t)}\mathrm{d}W_{S_f}^{\mathbb{Z}},$$

where $\mathbb{Q}$ and $\mathbb{Z}$ indicate the domestic-spot and foreign-spot measures, respectively. To make the process $y(t)S_f(t)/M_d(t)$ a martingale we set:

$$\mathrm{d}W_{S_f}^{\mathbb{Z}}(t) = \mathrm{d}W_{S_f}^{\mathbb{Q}} - \rho_{y,S_f}\sqrt{v(t)}\mathrm{d}t,$$

where $v(t)$ is the variance process of FX defined in (5.7).

Under the change of measure, from foreign-spot to domestic-spot, $S_f(t)$ has the following dynamics:

$$\begin{aligned} \mathrm{d}S_f(t)/S_f(t) &= r_f(t)\mathrm{d}t + \sqrt{\omega(t)}\mathrm{d}W_{S_f}^{\mathbb{Z}}(t) \\ &= \left(r_f(t) - \rho_{y,S_f}\sqrt{v(t)}\sqrt{\omega(t)}\right)\mathrm{d}t + \sqrt{\omega(t)}\mathrm{d}W_{S_f}^{\mathbb{Q}}(t). \end{aligned} \tag{5.27}$$

The variance process is correlated with the stock and by the Cholesky decomposition we find:

$$\begin{aligned}\mathrm{d}\omega(t) &= \kappa_f(\bar{\omega}-\omega(t))\mathrm{d}t + \gamma_f\sqrt{\omega(t)}\left(\rho_{S_f,\omega}\mathrm{d}\widetilde{W}^{\mathbb{Z}}_{S_f}(t) + \sqrt{1-\rho^2_{S_f,\omega}}\mathrm{d}\widetilde{W}^{\mathbb{Z}}_{\omega}(t)\right)\\ &= \left(\kappa_f(\bar{\omega}-\omega(t)) - \rho_{S_f,\omega}\rho_{S_f,y}\gamma_f\sqrt{\omega(t)}\sqrt{v(t)}\right)\mathrm{d}t + \gamma_f\sqrt{\omega(t)}\mathrm{d}W^{\mathbb{Q}}_{\omega}(t). \quad (5.28)\end{aligned}$$

$S_f(t)$ in (5.27) and $\omega(t)$ in (5.28) are governed by several non-affine terms. Assuming that the foreign stock, $S_f(t)$, is already calibrated to market data, we only need to simulate the foreign stock dynamics in the domestic market. Monte Carlo simulation of the foreign stock under domestic measure can be done as, for example, presented in [3]. The outstanding property of Andersen's QE Monte Carlo scheme is that the Heston model can be accurately simulated when the Feller condition is satisfied as well as when this condition is violated.

5.2.5 Numerical experiment for the FX-HHW model

In this section we check the errors resulting from the various approximations in the FX-HHW1 model. We use the set-up from [93], which means that the interest rate curves are modeled by ZCBs defined by $P_d(0,T) = \exp(-0.02T)$ and $P_f(0,T) = \exp(-0.05T)$. Furthermore,

$$\eta_d = 0.7\%,\;\; \eta_f = 1.2\%,\;\; \lambda_d = 1\%,\;\; \lambda_f = 5\%.$$

We choose [2]:

$$\kappa = 0.5,\;\; \gamma = 0.3,\;\; \bar{v} = 0.1,\;\; v(0) = 0.1.$$

The correlation structure, defined in (5.8), is given by:

$$\begin{pmatrix} 1 & \rho_{y,v} & \rho_{y,d} & \rho_{y,f}\\ \rho_{y,v} & 1 & \rho_{v,d} & \rho_{v,f}\\ \rho_{y,d} & \rho_{v,d} & 1 & \rho_{d,f}\\ \rho_{y,f} & \rho_{v,f} & \rho_{d,f} & 1\end{pmatrix} = \begin{pmatrix} 100\% & -40\% & -15\% & -15\%\\ -40\% & 100\% & 30\% & 30\%\\ -15\% & 30\% & 100\% & 25\%\\ -15\% & 30\% & 25\% & 100\%\end{pmatrix}. \quad (5.29)$$

The initial spot FX rate (Dollar, \$, per Euro, €) is set to 1.35. For the FX-HHW model we compute a number of FX option prices with many expiries and strikes, using two different pricing methods.

The first method is the plain Monte Carlo method, with 50.000 paths and $20T_i$ steps, for the full-scale FX-HHW model, without any approximations.

For the second pricing method, we have used the ChF, based on the approximations in the FX-HHW1 model in Section 5.2.3. Efficient pricing of plain vanilla products is then done by means of the COS method [32], based on a Fourier cosine series expansion of the probability density function, which is recovered by the ChF with 500 Fourier cosine terms.

We also define the experiments as in [93], with expiries given by $T_1, \ldots, T_{10}$, and the strikes are computed by the formula:

$$\begin{aligned} K_n(T_i) &= \mathrm{FX}^{T_i}(0)\exp\left(0.1c_n\sqrt{T_i}\right), \quad \text{with} \quad (5.30)\\ c_n &= \{-1.5,\ -1.0,\ -0.5,\ 0,\ 0.5,\ 1.0,\ 1.5\},\end{aligned}$$

[2] The model parameters do not satisfy the Feller condition, $\gamma^2 > 2\kappa\bar{v}$.

and $\text{FX}^{T_i}(0)$ as in (5.12) with $y(0) = 1.35$. This formula for the strikes is convenient, since for $n = 4$, strikes $K_4(T_i)$ with $i = 1, \ldots, 10$ are equal to the forward FX rates for time T_i. The strikes and maturities are presented in Table 5.4 in Appendix 5.A.

The option prices resulting from both models are expressed in terms of the implied Black volatilities. The differences between the volatilities are tabulated in Table 5.1. The approximation FX-HHW1 appears to be highly accurate for the parameters considered. We report a maximum error of about 0.1% volatility for at-the-money options with a maturity of 30 years and less than 0.07% for the other options.

Table 5.1: *Differences, in implied volatilities, between the FX-HHW and FX-HHW1 models. The corresponding FX option prices and the standard deviations are tabulated in Table 5.7. Strike $K_4(T_i)$ is the at-the-money strike.*

T_i	$K_1(T_i)$	$K_2(T_i)$	$K_3(T_i)$	$K_4(T_i)$	$K_5(T_i)$	$K_6(T_i)$	$K_7(T_i)$
6m	-0.03 %	-0.02 %	0.00 %	0.02 %	0.03 %	0.04 %	0.05 %
1y	-0.01 %	-0.01 %	-0.01 %	-0.01 %	-0.01 %	-0.01 %	-0.01 %
3y	0.05 %	0.04 %	0.02 %	-0.01 %	-0.03 %	-0.06 %	-0.09 %
5y	0.06 %	0.04 %	0.02 %	0.00 %	-0.03 %	-0.07 %	-0.10 %
7y	0.08 %	0.06 %	0.04 %	0.03 %	0.01 %	-0.01 %	-0.03 %
10y	-0.02 %	-0.03 %	-0.03 %	-0.05 %	-0.07 %	-0.09 %	-0.12 %
15y	-0.12 %	-0.10 %	-0.09 %	-0.09 %	-0.09 %	-0.09 %	-0.10 %
20y	0.09 %	0.09 %	0.09 %	0.08 %	0.08 %	0.07 %	0.06 %
25y	-0.15 %	-0.11 %	-0.08 %	-0.06 %	-0.05 %	-0.04 %	-0.04 %
30y	0.10 %	0.11 %	0.12 %	0.12 %	0.12 %	0.12 %	0.12 %

In the next subsection calibration results to FX market data are presented.

Calibration to market data

We discuss the calibration of the FX-HHW model to FX market data. In the simulation the reference market implied volatilities are taken from [93] and are presented in Table 5.5 in Appendix 5.A. In the calibration routine the approximate model FX-HHW1 was employed. The correlation structure is as in (5.29). In Figure 5.1 some of the calibration results are presented.

Our experiments show that the model can be well calibrated to the market data. For long maturities and for deep-in-the money options some discrepancy is present. This is however typical when dealing with the Heston model (not related to our approximation), since the skew/smile pattern in FX does not flatten for long maturities. This was sometimes improved by adding jumps to the model (Bates' model). In Appendix 5.A in Table 5.6 the detailed calibration results are tabulated.

Short-rate interest rate models can typically provide a satisfactory fit to at-the-money interest rate products. In the next section an extension of the framework, so that interest rate smiles and skews can be modeled as well, is presented.

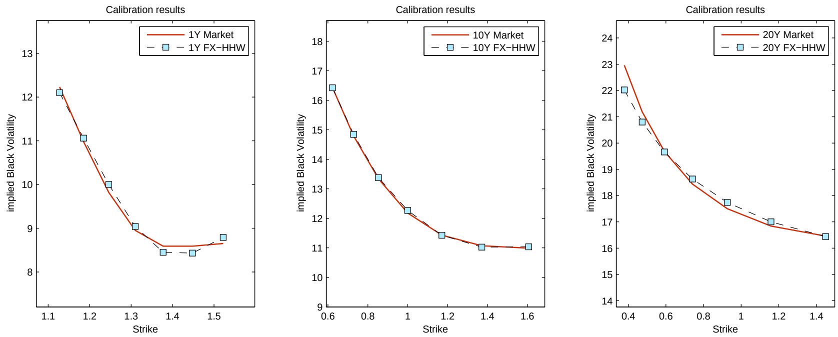

Figure 5.1: *Comparison of implied volatilities from the market and the FX-HHW1 model for FX European call options for maturities of 1, 10 and 20 years. The strikes are provided in Table 5.4 in Appendix 5.A.* $y(0) = 1.35$.

5.3 Multi-Currency model with interest rate smile

In this section we discuss a second extension of the multi-currency model, in which an interest rate smile is incorporated. This hybrid model models two types of smiles, the smile for the FX rate and the smiles in the domestic and foreign fixed income markets. We abbreviate the model by *FX-HLMM*. It is especially interesting for FX products that are exposed to interest rate smiles. A description of such FX hybrid products can be found in the handbook by Hunter [59].

A first attempt to model the FX by stochastic volatility and interest rates driven by a market model was proposed in [105], assuming independence between log-normal-Libor rates and FX. In our approach we define a model with *non-zero correlation* between FX and interest rate processes.

As in the previous sections, the stochastic volatility FX is of the Heston-type, which under domestic risk-neutral measure, $\mathbb{Q}$, follows the following dynamics:

$$\begin{aligned} \mathrm{d}y(t)/y(t) &= \quad (\dots)\mathrm{d}t + \quad \sqrt{v(t)}\mathrm{d}W_y^{\mathbb{Q}}(t), \quad y(0) > 0, \\ \mathrm{d}v(t) &= \kappa(\bar{v} - v(t))\mathrm{d}t + \gamma\sqrt{v(t)}\mathrm{d}W_v^{\mathbb{Q}}(t), \quad v(0) > 0, \end{aligned} \tag{5.31}$$

with the parameters as in (5.7). Since we consider the model under the forward measure the drift in the first SDE does not need to be specified (the dynamics of domestic-forward FX $y(t)P_f(t,T)/P_d(t,T)$ do not contain a drift term).

In the model we assume that the domestic and foreign currencies are independently calibrated to interest rate products available in their own markets. For simplicity, we also assume that the tenor structure for both currencies is the same, i.e., $\mathcal{T}_d \equiv \mathcal{T}_f = \{T_0, T_1, \dots, T_N \equiv T\}$ and $\tau_k = T_k - T_{k-1}$ for $k = 1 \dots N$. For $t < T_{k-1}$ we define the forward Libor rates $L_{d,k}(t) := L_d(t, T_{k-1}, T_k)$ and $L_{f,k}(t) := L_f(t, T_{k-1}, T_k)$ as

$$L_{d,k}(t) := \frac{1}{\tau_k}\left(\frac{P_d(t,T_{k-1})}{P_d(t,T_k)} - 1\right), \quad L_{f,k}(t) := \frac{1}{\tau_k}\left(\frac{P_f(t,T_{k-1})}{P_f(t,T_k)} - 1\right). \tag{5.32}$$

For each currency we choose the DD-SV Libor Market Model from [5] for the interest rates, under the T-forward measure generated by the numéraires $P_d(t,T)$ and $P_f(t,T)$, given by:

$$\begin{aligned} \mathrm{d}L_{d,k}(t) = &\quad v_{d,k}\phi_{d,k}(t)\sqrt{v_d(t)}\left(\mu_d(t)\sqrt{v_d(t)}\mathrm{d}t + \mathrm{d}W_k^{d,T}(t)\right), \\ \mathrm{d}v_d(t) = &\quad \lambda_d(v_d(0) - v_d(t))\mathrm{d}t + \eta_d\sqrt{v_d(t)}\mathrm{d}W_v^{d,T}(t), \end{aligned} \tag{5.33}$$

and

$$\begin{aligned} \mathrm{d}L_{f,k}(t) = &\quad v_{f,k}\phi_{f,k}(t)\sqrt{v_f(t)}\left(\mu_f(t)\sqrt{v_f(t)}\mathrm{d}t + \mathrm{d}\widehat{W}_k^{f,T}(t)\right), \\ \mathrm{d}v_f(t) = &\quad \lambda_f(v_f(0) - v_f(t))\mathrm{d}t + \eta_f\sqrt{v_f(t)}\mathrm{d}\widehat{W}_v^{f,T}(t), \end{aligned} \tag{5.34}$$

with

$$\mu_d(t) = -\sum_{j=k+1}^{N}\frac{\tau_j\phi_{d,j}(t)v_{d,j}}{1+\tau_j L_{d,j}(t)}\rho_{k,j}^d, \qquad \mu_f(t) = -\sum_{j=k+1}^{N}\frac{\tau_j\phi_{f,j}(t)v_{f,j}}{1+\tau_j L_{f,j}(t)}\rho_{k,j}^f,$$

where

$$\begin{aligned} \phi_{d,k} &= \beta_{d,k}L_{d,k}(t) + (1-\beta_{d,k})L_{d,k}(0), \\ \phi_{f,k} &= \beta_{f,k}L_{f,k}(t) + (1-\beta_{f,k})L_{f,k}(0). \end{aligned}$$

The Brownian motion, $\mathrm{d}W_k^{d,T}(t)$, corresponds to the k-th domestic Libor rate, $L_{d,k}(t)$, under the T-forward domestic measure, and the Brownian motion, $\mathrm{d}\widehat{W}_k^{f,T}(t)$, relates to the k-th foreign market Libor rate, $L_{f,k}(t)$, under the terminal foreign measure T.

In the model $v_{d,k}(t)$ and $v_{f,k}(t)$ determine the level of the interest rate volatility smile, the parameters $\beta_{d,k}(t)$ and $\beta_{f,k}(t)$ control the slope of the volatility smile, and λ_d, λ_f determine the speed of mean reversion for the variance and influence the speed at which the interest rate volatility smile flattens as the swaption expiry increases [92]. Parameters η_d, η_f determine the curvature of the interest rate smile.

The following correlation structure [3] is imposed, between

$$\begin{array}{lrl} \text{FX and its variance process, } v(t): & \mathrm{d}W_y^T(t)\mathrm{d}W_v^T(t) = & \rho_{y,v}\mathrm{d}t, \\ \text{FX and domestic Libors, } L_{d,j}(t): & \mathrm{d}W_y^T(t)\mathrm{d}W_j^{d,T}(t) = & \rho_{y,j}^d\mathrm{d}t, \\ \text{FX and foreign Libors, } L_{f,j}(t): & \mathrm{d}W_y^T(t)\mathrm{d}\widehat{W}_j^{f,T}(t) = & \rho_{y,j}^f\mathrm{d}t, \\ \text{Libors in domestic market:} & \mathrm{d}W_k^{d,T}(t)\mathrm{d}W_j^{d,T}(t) = & \rho_{k,j}^d\mathrm{d}t, \\ \text{Libors in foreign market:} & \mathrm{d}\widehat{W}_k^{f,T}(t)\mathrm{d}\widehat{W}_j^{f,T}(t) = & \rho_{k,j}^f\mathrm{d}t, \\ \text{Libors in domestic and foreign markets:} & \mathrm{d}W_k^{d,T}(t)\mathrm{d}\widehat{W}_j^{f,T}(t) = & \rho_{k,j}^{d,f}\mathrm{d}t. \end{array} \tag{5.35}$$

We prescribe a zero correlation between the remaining processes, i.e., between

[3] As it is insightful to relate the covariance matrix with the necessary model approximations, the correlation structure is introduced here by means of instantaneous correlation of the scalar diffusions.

Libors and their variance process,

$$\mathrm{d}W_k^{d,T}(t)\mathrm{d}W_v^{d,T}(t) = 0, \quad \mathrm{d}\widehat{W}_k^{f,T}(t)\mathrm{d}\widehat{W}_v^{f,T}(t) = 0,$$

Libors and the FX variance process,

$$\mathrm{d}W_k^{d,T}(t)\mathrm{d}W_v^{T}(t) = 0, \quad \mathrm{d}\widehat{W}_k^{f,T}(t)\mathrm{d}W_v^{T}(t) = 0,$$

all variance processes,

$$\mathrm{d}W_v^{T}(t)\mathrm{d}W_v^{d,T}(t) = 0, \quad \mathrm{d}W_v^{T}(t)\mathrm{d}\widehat{W}_v^{f,T}(t) = 0, \quad \mathrm{d}W_v^{d,T}(t)\mathrm{d}\widehat{W}_v^{f,T}(t) = 0,$$

FX and the Libor variance processes,

$$\mathrm{d}W_y^{T}(t)\mathrm{d}W_v^{d,T}(t) = 0, \quad \mathrm{d}W_y^{T}(t)\mathrm{d}\widehat{W}_v^{f,T}(t) = 0.$$

The correlation structure is graphically displayed in Figure 5.2.

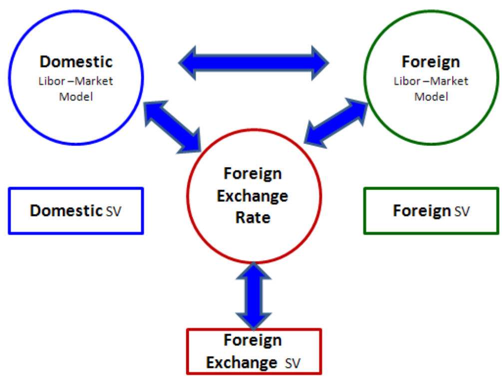

Figure 5.2: *The correlation structure for the FX-HLMM model. Arrows indicate non-zero correlations. SV is Stochastic Volatility.*

Throughout this chapter we assume that the DD-SV model in (5.33) and (5.34) is already in the *effective* parameter framework as developed in [92]. This means that approximate time-homogeneous parameters are used instead of the time-dependent parameters, i.e., $\beta_k(t) \equiv \beta_k$ and $v_k(t) \equiv v_k$.

With this correlation structure, we derive the dynamics for the forward FX, given by:

$$\mathrm{FX}^T(t) = y(t)\frac{P_f(t,T)}{P_d(t,T)}, \tag{5.36}$$

(see also (5.12)) with $y(t)$ the spot exchange rate and $P_d(t,T)$ and $P_f(t,T)$ zero-coupon bonds. Note that the bonds are not yet specified.

When deriving the dynamics for (5.36), we need expressions for the zero-coupon bonds, $P_d(t,T)$ and $P_f(t,T)$. With Equation (5.32) the following expression for the final bond can be obtained:

$$\frac{1}{P_i(t,T)} = \frac{1}{P_i(t,T_{m(t)})} \prod_{j=m(t)+1}^{N} \left(1+\tau_j L_{i,j}(t)\right), \quad \text{for } \; i=\{d,f\}, \tag{5.37}$$

with $T=T_N$ and $m(t)=\min(k : t \leq T_k)$ (empty products in (5.37) are defined to be equal to 1). The bond $P_i(t,T_N)$ in (5.37) is fully determined by the Libor rates $L_{i,k}(t),\ k=1,\ldots,N$ and the bond $P_i(t,T_{m(t)})$. Whereas the Libors $L_{i,k}(t)$ are defined by system (5.33) and (5.34), the bond $P_i(t,T_{m(t)})$ is not yet well-defined in the current framework.

To define continuous time dynamics for a zero-coupon bond. We consider here the linear interpolation scheme, proposed in [98], which reads:

$$\frac{1}{P_i(t,T_{m(t)})} = 1+(T_{m(t)}-t)L_{i,m(t)}(T_{m(t)-1}), \text{ for } \; T_{m(t)-1} < t < T_{m(t)}. \tag{5.38}$$

As it was shown in Chapter 4 (in the case of the equity hybrid model), this basic interpolation technique was very satisfactory within the calibration. By combining (5.38) with (5.37), we find for the domestic and foreign bonds:

$$\begin{aligned}
\frac{1}{P_d(t,T)} &= \left(1+(T_{m(t)}-t)L_{d,m(t)}(T_{m(t)-1})\right) \prod_{j=m(t)+1}^{N} \left(1+\tau_j L_d(t,T_{j-1},T_j)\right), \\
\frac{1}{P_f(t,T)} &= \left(1+(T_{m(t)}-t)L_{f,m(t)}(T_{m(t)-1})\right) \prod_{j=m(t)+1}^{N} \left(1+\tau_j L_f(t,T_{j-1},T_j)\right).
\end{aligned}$$

When deriving the dynamics for $\mathrm{FX}^T(t)$ in (5.36) we will not encounter any *dt*-terms (as $\mathrm{FX}^T(t)$ has to be a martingale under the numéraire $P_d(t,T)$).

For each zero-coupon bond, $P_d(t,T)$ or $P_f(t,T)$, the dynamics are determined under the appropriate T-forward measures (for $P_d(t,T)$ the domestic T-forward measure, and for $P_f(t,T)$ the foreign T-forward measure). The dynamics for the zero-coupon bonds, driven by the Libor dynamics in (5.33) and (5.34), are given by:

$$\begin{aligned}
\frac{\mathrm{d}P_d(t,T)}{P_d(t,T)} &= (\ldots)\mathrm{d}t - \sqrt{v_d(t)} \sum_{j=m(t)+1}^{N} \frac{\tau_j v_{d,j}\phi_{d,j}(t)}{1+\tau_j L_{d,j}(t)} \mathrm{d}W_j^{d,T}(t), \\
\frac{\mathrm{d}P_f(t,T)}{P_f(t,T)} &= (\ldots)\mathrm{d}t - \sqrt{v_f(t)} \sum_{j=m(t)+1}^{N} \frac{\tau_j v_{f,j}\phi_{f,j}(t)}{1+\tau_j L_{f,j}(t)} \mathrm{d}\widehat{W}_j^{f,T}(t),
\end{aligned}$$

and the coefficients were defined in (5.33) and (5.34).

By changing the numéraire from $P_f(t,T)$ to $P_d(t,T)$ for the foreign bond, only the drift terms will change. Since $\mathrm{FX}^T(t)$ in (5.36) is a martingale under the $P_d(t,T)$ measure, it is *not* necessary to determine the appropriate drift correction.

By taking Equation (5.13) for the general dynamics of (5.36) and neglecting all the dt-terms we get

$$\begin{aligned}\frac{\mathrm{dFX}^T(t)}{\mathrm{FX}^T(t)} &= \sqrt{v(t)}\mathrm{d}W_y^T(t) + \sqrt{v_d(t)}\sum_{j=m(t)+1}^{N}\frac{\tau_j v_{d,j}\phi_{d,j}(t)}{1+\tau_j L_{d,j}(t)}\mathrm{d}W_j^{d,T}(t)\\ &\quad -\sqrt{v_f(t)}\sum_{j=m(t)+1}^{N}\frac{\tau_j v_{f,j}\phi_{f,j}(t)}{1+\tau_j L_{f,j}(t)}\mathrm{d}W_j^{f,T}(t). \qquad (5.39)\end{aligned}$$

Note that the *hat* in $\widehat{W}$, disappeared from the Brownian motion $\mathrm{d}W_j^{f,T}(t)$ in (5.39) which is an indication for the change of measure from the foreign to the domestic measure for the foreign Libors.

Since the stochastic volatility process, $v(t)$, for FX is independent of the domestic and foreign Libors, $L_{d,k}(t)$ and $L_{f,k}(t)$, the dynamics under the $P_d(t,T)$-measure do not change [4] and are given by:

$$\mathrm{d}v(t) = \kappa(\bar{v} - v(t))\mathrm{d}t + \gamma\sqrt{v(t)}\mathrm{d}W_v^T(t). \qquad (5.40)$$

The model given in (5.39), with the stochastic variance in (5.40) and the correlations between the main underlying processes, is not affine. In the next section we discuss the linearization.

5.3.1 Linearization and forward characteristic function

The model in (5.39) is not of the affine form, as it contains terms like $\phi_{i,j}(t)/(1+\tau_{i,j}L_{i,j}(t))$ with $\phi_{i,j} = \beta_{i,j}L_{i,j}(t) + (1-\beta_{i,j})L_{i,j}(0)$ for $i = \{d,f\}$. In order to derive a characteristic function, we *freeze* the Libor rates, which is standard practice (see for example [44, 58, 61]), i.e.:

$$\begin{aligned} L_{d,j}(t) \approx L_{d,j}(0) &\quad\Rightarrow\quad \phi_{d,j} \equiv L_{d,j}(0),\\ L_{f,j}(t) \approx L_{f,j}(0) &\quad\Rightarrow\quad \phi_{f,j} \equiv L_{f,j}(0). \qquad (5.41)\end{aligned}$$

This approximation gives the following $\mathrm{FX}^T(t)$-dynamics:

$$\begin{aligned}\frac{\mathrm{dFX}^T(t)}{\mathrm{FX}^T(t)} &\approx \sqrt{v(t)}\mathrm{d}W_y^T(t) + \sqrt{v_d(t)}\sum_{j\in\mathcal{A}}\psi_{d,j}\mathrm{d}W_j^{d,T}(t) - \sqrt{v_f(t)}\sum_{j\in\mathcal{A}}\psi_{f,j}\mathrm{d}W_j^{f,T}(t),\\ \mathrm{d}v(t) &= \kappa(\bar{v} - v(t))\mathrm{d}t + \gamma\sqrt{v(t)}\mathrm{d}W_v^T(t),\\ \mathrm{d}v_i(t) &= \lambda_i(v_i(0) - v_i(t))\mathrm{d}t + \eta_i\sqrt{v_i(t)}\mathrm{d}W_v^{i,T}(t),\end{aligned}$$

with $i = \{d,f\}$, $\mathcal{A} = \{m(t)+1,\dots N\}$, the correlations are given in (5.35) and

$$\psi_{d,j} := \frac{\tau_j v_{d,j}L_{d,j}(0)}{1+\tau_j L_{d,j}(0)}, \quad \psi_{f,j} := \frac{\tau_j v_{f,j}L_{f,j}(0)}{1+\tau_j L_{f,j}(0)}. \qquad (5.42)$$

[4] In Chapter 4 the proof for this statement was given when a single yield curve is considered.

We derive the dynamics for the logarithmic transformation of $\mathrm{FX}^T(t)$, $x^T(t) = \log \mathrm{FX}^T(t)$, for which we need to calculate the square of the diffusion coefficients [5].

With the notation,

$$a := \sqrt{v(t)}\mathrm{d}W_y^T(t),\ b := \sqrt{v_d(t)}\sum_{j\in\mathcal{A}}\psi_{d,j}\mathrm{d}W_j^{d,T}(t),\ c := \sqrt{v_f(t)}\sum_{j\in\mathcal{A}}\psi_{f,j}\mathrm{d}W_j^{f,T}(t), \tag{5.43}$$

we find, for the square diffusion coefficient $(a+b-c)^2 = a^2+b^2+c^2+2ab-2ac-2bc$. So, the dynamics for the log-forward, $x^T(t) = \log \mathrm{FX}^T(t)$, can be expressed as:

$$\begin{aligned} \mathrm{d}x^T(t) \quad &\approx \quad -\frac{1}{2}(a+b-c)^2 + \sqrt{v(t)}\mathrm{d}W_y^T(t) + \sqrt{v_d(t)}\sum_{\mathcal{A}}\psi_{d,j}\mathrm{d}W_j^{d,T}(t) \\ &\quad -\sqrt{v_f(t)}\sum_{\mathcal{A}}\psi_{f,j}\mathrm{d}W_j^{f,T}(t), \end{aligned} \tag{5.44}$$

with the coefficients a, b and c given in (5.43). Since

$$\Big(\sum_{j=1}^{N} x_j\Big)^2 = \sum_{j=1}^{N} x_j^2 + \sum_{\substack{i,j=1,\ldots,N\\ i\neq j}} x_i x_j, \quad \text{for } N>0,$$

we find:

$$\begin{aligned} a^2 &= v(t)\mathrm{d}t, \\ b^2 &= v_d(t)\Big(\sum_{j\in\mathcal{A}}\psi_{d,j}^2 + \sum_{\substack{i,j\in\mathcal{A}\\ i\neq j}}\psi_{d,i}\psi_{d,j}\rho_{i,j}^d\Big)\mathrm{d}t \quad =: \quad v_d(t)A_d(t)\mathrm{d}t, \qquad (5.45) \\ c^2 &= v_f(t)\Big(\sum_{j\in\mathcal{A}}\psi_{f,j}^2 + \sum_{\substack{i,j\in\mathcal{A}\\ i\neq j}}\psi_{f,i}\psi_{f,j}\rho_{i,j}^f\Big)\mathrm{d}t, \quad =: \quad v_f(t)A_f(t)\mathrm{d}t, \qquad (5.46) \\ ab &= \sqrt{v(t)}\sqrt{v_d(t)}\sum_{j\in\mathcal{A}}\psi_{d,j}\rho_{j,x}^d\mathrm{d}t, \\ ac &= \sqrt{v(t)}\sqrt{v_f(t)}\sum_{j\in\mathcal{A}}\psi_{f,j}\rho_{j,x}^f\mathrm{d}t, \\ bc &= \sqrt{v_d(t)}\sqrt{v_f(t)}\sum_{j\in\mathcal{A}}\psi_{d,j}\sum_{k\in\mathcal{A}}\psi_{f,k}\rho_{j,k}^{d,f}\mathrm{d}t, \end{aligned}$$

with $\rho_{j,x}^d$, $\rho_{j,x}^f$ the correlation between the FX and j-th domestic and foreign Libor, respectively. The correlation between the k-th domestic and j-th foreign Libor is $\rho_{k,j}^{d,f}$.

[5] As in the standard Black-Scholes analysis for $\mathrm{d}S(t) = \sigma_1 S(t)\mathrm{d}W(t)$, the log-transform gives $\mathrm{d}\log S(t) = -\frac{1}{2}\sigma_1^2\mathrm{d}t + \sigma_1\mathrm{d}W(t)$.

By setting $f\big(t, \sqrt{v(t)}, \sqrt{v_d(t)}, \sqrt{v_f(t)}\big) := (2ab - 2ac - 2bc)/\mathrm{d}t$, we can express the dynamics for $\mathrm{d}x^T(t)$ in (5.44) by:

$$\begin{aligned} dx^T(t) &\approx -\frac{1}{2}\left(v(t) + A_d(t)v_d(t) + A_f(t)v_f(t) + f\big(t, \sqrt{v(t)}, \sqrt{v_d(t)}, \sqrt{v_f(t)}\big)\right)\mathrm{d}t \\ &\quad + \sqrt{v(t)}\mathrm{d}W_y^T(t) + \sqrt{v_d(t)}\textstyle\sum_{\mathcal{A}}\psi_{d,j}\mathrm{d}W_j^{d,T}(t) - \sqrt{v_f(t)}\textstyle\sum_{\mathcal{A}}\psi_{f,j}\mathrm{d}W_j^{f,T}(t). \end{aligned}$$

The coefficients $\psi_{d,j}$, $\psi_{f,j}$, A_d and A_f in (5.42), (5.45), and (5.46) are deterministic and piecewise constant.

In order to make the model affine, we *linearize* the non-affine terms in the drift in $f(t, \sqrt{v(t)}, \sqrt{v_d(t)}, \sqrt{v_f(t)})$ by a projection on the first moments, i.e.,

$$f\big(t, \sqrt{v(t)}, \sqrt{v_d(t)}, \sqrt{v_f(t)}\big) \approx f\big(t, \mathbb{E}(\sqrt{v(t)}), \mathbb{E}(\sqrt{v_d(t)}), \mathbb{E}(\sqrt{v_f(t)})\big) =: f(t). \tag{5.47}$$

The variance processes $v(t)$, $v_d(t)$ and $v_f(t)$ are independent CIR-type processes [25], so the expectation of their products equals the product of the expectations. Function $f(t)$ can be determined with the help of the formula in Lemma 2.3.1 in Chapter 2.

The approximation in (5.47) linearizes all non-affine terms in the corresponding PDE. As before, the forward characteristic function, $\phi^T := \phi^T(u, x^T(t), t, T)$, is defined as the solution of the following backward PDE:

$$\begin{aligned} 0 &= \frac{\partial \phi^T}{\partial t} + \frac{1}{2}\left(v + A_d(t)v_d + A_f(t)v_f + f(t)\right)\left(\frac{\partial^2 \phi^T}{\partial x^2} - \frac{\partial \phi^T}{\partial x}\right) \\ &\quad + \lambda_d(v_d(0) - v_d)\frac{\partial \phi^T}{\partial v_d} + \lambda_f(v_f(0) - v_f)\frac{\partial \phi^T}{\partial v_f} + \kappa(\bar{v} - v)\frac{\partial \phi^T}{\partial v} \\ &\quad + \frac{1}{2}\eta_d^2 v_d \frac{\partial^2 \phi^T}{\partial v_d^2} + \frac{1}{2}\eta_f^2 v_f \frac{\partial^2 \phi^T}{\partial v_f^2} + \frac{1}{2}\gamma^2 v \frac{\partial^2 \phi^T}{\partial v^2} + \rho_{y,v}\gamma v \frac{\partial^2 \phi^T}{\partial x \partial v}, \end{aligned} \tag{5.48}$$

with the final condition $\phi^T(u, x^T(T), T, T) = \mathrm{e}^{iux^T(T)}$. Since all coefficients in this PDE are linear, the solution is of the following form:

$$\begin{aligned} \phi^T(u, x^T(t), t, T) &= \exp\big(A(u,\tau) + B(u,\tau)x^T(t) + C(u,\tau)v(t) \\ &\quad + D_d(u,\tau)v_d(t) + D_f(u,\tau)v_f(t)\big), \end{aligned} \tag{5.49}$$

with $\tau := T - t$. Substitution of (5.49) in (5.48) gives us the following system of ODEs for the functions $A(\tau) := A(u,\tau)$, $B(\tau) := B(u,\tau)$, $C(\tau) := C(u,\tau)$, $D_d(\tau) := D_d(u,\tau)$ and $D_f(\tau) := D_f(u,\tau)$:

$$\begin{aligned} A'(\tau) &= f(t)(B^2(\tau) - B(\tau))/2 + \lambda_d v_d(0)D_1(\tau) + \lambda_f v_f(0)D_2(\tau) + \kappa\bar{v}C(\tau), \\ B'(\tau) &= 0, \\ C'(\tau) &= (B^2(\tau) - B(\tau))/2 + \left(\rho_{y,v}\gamma B(\tau) - \kappa\right)C(\tau) + \gamma^2 C^2(\tau)/2, \\ D_d'(\tau) &= A_d(t)(B^2(\tau) - B(\tau))/2 - \lambda_d D_d(\tau) + \eta_d^2 D_d^2(\tau)/2, \\ D_f'(\tau) &= A_f(t)(B^2(\tau) - B(\tau))/2 - \lambda_f D_f(\tau) + \eta_f^2 D_f^2(\tau)/2, \end{aligned}$$

with initial conditions $A(0) = 0$, $B(0) = iu$, $C(0) = 0$, $D_d(0) = 0$, $D_f(0) = 0$ with $A_d(t)$ and $A_f(t)$ from (5.45), (5.46), respectively, and $f(t)$ as in (5.47).

With $B(\tau) = iu$, the solution for $C(\tau)$ is analogous to the solution of the ODE for the FX-HHW1 model in Equation (5.24). As the remaining ODEs contain the piecewise constant functions $A_d(t)$, $A_f(t)$ the solution must be determined iteratively, like for the pure Heston model with piecewise constant parameters in [4]. For a given grid $0 = \tau_0 < \tau_1 < \cdots < \tau_N = \tau$, the functions $D_d(u, \tau)$, $D_f(u, \tau)$ and $A(u, \tau)$ can be expressed as:

$$\begin{aligned} D_d(u, \tau_j) &= D_d(u, \tau_{j-1}) + \chi_d(u, \tau_j), \\ D_f(u, \tau_j) &= D_f(u, \tau_{j-1}) + \chi_f(u, \tau_j), \end{aligned}$$

for $j = 1, \ldots, N$, and

$$A(u, \tau_j) = A(u, \tau_{j-1}) + \chi_A(u, \tau_j) \; - \; \frac{1}{2}(u^2 + u) \int_{\tau_{j-1}}^{\tau_j} f(s) \mathrm{d}s,$$

with $f(s)$ in (5.47) and analytically known functions $\chi_k(u, \tau_j)$, for $k = \{d, f\}$ and $\chi_A(u, \tau_j)$:

$$\chi_k(u, \tau_j) := \left(\lambda_k - \delta_{k,j} - \eta_k^2 D_k(u, \tau_{j-1})\right) (1 - \mathrm{e}^{-\delta_{k,j} s_j}) / (\eta_k^2 (1 - \ell_{k,j} \mathrm{e}^{-\delta_{k,j} s_j})),$$

and

$$\begin{aligned} \chi_A(u, \tau_j) \;\; = \;\; & \frac{\kappa \bar{v}}{\gamma^2} \left((\kappa - \rho_{y,v} \gamma i u - d_j) s_j - 2 \log \left((1 - g_j \mathrm{e}^{-d_j s_j}) / (1 - g_j) \right) \right) \\ & + v_d(0) \frac{\lambda_d}{\eta_d^2} \left((\lambda_d - \delta_{d,j}) s_j - 2 \log \left((1 - \ell_{d,j} \mathrm{e}^{-\delta_{d,j} s_j}) / \, (1 - \ell_{d,j}) \right) \right) \\ & + v_f(0) \frac{\lambda_f}{\eta_f^2} \left((\lambda_f - \delta_{f,j}) s_j - 2 \log \left((1 - \ell_{f,j} \mathrm{e}^{-\delta_{f,j} s_j}) / \, (1 - \ell_{f,j}) \right) \right), \end{aligned}$$

where

$$\begin{aligned} d_j = & \sqrt{(\rho_{y,v} \gamma i u - \kappa)^2 + \gamma^2 (iu + u^2)}, \quad & g_j = \frac{(\kappa - \rho_{y,v} \gamma i u) - d_j - \gamma^2 C(u, \tau_{j-1})}{(\kappa - \rho_{y,v} \gamma i u) + d_j - \gamma^2 C(u, \tau_{j-1})}, \\ \delta_{k,j} = & \sqrt{\lambda_k^2 + \eta_k^2 A_k(t)(u^2 + iu)}, & \ell_{k,j} = \frac{\lambda_k - \delta_{k,j} - \eta_k^2 D_k(u, \tau_{j-1})}{\lambda_k + \delta_{k,j} - \eta_k^2 D_k(u, \tau_{j-1})}, \end{aligned}$$

with $s_j = \tau_j - \tau_{j-1}$, $j = 1, \ldots, N$, $A_d(t)$ and $A_f(t)$ are from (5.45) and (5.46).

The resulting approximation of the full-scale FX-HLMM model is called *FX-LMM1* here.

5.3.2 Foreign stock in the FX-HLMM framework

We also consider a foreign stock, $S_f(t)$, driven by the Heston stochastic volatility model, with the interest rates driven by the market model. The stochastic processes of the stock model are assumed to be of the same form as the FX (with one, foreign, interest rate curve) with the dynamics, under the forward foreign measure, given by:

$$\begin{aligned}\frac{\mathrm{d}S_f^T(t)}{S_f^T(t)} &= \sqrt{\omega(t)}\mathrm{d}W_{S_f}^{f,T}(t) + \sqrt{v_f(t)}\sum_{j=m(t)+1}^{N}\frac{\tau_j v_{f,j}\phi_{f,j}(t)}{1+\tau_j L_{f,j}(t)}\mathrm{d}W_j^{f,T}(t),\\ \mathrm{d}\omega(t) &= \kappa_f(\bar{\omega}-\omega(t))\mathrm{d}t + \gamma_f\sqrt{\omega(t)}\mathrm{d}W_\omega^{f,T}(t).\end{aligned} \tag{5.50}$$

Variance process, $\omega(t)$, is correlated with forward stock $S_f^T(t)$.

We move to the domestic-forward measure. The forward stock, $S_f^T(t)$, and forward foreign exchange rate, $\mathrm{FX}^T(t)$, are defined by

$$S_f^T(t) = \frac{S_f(t)}{P_f(t,T)}, \quad \mathrm{FX}^T(t) = y(t)\frac{P_f(t,T)}{P_d(t,T)}.$$

The quantity

$$S_f^T(t)\mathrm{FX}^T(t) = \frac{S_f(t)}{P_f(t,T)}y(t)\frac{P_f(t,T)}{P_d(t,T)} = \frac{S_f(t)}{P_d(t,T)}y(t), \tag{5.51}$$

is therefore a tradable asset. So, foreign stock exchanged by a foreign exchange rate and denominated in the domestic zero-coupon bond is a tradable quantity, which implies that $S_f^T(t)\mathrm{FX}^T(t)$ is a martingale. By Itô's lemma, one finds:

$$\frac{\mathrm{d}\left(S_f^T(t)\mathrm{FX}^T(t)\right)}{S_f^T(t)\mathrm{FX}^T(t)} = \frac{\mathrm{dFX}^T(t)}{\mathrm{FX}^T(t)} + \frac{\mathrm{d}S_f^T(t)}{S_f^T(t)} + \left(\frac{\mathrm{dFX}^T(t)}{\mathrm{FX}^T(t)}\right)\left(\frac{\mathrm{d}S_f^T(t)}{S_f^T(t)}\right). \tag{5.52}$$

The two first terms at the RHS of (5.52) do not contribute to the drift. The last term contains all $\mathrm{d}t$-terms, that, by a change of measure, will enter the drift of the variance process $\mathrm{d}\omega(t)$ in (5.50).

5.3.3 Numerical experiments with the FX-HLMM model

We here focus on the FX-HLMM model covered in Section 5.3 and consider the errors generated by the various approximations that led to the model FX-HLMM1 by some numerical experiments.

We have performed basically two linearization steps to define FX-HLMM1: We have frozen the Libors at their initial values and projected the non-affine covariance terms on a deterministic function. We check, by a numerical experiment, the size of the errors of these approximations.

We have chosen the following interest rate curves $P_d(0,T) = \exp(-0.02T)$, $P_f(0,T) = \exp(-0.05T)$, and, as before, for the FX stochastic volatility model we set:

$$\kappa = 0.5, \quad \gamma = 0.3, \quad \bar{v} = 0.1, \quad v(0) = 0.1.$$

In the simulation we have chosen the following parameters for the domestic and foreign markets:

$$\beta_{d,k} = 95\%, \quad \upsilon_{d,k} = 15\%, \quad \lambda_d = 100\%, \quad \eta_d = 10\%,$$
$$\beta_{f,k} = 50\%, \quad \upsilon_{f,k} = 25\%, \quad \lambda_f = 70\%, \quad \eta_f = 20\%.$$

In the correlation matrix a number of correlations need to be specified. For the correlations between the Libor rates in each market, we prescribe large positive values, as frequently observed in fixed income markets (see for example [19]), $\rho^d_{i,j} = 90\%$, $\rho^f_{i,j} = 70\%$, for $i, j = 1, \ldots, N$ $(i \neq j)$. In order to generate skew for FX, we prescribe a *negative* correlation between $\mathrm{FX}^T(t)$ and its stochastic volatility process, $v(t)$, i.e., $\rho_{y,v} = -40\%$. The correlation between the FX and the domestic Libors is set as $\rho^d_{y,k} = -15\%$, for $k = 1, \ldots, N$, and the correlation between FX and the foreign Libors is $\rho^f_{y,k} = -15\%$. The correlation between the domestic and foreign Libors is $\rho^{d,f}_{i,j} = 25\%$ for $i, j = 1, \ldots, N$ $(i \neq j)$. The following block correlation matrix results:

$$\mathbf{C} = \begin{bmatrix} \mathbf{C}_d & \mathbf{C_{d,f}} & \mathbf{C_{y,d}} \\ \mathbf{C}^{\mathrm{T}}_{d,f} & \mathbf{C_f} & \mathbf{C_{y,f}} \\ \mathbf{C}^{\mathrm{T}}_{y,d} & \mathbf{C}^{\mathrm{T}}_{y,f} & 1 \end{bmatrix},$$

with the domestic Libor correlations given by

$$\mathbf{C_d} = \begin{bmatrix} 1 & \rho^d_{1,2} & \ldots & \rho^d_{1,N} \\ \rho^d_{1,2} & 1 & \ldots & \rho^d_{2,N} \\ \vdots & \vdots & \ddots & \vdots \\ \rho^d_{1,N} & \rho^d_{2,N} & \ldots & 1 \end{bmatrix} = \begin{bmatrix} 1 & 90\% & \ldots & 90\% \\ 90\% & 1 & \ldots & 90\% \\ \vdots & \vdots & \ddots & \vdots \\ 90\% & 90\% & \ldots & 1 \end{bmatrix}_{N\times N},$$

the foreign Libors correlations given by:

$$\mathbf{C_f} = \begin{bmatrix} 1 & \rho^f_{1,2} & \ldots & \rho^f_{1,N} \\ \rho^f_{1,2} & 1 & \ldots & \rho^f_{2,N} \\ \vdots & \vdots & \ddots & \vdots \\ \rho^f_{1,N} & \rho^f_{2,N} & \ldots & 1 \end{bmatrix} = \begin{bmatrix} 1 & 70\% & \ldots & 70\% \\ 70\% & 1 & \ldots & 70\% \\ \vdots & \vdots & \ddots & \vdots \\ 70\% & 70\% & \ldots & 1 \end{bmatrix}_{N\times N},$$

the correlation between Libors from the domestic and foreign markets given by:

$$\mathbf{C_{df}} = \begin{bmatrix} 1 & \rho^{d,f}_{1,2} & \ldots & \rho^{d,f}_{1,N} \\ \rho^{d,f}_{1,2} & 1 & \ldots & \rho^{d,f}_{2,N} \\ \vdots & \vdots & \ddots & \vdots \\ \rho^{d,f}_{1,N} & \rho^{d,f}_{2,N} & \ldots & 1 \end{bmatrix} = \begin{bmatrix} 1 & 25\% & \ldots & 25\% \\ 25\% & 1 & \ldots & 25\% \\ \vdots & \vdots & \ddots & \vdots \\ 25\% & 25\% & \ldots & 1 \end{bmatrix}_{N\times N},$$

and the vectors $\mathbf{C}_{y,d}$ and $\mathbf{C}_{y,f}$, as used in [93], are given by:

$$\mathbf{C_{y,d}} = \begin{bmatrix} \rho^d_{y,1} \\ \rho^d_{y,2} \\ \vdots \\ \rho^d_{y,N} \end{bmatrix} = \begin{bmatrix} -15\% \\ -15\% \\ \vdots \\ -15\% \end{bmatrix}_{N\times 1}, \mathbf{C_{y,f}} = \begin{bmatrix} \rho^f_{y,1} \\ \rho^f_{y,2} \\ \vdots \\ \rho^f_{y,N} \end{bmatrix} = \begin{bmatrix} -15\% \\ -15\% \\ \vdots \\ -15\% \end{bmatrix}_{N\times 1}.$$

Since in both markets the Libor rates are assumed to be independent of their variance processes, we can neglect these correlations here.

Now we find the prices of plain vanilla options on FX in (5.36). The simulation is performed in the same spirit as in Section 5.2.5 where the FX-HHW model was considered. In Table 5.2 we present the differences, in terms of the implied volatilities between the models FX-HLMM and FX-HLMM1. While the prices for the FX-HLMM were obtained by Monte Carlo simulation (20.000 paths and 20 intermediate points between the dates T_{i-1} and T_i for $i = 1, \ldots, N$), the prices for FX-HLMM1 were obtained by the Fourier-based COS method [32] with 500 cosine series terms.

Table 5.2: *Differences, in implied Black volatilities, between the FX-HLMM and FX-LMM1 models. The corresponding strikes $K_1(T_i), \ldots, K_7(T_i)$ are tabulated in Table 5.4. The prices and associated standard deviations are presented in Table 5.8.*

T_i	$K_1(T_i)$	$K_2(T_i)$	$K_3(T_i)$	$K_4(T_i)$	$K_5(T_i)$	$K_6(T_i)$	$K_7(T_i)$
2y	0.19 %	0.14 %	0.09 %	0.05 %	0.00 %	-0.05 %	-0.10 %
3y	0.29 %	0.25 %	0.21 %	0.16 %	0.11 %	0.06 %	0.02 %
5y	0.32 %	0.28 %	0.23 %	0.17 %	0.10 %	0.05 %	0.00 %
7y	0.30 %	0.28 %	0.25 %	0.21 %	0.18 %	0.14 %	0.10 %
10y	0.39 %	0.32 %	0.25 %	0.18 %	0.12 %	0.05 %	-0.03 %
15y	0.38 %	0.29 %	0.21 %	0.13 %	0.05 %	-0.04 %	-0.14 %
20y	0.02 %	-0.09 %	-0.18 %	-0.27 %	-0.34 %	-0.40 %	-0.44 %
25y	0.08 %	0.04 %	-0.14 %	-0.25 %	-0.34 %	-0.40 %	-0.46 %
30y	0.11 %	0.07 %	0.00 %	-0.09 %	-0.18 %	-0.21 %	-0.24 %

The FX-HLMM1 model performs very well, as the maximum difference in terms of implied volatilities is between $0.2\% - 0.5\%$.

Sensitivity to the interest rate skew

Approximation FX-HLMM1 was based on freezing the Libor rates. By freezing the Libors, i.e.: $L_{d,k}(t) \equiv L_{d,k}(0)$ and $L_{f,k}(t) \equiv L_{f,k}(0)$ we have

$$\begin{aligned}
\phi_{d,k}(t) &= \beta_{d,k} L_{d,k}(t) + (1 - \beta_{d,k}) L_{d,k}(0) = L_{d,k}(0), \qquad (5.53)\\
\phi_{f,k}(t) &= \beta_{f,k} L_{f,k}(t) + (1 - \beta_{f,k}) L_{f,k}(0) = L_{f,k}(0). \qquad (5.54)
\end{aligned}$$

In the DD-SV models for the Libor rates $L_{d,k}(t)$ and $L_{f,k}(t)$ for any k, the parameters $\beta_{d,k}$, $\beta_{f,k}$ control the slope of the interest rate volatility smiles. Freezing the Libors to $L_{d,k}(0)$ and $L_{f,k}(0)$ is equivalent to setting $\beta_{d,k} = 0$ and $\beta_{f,k} = 0$ in (5.53) and (5.54) in the approximation FX-HLMM1.

By a Monte Carlo simulation, we obtain the FX implied volatilities from the full-scale FX-HLMM model for different values of β and by comparing them to those from FX-HLMM1 with $\beta = 0$ we check the influence of the parameters $\beta_{d,k}$ and $\beta_{f,k}$ on the FX. In Table 5.3 the implied volatilities for the FX European call options for FX-HLMM and FX-HLMM1 are presented. The experiments are performed for different combinations of the interest rate skew parameters, β_d and β_f.

Table 5.3: *Implied volatilities of the FX options from the FX-HLMM and FX-HLMM1 models, $T = 10$ and parameters were as in Section 5.3.3. The numbers in parentheses correspond to the standard deviations (the experiment was performed 20 times with $20T$ time steps).*

strike	FX-HLMM (Monte Carlo simulation)					FX-HLMM1 (Fourier)
	$\beta_f = 0.5$			$\beta_d = 0.5$		$\beta_d = 0$
(5.30)	$\beta_d = 0$	$\beta_d = 0.5$	$\beta_d = 1$	$\beta_f = 0$	$\beta_f = 1$	$\beta_f = 0$
0.6224	31.98 % (0.20)	31.91 % (0.17)	31.98 % (0.17)	31.99 % (0.15)	31.96 % (0.18)	31.56 %
0.7290	31.49 % (0.21)	31.43 % (0.16)	31.48 % (0.19)	31.51 % (0.15)	31.46 % (0.18)	31.12 %
0.8538	31.02 % (0.21)	30.96 % (0.17)	31.01 % (0.20)	31.04 % (0.15)	30.97 % (0.18)	30.69 %
1.0001	30.58 % (0.21)	30.53 % (0.17)	30.56 % (0.22)	30.61 % (0.15)	30.52 % (0.17)	30.30 %
1.1714	30.16 % (0.20)	30.11 % (0.17)	30.15 % (0.24)	30.20 % (0.15)	30.08 % (0.16)	29.93 %
1.3721	29.77 % (0.22)	29.73 % (0.16)	29.77 % (0.26)	29.82 % (0.16)	29.68 % (0.17)	29.60 %
1.6071	29.41 % (0.24)	29.38 % (0.17)	29.43 % (0.28)	29.48 % (0.17)	29.31 % (0.18)	29.30 %

The experiment indicates that there is only a small impact of the different $\beta_{d,k}-$ and $\beta_{f,k}-$values on the FX implied volatilities, implying that the approximate model, FX-HLMM1 with $\beta_{d,k} = \beta_{f,k} = 0$, is useful for the interest rate modelling, for the parameters studied. With $\beta_{d,k} \neq 0$ and $\beta_{f,k} \neq 0$ the implied volatilities obtained by the FX-HLMM model appear to be somewhat higher than those obtained by FX-HLMM1, a difference of approximately $0.1\% - 0.15\%$, which is considered highly satisfactory.

5.4 Conclusion

In this chapter we have presented two FX models with stochastic volatility and correlated stochastic interest rates. Both FX models were based on the Heston FX model and differ with respect to the interest rate processes.

In the first model we considered a model in which the domestic and foreign interest rates were driven by single factor Hull-White short-rate processes. This model enables pricing of FX-interest rate hybrid products that are not exposed to the smile in the fixed income markets.

For hybrid products sensitive to the interest rate skew a second model was presented in which the interest rates were driven by the stochastic volatility Libor Market Model.

For both hybrid models we have developed approximate models for the pricing of European options on the FX. These pricing formulas form the basis for model calibration strategies.

The approximate models are based on the linearization of the non-affine terms in the corresponding pricing PDE, in a very similar way as presented in Chapter 4 for equity-interest rate options. The approximate models perform very well in the world of foreign exchange, for the experiments considered.

The solution to these models can also be used to obtain an initial guess when the full-scale models are used.

5.A Appendix: Tables

In this appendix we present tables with details for the numerical experiments.

T_i	$K_1(T_i)$	$K_2(T_i)$	$K_3(T_i)$	$K_4(T_i)$	$K_5(T_i)$	$K_6(T_i)$	$K_7(T_i)$
6m	1.1961	1.2391	1.2837	1.3299	1.3778	1.4273	1.4787
1y	1.1276	1.1854	1.2462	1.3101	1.3773	1.4479	1.5221
3y	0.9515	1.0376	1.1315	1.2338	1.3454	1.4671	1.5999
5y	0.8309	0.9291	1.0390	1.1620	1.2994	1.4531	1.6250
7y	0.7358	0.8399	0.9587	1.0943	1.2491	1.4257	1.6274
10y	0.6224	0.7290	0.8538	1.0001	1.1714	1.3721	1.6071
15y	0.4815	0.5844	0.7093	0.8608	1.0447	1.2680	1.5389
20y	0.3788	0.4737	0.5924	0.7409	0.9265	1.1587	1.4491
30y	0.2414	0.3174	0.4174	0.5489	0.7218	0.9492	1.2482

Table 5.4: *Expiries and strikes of FX options used in the FX-HHW model. Strikes $K_n(T_i)$ were calculated as given in (5.30) with $y(0) = 1.35$.*

T_i	$K_1(T_i)$	$K_2(T_i)$	$K_3(T_i)$	$K_4(T_i)$	$K_5(T_i)$	$K_6(T_i)$	$K_7(T_i)$
6m	11.41 %	10.49 %	9.66 %	9.02 %	8.72 %	8.66 %	8.68 %
1y	12.23 %	10.98 %	9.82 %	8.95 %	8.59 %	8.59 %	8.65 %
3y	12.94 %	11.35 %	9.89 %	8.78 %	8.34 %	8.36 %	8.46 %
5y	13.44 %	11.84 %	10.38 %	9.27 %	8.76 %	8.71 %	8.83 %
7y	14.29 %	12.68 %	11.23 %	10.12 %	9.52 %	9.37 %	9.43 %
10y	16.43 %	14.79 %	13.34 %	12.18 %	11.43 %	11.07 %	10.99 %
15y	20.93 %	19.13 %	17.56 %	16.27 %	15.29 %	14.65 %	14.29 %
20y	22.96 %	21.19 %	19.68 %	18.44 %	17.50 %	16.84 %	16.46 %
30y	25.09 %	23.48 %	22.17 %	21.13 %	20.35 %	19.81 %	19.48 %

Table 5.5: *Market implied Black volatilities for FX options as given in [93]. The strikes $K_n(T_i)$ were tabulated in Table 5.4.*

T_i	$K_1(T_i)$	$K_2(T_i)$	$K_3(T_i)$	$K_4(T_i)$	$K_5(T_i)$	$K_6(T_i)$	$K_7(T_i)$
6m	0.12 %	-0.12 %	-0.25 %	-0.23 %	-0.01 %	0.20 %	0.22 %
1y	0.13 %	-0.08 %	-0.18 %	-0.09 %	0.14 %	0.16 %	-0.14 %
3y	0.16 %	-0.07 %	-0.17 %	-0.08 %	0.18 %	0.22 %	-0.14 %
5y	0.11 %	-0.06 %	-0.12 %	-0.07 %	0.10 %	0.13 %	-0.14 %
7y	0.07 %	-0.03 %	-0.06 %	-0.03 %	0.06 %	0.10 %	-0.08 %
10y	0.04 %	-0.01 %	-0.01 %	-0.02 %	0.02 %	0.05 %	-0.02 %
15y	0.11 %	-0.05 %	-0.09 %	-0.04 %	0.03 %	0.09 %	-0.05 %
20y	0.94 %	0.39 %	0.02 %	-0.19 %	-0.24 %	-0.16 %	0.02 %
30y	1.65 %	0.70 %	0.00 %	-0.48 %	-0.74 %	-0.82 %	-0.74 %

Table 5.6: *The calibration results for the FX-HHW model, in terms of the differences between the market (given in Table 5.5) and FX-HHW model implied volatilities. Strikes $K_n(T_i)$ are given in Table 5.4.*

T_i	method	$K_1(T_i)$	$K_2(T_i)$	$K_3(T_i)$	$K_4(T_i)$	$K_5(T_i)$	$K_6(T_i)$	$K_7(T_i)$
6m	MC	0.1907	0.1636	0.1382	0.1148	0.0935	0.0748	0.0585
	std dev	0.0004	0.0004	0.0005	0.0004	0.0004	0.0004	0.0004
	COS	0.1908	0.1637	0.1382	0.1147	0.0934	0.0746	0.0583
1y	MC	0.2566	0.2209	0.1870	0.1553	0.1264	0.1008	0.0785
	std dev	0.0007	0.0007	0.0007	0.0007	0.0007	0.0007	0.0007
	COS	0.2567	0.2210	0.1870	0.1554	0.1265	0.1008	0.0786
3y	MC	0.3768	0.3281	0.2805	0.2349	0.1923	0.1538	0.1200
	std dev	0.0014	0.0015	0.0015	0.0015	0.0015	0.0015	0.0014
	COS	0.3765	0.3279	0.2804	0.2349	0.1926	0.1543	0.1207
5y	MC	0.4216	0.3709	0.3205	0.2713	0.2246	0.1816	0.1432
	std dev	0.0021	0.0021	0.0021	0.0020	0.0020	0.0019	0.0018
	COS	0.4212	0.3706	0.3203	0.2713	0.2249	0.1822	0.1441
10y	MC	0.4310	0.3871	0.3420	0.2967	0.2521	0.2096	0.1702
	std dev	0.0033	0.0033	0.0033	0.0033	0.0033	0.0031	0.0030
	COS	0.4311	0.3873	0.3423	0.2971	0.2528	0.2106	0.1714
20y	MC	0.3362	0.3109	0.2838	0.2553	0.2260	0.1966	0.1677
	std dev	0.0037	0.0037	0.0037	0.0037	0.0037	0.0036	0.0036
	COS	0.3358	0.3104	0.2833	0.2548	0.2254	0.1960	0.1672
30y	MC	0.2322	0.2191	0.2046	0.1888	0.1720	0.1545	0.1367
	std dev	0.0050	0.0050	0.0050	0.0050	0.0049	0.0048	0.0048
	COS	0.2319	0.2188	0.2042	0.1883	0.1714	0.1539	0.1359

Table 5.7: *Average FX call option prices obtained by the FX-HHW model with 20 Monte Carlo simulations, 50.000 paths and $20 \times T_i$ steps; MC stands for Monte Carlo and COS for Fourier Cosine expansion technique ([32]) for the FX-HHW1 model with 500 expansion terms. The strikes $K_n(T_i)$ are tabulated in Table 5.4.*

T_i	method	$K_1(T_i)$	$K_2(T_i)$	$K_3(T_i)$	$K_4(T_i)$	$K_5(T_i)$	$K_6(T_i)$	$K_7(T_i)$
2y	MC	0.3336	0.2889	0.2456	0.2046	0.1667	0.1327	0.1030
	std dev	0.0008	0.0009	0.0010	0.0010	0.0011	0.0011	0.0012
	COS	0.3326	0.2880	0.2450	0.2043	0.1667	0.1330	0.1037
3y	MC	0.3786	0.3299	0.2823	0.2366	0.1939	0.1553	0.1213
	std dev	0.0006	0.0007	0.0008	0.0009	0.0011	0.0012	0.0013
	COS	0.3768	0.3282	0.2808	0.2354	0.1931	0.1548	0.1212
5y	MC	0.4243	0.3738	0.3234	0.2743	0.2274	0.1843	0.1457
	std dev	0.0012	0.0013	0.0014	0.0015	0.0016	0.0016	0.0016
	COS	0.4222	0.3717	0.3215	0.2727	0.2265	0.1838	0.1457
10y	MC	0.4363	0.3928	0.3482	0.3031	0.2587	0.2162	0.1764
	std dev	0.0012	0.0016	0.0019	0.0023	0.0026	0.0027	0.0028
	COS	0.4338	0.3905	0.3461	0.3014	0.2576	0.2157	0.1767
20y	MC	0.3417	0.3171	0.2907	0.2629	0.2342	0.2052	0.1768
	std dev	0.0010	0.0013	0.0015	0.0018	0.0021	0.0025	0.0030
	COS	0.3416	0.3176	0.2918	0.2647	0.2367	0.2085	0.1806
30y	MC	0.2396	0.2281	0.2152	0.2011	0.1858	0.1699	0.1534
	std dev	0.0012	0.0015	0.0018	0.0021	0.0024	0.0029	0.0035
	COS	0.2393	0.2279	0.2152	0.2014	0.1866	0.1710	0.1548

Table 5.8: *Average FX call option prices obtained by the FX-HLMM model with 20 Monte Carlo simulations, 50.000 paths and $20 \times T_i$ steps; MC stands for Monte Carlo and COS for the Fourier Cosine expansion technique described in Chapter 1 for the FX-HLMM1 model with 500 expansion terms. Values of the strikes $K_n(T_i)$ are tabulated in Table 5.4.*

CHAPTER 6

Conclusions and Outlook

Bud Fox: How much is enough?
Gordon Gekko: It's not a question of enough, pal. It's a zero sum game, somebody wins, somebody loses. Money itself isn't lost or made, it's simply transferred from one perception to another.

Gordon Gekko ("Wall Street")

6.1 Conclusions

In this thesis we have presented novel approaches for modelling long-term hybrid derivatives involving equity, foreign exchange, and interest rates asset classes. No restrictions regarding the choice of correlation structure between the different Wiener processes appearing had to be made.

We have defined hybrid models that belong to the class of affine diffusion models and we have shown that the Schöbel-Zhu-Hull-White model fits in this category. Due to the resulting semi-closed form of the Schöbel-Zhu-Hull-White characteristic function, we were able to calibrate the model in an efficient way.

We have also investigated models with more advanced volatility structure, like the Heston-Hull-White and the Heston-Cox-Ingersoll-Ross hybrid models. By approximations of the non-affine terms in the corresponding instantaneous covariance matrix, we placed the approximate hybrid models in the framework of affine diffusion processes. For those models we have determined the characteristic functions. The approximations in the models have been validated by comparing the obtained implied volatilities to those of the full-scale hybrid models.

For the affine Heston-Gaussian multi-factor model we have discussed an efficient Monte Carlo simulation scheme and a way to calculate the Greeks of plain vanilla options. We have also shown that the model provides option prices similar to the (non-affine) Heston-Gaussian multi-factor model and superior to Schöbel-Zhu variants, if the Feller condition is violated.

Moreover, we have proposed an equity-interest rate hybrid model with stochastic volatility for stock and for the interest rates modelled by the Libor Market Models. By changing the measure from the risk-neutral to the forward measure, associated with the zero-coupon bond as the numéraire, the dimension of the approximating characteristic function has been significantly reduced. This, combined with *freezing* the Libor rates and appropriate linearizations of the non-affine terms arising in the corresponding instantaneous covariance matrix, enabled us to derive a closed-form iterative forward characteristic function. By this, the approximate hybrid model can be used for calibration.

The main advantage of the latter model, the Heston-Libor Market Model, developed lies in its ability to price hybrid products that are exposed to the interest rate smile accurately and efficiently.

Finally, we have presented two foreign exchange models with stochastic volatility and correlated stochastic interest rates. Both cross-currency models were based on the Heston model and differ with respect to the interest rate processes. In the first model we considered the domestic and foreign interest rates to be driven by single factor short-rate processes. This model enabled pricing of Foreign Exchange-Interest Rate hybrid products that were not exposed to the smile in fixed income markets. For hybrid products sensitive to the interest rate skew a second model was presented in which the interest rates were driven by the stochastic volatility Libor Market Model.

The resulting efficient pricing methods may form the basis for the modelling of complex structured hybrid products to be defined in the near future.

6.2 Outlook

Hybrid derivatives with equity structure that, beside interest rates also, depend on the creditworthiness and performance of the underlying equity can be an interesting extension of the models presented in this thesis. The hybrid model, as such, would allow the valuation, in a single consistent model, of debt-equity securities which are vulnerable to default, as well as of derivatives depending on interest rates, equity and credit.

Extended equity-interest rate hybrid models could additionally take into account the risk of default that a counterparty would bear if the reference entity would not honor its financial obligations. In the case of an equity default swap, for example, such a hybrid product could provide protection against some possible events related to a specified reference asset.

Another interesting topic for future research could be the investigation on estimating, from historical data, of the correlation between different asset classes. Contrary to the case of the *pure* Heston model, where the correlation between a stock and the variance process is obtained via model calibration to a volatility surface from plain vanilla options, estimation of a correlation between stock and interest rate, for example, is not well studied in the literature so far. It is particularly difficult as multiple interest rates (with different maturities) are available in the market.

Additional improvement in hybrid modelling could be achieved if analytic formulas for implied volatilities, for the models considered in this thesis, would be derived. A modeling framework in which analytic, closed-form, expressions for implied volatilities can be determined, could provide a significant reduction of the computational time needed in the model calibration.

Alternatively, the stochastic volatility model of Heston could be replaced by dynamics for which analytic approximations for implied volatilities are already well established, like the SABR model [51].

The future for hybrid models and efficient calibration seems bright.

References

[1] M. Abramowitz and I.A. Stegun. *Modified Bessel Functions* **I** *and* **K**. Handbook of Mathematical Functions with Formulas, Graphs, and Mathematical Tables, 9th edition, 1972.

[2] S. Amstrup, L. MacDonald, and B. Manly. *Handbook of Capture-Recapture Analysis*. Princeton University Press, 2006.

[3] L.B.G. Andersen. Simple and efficient simulation of the Heston stochastic volatility model. *J. of Comp. Finance*, 11:1–42, 2007.

[4] L.B.G. Andersen and J. Andreasen. Volatility skews and extensions of the Libor Market Model. *Appl. Math. Finance*, 1(7):1–32, 2000.

[5] L.B.G. Andersen and J. Andreasen. Volatile volatilities. *Risk*, 15(12):163–168, 2002.

[6] J. Andreasen. Closed form pricing of FX options under stochastic rates and volatility. Presentation at Global Derivatives Conference, Paris, 9-11 May, 2006.

[7] A. Antonov. Effective approximation of FX/EQ options for the hybrid models: Heston and correlated Gaussian interest rates. Presentation at MathFinance Conference, Derivatives and Risk Management in Theory and Practice, Frankfurt, 26-27 May, 2007.

[8] A. Antonov, M. Arneguy, and N. Audet. Markovian projection to a displaced volatility Heston model. SSRN working paper, 2008.

[9] A. Antonov and T. Misirpashaev. Efficient calibration to FX options by Markovian projection in cross-currency Libor Market Models. SSRN working paper, 2006.

[10] L. Arnold. *Stochastic Differential Equations, Theory and Applications.* Wiley, New York, 1973.

[11] G. Bakshi, C. Cao, and Z. Chen. Empirical performance of alternative option pricing models. *J. Finance*, 52(6):2003–2049, 1997.

[12] G. Bakshi, C. Cao, and Z. Chen. Pricing and hedging long-term options. *J. Econometrics*, 97:277–318, 2000.

[13] E. Benhamou, A. Rivoira, and A. Gruz. Stochastic interest rates for local volatility hybrid models. *Wilmott Magazine*, 2008.

[14] C. Beveridge and M. Joshi. Interpolation schemes in the displaced-diffusion Libor Market Model and the efficient pricing and greeks for callable range accruals. SSRN working paper, 2010.

[15] F. Black and P. Karasinski. Bond and option pricing when short rates are lognormal. *Financial Analysts J.*, 4(47):52–59, 1991.

[16] F. Black and M. Scholes. The pricing of options and corporate liabilities. *J. Polit. Economy*, 81:637–654, 1973.

[17] M. Bouzoubaa and A. Osseiran. *Exotic Options and Hybrids. A Guide to Structuring, Pricing and Trading.* Willey Finance, United Kingdom, 2010.

[18] A. Brace, D. Gatarek, and M. Musiela. The market model of interest rate dynamics. *Math. Fin.*, 7(2):127–155, 1997.

[19] D. Brigo and F. Mercurio. *Interest Rate Models- Theory and Practice: With Smile, Inflation and Credit.* Springer Finance, 2nd edition, 2007.

[20] M. Broadie and Ö. Kaya. Exact simulation of stochastic volatility and other affine jump diffusion processes. *Operations Research*, 54:217–231, 2006.

[21] M. Broadie and Y. Yamamoto. Application of the fast Gauss transform to option pricing. *Management Science*, 49:1071–1088, 2003.

[22] O. Caps. On the valuation of power-reverse duals and equity-rates hybrids. Presentation at MathFinance Conference, Derivatives and Risk Management in Theory and Practice, Frankfurt, 26-27 May, 2007.

[23] P.P. Carr and D.B. Madan. Option valuation using the fast Fourier transform. *J. Comp. Finance*, 2:61–73, 1999.

[24] P. Cheng and O. Scaillet. Linear-quadratic jump-diffusion modelling. *Math. Fin.*, 17(4):575–598, 2007.

[25] J.C. Cox, J.E. Ingersoll, and S.A. Ross. A theory of the term structure of interest rates. *Econometrica*, 53:385–407, 1985.

[26] M.H.A. Davis and V. Mataix-Pastor. Arbitrage-free interpolation of the swap curve. *IJTAF*, 12(7):969–1005, 2009.

[27] E. Derman and I. Kani. Stochastic implied trees: Arbitrage pricing with stochastic term and strike structure of volatility. *IJTAF*, 1:61–110, 1998.

[28] D. Duffie, J. Pan, and K. Singleton. Transform analysis and asset pricing for affine jump-diffusions. *Econometrica*, 68:1343–1376, 2000.

[29] D.J. Duffy. *Finite Difference Methods in Financial Engineering. A partial Differential Equation Approach.* John Wiley & Sons, Ltd, 2006.

[30] D. Dufresne. The integrated square-root process. Working paper, University of Montreal, 2001.

[31] B. Dupire. Pricing with a smile. *Risk*, 7:18–20, 1994.

[32] F. Fang and C.W. Oosterlee. A novel pricing method for european options based on Fourier-cosine series expansions. *SIAM J. Sci. Comput.*, 31:826–848, 2008.

[33] F. Fang and C.W. Oosterlee. Pricing options under stochastic volatility with Fourier cosine expansions. 15(3):833–838, 2010. Progress in Industrial Mathematics at ECMI 2008.

[34] W. Feller. *An Introduction to Probability Theory and its Applications.* Wiley Chicester, 2nd edition, 1971.

[35] R.A. Fisher. On the interpretation of χ^2 from contingency tables and calculations of P. *J. R. Statist. Soc.*, 85:89–94, 1922.

[36] G. Forsythe, M.Malcolm, and C. Moler. *Computer Methods for Mathematical Computations.* Prentice-Hall, New Jersey, 1977.

[37] J.P. Fouque, G. Papanicolaou, and K.R. Sircar. *Derivatives in Financial Markets with Stochastic Volatility.* Cambridge University Press, 2000.

[38] R. Frey and D. Sommer. A systematic approach to pricing and hedging international derivatives with interest rate risk: Analysis of international derivatives under stochastic interest rates. *Appl. Math. Finance*, 3(4):295–317, 1996.

[39] R. Gaspar. General quadratic term structures of bond, futures and forward prices. Working paper series in economics and finance, Stockholm School of Economics, Sweden, 2004.

[40] J. Gatheral. *The Volatility Surface. A Practitioner's Guide.* John Wiley & Sons, Ltd, 2006.

[41] H. Geman, N. El Karoui, and J.C. Rochet. Changes of numéraire, changes of probability measures and pricing of options. *J. Appl. Prob.*, 32:443–458, 1995.

[42] M.B. German and S.W. Kohlhagen. Foreign currency option values. *J. Int. Money Finance*, 3:231–237, 1983.

[43] A. Giese. On the pricing of auto-callable equity securities in the presence of stochastic volatility and stochastic interest rates. Presentation at MathFinanceWorkshop: Derivatives and Risk Management in Theory and Practice, Frankfurt, 2006.

[44] P. Glasserman and X. Zhao. Fast greeks by simulation in forward Libor models. *J. Comp. Fin.*, 3(1):5–39, 1999.

[45] I.S. Gradshteyn and I.M. Ryzhik. *Table of Integrals, Series, and Products*. Academic Press San Diego, 5th edition, 1996.

[46] L.A. Grzelak and C.W. Oosterlee. An equity-interest rate hybrid model with stochastic volatility and the interest rate smile. Submitted for publication. Available at SSRN: `http://ssrn.com/abstract=1543704`, 2010.

[47] L.A. Grzelak and C.W. Oosterlee. On cross-currency models with stochastic volatility and correlated interest rates. *Forthcoming in Appl. Math. Finance.*, 2011.

[48] L.A. Grzelak and C.W. Oosterlee. On the Heston model with stochastic interest rates. *SIAM J. Fin. Math.*, 2(1):255–286, 2011.

[49] L.A. Grzelak, C.W. Oosterlee, and S. van Weeren. The affine Heston model with correlated Gaussian interest rates for pricing hybrid derivatives. Submitted for publication. Available at SSRN: `http://ssrn.com/abstract=1434829`, 2009.

[50] L.A. Grzelak, C.W. Oosterlee, and S. van Weeren. Extension of stochastic volatility equity models with Hull-White interest rate process. *Quant. Fin.*, pages 1469–7696, 2009.

[51] P.S. Hagan, D. Kumar, A.S. Leśniewski, and D.E Woodward. Managing smile risk. *Wilmott Magazine*, pages 84–108, 2002.

[52] C. He, J.S. Kennedy, T. Coleman, P.A. Forsyth, Y. Li, and K. Vetzal. Calibration and hedging under jump diffusion. *Rev. Derivatives Res.*, 9:1–35, 2006.

[53] D. Heath, R.A. Jarrow, and A. Morton. Bond pricing and the term structure of interest rates: A new methodology for contingent claims valuation. *Econometrica*, 1(60):77–105, 1992.

[54] S. Heston. A closed-form solution for options with stochastic volatility with applications to bond and currency options. *Rev. Fin. Studies*, 6:327–343, 1993.

[55] J. Hull and A. White. The pricing of options on assets with stochastic volatilities. *J. Fin.*, 42(2):281–300, 1987.

[56] J. Hull and A. White. Pricing interest-rate derivative securities. *Rev. Fin. Studies*, 3:573–592, 1990.

[57] J. Hull and A. White. Numerical procedures for implementing term structure models II: Two-factor models. *J. Derivatives*, 2:37–47, 1994.

[58] J. Hull and A. White. Forward rate volatilities, swap rate volatilities and the implementation of the Libor Market Model. *J. Fixed Income*, 10(2):46–62, 2000.

[59] C. Hunter and G. Picot. Hybrid derivatives- financial engines of the future. The Euromoney- Derivatives and Risk Management Handbook, BNP Paribas, 2006.

[60] P. Jäckel. Stochastic volatility models: Past, present and future. *The Best of Wilmott I: Incorporating the Quantitative Finance Review*, pages 379–390, 2004.

[61] P. Jäckel and R. Rebonato. Linking caplet and swaption volatilities in a BGM framework: Approximate solutions. *J. Comp. Fin.*, 6(4):41–60, 2000.

[62] F. Jamshidian. Bond and option evaluation in the Gausian interest rate model. *Research in Finance*, 9:131–170, 1991.

[63] F. Jamshidian. Libor and swap market models and measures. *Financ. Stoch.*, 1(4):293–330, 1997.

[64] R. Jarrow and Y. Yildirim. Pricing treasury inflation protected securities and related derivatives using an HJM model. *J. Finan. Quant. Anal.*, 38(2):409–430, 2003.

[65] N.L. Johnson, S. Kotz, and N. Balakrishnan. *Continuous Univariate Distributions.* Wiley, New York, 2nd edition, 1994.

[66] D. Kahaner, C. Moler, and S. Nash. *Numerical Methods and Software.* Prentice-Hall, New Jersey, 1989.

[67] A. Kawai and P. Jäckel. An asymptotic FX option formula in the cross currency Libor Market Model. *Wilmott Magazine*, pages 74–84, 2007.

[68] W. Koepf. *Hypergeometric Summation: An Algorithmic Approach to Summation and Special Function Identities.* Braunschweig, Germany: Vieweg, 1998.

[69] E.E. Kummer. Über die hypergeometrische Reihe $F(a; b; x)$. *J. reine angew. Math.*, 15:39–83, 1936.

[70] R. Lee. Option pricing by transform methods: Extensions, unification, and error control. *J. Comp. Finance*, 7(3):51–86, 2004.

[71] A. Lewis. Option valuation under stochastic volatility. Finance Press, Newport Beach, 2001.

[72] A. Lewis. A simple option formula for general jump-diffusion and other exponential Lévy processes. SSRN working paper, 2001.

[73] R. Lord. *Private communication*, 2008.

[74] R. Lord and C. Kahl. Why the rotation count algorithm works. Tinbergen Institute Discussion Paper No. 2006-065/2, 2006.

[75] R. Lord, R. Koekkoek, and D.Dijk. A comparison of biased simulation schemes for stochastic volatility models. *Quant. Fin.*, 10(2):177–194, 2010.

[76] K. Mayrhofer and F.D. Fischer. Analytical solutions and a numerical algorithm for the Gauss's hypergeometric function ${}_2F_1$ (a, b; c; z). *Z. Angew. Math. Mech. (ZAMM)*, 74:265–273, 1996.

[77] F. Mercurio and M. Morini. *No-Arbitrage Dynamics for a Tractable SABR Term Structure Libor Model.* Risk Books, modelling interest rates: latest advances for derivatives pricing edition, 2009.

[78] P. Mikkelsen. Cross-currency Libor Market Models. Center for Analytica Finance Aarhus School of Business working paper no.85, 2001.

[79] K.R. Miltersen, K. Sandmann, and D. Sondermann. Closed form solutions for term structure derivatives with lognormal interest rates. *J. Finance*, 52(1):409–430, 1997.

[80] K.W. Morton and D.F. Mayers. *Numerical Solution of Partial Differential Equations, An Introduction.* Cambridge University Press, 2005.

[81] S.M. Moser. Some expectations of a non-central chi-square distribution with an even number of degrees of freedom. TENCON 2007 - 2007 IEEE Region 10 Conference, Oct.30- Nov.2 2007.

[82] M. Musiela and M. Rutkowski. *Martingale Methods in Financial Modelling.* Springer Finance, 1997.

[83] M. Muskulus, K. in't Hout, J. Bierkens, A.P.C. van der Ploeg, J. in't Panhuis, F. Fang, B. Janssens, and C.W. Oosterlee. The ING problem- a problem from financial industry; three papers on the Heston-Hull-White model. Proc. Math. with Industry, Utrecht, Netherlands, 2007.

[84] G.W. Oehlert. A note on the delta method. *Amer. Statistician*, 46:27–29, 1992.

[85] B. Oksendal. *Stochastic Differential Equations; An Introduction with Applications.* Springer-Verlag, New York, 5th edition, 2000.

[86] A. Osseiran and M. Bouzoubaa. *Exotic Options and Hybrids: A Guide to Structuring, Pricing and Trading.* John Wiley and Sons Ltd, 2010.

[87] M. Overhaus, A. Bermudez, H. Buehler, A. Ferraris, C. Jordinson, and A. Lamnouar. *Equity Hybrid Derivatives.* John Wiley and Sons Ltd, 2007.

[88] P.B. Patnaik. The non-central χ^2 and F-distributions and their applications. *Biometrika*, 36:202–232, 1949.

[89] A. Pelsser. A tractable interest rate model that guarantees positive interest rates. *Rev. Derivatives Res.*, 1:269–284, 1997.

[90] A. Pelsser. *Efficient Methods for Valuing Interest Rate Derivatives.* Springer-Verlag London, 2000.

[91] V.V. Piterbarg. Computing deltas of callable Libor exotics in forward Libor models. *J. Comp. Fin.*, 7(2):107–144, 2004.

[92] V.V. Piterbarg. Time to smile. *Risk*, 18(5):71–75, 2005.

[93] V.V. Piterbarg. Smiling hybrids. *Risk*, 19:66–71, 2006.

[94] R. Rebonato. *Modern Pricing of Interest Rate Derivatives: the Libor Market Model and Beyond.* Princeton University Press, UK, 2002.

[95] R. Rebonato. *Volatility and Correlation. The Perfect Hedger and the Fox.* John Wiley & Sons, Ltd, 2nd edition, 2004.

[96] L.C.G. Rogers. Which model for term-structure of interest rates should one use? *Math. Fin.*, 65:93–115, 1995.

[97] M. Rubinstein. Implied binomial trees. *J. Finance*, 49:771–818, 1994.

[98] E. Schlögl. *Advances in Finance and Stochastics: Essays in Honour of Dieter Sondermann*, chapter Arbitrage-Free Interpolation in Models of A Market Observable Interest Rates, pages 197–218. Springer Verlag, Heidelberg, 2002.

[99] E. Schlögl. A multicurrency extension of the lognormal interest rate market models. *Finance and Stochastics*, 6(2):171–196, 2002.

[100] R. Schöbel and J. Zhu. Stochastic volatility with an Ornstein-Uhlenbeck process: An extension. *Europ. Fin. Review*, 3:23–46, 1999.

[101] H. Schurz. Asymptotical mean square stability of an equilibrium point of some linear numerical solutions with multiplicative noise. *Stoch. Anal. App.*, 14:313–353, 1996.

[102] S. Shreve. *Stochastic Calculus for Finance II: Continuous-Time Models.* New York: Springer, 2004.

[103] J. Sippel and S. Ohkoshi. All power to PRDC notes. *Risk*, 15(11):531–533, 2002.

[104] J.C. Stein and E.M. Stein. Stock price distributions with stochastic volatility: An analytic approach. *Rev. Fin. Studies*, 4:727–752, 1991.

[105] A. Takahashi and K. Takehara. Fourier transform method with an asymptotic expansion approach: an application to currency options. *IJTAF*, 11(4):381–401, 2008.

[106] A. van Haastrecht, R. Lord, A. Pelsser, and D. Schrager. Pricing long-maturity equity and FX derivatives with stochastic interest and stochastic volatility. *Ins.: Mathematics Econ.*, 45(3):436–448, 2009.

[107] A. van Haastrecht and A. Pelsser. Generic pricing of FX, inflation and stock options under stochastic interest rates and stochastic volatility. *Forthcoming in Quant. Fin., 2011.*

[108] O.A. Vašiček. An equilibrium characterization of the term structure. *J. Financial Econ.*, 5:177–188, 1977.

[109] P. Wilmott. Cliquet options and volatility models. *Wilmott Magazine*, pages 78–83, 2002.

[110] B. Wong and C.C. Heyde. On changes of measure in stochastic volatility models. *J. App. Math. Stoch. Anal.*, pages 1–13, 2006.

[111] L. Wu and F. Zhang. Fast swaption pricing under the market model with a square-root volatility process. *Quant. Fin.*, 8(2):163–180, 2008.

[112] J. Zhu. *Modular Pricing of Options*. Springer Verlag, Berlin, 2000.

Curriculum Vitae

Lech Aleksander Grzelak was born in Zielona Góra, Poland, on March 12, 1982. After finishing high school he begun his studies in Econometrics and Computer Science at the University of Zielona Góra. After three years of studies in Poland, he moved to the Netherlands to continue the scientific career in the masters programme in Applied Mathematics at the Delft University of Technology. In 2006 he received with honors (Cum Laude) his Master of Science diploma with his thesis entitled "A statistical approach to determine microbiologically influenced corrosion (MIC) rates of underground gas pipelines" under supervision of Roger M. Cooke and in 2007 he received his second Master of Science title at the University of Zielona Góra with a thesis titled: "Stochastic processes for price dynamics" under supervision of Jolanta Misiewicz. In 2007 he continued his research at the Delft University of Technology as a PhD candidate in Numerical Analysis Group under supervision of Cornelis W. Oosterlee.

List of Publications

1. L.A. Grzelak and C.W. Oosterlee. On the Heston model with stochastic interest rates. *SIAM J. Fin. Math.*, 2(1):255–286, 2011.

2. L.A. Grzelak and C.W. Oosterlee. On cross-currency models with stochastic volatility and correlated interest rates. *Forthcoming in Appl. Math. Finance.*, 2011.

3. L.A. Grzelak, C.W. Oosterlee, and S.van Weeren. Extension of stochastic volatility equity models with Hull-White interest rate process. *Quant. Finance*, pages 1469–7696, 2009.

4. C.W. Oosterlee and L.A. Grzelak. Fast pricing of hybrid derivative products. *ERCIM News 78,* July 2009.

5. L.A. Grzelak and C.W. Oosterlee. An equity-interest rate hybrid model with stochastic volatility and the interest rate smile. Submitted for publication, 2010.

6. L.A. Grzelak, C.W. Oosterlee, and S.van Weeren. The affine Heston model with correlated Gaussian interest rates for pricing hybrid derivatives. Submitted for publication, 2009.